THE SEDIMENTOLOGY OF THE CAMBRIAN CLASTIC SEDIMENTS OF NORTHWEST SCOTLAND

A thesis submitted for the degree of
Doctor of Philosophy

by Thomas Mckie B.Sc. (Strathclyde)

Department of Applied Geology,
University of Strathclyde.

February 1988

ABSTRACT

The Cambrian clastic sediments of northwest Scotland crop-out along the line of the Moine Thrust Zone between Skye in the south and Loch Eriboll in the north and form the basal 250m of a broadly transgressive Cambro-Ordovician sequence of clastic and carbonate sediments. These sediments were deposited on the passive western margin of the Iapetus Ocean. The clastic stratigraphy consists of four members; the Lower Member, Pipe Rock, Fucoid Beds and Salterella Grit. The Lower Member consists of 100-125m of mature, cross-bedded quartzarenites which have been subdivided into three facies associations. The lowest association is a 10m thick series of cross-bedded channel sands interpreted as mesotidal barrier inlet deposits. This association is erosively overlain by 10m of thinly bedded, cross-bedded and parallel laminated sands interpreted as lower shoreface sediments. The remainder of the Lower Member comprises compound cross-bedded cosets 1-10m thick interpreted as tidal sandwave deposits. The sudden appearance of numerous Skolithos burrows at the Lower Member-Pipe Rock boundary is interpreted as an evolutionary event representing the colonisation of the Cambrian shelf by suspension feeding annelids. The Pipe Rock is an 85-100m thick sequence of mature, highly burrowed quartzarenites considered to have been deposited in a tidal shelf to outer shelf tempestite setting. The Fucoid Beds consists of 20m of a mixed clastic-carbonate sequence of thinly bedded wave rippled tempestites interbedded with fairweather echinoderm grainstones. The Salterella Grit is a 0-15m thick coarsening upwards sequence of muds and quartzarenites interpreted as having been deposited as tidal sandridges which went through active and moribund stages of development before being buried under carbonate platform sediments. The dominant controls on the facies developed in this sequence were thermal subsidence, eustatic sea level rise and tidal resonant effects. Two rapid shallowing events, in the middle of the Pipe Rock and at the top of the Fucoid Beds, may have been produced by variations in the spreading rate of the Iapetus Ocean.

ACKNOWLEDGEMENTS

I thank Dr. Roger Anderton for supervising this project and for first stimulating my interest in sedimentology. Prof. M J Russell, Dr. I Allison and Dr. R S Haszeldine are thanked for many useful discussions on Northwest Highlands geology, Lower Palaeozoic potassium feldspar authigenesis and sedimentology in general. I am also indebted to Dr. G Bowes who coped admirably with my computer illiteracy and to Dr. A J Hall for advice on mineralogy. Murdoch Macleod and Dugald Turner provided the X-ray diffraction analyses and Peter Wallace and John Gilleece produced endless thin sections and Fucoid Beds slabs. My thanks also go to John Brint, Calum Macaulay, Russell van Claydon, Clark Fenton and Lindsay Ferguson for proof reading this thesis. This research was carried out during the tenure of a N.E.R.C. postgraduate studentship, which is gratefully acknowledged.

CONTENTS

Chapter 1

Introduction

1.1 LOCATION AND REGIONAL GEOLOGY

The Cambro-Ordovician sediments of the northwest Highlands of Scotland crop-out in a linear tract extending from Loch Eriboll in the north to Kishorn in the south, with a faulted outlier occurring on the Sleat peninsula of Skye (Fig. 1.1). The stratigraphy is that of a classical "orthoquartzite-carbonate suite", typical of many Lower Palaeozoic transgressive sequences worldwide. The Scottish sequence consists of a basal 250m of clastic sediments overlain by over 1,000m of carbonate sediments (Fig. 1.2). The clastic sediments, which are the subject of this study, rest with angular unconformity on the Archaean Lewisian gneisses and the Proterozoic Torridonian sandstones. The unconformity is best displayed along the undisturbed western margin of this linear outcrop and is planar wherever it crops out. The eastern margin is defined by a series of major Caledonian thrusts, the Moine Thrust Zone, which may either consist of a narrow series of simple thrusts or, in some areas, may be a complex imbricate zone many kilometres wide. The foreland succession in the west is generally intact but may exhibit evidence of slight movement, particularly within less competent lithologies.

These Cambro-Ordovician sediments may be correlated on faunal and lithological grounds with similar sequences on Spitzbergen, eastern Greenland and western Newfoundland (Swett and Smit 1972, Cowie 1974) which were deposited on the western margin of the Iapetus Ocean during a period of global sea level rise (Matthews and Cowie 1979). Palaeogeographical reconstructions of the Lower Cambrian of the North American craton generally place Scotland opposite southeastern Greenland at a palaeolatitude of approximately twenty degrees south (Jell 1974, Briden et al. 1974, Smith et al. 1981).

1.2 STRATIGRAPHY

Various stratigraphic schemes have been applied to these sediments (Table 1.1). The stratigraphic nomenclature used here follows that of Swett (1969). Although this scheme was not formally proposed and is only partly in accordance with the American Code of

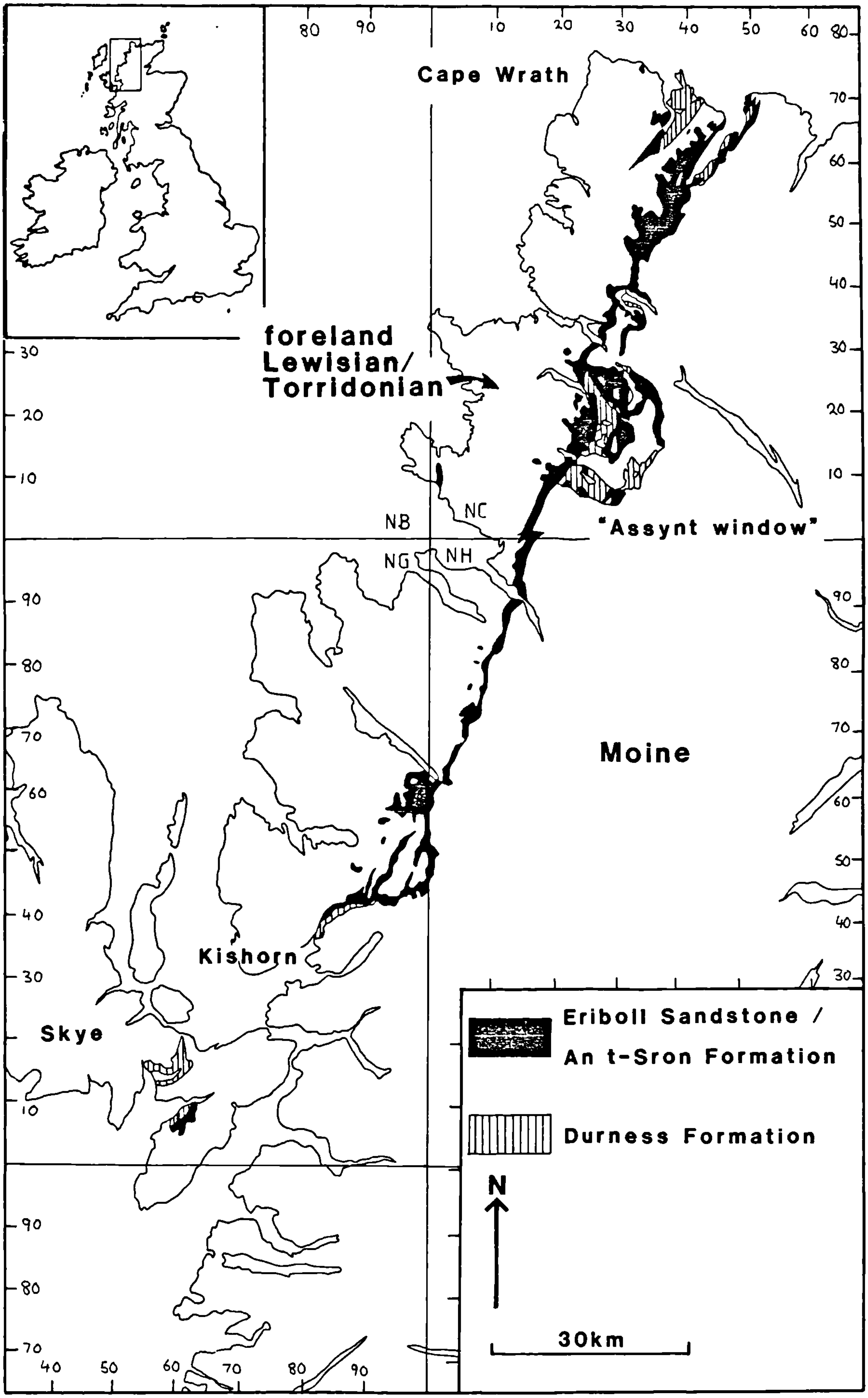

Fig. 1.1 Location map of the Cambrian clastic sediments.

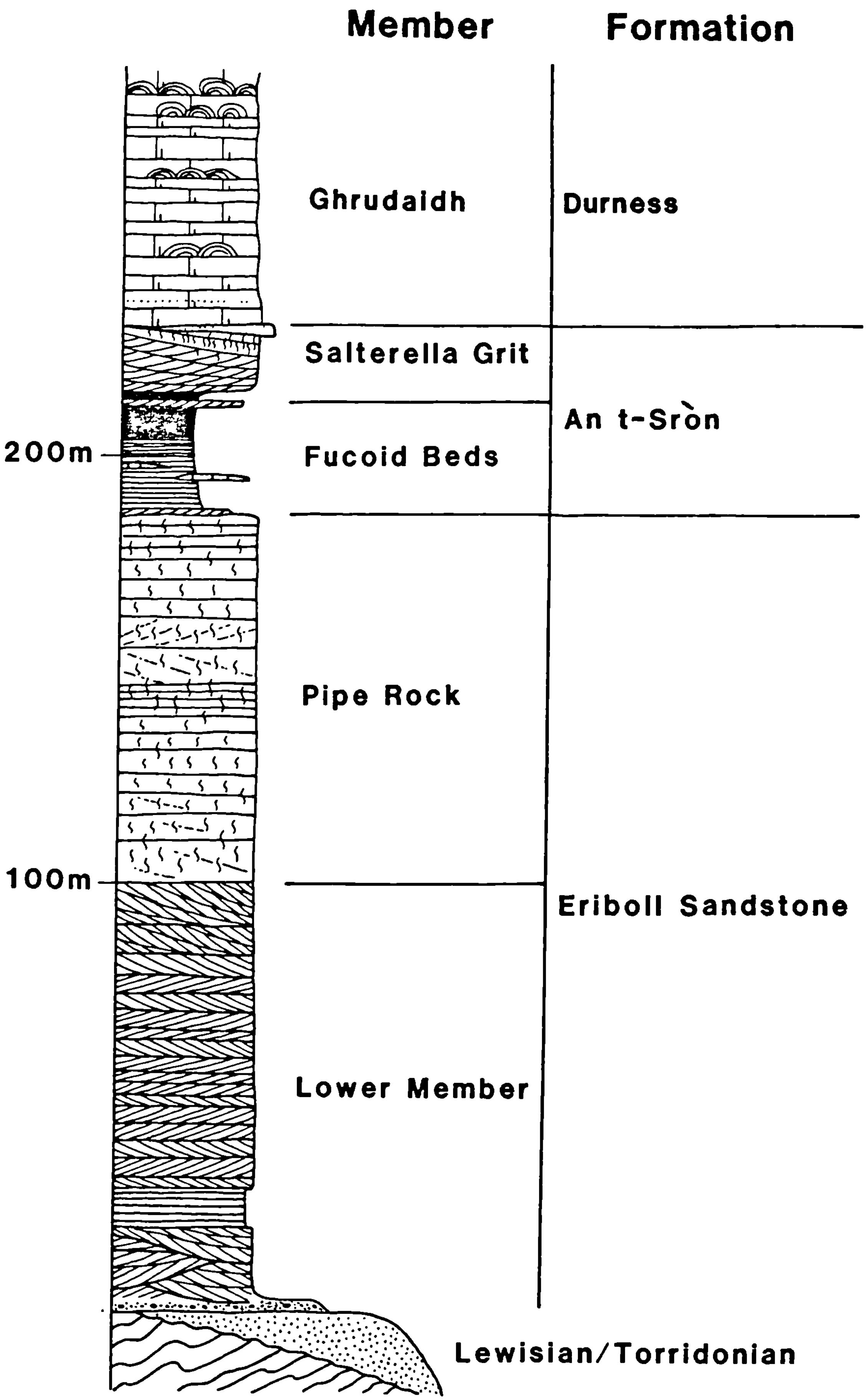

Fig. 1.2 Stratigraphic log of the Cambrian clastic sediments

Peach et al. (1907)	Swett (1969)	Cowie et al. (1972)	This thesis
Serpulite Grit	Serpulite Grit	Salterella Grit	Salterella Grit
Fucoid Beds	Fucoid Beds	Fucoid Beds	Fucoid Beds
Pipe Rock	Pipe Rock	Pipe Rock	Pipe Rock
Basal Quartzite	Lower Member	False Bedded Quartzite	Lower Member

Table 1.1 Stratigraphic nomenclature of the Cambrian clastic sediments.

Stratigraphic Nomenclature (Cowie 1974) it is felt that it is preferable in two respects; it avoids the terms "false bedded", an archaic term for a sedimentological study, and "quartzite", a misnomer for these unmetamorphosed rocks. For this study however the Serpulite Grit will be referred to as the Salterella Grit since Serpulites does not occur within the clastic sequence.

The Eriboll Sandstone Formation consists of the Lower Member and the Pipe Rock Member. This formation correlates with the Kløftelv Formation of eastern Greenland and the Bradore Formation of western Newfoundland (Cowie et al. 1972). The Lower Member consists of 75-125m of unfossiliferous, cross-bedded quartzarenites with minor arkoses and subarkoses mainly concentrated near the base. The Pipe Rock Member is 75-100m thick and is lithologically similar to the Lower Member but differs in that virtually all physical sedimentary structures are obscured by Skolithos burrows. Monocraterion is locally abundant near the middle of the sequence.

The An t-Sròn Formation comprises the Fucoid Beds Member and the Salterella (Serpulite) Grit Member. The Fucoid Beds Member is a 12-27m thick sequence of thinly bedded dolomitic silts and muds with a diverse faunal assemblage. This member may be correlated with the Bastion Formation of eastern Greenland and the Forteau Formation of western Newfoundland. The Salterella Grit Member forms a 5-15m thick, generally coarsening upwards, sequence of muds, silts and cross-bedded sands with Skolithos and Salterella locally abundant. The Salterella Grit may be correlated with the Hawke Bay Formation of western Newfoundland.

1.3 AGE OF THE CLASTIC SEDIMENTS

The presence of olenellid trilobites within the Fucoid Beds (Peach et al. 1907) indicates a Lower Cambrian age for this member, probably within the younger part of the North American Bonnia-Olenellus zone (Cowie and McNamara 1978). Downie (1982), using acritarchs from the top of the Pipe Rock and the Fucoid Beds, made a more precise dating of the Eriboll Sandstone as being equivalent to the Russian Lükati or Vergale Horizons and the An t-Sròn Formation as equivalent to the Lükati Horizon. Peach et al. (1907) record Salterella near the middle of the Pipe Rock in one locality which Yochelson (1983) has suggested is indicative of younger Lower Cambrian age. Although no fossils have yet been recorded from the Lower Member it is likely that the entire clastic sequence is of younger Lower Cambrian age as Downie has suggested. Using the revised Cambrian stage scale of Spizharski et al. (1986) it is reasonable to assume that the Lower Member is at least Atdabanian in age and may even be of Botomian age, and that the Salterella Grit is of Botomian or Tohojian age.

1.4 PREVIOUS RESEARCH

Research on the geology of the northwest Highlands has mostly concentrated on structural studies of the Moine Thrust Zone. Although outcrop is now restricted to a narrow linear belt, Peach et al. (1907) demonstrated that the Cambro-Ordovician sediments within the thrust zone must have extended far to the east of the present area of outcrop. Balanced sections by Butler and Coward (1984) suggest that in the area of Sutherland these sediments restore to a width of roughly 54km, indicating a Cambrian shelf width of at least this value.

Swett et al. (1971) demonstrated a tidal origin for the Eriboll Sandstone based on palaeocurrent evidence and comparable structures in the recent sediments of the Bay of Fundy. They considered the mineralogical maturity of these sands to be the result of prolonged transport in a tidal environment. Russell and Allison (1985) examined weathered Lewisian profiles underlying the Lower Member in the Loch Eriboll area which may represent a Precambrian palaeosol. They suggested that the maturity of the Eriboll Sandstone, and also the Dalradian Appin and Argyll Groups, to be a result of reworking of this quartzose palaeosol.

The Fucoid Beds have generally been considered to represent a more offshore facies than the sands of the Eriboll Sandstone. Peach et al. (1907) likened these beds to muds accumulating in a deep water, offshore environment. Swett (1969) also suggested an offshore environment for the Fucoid Beds but considered the possibilty that the fine-grained, muddy nature was due to increasing distance from the shoreline without necessarily being in deeper water than the Eriboll Sandstone. Bowie et al. (1966), in the course of a geochemical survey of the northwest Highlands, discovered anomalously high concentrations of potassium feldspar in the muds of the Fucoid Beds. The feldspar was considered to be the result of absorption of seawater derived potassium by clay minerals in the sediments during or after deposition. In an alternative hypothesis Swett (1968) suggested that the feldspar was the result of dolomitisation of illitic limestones in the Durness Formation producing diagenetic solutions saturated with respect to K-feldspar which migrated downwards into the Fucoid Beds. Following the discovery of anhydrite in the Fucoid Beds Allison and Russell (1985) suggested an evaporitic lagoonal setting in which the feldspar was precipitated in-situ from alkaline brackish brines derived from weathering of the Lewisian due to mixing with sea water.

Little work has been done on the Salterella Grit and it is generally considered to be a result of a marine regression producing a return to conditions similar to those which produced the Eriboll Sandstone (Swett 1969, Swett and Smit 1972, Cowie and Rushton 1974).

1.5 THE CAMBRIAN PALAEOSHORELINE

Swett et al. (1971) suggested that the Cambrian palaeoshoreline was aligned roughly parallel and to the west of the line of the Moine Thrust Zone on the basis of the lack of facies changes, uniformity of formation thicknesses and palaeocurrent orientations along this line. During this study further palaeocurrents derived from a large variety of facies from all four members of the Cambrian sequence substantiate the palaeoshoreline orientation suggested by Swett et al. Therefore, unless otherwise stated, an outcrop parallel shoreline at some unknown distance to the west is assumed when interpreting individual members.

Chapter 2

The sedimentology of the Lower Member

2.1 INTRODUCTION

The Lower Member forms the basal 75-125m of the clastic sequence and lies with angular unconformity on the Precambrian Lewisian and Torridonian. Where the unconformity crops out it is seen to be planar over a distance of several kilometres (Fig. 2.1). On a larger scale, published maps indicate that the unconformity is probably planar over the whole outcrop length (Peach et al. 1907). The Lower Member rests on the Lewisian mainly north of Loch Assynt, and mainly Torridonian south of this area. There is no evidence of a break in the plane of unconformity at the contact between Lewisian and Torridonian.

The base of this member is conglomeratic and arkosic to subarkosic in composition, the rest of the sequence consisting of cross-bedded quartzarenites, although subarkosic beds occasionally occur. Muds are uncommon and rarely exceed a few centimetres in thickness.

A bimodal palaeocurrent pattern and associated features comparable to those in the modern Bay of Fundy led Swett et al. (1971) to suggest a tidal origin for the Eriboll Sandstone. Recent work in the last fifteen years on modern tidal shelves has shown that there exists a wide variety of tidally produced bedforms which may attain heights of ten's of metres and wavelengths of up to hundreds of metres (Belderson et al. 1982). In order to see if the deposits of such large scale bedforms are present in the Cambrian clastic succession outcrops of a comparable scale were examined. Following Anderton (1985), these large outcrops were photographed and all possible sedimentary structures traced from the photographs. Tracings of the sections were taken into the field and palaeocurrent data, graphic logs and sample locations superimposed on them, thus allowing the large scale geometry and facies variations to be deduced which are not immediately apparent on the limited scale visible in the field.

A close examination of the sequence reveals that it can be subdivided into three stratigraphically defined facies associations (Fig. 2.2) which can be traced along the whole length of outcrop.

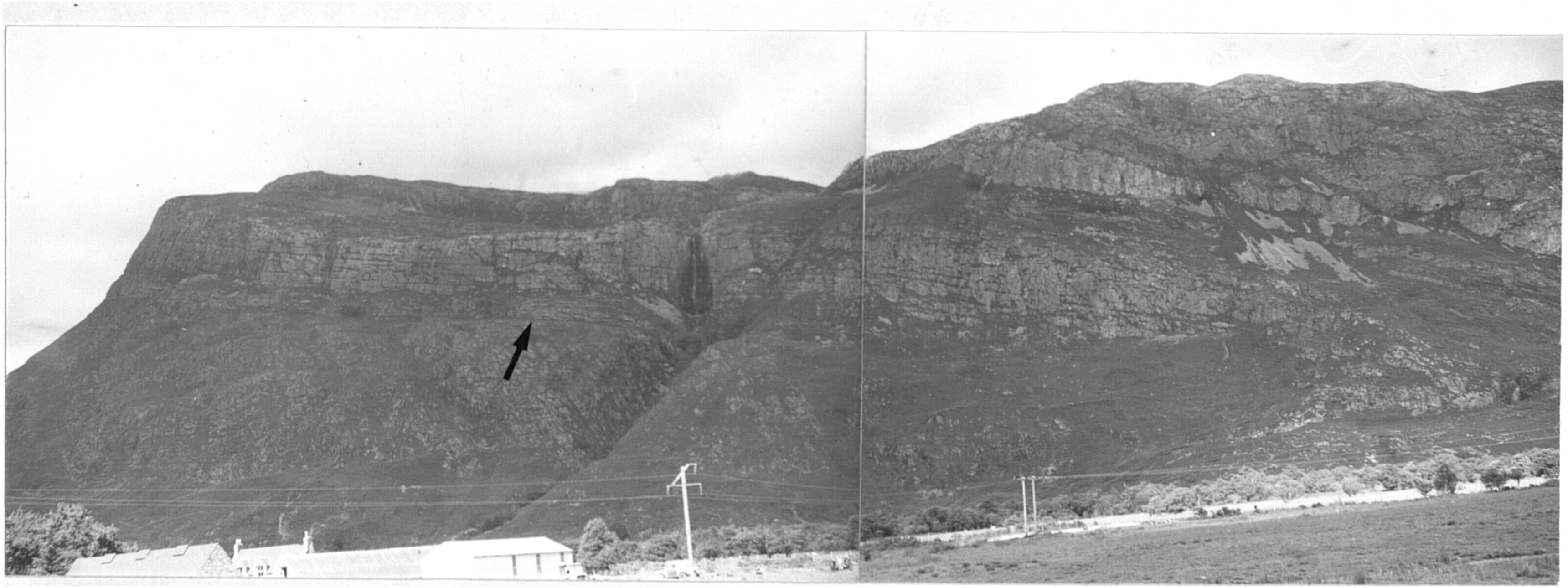

Fig. 2.1 The Torridonian/Cambrian unconformity (arrowed). Kinlochewe, NH 025 645.

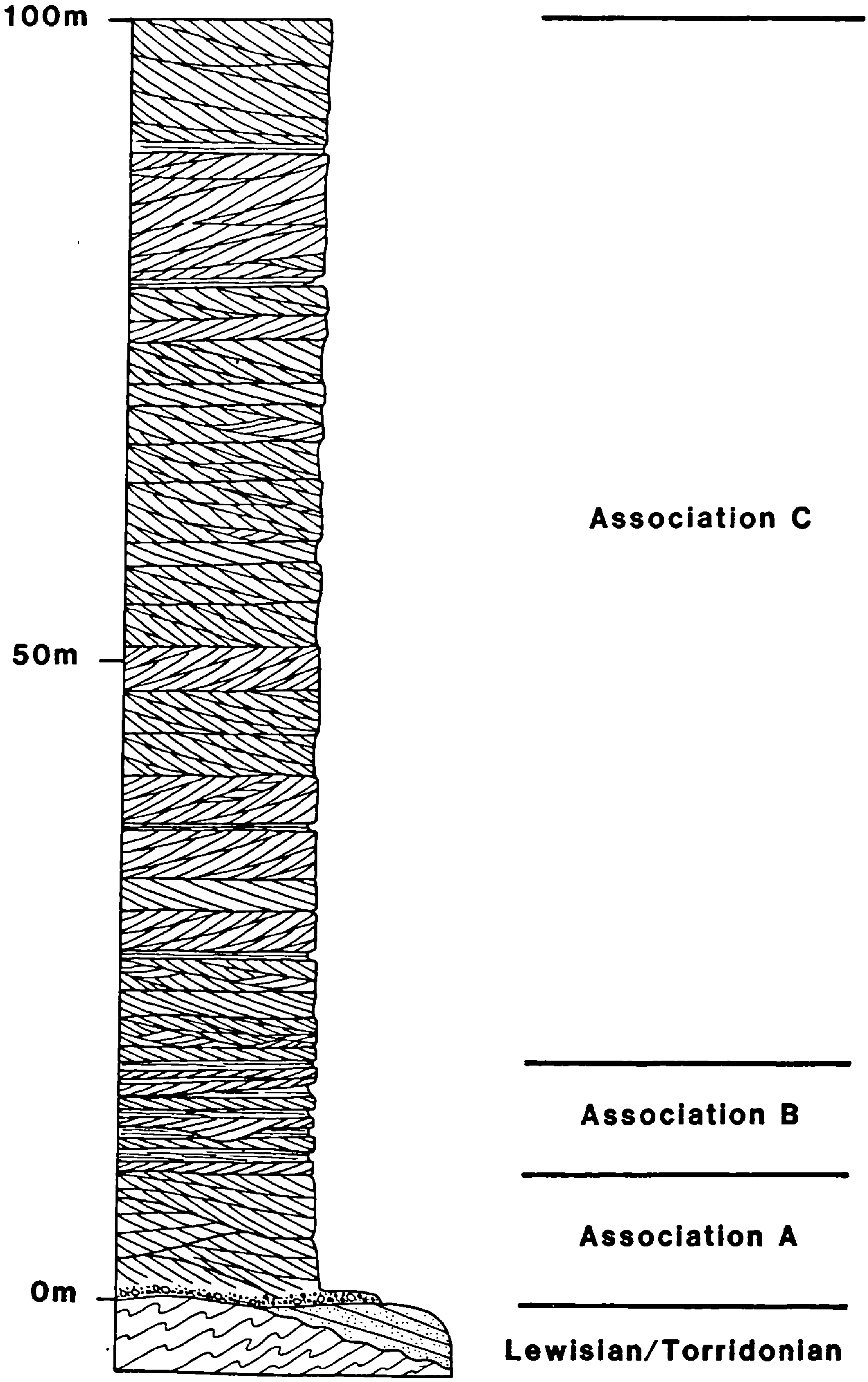

Fig. 2.2 Stratigraphic log of the Lower Member.

Facies association A forms the basal 15-20m of the Lower Member and consists of decimetre thick cross-bedded sands with occasional large channel forms visible. Facies association B comprises the next 10m and is made up of decimetre thick, laterally persistant cross-bedded sands interbedded with centimetre thick parallel laminated sands. The contact with association A is abrupt and is marked by a laterally persistant erosion plane traceable over distances of a kilometre scale in large outcrops. Association B passes gradationally upwards into facies association C. This association consists of a 60-80m thick sequence of cross-bedded sands which form metre scale cosets with a complex internal structure. The laminated sands of association B gradually decrease in frequency upwards through association C. The top 10-20m of this association consists of decimetre thick cross-bedded sands forming up to 10m thick complex bedded cosets. In addition to the sedimentological differences between these facies associations the palaeocurrent distributions for each association also show differences in orientation and modality.

Facies	Typical log	Grain size	Coset/set thickness	Coset/set length	Internal structure	Set surfaces	Other features	Interpretation
6A	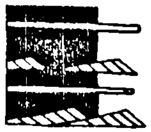	Silt-VFS + mud	40cm cm	10m	Wavy bedding	Bottom planar non erosive. Top not preserved	Up to 30% collophane in muds	Abandoned channel with weak tidal access
5A	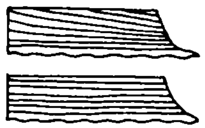	MS-CS	2-10cm	30m	Planar or low angle laminations	Base erosive, top rarely preserved		Storm deposition from surge currents
4A	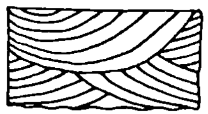	VCS-Granule	25-50cm	<10m	Trough cross bedding	Base erosive, top not preserved	Isolated troughs or persistant sets	Migration of 3-D dunes within barrier inlet
3A	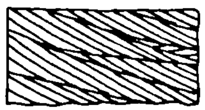	MS-VCS	Cosets 25-100, sets up to 20 cm	10m	Compound cosets. Sets dip at <10°	Base erosive, top not preserved	Sets mostly tabular cross bedded	Migration of small sandwaves within barrier inlet
2A	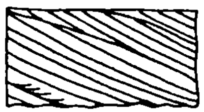	MS-VCS	10-100cm	20m	Tabular cross bedding	Base erosive, top rarely preserved	Abundant reactivation surfaces	Migration of dunes or sandwaves in barrier inlet
1A	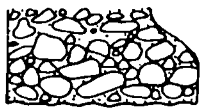	Granule - pebble	2-30cm	Continuous along outcrop	Rare imbrication	Base erosive, top grades into facies 2A		Barrier inlet channel lag

Table 2.1

2.2 FACIES ASSOCIATION A

2.2.1 Facies descriptions

The facies descriptions for facies association A are summarised in table 2.1 and expanded upon below.

Facies 1A: Basal conglomerate

This conglomerate occurs along the full length of outcrop and varies from a few centimetres up to several decimetres in thickness. Clasts range in size from granules to pebbles and are supported in a matrix of medium to very coarse sand (Fig. 2.3). Polycrystalline quartz, with rutile inclusions of probable Lewisian origin, and altered microcline form the bulk of the clasts, although some plagioclase is normally present. The matrix tends to be arkosic in composition and may contain accessory pyroxene grains. There is an absence of current structures in this facies, although in more matrix-free portions the clasts may be imbricated.

Facies 2A: Tabular cross-bedded sands

This facies forms more than 90% of the beds in facies association A. There are sufficient variations within it to merit division into two subfacies on the basis of lateral changes in set geometry.

Subfacies 2Ai: Planar tabular sets

This subfacies consists of 10-100cm thick planar beds of tabular cross-bedded sands (Fig. 2.4a). Foresets range from a few millimetres up to 0.5cm in thickness, a parameter which shows no variation throughout all the Lower Member facies, with either tangential or angular bottomsets, tangential forms being more common. The grain-size of foresets varies from medium to very coarse sand with occasional granule gravels. Granules are also occasionally concentrated at the tops of beds as a winnowed layer a few grains thick. Counterflow ripple laminations occur rarely on bottomsets.

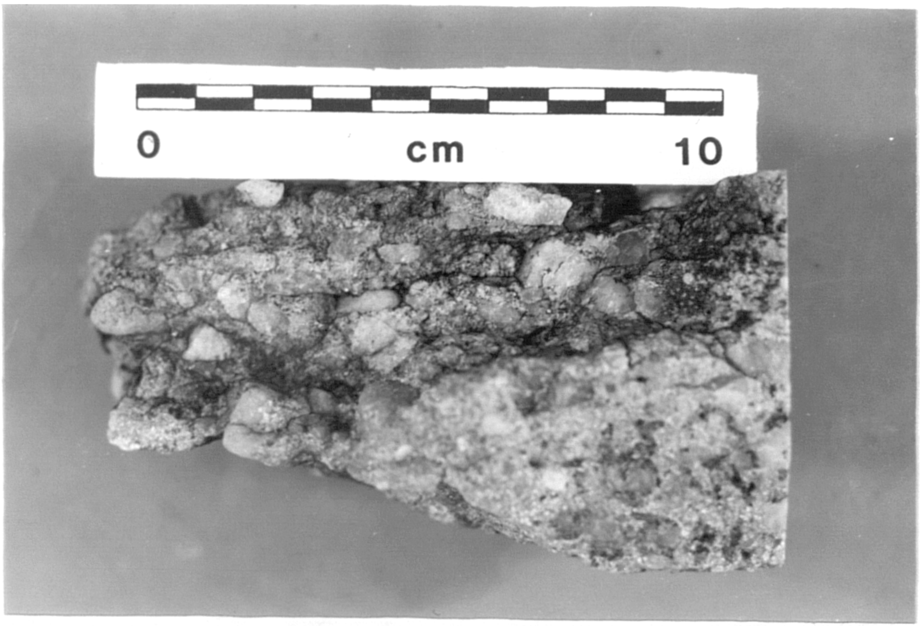

Fig. 2.3 Facies 1A, basal conglomerate (Meall a' Ghiubhais, NG 985 653).

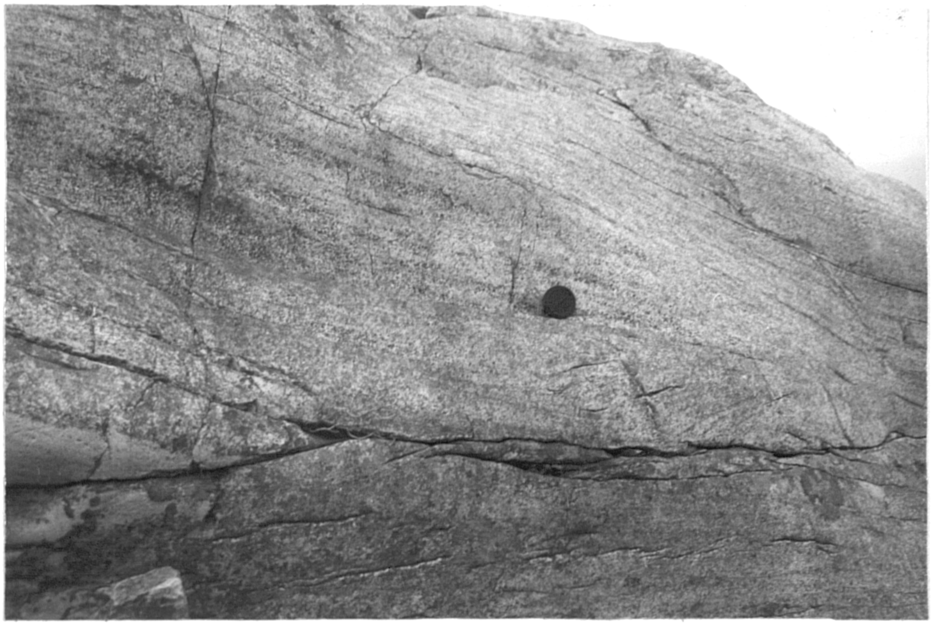

Fig. 2.4a Tabular cross-bedded sets of facies 2A (Creag na Feòla, NH 130 963). Set 70cm thick.

Fig. 2.4b Tabular cross-bedded sets of facies 2A with R3-type reactivation surfaces (Creag na Feòla, NH 130 963). Lens cap 5cm wide.

Individual beds can be traced laterally over distances of up to 20m and are initiated along concave-up erosion surfaces (Fig. 2.5a, R1 surfaces) similar to those of Allen (1973). Beds are terminated by low angle, convex-up reactivation surfaces (Fig. 2.5a, R2 surfaces) which have dips of 0-20 degrees. Overlying sets may thicken over these surfaces to assume the thickness of both sets. Between these larger reactivation surfaces are steeper, more discontinuous forms (Fig. 2.5a, R3 surfaces) which occur as convex-up erosion surfaces in the upper half of foresets, with the lower half parallel to subparallel to the cross-bedding. Within some beds these surfaces are very common and show a cyclic variation in spacing (see section 2.3.2) over a distance of a few metres. In shorter outcrops similar surfaces show a progressive increase or decrease in spacing which may represent portions of a larger periodic variation.

Subfacies 2Aii: Discontinuous tabular sets

This facies is much less common than subfacies 2Ai It is similar in composition and set thickness to subfacies 2Ai but differs in that set boundaries are not planar but frequently preserve dune topography (Fig. 2.5b). Reactivation surfaces are very common, especially the large undulose R1 and R2 forms. Individual sets may be traced laterally over distances of a few metres.

Facies 3A: Compound cross-bedded cosets

This facies comprises 25-100cm thick beds which consist of ripple and dune cross-stratified sets from a few centimetres up to 20cm thick enclosed between gently inclined bounding surfaces. These bounding surfaces are planar with erosively based tangential bottomsets and have dips of up to 10 degrees (Fig. 2.6). The cross-bedding is predominantly oriented down these inclined surfaces and may be enclosed by subhorizontal surfaces which are in turn enclosed by the large dipping surfaces. Up-dip oriented cross-bedding occasionally occurs in some cosets. Grainsize and thickness of foresets are similar to facies 2A. These beds may be traced laterally over many metres where they are invariably terminated by low angle

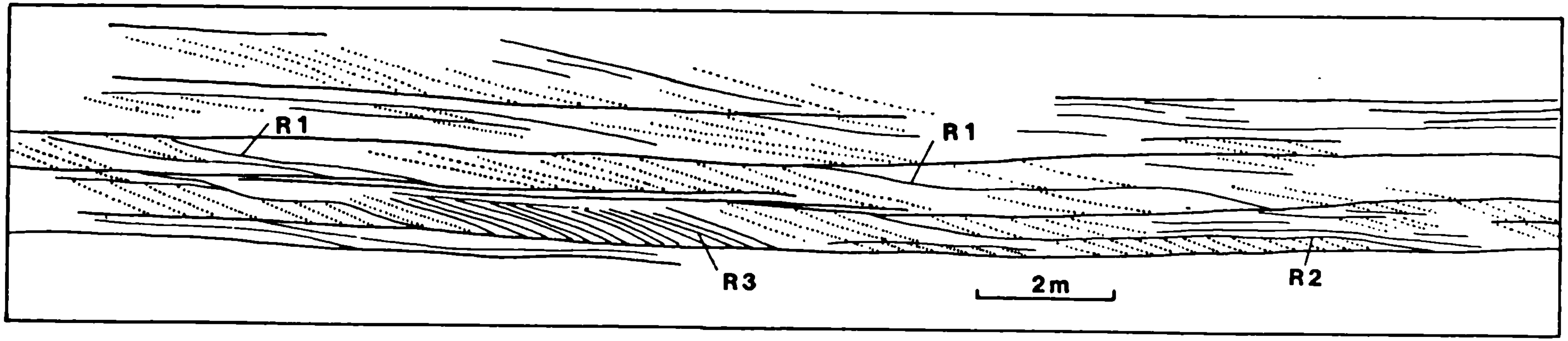

Fig. 2.5a Lateral changes in facies 2A. Facies 2Ai, Creag na Feòla, NH 130 963.

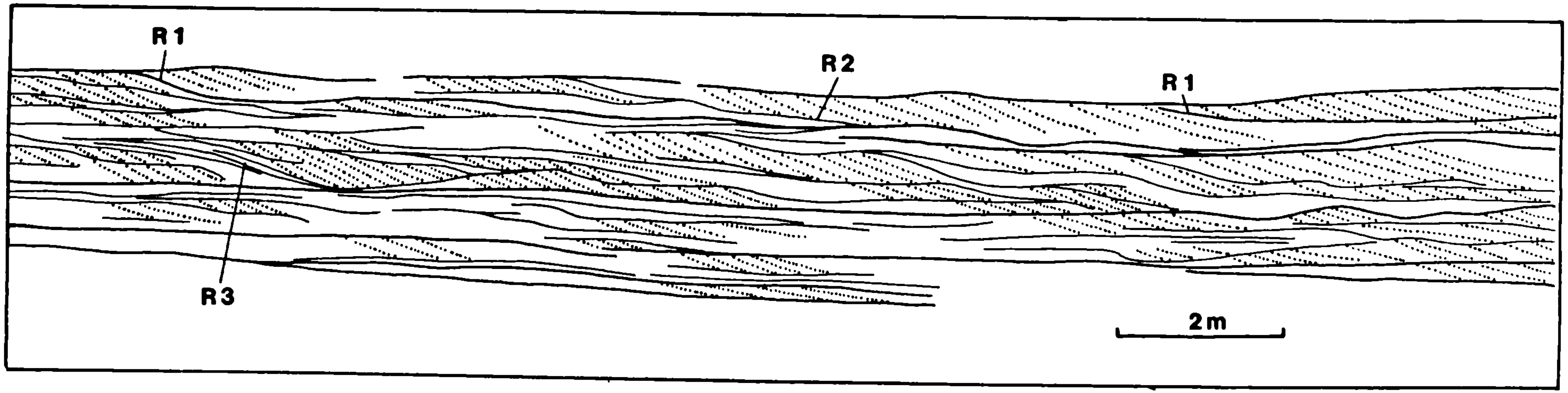

Fig. 2.5b Lateral changes in facies 2A. Facies 2Aii, Tràigh na h-Uamhag, NC 440 661.

Fig. 2.6 Compound coset of facies 3A showing inclined bounding surfaces.
Creag na Feòla, NH 130 963. Scale 50cm long.

reactivation surfaces extending over the full set height and are then followed by facies 2A sets. No transition from other facies into facies 3A has been observed.

Facies 4A: Trough cross-bedded sets

Trough cross-bedded sets are rare in association A. They range in thickness from 25-50cm and consist of very coarse sand to granule sized grains. The cross-bedding may be either concordant or discordant (nomenclature of Allen 1982a, p348). Trough cross-bedded sets may form beds which can be traced over several metres laterally or may occur as isolated troughs within beds of other facies.

Facies 5A: Parallel laminated sands

These beds occur every 50-100cm vertically through association A and are interbedded with facies 2A,3A and 4A. Individual beds range in thickness from 2-10cm and consist of parallel or low angle laminated, ungraded, muddy, medium to coarse sand (Fig. 2.7). Graded examples may occur with a lag of very coarse sand and with mud concentrated at the bed top. The bases of these beds are generally erosive. Current ripple laminations are only rarely present in the top few centimetres of beds. These beds may take on a lenticular aspect due to overlying beds of facies 2A and 3A eroding into them, often removing all of the thinner beds and leaving metre-long lenses preserved. Despite the erosion by overlying beds facies 5A sands can be traced up to 30m laterally.

Facies 6A: Wavy bedded silts

Three examples of this facies have been found at Cnoc a' Bhaic (NC 240 297), Creag na Feòla (NH 002 845), and Coir' a' Ghuibhsachain (NH 002 845). It consists of up to 40cm of quartzose, wavy bedded and thinly laminated silts and fine sands interbedded with dark grey, very fine sands and muds (Fig. 2.8a and b). The wavy bedded sands have current ripple laminations and tend to pass vertically into millimetre thick laminae as the proportion of intervening muds increases, although the reverse situation also occurs. The

Fig. 2.7a Facies 5A parallel laminated sands, Creag na Feòla, NH 130 963. Lens cap 5cm wide.

Fig. 2.7b Facies 5A bed with low angle laminations. Creag na Feòla, NH 130 963.

Fig. 2.8a Facies 6A, wavy silts. Ripple laminated silts interbedded with laminated muds. Coir' a' Ghuibhsachain, NH 002 845. Lens cap 5cm wide.

Fig. 2.8b Facies 6A ripple and plane bedded silts interbedded with laminated muds. Creag na Feòla, NH 130 963. Lens cap 5cm wide.

Fig. 2.8c Thin section of facies 6A muds showing carbonaceous laminae, mica laths and equant dahlite crystals in a collophane matrix. Creag na Feòla. Field of view 1.74mm x 2.78mm.


SIGMA


SIGMA

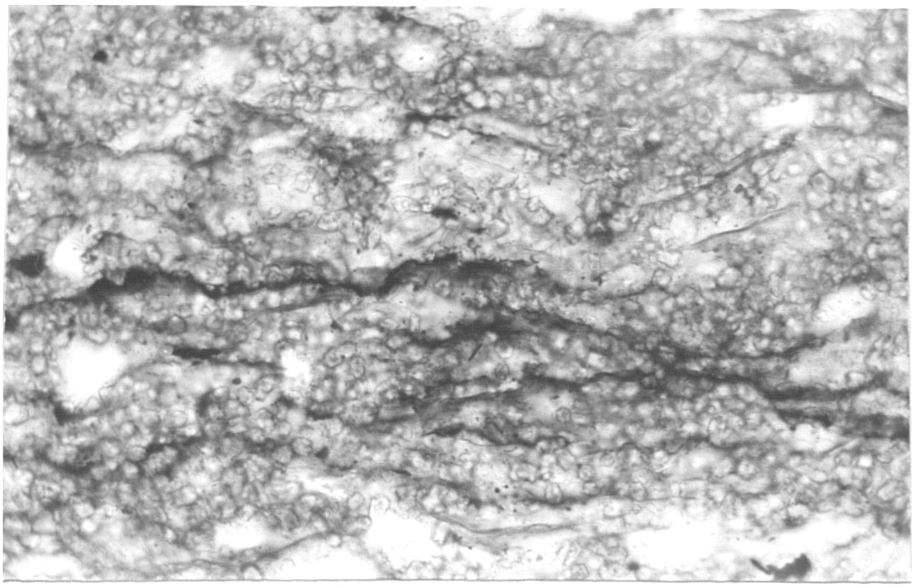

intervening muds contain up to 30% collophane, which is partially recrystallised to dahlite, with isolated "floating" grains of silt sized quartz and feldspar. Thin filaments of carbonaceous material occur parallel to bedding (Fig. 2.8c). These sequences are overlain by erosive-based beds of facies 2A,3A and 4A which cut down into them, resulting in small preserved lenses which can rarely be traced over 10m laterally. The example at Creag na Feòla appears to have been deposited on a gently inclined surface dipping westwards.

2.2.2 Channel forms

Three examples of channel-like forms occur; at Traigh na Uamhag (NC 440 661 , Coire a' Ghuibhsachain (NH 003 848) and Meal a' Ghuibhais (NG 977 655 . In each case only one margin is visible therefore the lateral extent of these forms is unknown (Fig. 2.9). Channels range from 4-7m in depth and are infilled by sands of facies 2A to 5A. Lateral accretion surfaces within the channels are gently inclined at up to 15 degrees along the margins, but may be near horizontal along the base. The three examples are not restricted to a particular stratigraphic level within association A but occur from the unconformity to the top of the sequence. In addition, correction for tectonic tilt in beds of association A, where channels are not visible revealed, that the majority of bounding surfaces of sets or cosets have an inclination similar in steepness and orientation to the inclined beds within the channels suggesting that much of the bedding planes in facies association A may be channel accretion surfaces. Cross-bedding measurements indicate dune migration along these inclined surfaces.

2.2.3 Palaeocurrents

Palaeocurrent measurements were taken on cross-bedding of facies 2A to 4A and on the inclined bounding surfaces of facies 3A (Fig. 2.10). The orientation of channel margins and lateral accretion surfaces were also noted in three areas. The palaeocurrents for facies 2A to 4A show a pronounced easterly, unimodal distribution

Fig. 2.9 Lower Member channel forms, lateral accretion surfaces indicated. Scale bars 5m long.

Fig. 2.9a Channel form resting on unconformity, Tràigh na Uamhag, NC 440 661.

Fig. 2.9b Channel 5-10m above unconformity. Coire a' Ghuibhsachain, NH 003 848.

Fig. 2.9c Lateral accretion surfaces in channel unit, Meal a' Ghuibhais, NG 977 655.

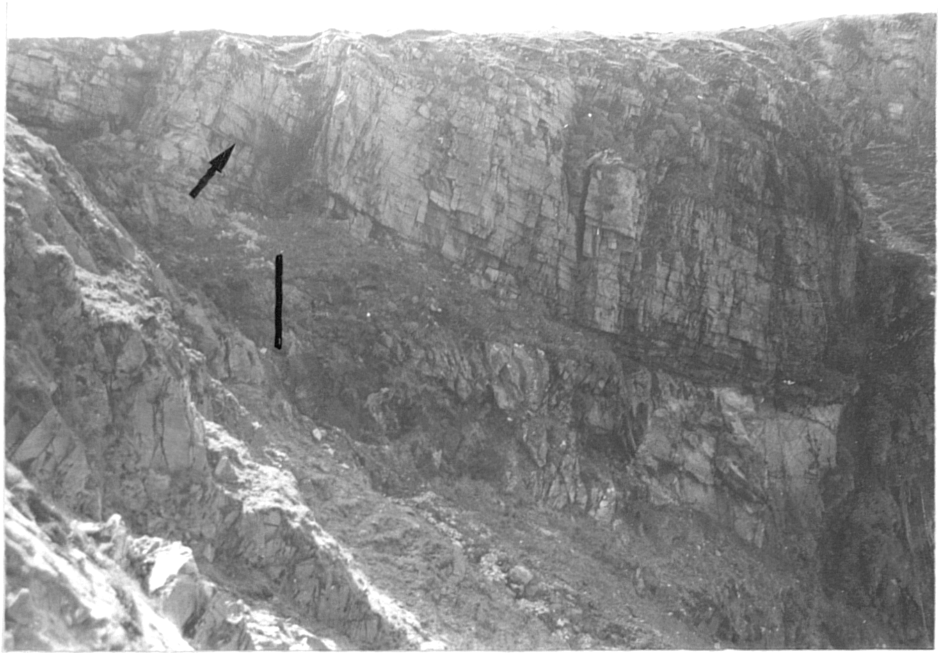

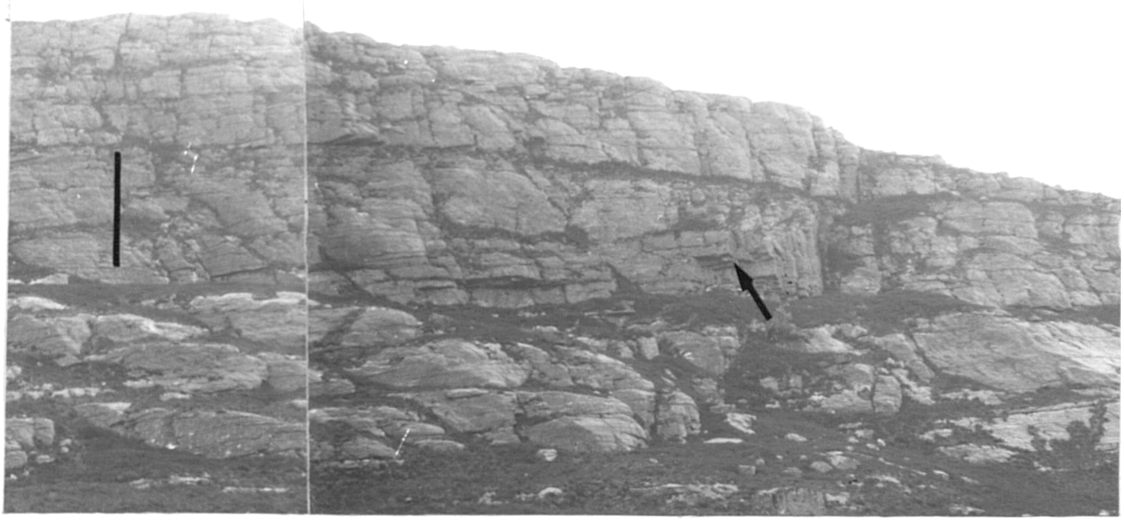

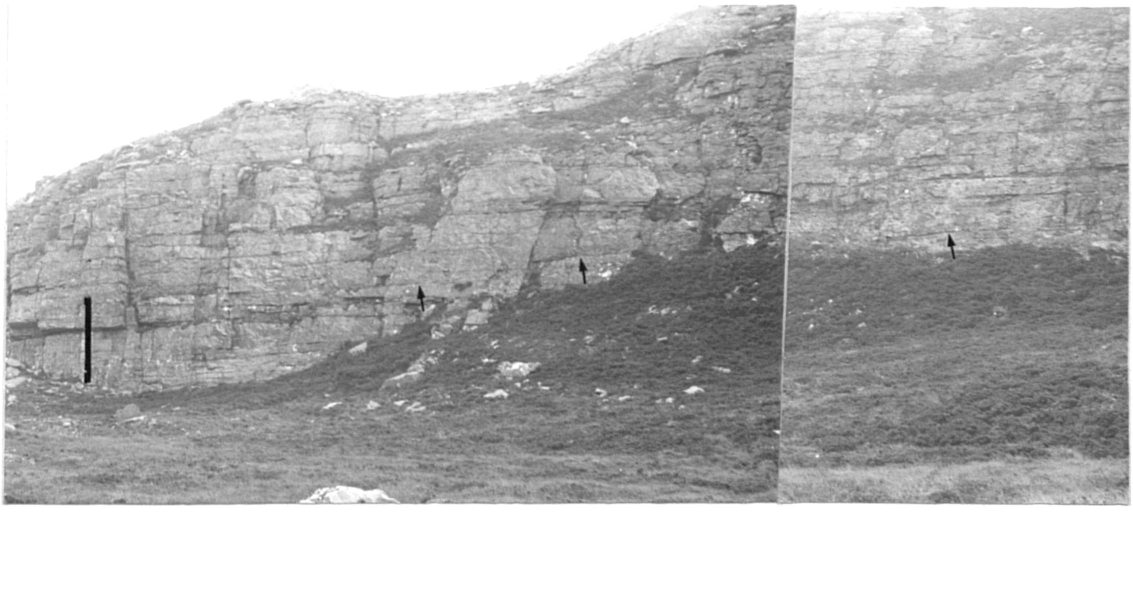

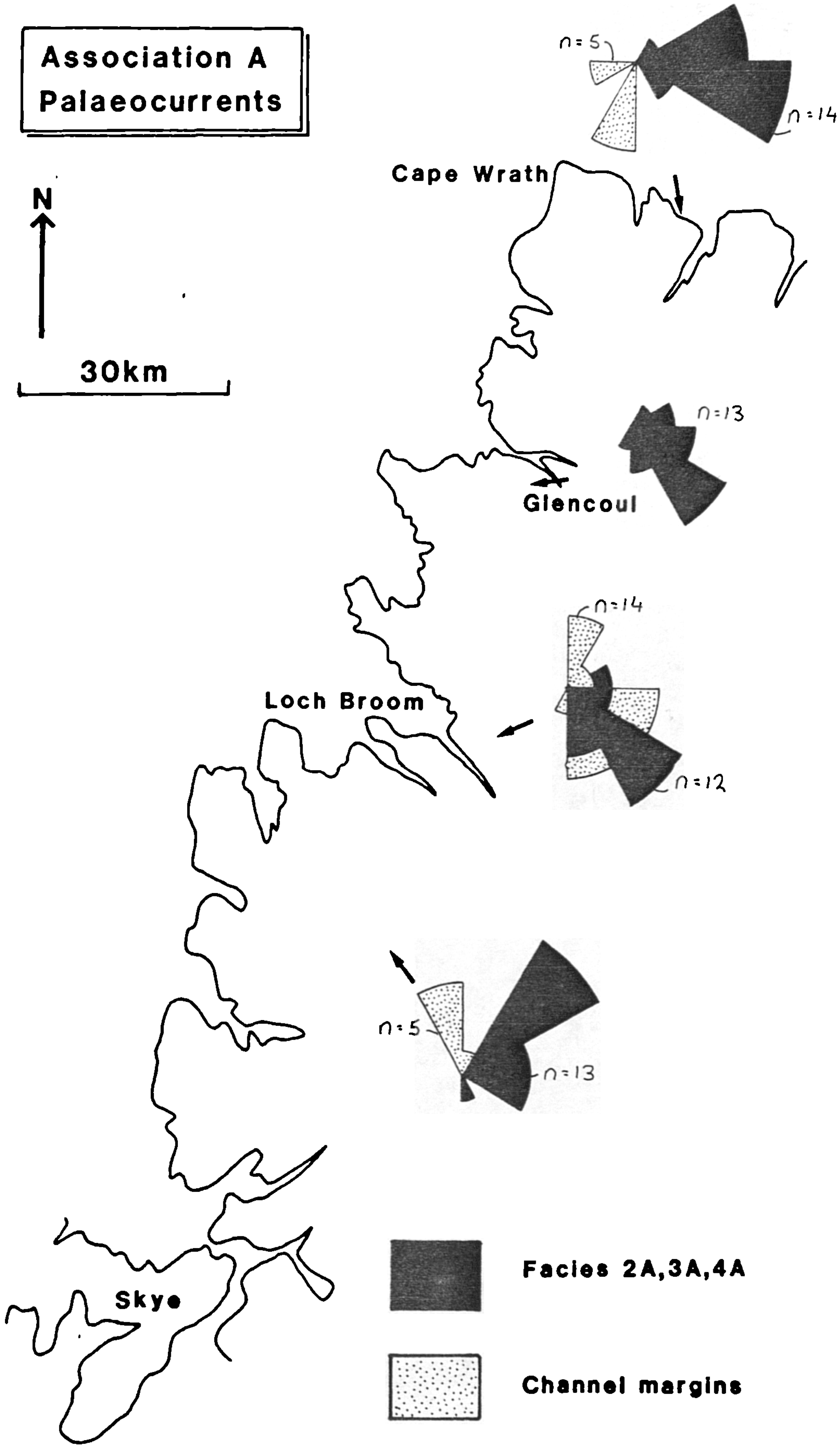

Fig. 2.10 Palaeocurrents for Association A

with an occasional northwards deflection. The channel margins generally dip in a direction perpendicular to the facies 2A to 4A palaeocurrents indicating channel orientations similar to those derived from the cross-bedding.

2.2.4 Interpretation of association A

Association A has a consistent thickness and a lack of any facies variation suggesting that it was all deposited in a similar environment throughout it's outcrop length. Channel forms are present at all levels in the sequence infilled by facies 1A to 5A and the presence of inclined surfaces, which may be channel accretion surfaces, suggests that facies association A consists entirely of channel infill deposits. The abundance of reactivation surfaces, some with cyclic variations in spacing, may imply that these channels were produced by tidal currents. The fact that association A forms the basal portion of the transgressive sequence suggests that these were probably coastal channel systems, in which case an estuarine or barrier island interpretation is most likely. A barrier island interpretation is favoured because of association A's relation to facies association B, the great lateral extent of this facies association and the absence of identifiable estuarine bank and tidal flat deposits. These channels must have migrated laterally to rework any thin deposits of terrestrial or associated barrier sediments down to the unconformity, and to deposit a thin lag of conglomeratic material (facies 1A) and a continuous sheet of inlet filling sands. This mechanism has been demonstrated for recent transgressive barrier systems (Hoyt and Henry 1967, Kumar and Sanders 1970, Kumar 1973) where lateral migration of the deeper ebb channels produces a sheet of inlet sands which has a high preservation potential and is volumetrically the most important part of a barrier depositional system (Moslow and Tye 1985).

Assuming a Cambrian coastline running roughly north-south with a palaeoslope to the east (Swett et al. 1971) the palaeocurrents within association A imply a consistent ebb dominance suggesting a mesotidal regime (Hubbard et al. 1979). Facies 2A, 3A and 4A represent dune or sandwave migration under various strengths of ebb and flood currents within these ebb channels. Subfacies 2Ai was probably deposited by straight to sinuous crested dunes which migrated for considerable distances in an ebb direction. Occasionally the crests and the lee slopes were eroded (R2 surfaces) by infrequent, abnormally large flood currents induced by storms or by the lee vortex of dunes with a greater celerity advancing over them (Allen 1973, DeMowbray and Visser 1984). Periodically, normal flood currents were sufficiently strong to erode dune crests to produce the shorter R3 type reactivation surfaces. This may have been related to the changing hydraulic efficiency of the ebb channels in permitting the ingress of flood currents. In contrast facies 2Aii must have been deposited under currents which were much more unsteady than those responsible for facies 2Ai. This unsteadiness led to the production of abundant reactivation surfaces and preservation of form sets by dune overtaking. Similar bedding sequences to facies 2A have been observed or proposed for modern inlets (Kumar and Sanders 1974, Hayes 1980, Moslow and Tye 1985).

Facies 3A was deposited by dunes or sandwaves with low angle lee slopes on which migrated superimposed dunes and ripples. The lateral extent and shallow dip of the inclined surfaces and the small size of the cross-bedded sets relative to the coset height suggests that these surfaces were not produced by erosion during the subordinate tide but possibly by erosion by the lee vortex of superimposed downcurrent descending ripples. Occasionally the subordinate current was strong enough to produce up dip oriented ripples. These bedforms may be analagous to those described from channels in Lily Bank in the Bahamas (Hine 1977), from the Bay of Fundy (Dalrymple 1984) and from inlets to the Georgia and South Carolina barrier islands (Hubbard et al. 1979).

Facies 4A represents the migration of lunate dunes within the ebb tidal channels. Such dune forms are a common feature of recent inlet sequences (Hayes 1980, Moslow and Tye 1985). Although association A is dominated by facies 2Ai the random distribution of facies 2A, 3A and 4A reflects the unsteady and changing nature of tidal currents within these tidal channels coupled with random wind effects which would have served to enhance tidal currents. The implied greater celerity of facies 2Aii bedforms may have been the result of deposition in more hydraulically efficient channels than the facies 2Ai, 3A and 4A.

The erosive nature, thinness and great lateral extent of the parallel laminated sands of facies 5A suggests a storm origin for these sediments. The erosive base of these beds probably represents scour of the channel floor during peak storm currents, with deposition of suspended material during the waning stage of storm currents. The ungraded nature and mix of mud and sand-sized grains suggests that deposition was rapid. Cacchione and Drake (1982) have shown that rapid deposition of storm suspended material results from the rapid drop in bed shear stress as the near bed suspended sediment concentration increases during waning storm currents. The physical location of these beds within barrier inlet channels would not have been conducive to deposition from gradient or geostrophic storm currents and it is likely that the very rapid deposition of these beds took place from storm surge ebb currents (Hayes 1967) as back barrier ponded storm surge waters were rapidly released through the inlet channels as storms waned. During fairweather periods these beds were particularly vulnerable to reworking by tidal dunes and sandwaves.

Facies 6A occurs in close association with the channel facies and in the example at Creag na Feòla, may have been deposited on an inclined lateral accretion surface. This facies is therefore interpreted as temporarily abandoned channel deposits. The presence of wavy bedding suggests that weak tidal currents were still present (DeRaaf and Boersma 1971). When tidal currents were not forming sandy ripples these abandoned channels would have received some suspended mud and wind blown silt. The presence of carbonaceous laminae and phosphatic material suggests that algal mats were abundant in these channels. Similar abandoned channel sequences have been observed in South Carolina (Tye 1984, Moslow and Tye 1985) and northwest Spain (Villas et al. 1985). The lateral migration of active channels reworked these abandoned channel sequences resulting in the very poor preservation of this facies. Since the observed channel thicknesses are less than the total thickness of association A then vertical accretion of channels must have taken place. This suggests that after initial transgression into the area of outcrop a barrier stillstand took place, allowing total reworking of terrestrial and backbarrier sediments and vertical growth. Vertical growth of the barrier was slow enough to allow reworking of all barrier facies, leaving a continuous sheet of of inlet facies several channel thicknesses deep. Continuous barrier retreat, rather than in-situ barrier drowning, would have been favoured by a low relief coastal plain (Glaeser 1978, Leatherman 1983). The planar nature of the Precambrian-Cambrian unconformity, regardless of underlying geology, suggests that it represents a peneplained surface which would have resulted in wide coastal plains conducive to continuous barrier retreat.

The possible northwards deflection of some channels may have been the result of sediment accretion on the southern margins of channels due to northwards flowing longshore currents. This has been observed in the recent inlets of South Carolina (Barwis and Makurath 1978, Tye 1984) where spit accretion on the downdrift barrier island has resulted in shore parallel aligned channels.

2.2.5 Palaeotidal model for association A

2.2.5.a Introduction

Recent work by Allen (1981), Siegenthaler (1982), Nio et al. (1982), Allen (1984) and Teyssen (1984) has shown that it is possible to model palaeotidal currents from cross-bedded sets which show a periodic variation in structure which can be attributed to a spring-neap cyclicity.

Within association A the small scale (R3) reactivation surfaces at Creag na Feòla show a cyclic variation in spacing (Fig. 2.11), similar to those observed by Terwindt (1981) from the recent sediments of the Oosterschelde, which may indicate a tidal influence. The cross-bedding is ebb oriented and the reactivation surfaces probably represent erosion of dune crests during flood tides. Similar series of reactivation surfaces occur throughout association A but

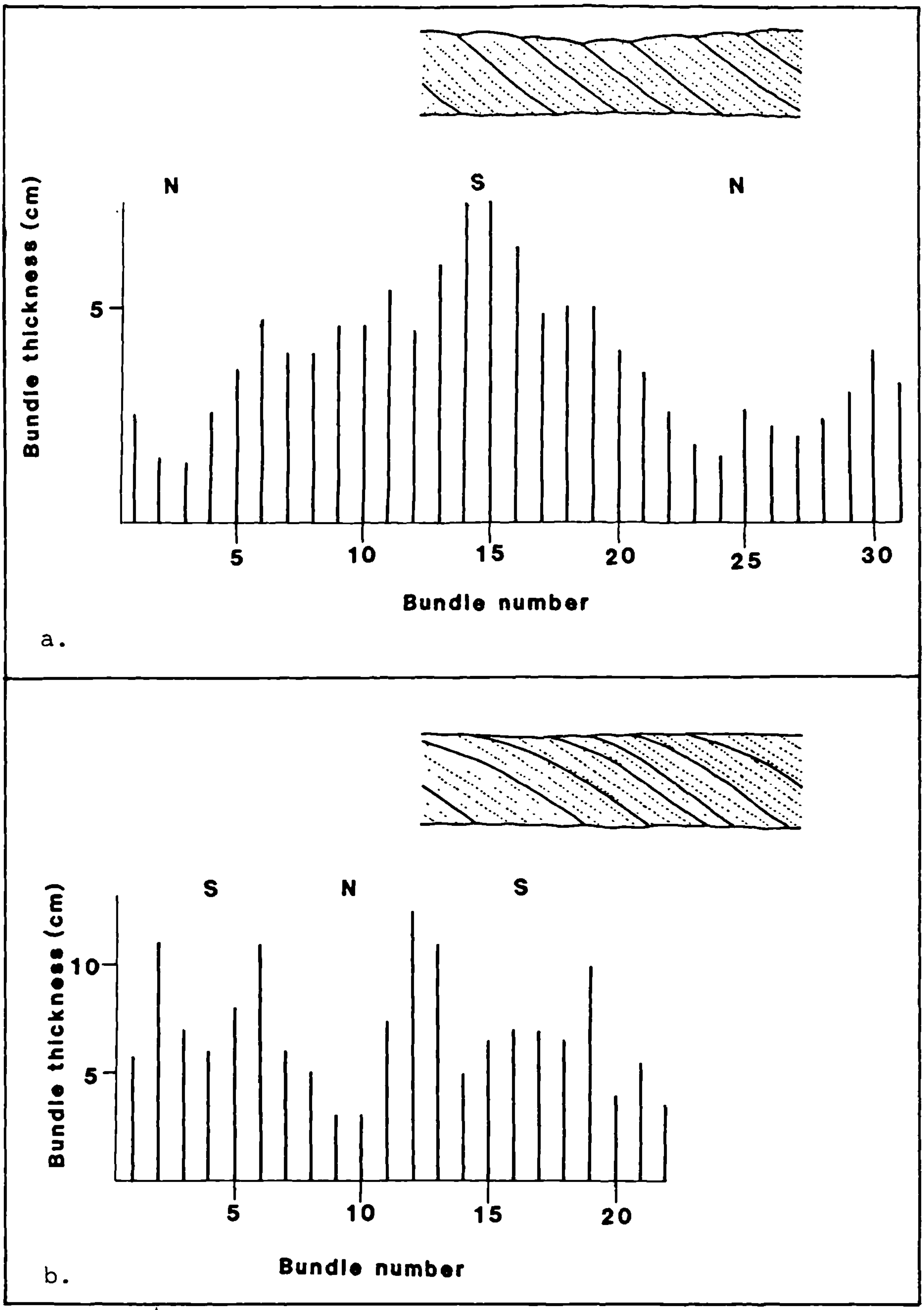

Fig. 2.11 Periodic structure spacing within set of Association A. 2.11a Meall a' Ghuibhais, 2.11b Creag na Feòla.

they lack the lateral extent required to determine whether their spacings are cyclic in distribution. However, many do show a consistent increase or decrease in spacing suggesting that perhaps they may form part of a larger scale periodicity. Other cross-bedded units lack persistent reactivation surfaces, but show a cyclic variation in the thickness of well cemented, coarse grained "bundles" of foresets which are separated by foreset parallel joints (Fig. 2.11). These joints are an unusual feature within the cross-bedding of the Lower Member and probably utilised weaker foreset parallel planes which reflect some depositional feature. The overlying beds show up to 1cm of erosion at the sites of these joints, suggesting that the unconsolidated sediment was more easily eroded in these areas. These planes probably represent slack water periods between tides when a limited amount of fines were deposited along dune slipfaces, and the intervening "bundles" the migration of these dunes during full ebb currents. Plots of bundle spacing, grainsize and set thicknesses are presented in table 2.1.

Lambeck (1978) has shown that the Cambrian lunar month was probably 30-31 days long and therefore the presence of spring-neap cycles in association A (Fig. 2.11) with more than 15 bundles is indicative of a semidiurnal tidal system. The fact that no sequence has 30-31 bundles per cycle implies that during neap tides currents were below threshold values.

Estimation of tidal current velocities were made using the FORTRAN IV program of Teyssen (1984), which is a variation on the method of Allen (1981), and the method of Nio et al. (1983). In each case the formulae were corrected for a Cambrian semi-diurnal tidal period of approximately ten hours (Scrutton 1978). In the example used with reactivation surfaces spacings were measured where the surfaces were parallel to the foresets and it was assumed that negligible erosion had taken place in proportion to the total bundle thickness. Threshold current data were derived from Miller et al. (1977). The results are presented in table 2.1.

Location	Bundle thickness (m)	Grain size (cm)	Set thickness (m)	Tide*	Velocity (m/s) Teyssen model	Velocity(m/s) Nio et al. model
NG130963	0.080	0.06	0.68	P	1.1	0.95
NG130963	0.070	0.03	0.68	P	1.4	0.70
NG130963	0.030	0.04	0.68	W	1.3	0.80
NG977657	0.015	0.05	0.40	W	1.4	0.63
NG977657	0.070	0.07	0.45	P	1.2	0.70
NG977657	0.020	0.05	0.30	W	1.4	0.66
NG978658	0.130	0.04	0.47	P	1.3	0.93
NG978658	0.040	0.04	0.33	W	0.9	0.70

* P -maximum bundle thickness therefore probably peak spring tides
  W -minimum bundle thickness reflects tides just above threshold velocities and not neap tides

A channel depth of 10m is assumed for the Nio et al. model

Table 2.1 Estimates of palaeotidal velocities for association A

2.2.4b **Results**

Spring ebb tidal currents were calculated to range from 0.65-1.0m/s (method of Nio et al. 1982) or 0.9-1.4m/s (method of Teyssen 1984). The method of Nio et al. is considered more reliable since it is largely a function of bundle thickness as opposed to Teyssen's program which is more sensitive to grain-size variations, a parameter which varies little in these bundle sequences. Values of 0.6-1.0m/s are comparable to velocities within the South Carolina inlet ebb channels (Hubbard et al. 1979).

Spring flood tidal currents must have ranged from below the threshold velocity of medium sand sized grains in bundles without reactivation surfaces to just above threshold values in sequences with reactivation surfaces. During neap tides currents were consistently below threshold values for both ebb and flood tides. M_2 spring tidal curves for bundle sequences at Creag na Feòla and Meall a' Ghiubhais are presented in Fig. 2.12. For the M_f tidal curves, the number of bundles present indicate the number of days in a fifteen day spring-neap cycle when velocities were below threshold values (Fig. 2.12). These tidal curves represent velocity asymmetric currents within the deep ebb dominated channels of the tidal inlets. Flood tidal currents would presumably have been greater within the shallower marginal flood channels (Hayes 1980) which have not been preserved. A time-velocity asymmetry (Hayes 1980) within these deep channels due to residual ebb currents during flood tides is impossible to ascertain, but probably existed. The differences in M_2 ebb and flood tidal velocities and duration of currents above threshold values for the M_f tide in the two examples is probably related to the relative hydraulic efficiency of the channels and the amount of "leakage" between ebb and flood channels. Abnormally thick bundles within these spring-neap cycles probably represent tidal currents enhanced by wind forced currents produced by smaller storms than those responsible for deposition of facies 5A.

Using the method of Nio et al. a tidal range of 1.2-3.0m was calculated for spring tide bundles, confirming the mesotidal interpretation suggested by the ebb dominance of the palaeocurrents.

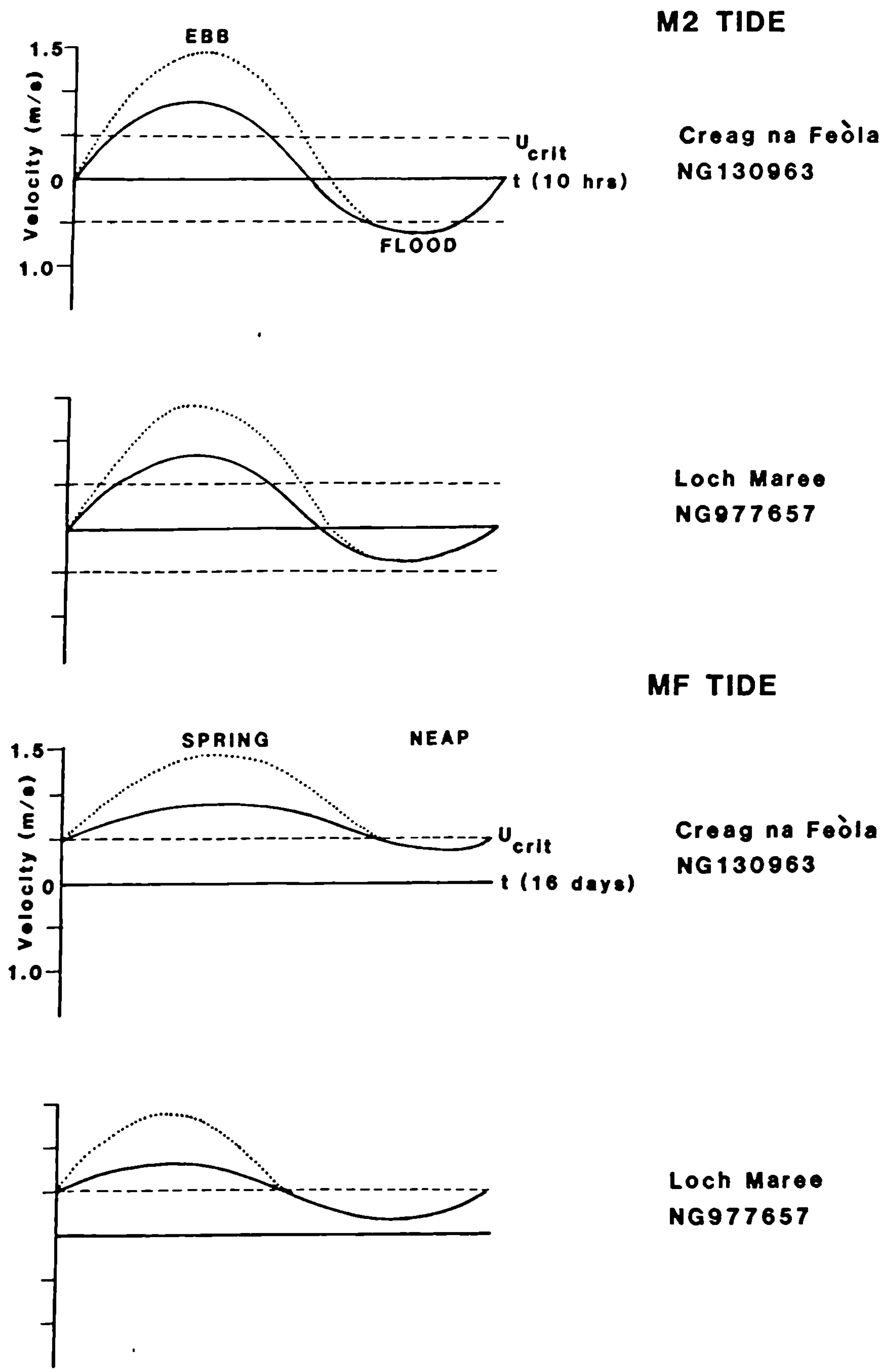

Fig. 2.12 Idealised palaeotidal curves for the M_2 and M_f tides for two specific channels in which spring-neap cyclicity is displayed.

Facies	Typical log	Grain size	Coset/set thickness	Coset/set length	Internal structure	Set surfaces	Other features	Interpretation
4B	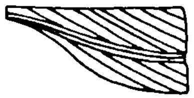	Infilled by facies 1B or 3B	40cm	4m	Channel form	Base channeled, top planar		Large gutter casts produced by storm rip-currents
3B	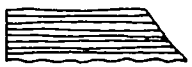	FS-CS	3-20cm	30m	Planar lamination	Base erosive, top rarely preserved	May be amalgamated into units up to 50cm thick	Shoreface storm deposits
2B	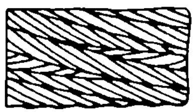	CS-VCS	Cosets 50-150 sets 5-25cm	10m	Compound cosets. Sets dip at 5-15	Base erosive, top rarely preserved	Sets mostly tabular cross bedded	Fairweather tidal sandwaves on shoreface
1B		CS-VCS	5-40cm	15m	Tabular cross bedding	Base erosive, top rarely preserved	Deformation structures at one locality	Fairweather and storm produced shoreface dunes

Table 2.3

2.3 FACIES ASSOCIATION B

2.3.1 Contact with association A

Facies association A passes abruptly into facies association B. Where visible, this contact is planar over distances of several kilometres (Fig. 2.13). Also, it does not vary in height above the basal unconformity over a lateral scale of a few ten's of kilometres, although variations of up to 5m may occur throughout the whole outcrop length. The facies descriptions for facies association B are summarised in table 2.3.

2.3.2 Facies descriptions

Facies 1B: Tabular cross-bedded sets

This facies is volumetrically the most abundant in association B. Beds range in thickness from 5-40cm, are erosive based and are generally ungraded (Fig. 2.14). Foresets range from coarse to very coarse sand, with occasional granule foresets present. The cross-bedding is tabular with dips of generally 15-20 degrees, although dips of up to 25 degrees occur. Bottomsets are mostly tangential with a subordinate number of angular examples. Form sets are rarely preserved and have vertical form indices ranging from 35-60, although these values are probably slightly larger than the original values due to erosion by overlying beds. At one locality (NH 130 963) this facies shows evidence of soft sediment deformation (Fig. 2.15). The disturbed bed is 5m wide and forms a flat-based convex-up lens with an undulose upper surface.

Facies 2B: Compound cross-bedded cosets

Cosets of this facies range from 50-150cm in thickness and are defined by erosive horizontal (E1) bounding surfaces (Fig. 2.16). These cosets are composed internally of gently dipping sets inclined at 5-15 degrees defined by inclined (E2) bounding surfaces up to 75cm long. Sets are composed of ripple and parallel laminated coarse to

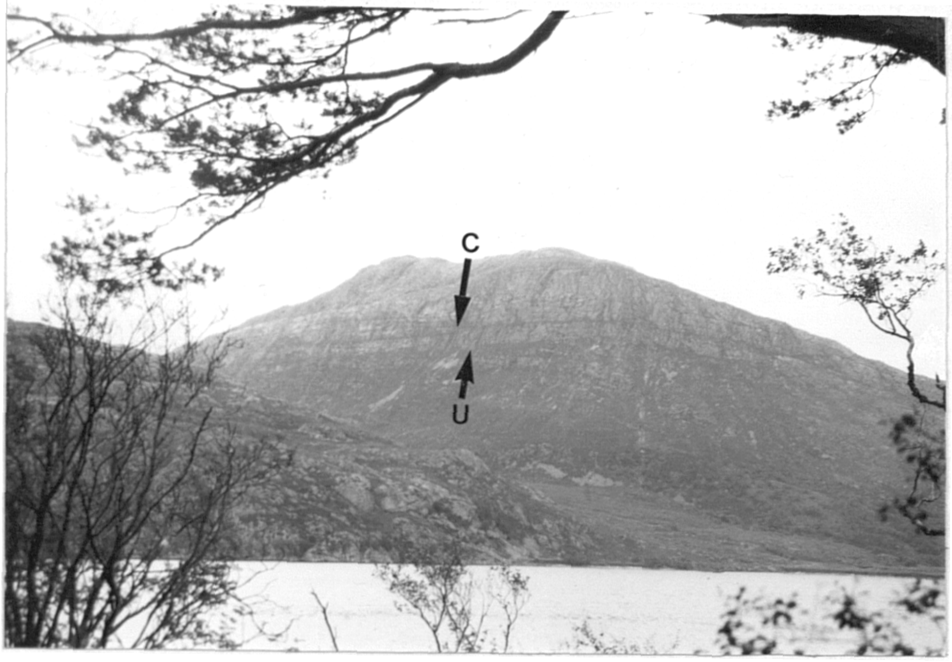

Fig. 2.13 Planar contact of associations A and B, Coille na Dubh Chlaise, NH 022 655.
U-unconformity, C-associations A and B contact.

Fig. 2.14a Tabular cross-bedded sets of facies 1B, Druim na h-Uamha Móire, NC 235 292. Note erosive set bases and opposed migration directions. Hammer 40cm long.

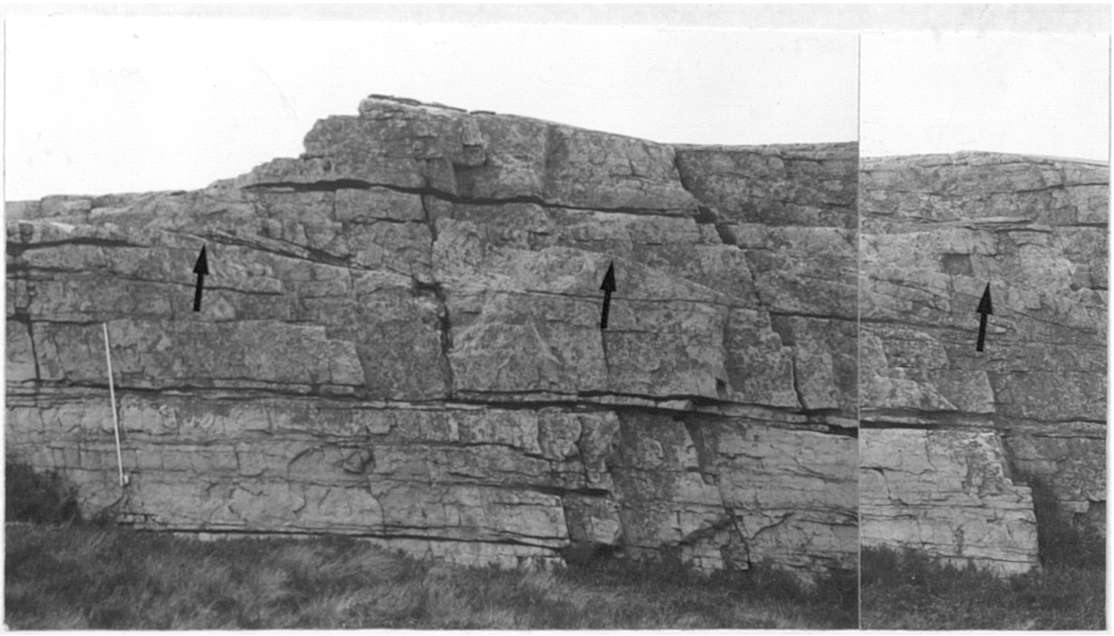

Fig. 2.14b Sets of facies 1B, Creag na Feòla, NH 132 963. Note spaced sigmoidal reactivation surfaces. Scale 50cm.

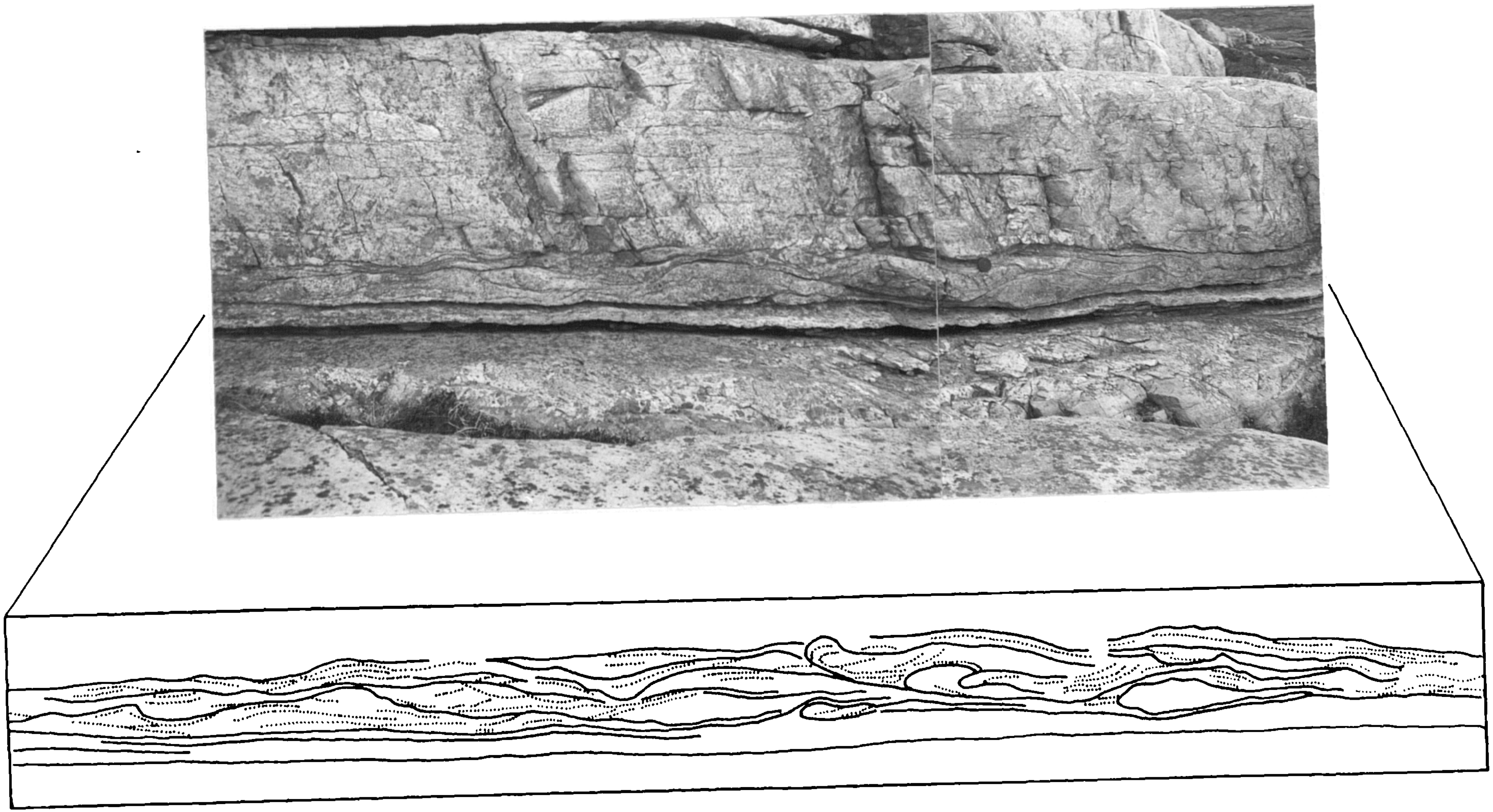

Fig. 2.15 Deformed facies 1B set (NH 132 963). Lens cap 5cm wide.

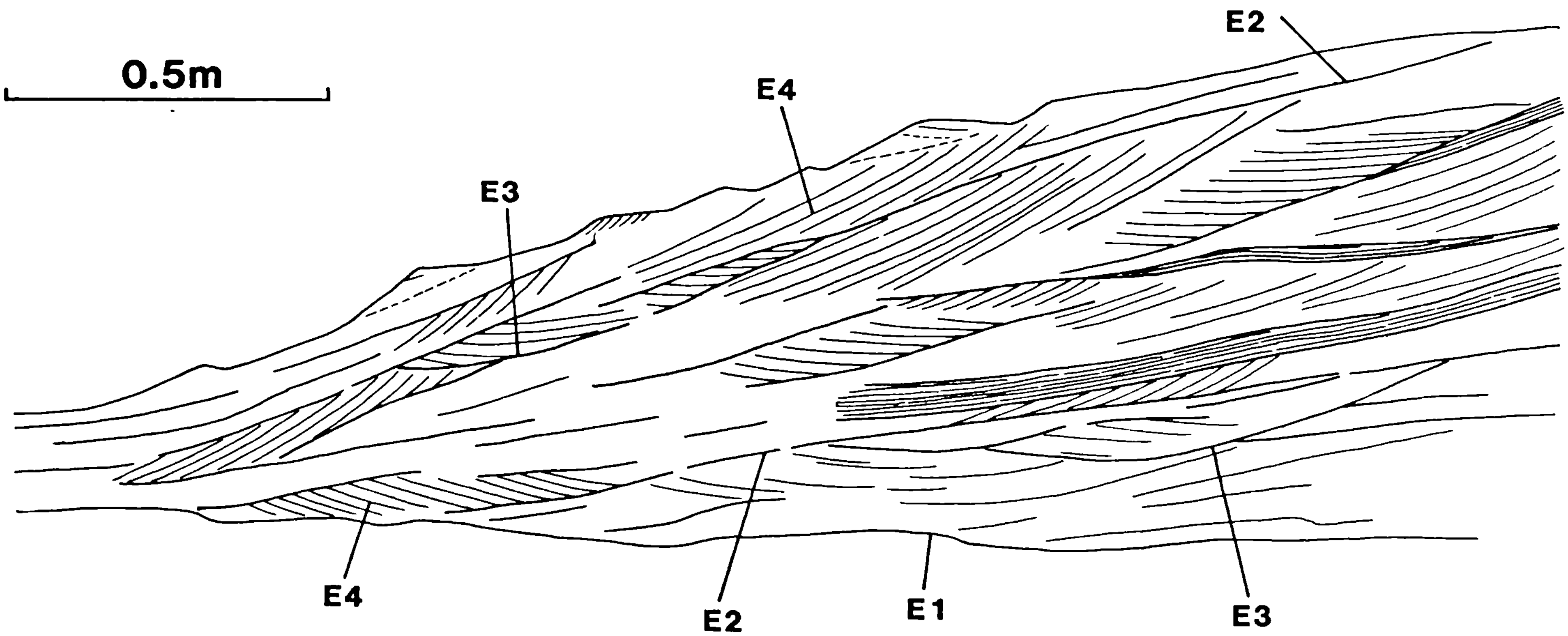

Fig. 2.16 Compound coset of facies 2B (Druim na h-Uamha Móire, NC 235 292) traced from a field photograph. The dip of the inclined set is exaggerated. Note the presence of parallel laminated beds of facies 3B.

very coarse sand. Ripple laminations are further enclosed by horizontal to subhorizontal third order (E3) bounding surfaces. Occasional erosive second order surfaces cross-cut all other structures and have dips of 0-15 degrees, and extend the full coset height. These cosets are occasionally seen to be initiated on rare low angle reactivation surfaces of facies 1B and are terminated by burial of the lee slope by descending facies 1B cross-beds which assume the full set height.

Facies 3B: Parallel laminated sands

This facies consists of 3-20cm thick beds of parallel laminated, muddy, fine to coarse sand. Beds are frequently erosive-based and may be graded or ungraded. The top few centimetres of some beds may show current or wave ripple laminations. The wave ripple laminations are very similar to the "swell and pinch" type of DeRaaf et al. (1977). Vertically through association B these beds are very frequent (Fig. 2.17) and may be amalgamated in some cases. Laterally, individual beds can be traced for many tens of metres before being eroded by overlying beds of facies 1B and 2B. Frequently the resultant erosion plane can be traced over many metres, where occasional lenses may be preserved of facies 3B beds. Less commonly these beds occur draping erosional surfaces, inclined planes and rippled surfaces within beds of facies 1B and 2B (Fig. 2.16).

Facies 4B: Small channels

Channel forms sporadically occur throughout association B. These channels are symmetrical in cross-section and may be up to 50cm deep and 400cm wide (Fig. 2.18). Channels are infilled by laminated sands of facies 3B or by vaguely cross-bedded sands of facies 1B. Where infill is by facies 3B the laminated beds are thin and the remainder of the channel is infilled by facies 1B.

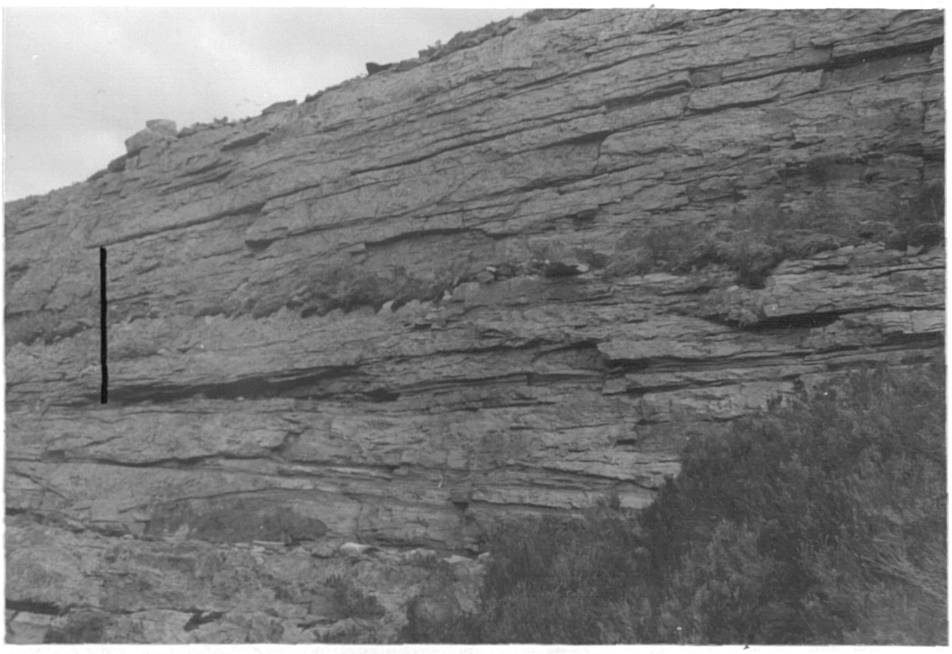

Fig. 2.17 Vertical sequence of facies 1B and 3B sets, Meall a'Ghuibhais, NG 977 655. Facies 2B setsare generally unweathered in contrast to the inweathered sets of facies 3B. Scale bar is 1m long.

Fig. 2.18a Facies 4B small channel approximately 0.5m deep. Strath Beag, NC 538 379.

Fig. 2.18b Small channel approximately 40cm deep, Meal a' Ghuibhais, NG 977 655. Note that this channel is also visible in Fig. 2.17, bottom left.

2.3.3 Palaeocurrents

Palaeocurrent data was taken predominantly from the foresets of facies 1B. A wide spread of directions exists which may be subdivided into a north-south trending, shore parallel, bimodal component and a subordinate east-west trending componant (Fig. 2.19), probably perpendicular to the palaeoshoreline.

2.3.4 Facies distribution

Virtually the entire vertical sequence of association B consists of a regular alternation of facies 1B and facies 3B (Fig. 2.20). Facies 2B becomes more common near the top of the sequence and is associated with a decrease in the frequency of facies 3B sets. Facies 4B is uncommon but was only observed in the lower half of the sequence.

2.3.5 Interpretation of association B

The bimodal palaeocurrent pattern for facies 1B suggests that much of this facies was produced by tidal currents. The bedforms would have been straight crested or sinuous dunes or sandwaves; the vertical form indices and low angle of foresets for some examples suggesting a sandwave origin (Allen 1982a, p454). These sandwaves migrated in an alongshore direction, perpendicular to the orientation of the channels of association A, with a minor number migrating on or offshore.

The internal structure of cosets of facies 2B conform closely to the theoretical structures of Allen's (1980) type IVB and V sandwaves produced by near symmetrical tidal currents. The reversing nature of the currents responsible for facies 2B is indicated by the presence of opposed ripple laminated sets and large low angle reactivation surfaces. Large erosive second order surfaces were produced by erosive storm currents. The association of erosive based graded beds with wave ripple laminations suggests a storm origin for facies 3B. These laminated sands are very similar to the shoreface

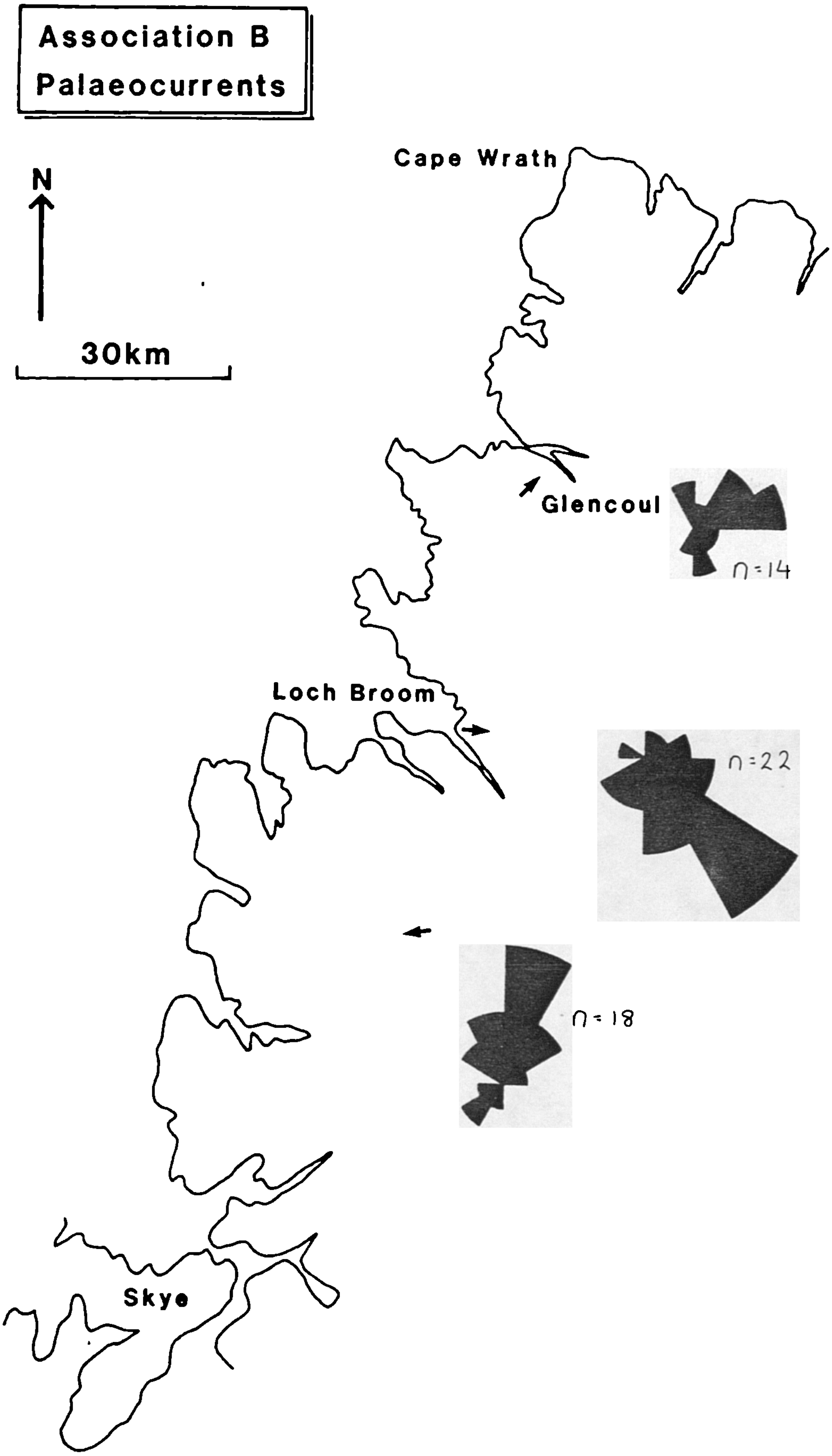

Fig. 2.19 Association B palaeocurrents.

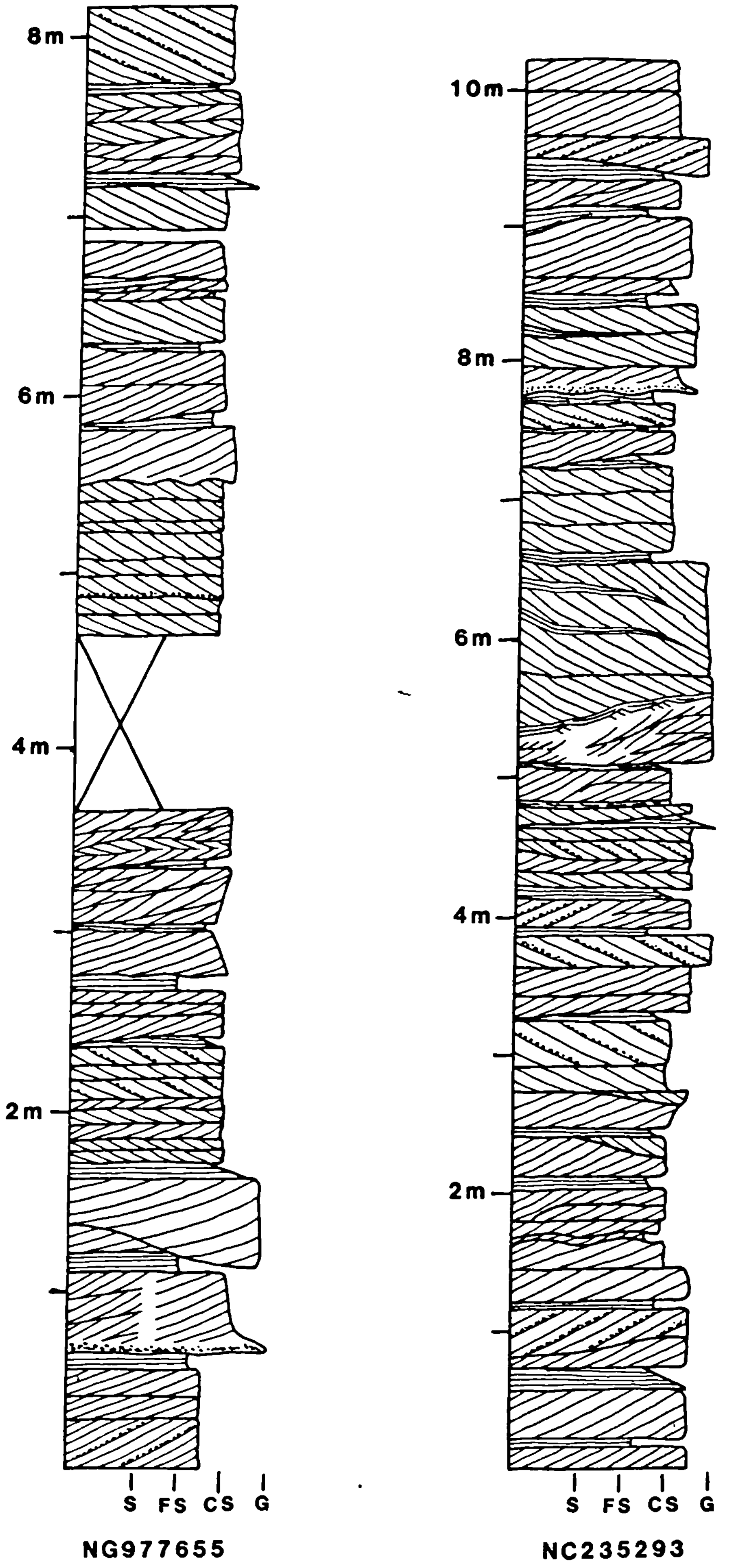

Fig. 2.20 Representative logs of association B sequences.

storm sands of Aigner and Reineck (1982) and Aigner (1985). Kumar and Sanders (1976) attributed such beds to deposition of storm suspended sediment under conditions of intense bottom shear. The mix of sand and mud sized particles in facies 3B suggests that suspended sediment concentrations were high and that deposition was very rapid as storm currents waned, with the latest stages of deposition under weaker ripple producing currents or oscillatory wave currents.

The sheet-like morphology and lateral persistence of the beds of this association and the inferred regular interaction of storm and shelf tidal processes is suggestive of a shoreface environment. Similar associations of facies have been observed in both recent (Howard and Reineck 1972, Chowdhuri and Reineck 1978) and ancient shoreface environments (Tavener-Smith 1982). The coarse grainsize, relative scarcity of ripple and planar laminations indicative of an upper shoreface environment compared to the abundance of large dune and sandwave structures suggests that association B represents the lower shoreface.

Swift et al. (1971) and Kumar and Sanders (1976) have suggested that the lower shoreface record is dominated by a storm hydraulic regime, which is borne out by the facies of association B. Maximum storm effects are recorded by the widespread erosion surfaces and scour channels, which were probably produced by strong offshore flowing coastal jets (Swift 1976), with waning stages dominated by fallout of suspended sediment. Smaller storm effects are recorded by the on/offshore directed palaeocurrents of facies 1B in response to offshore flowing gradient currents (Allen 1982) or onshore wind drift currents (Aigner 1985), although most facies 1B bedforms were probably tidally produced. The internal structures of facies 3B show a variety of scales of flow strengths. Daily tidal currents would have produced ripples and small dunes on the stoss and lee slopes of these sandwaves (eg. Fig. 2.16). However the internal structures indicate a range of bedforms from large dune cross-bedding and planar laminations produced by large spring tides or storm enhanced tidal flows, to large erosion surfaces with facies 3B drapes. The disturbed bed in facies 1B may have been produced by exceptionally large storm waves. The rarity of this feature and short lateral extent implies that it is not seismic in origin and the lenticular, convex-up shape may imply that it was a single slumped dune. Dune liquefaction by storm waves has been noted in Norton Sound, Alaska, by Olsen et al. (1982).

In summary therefore, although fairweather conditions in association B were dominated by tidal processes, a wide range of wind-induced flows are indicated from slight enhancement of tidal currents to widespread erosion and scouring. The presence of these shoreface sediments overlying the tidal channel deposits of association A indicates the former presence of a barrier island system, implying that these channels were tidal inlet ebb channels as previously discussed. The removal of the upper portions of the barrier lithosome by erosional shoreface retreat during transgression (Bruun 1962) is well documented from the recent sediments of the eastern seaboard of North America (Belknap and Kraft 1981, Swift et al. 1981, Belknap and Kraft 1985, Panageotou and Leatherman 1986) and in the ancient record by Barwis and Makurath (1978). This erosional retreat leaves a laterally persistant erosion plane, the ravinement surface of Swift (1965). The widespread, laterally persistant plane separating associations A and B (Fig. 2.13) may be the ravinement surface caused by erosional retreat of the barrier foreshore and upper shoreface to leave inlet facies juxtaposed against lower shoreface sediments in the Lower Member. The upper shoreface/ lower shoreface transition occurs at water depths of 10-15m (Swift et al. 1985) which may indicate the approximate depth of wave erosion during retreat of the Lower Member shoreface. Penland et al. (1985) have shown that the depth of wave erosion is a function of wave energy and the angle of approach of storm waves. The height of the Lower Member ravinement surface above the unconformity is constant, therefore assuming that the angle of wave approach and wave energy was similar along the length of present outcrop, this suggests that the palaeoshoreline may have been linear.

Facies	Typical log	Grain size	Coset/set thickness	Coset/set length	Internal structure	Set surfaces	Other features	Interpretation
4C		MS-CS	Cosets 5-10m sets 0.2-2m at top, 0.05 -0.2m at base	50m	Asymptotic sets dipping at 0-10	Base planar, top rarely preserved	Sets mostly tabular cross bedded	Large tidal sandwaves
3C	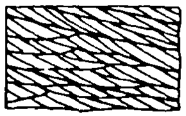	MS-CS	Cosets 1-2m sets 5-15cm thick	15m	Sets dip at up to 10°	Base planar, top rarely preserved	Sets mostly tabular cross bedded	Small tidal sandwaves
2C	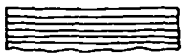	MS-CS	5cm	5m	Parallel lamination	Base erosive, top rarely preserved	Occasional wave rippled tops	Shelf tempestite
1C	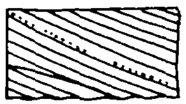	CS-VCS	10-50cm	7m	Tabular cross bedding	Base erosive, top rarely preserved	Aulichnites and monocraterion present	Small tidal dunes or sandwaves

Table 2.4

2.4 FACIES ASSOCIATION C

2.4.1 Introduction

Facies association B passes gradationally into association C with a decrease in the proportion of parallel laminated beds (facies 3B) and an overall increase in mean set thickness. Parallel laminated sands are eventually absent approximately 70m above the unconformity. The facies for this association are summarised in table 2.4.

2.4.2 Facies descriptions

Facies 1C: Tabular cross-bedded sets

This facies is similar to facies 1B in grainsize and foreset geometry. Individual beds may be up to 50cm thick and may be traced up to 7m laterally before being truncated by low angle, convex-up reactivation surfaces with dips of up to 10 degrees. Reactivation surfaces occuring as convex-up erosion surfaces in the upper half of foresets occur, but do not show any evidence of periodicity in spacing. Hanging set boundaries (Allen 1973) are a common feature of this facies. Undulose erosion surfaces occasionally occur and may be traceable over many tens of metres. These surfaces frequently have a winnowed granule or pebble lag and may have topographies of up to 50cm (Fig. 2.21). Beds of this facies generally occur interspersed with beds of other facies and rarely form cosets. Aulichnites and vertical burrows with a concentric structure in plan veiw (Monocraterion?) occur extremely rarely within this facies (Fig. 2.22) at Loch Eriboll (NC 430 607), Ullapool (NH 131 965) and Sgurr Bàn (NH 055 745).

Facies 2C: Parallel laminated sands

This facies consists of parallel laminated beds of medium to coarse sand very similar to facies 3B. Beds are generally only a few centimetres thick and are discontinuous over a few metres laterally due to the erosional bases of overlying beds. Beds may be

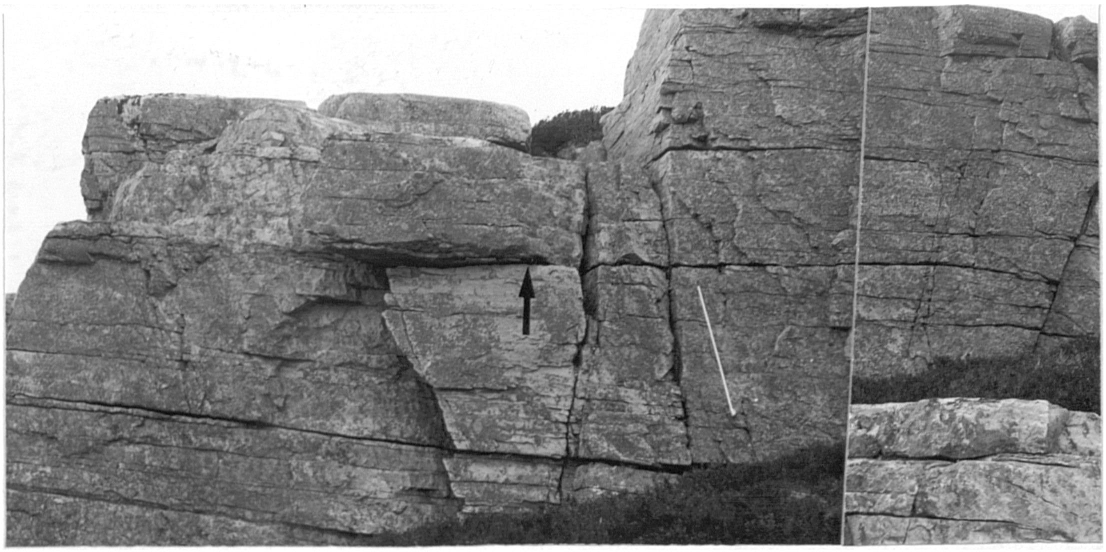

Fig. 2.21a Undulose erosion surface within sets of facies 1C. Creag na Feòla, NH 132 967. Scale 1m long.

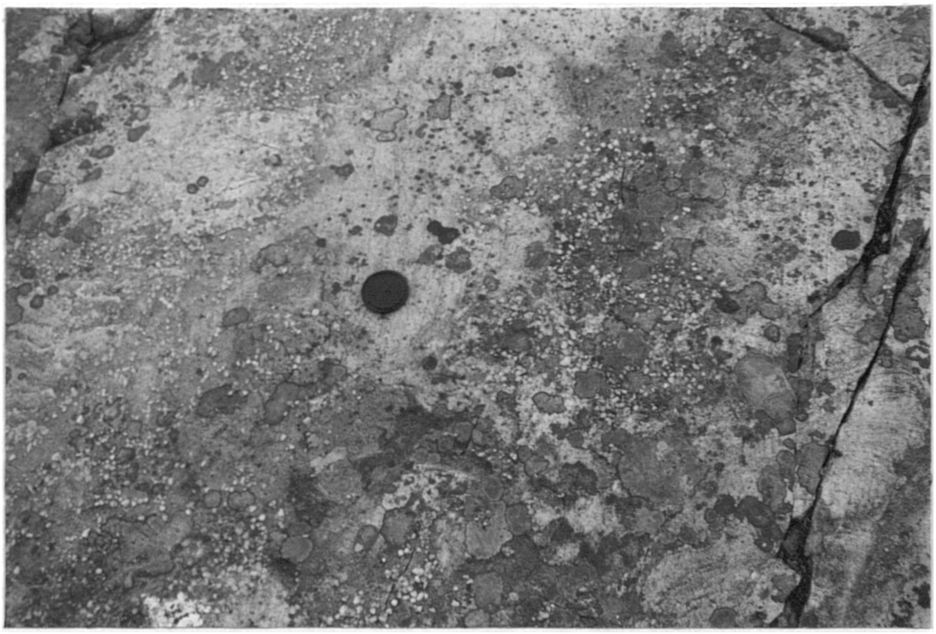

Fig. 2.21b Winnowed granule lag on erosion surface, Creag na Feòla, NH 132 967. Lens cap 5cm wide.

Fig. 2.22a Vertical burrows with concentric structure in plan view, Creag na Feòla, NH 132 967. Lens cap 5cm wide.

Fig. 2.22b Bilobed trail (Aulichnites?), Creag na Feòla, NH 132 967.

amalgamated, reaching a maximum thickness of 20cm (Fig. 2.23a), although more commonly they occur every few metres vertically. This facies gradually decreases in frequency vertically and is virtually absent in the top 30m of the Lower Member. Where this facies occurs in the upper 30m, beds tend to be very discontinuous with little detrital mud present. On rare occasions, where bed tops are preserved, form concordant wave ripple laminations are present (Fig. 2.23b).

Facies 3C: Small compound cross-bedded cosets

This is the most abundant facies within association C, comprising more than 60% of the vertical sequence. Cosets range from 1-2m in thickness and consist internally of a complex arrangement of ripple and parallel laminated sets (Fig. 2.24). Sets range in thickness from 5-15cm and are enclosed by inclined bounding surfaces (Fig. 2.24, E2 surfaces) 20-300cm in length dipping at up to ten degrees. Shorter horizontal to subhorizontal (E3) surfaces occur within the inclined E2 surfaces and enclose tabular cross laminations which vary in grainsize from medium to coarse sand and are generally directed down dip, although the proportion of up dip oriented examples may be up to 50%. Foreset dips vary from 20-30 degrees. This facies shows no vertical increase or decrease in grainsize or bed thickness. Occasionally this facies grades laterally into facies 1C sets by the progressive down dip increase in thickness of one cross-laminated set from the top of the coset towards the base (Fig. 2.25).

Facies 4C: Large compound cross-bedded cosets

This facies occurs exclusively within the top 20m of the Lower Member. Cosets range from 5-10m in thickness and are defined by laterally persistent horizontal (E1) bounding surfaces. These cosets consist of sets 20-100cm thick enclosed by inclined bounding surfaces (Fig. 2.26a, E2 surfaces) 3-6m long and dipping at 5-10 degrees. These sets are initiated along concave-up reactivation surfaces similar to to the R1 surfaces of facies 2A and are truncated by R2

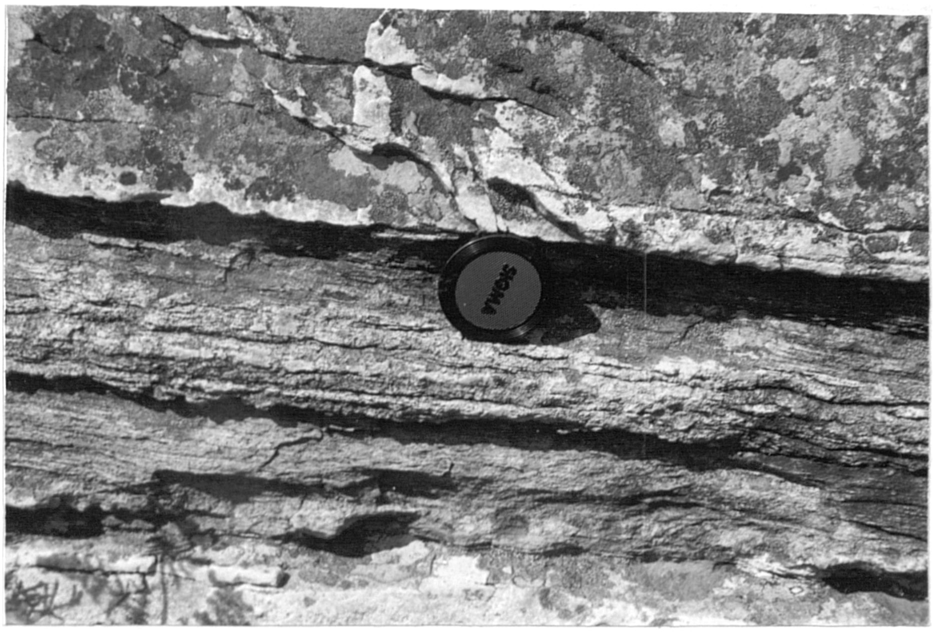

Fig. 2.23a Parallel laminated bed of facies 2C, Creag na Feòla, NH 132 967. This bed is particularly thick and may be amalgamated. Lens cap 5cm wide.

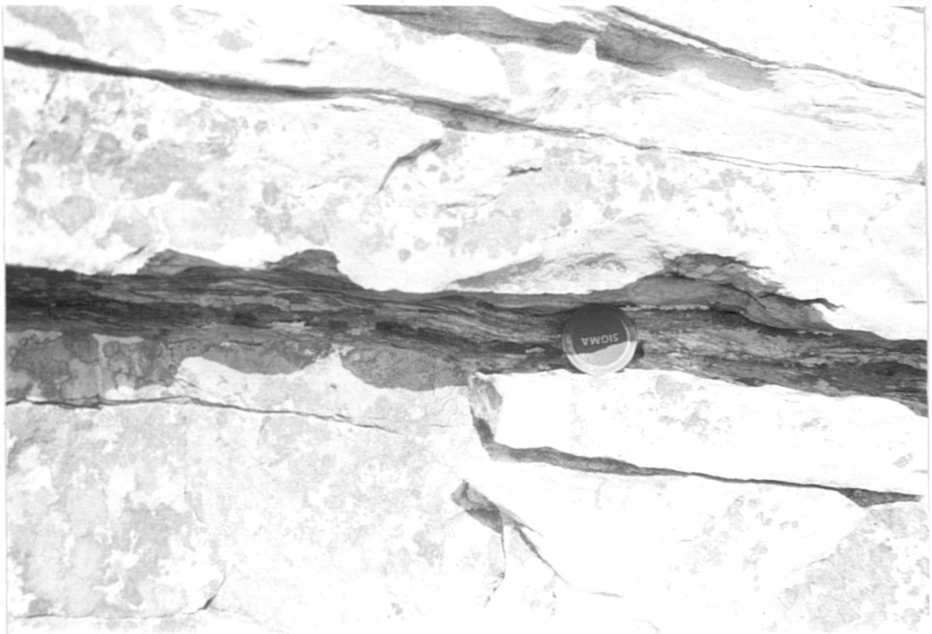

Fig. 2.23b Parallel laminated bed of facies 2C with wave rippled top, Creag na Feòla, NH 135 967.

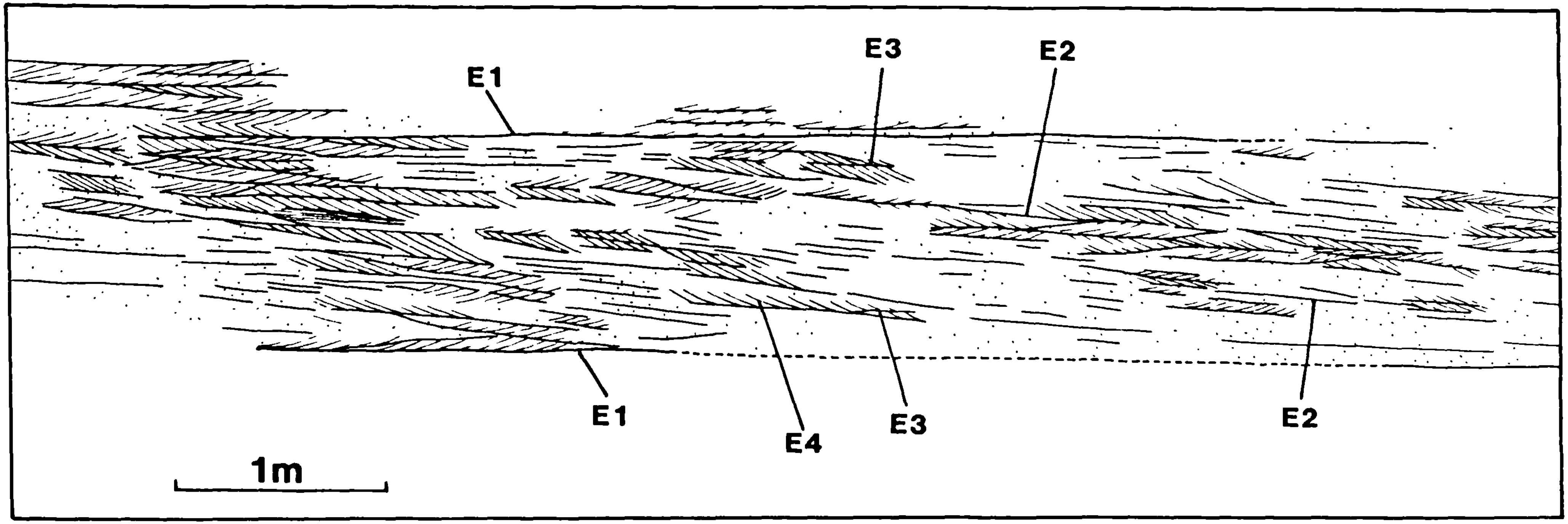

Fig. 2.24 Small coset of facies 3C, Port Chamuil, NC 431 609. Note rare parallel laminated sets of facies 2C.

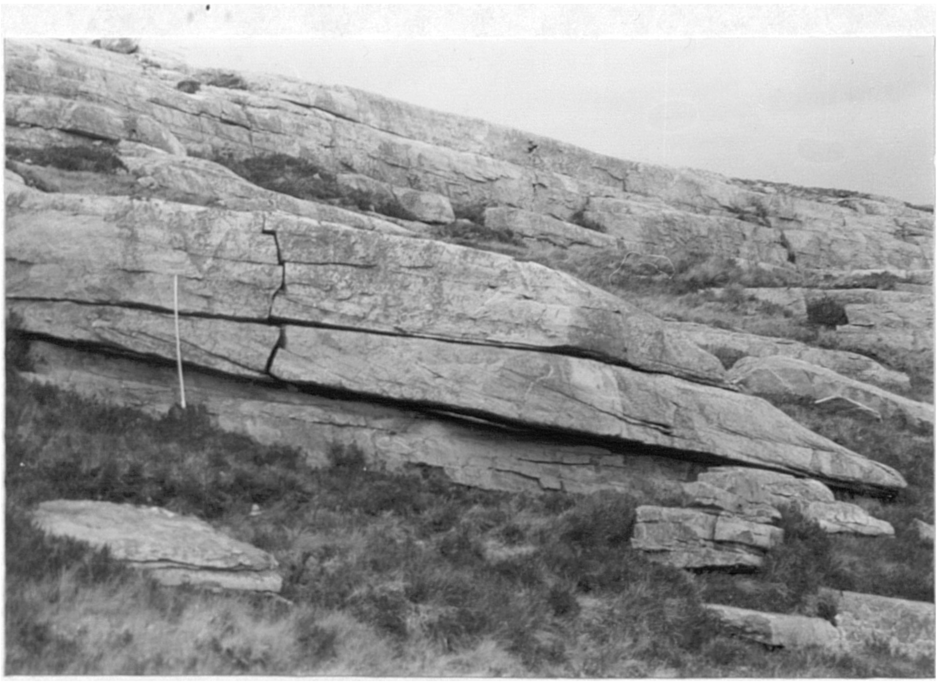

Fig. 2.25 Facies 1C set thickening down the lee slope of a facies 3C coset, Creag na Feòla, NH 132 967. Scale 1m long.

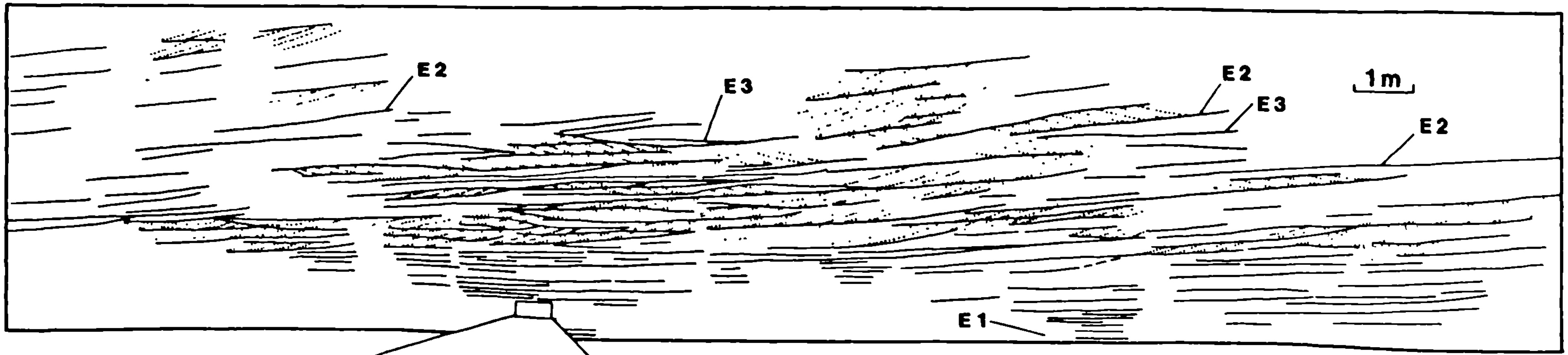

Fig. 2.26a Large coset of facies 4C, Port Chamuil, NC 431 607. Note parallel laminated sets

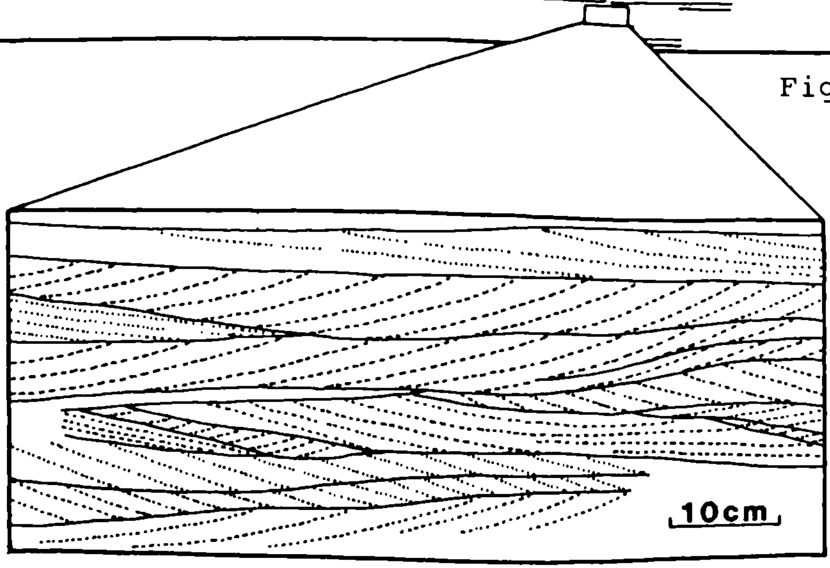

Fig. 2.26b Enlarged sketch of ripple laminated bottomsets.

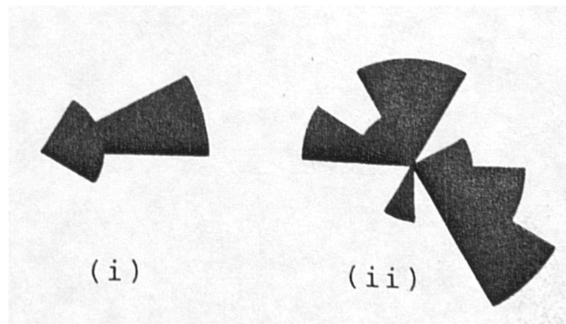

Fig. 2.26c (i) inclined set orientations.
(ii) rippled bottomsets.

type reactivation surfaces. The inclined sets thin down-dip towards tangential bottomsets 5-20cm thick (Fig. 2.26b). Both inclined sets and bottomsets consist of tabular cross-bedded medium to coarse sand, with occasional very coarse sand to granule foresets and set tops restricted to the inclined sets. Trough cross-bedding is relatively rare. Third order (E3) bounding surfaces enclose the cross-bedding between the inclined E2 surfaces. These third order surfaces are generally horizontal but may dip in the same direction or in the opposite direction to the second order surfaces with inclinations of a few degrees. In general the cross-bedding is directed down the inclined E2 surfaces, but occasionally it may have a wide scatter, with modes also oriented up and along these surfaces (Fig. 2.26c), particularly on the tangential bottomsets.

2.4.3 Palaeocurrents

Palaeocurrents for association C show a regional bimodality parallel to subparallel to the Moine Thrust Zone, and presumably the palaeoshoreline (Fig. 2.27), and conform with the more extensive palaeocurrent data of Swett et al. (1971).

2.4.4 Interpretation of association C

The bimodal palaeocurrents, trace fossil assemblage and absence of channels suggests that association C represents an open shelf tidal environment. Within this context facies 1C could have been deposited by the migration of small dunes or sandwaves under predominantly tidal currents, although random wind effects and storm-forced migration must have played a part in bedform migration. The large undulose erosion surfaces are similar to the Type 1 and 2 erosion surfaces of Anderton (1976) and may have been the result of widespread shelf erosion during major storms. The smaller reactivation surfaces may have resulted from tidal current reversals or smaller storm current erosion. The parallel laminated sands of facies 2C are similar to the storm sands of associations A and B. The vertical grading and transition from parallel laminations to wave

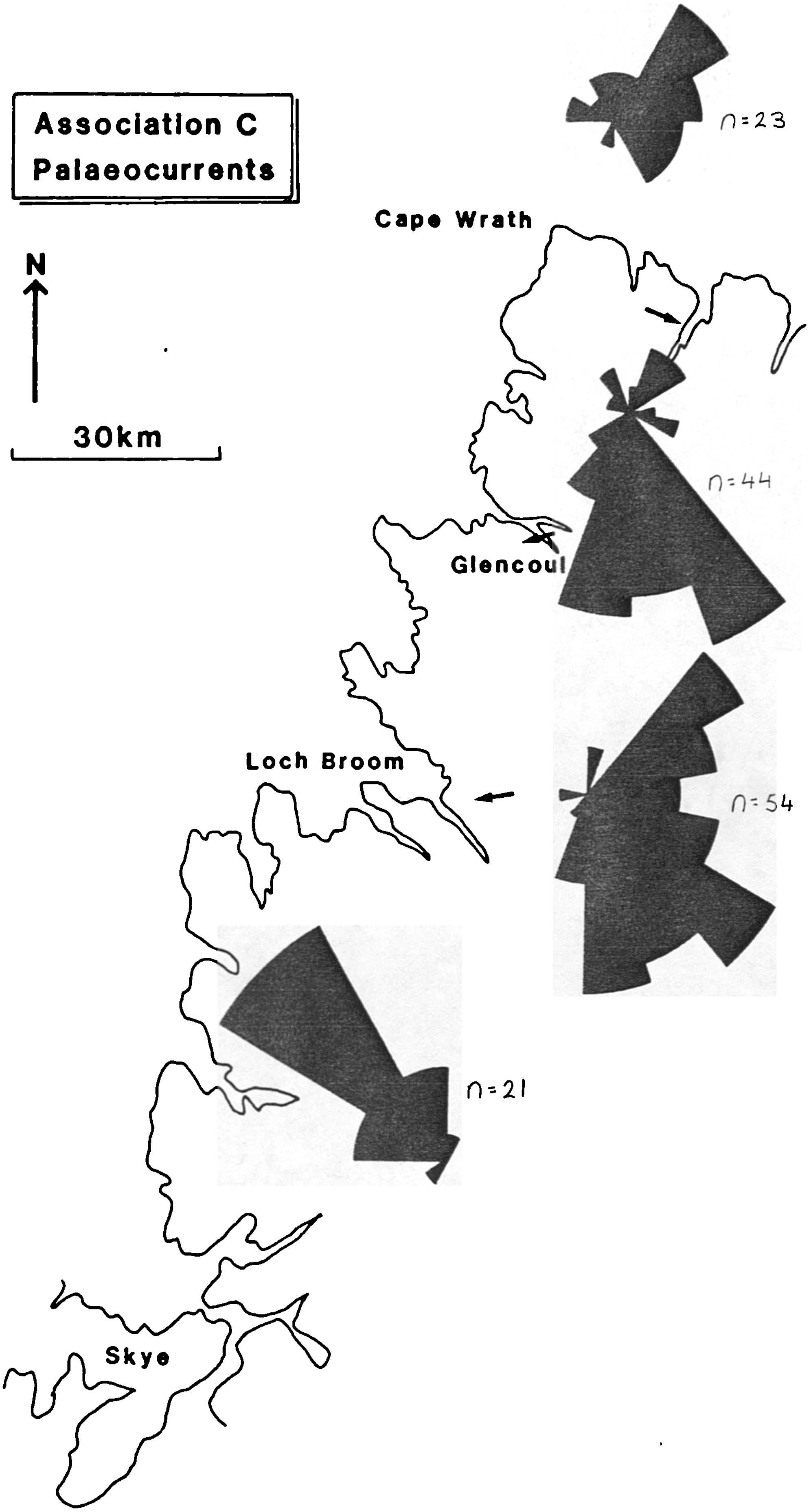

Fig. 2.27 Association C palaeocurrents.

rippling suggests that this facies was derived from storm suspended material derived from the barrier shoreface. Vertically through association C this facies shows a progressive increase in degree of reworking, presumably by "fairweather" tidal currents, until it is virtually absent in the upper part of this association.

Facies 3C cosets are similar to the type VI sandwaves of Allen (1980) and those of Lily Bank (Hine 1977). The abundant opposed ripple laminations suggests velocity symmetrical tidal currents which caused ripples and small dunes to migrate both up and down the sandwave lee face, producing more symmetrical sandwaves than in association B (Fig. 2.28). The absence of any pattern to the internal structure of these cosets suggests that sandwave migration was probably sporadic and may be a record of larger events than daily tides. Erosion in the lee of downcurrent migrating dunes, storm erosion or erosion by the subordinate tide would have produced the short inclined E2 surfaces, and E3 surfaces as ripples and dunes migrated over the stoss slopes of underlying dunes to produce "climbing sets". Longer E2 surfaces may have been the result of large scale storm erosion of sandwave lee slopes (Fig. 2.28). In contrast to the similar cosets of facies 2B, sets are shorter in length and less regularly arranged, probably as a result of random wind effects on tidal currents and greater reworking by superimposed ripples and dunes. The occasional thin sets of parallel laminated sands within these cosets were probably deposited by storms, but were extensively reworked by fairweather tidal dunes and ripples.

The large cosets of facies 4C are again similar to the type VI sandwaves of Allen (1980), of Hine (1977) and of the Permian Rancho Rojo Member (Blakey 1984) and are essentially larger versions of the facies 3C cosets. The longer E2 surfaces in these cosets suggest that storms played a greater role in the migration of these larger bedforms, or perhaps were less able to recover from erosive storm events. In contrast to the smaller cosets this facies shows a vertical increase in bed thickness and number of winnowed pebble lags. This suggests that these bedforms were sufficiently large in proportion to water depth to cause strong flow acceleration over the sandwave crests to produce larger dunes and greater winnowing near

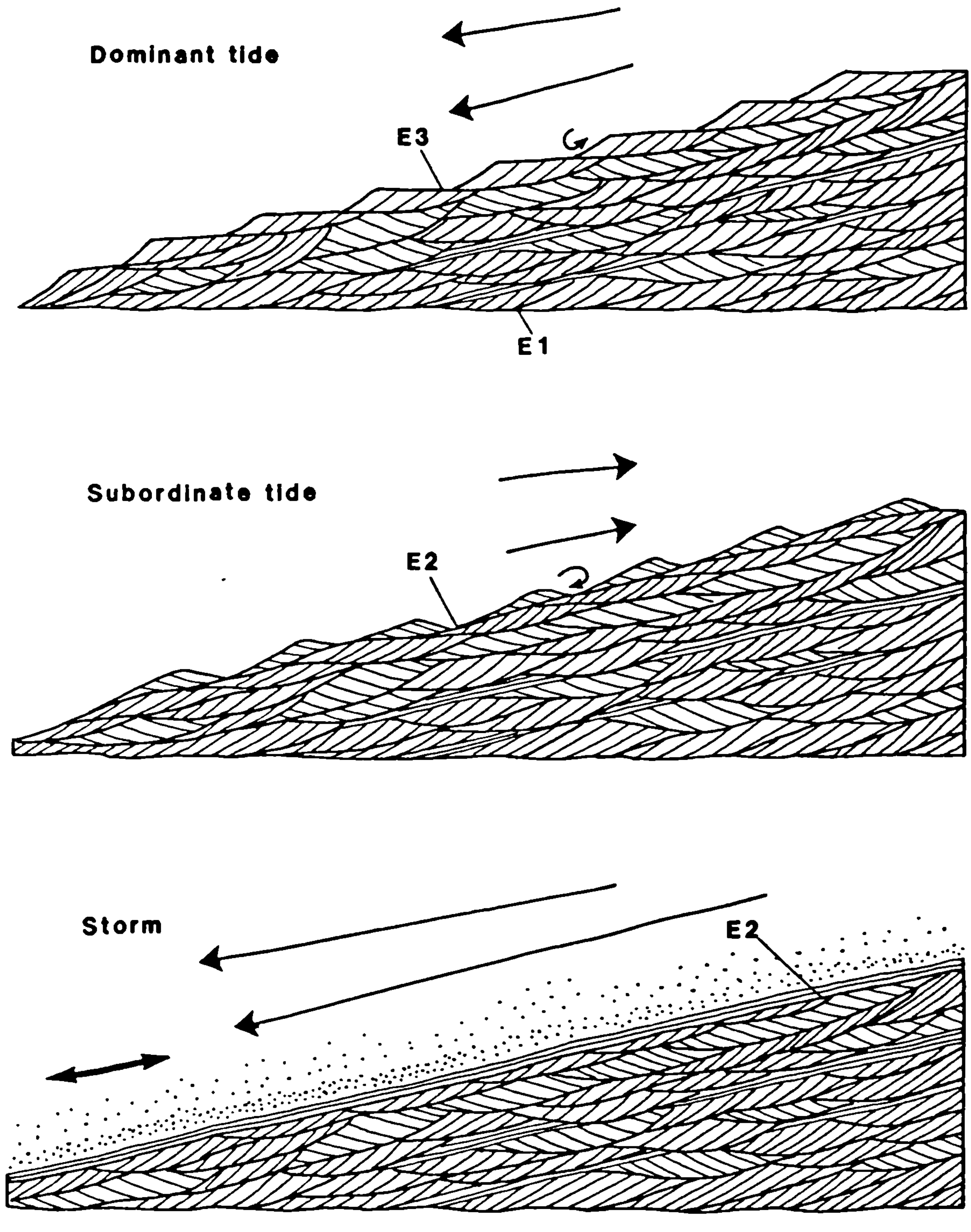

Fig. 2.28 Summary diagram of processes involved in constructing cosets of facies 3C and 4C.

the crestline. The pronounced palaeocurrent mode parallel to the sandwave lee slopes in Fig. (2.26) may have been the result of currents being partially constrained within sandwave troughs during low tides when the sandwave crests were closest to the sea surface. The transition from the relatively small sandwaves of facies 3C to the large facies 4C sandwaves indicates an increase in tidal current velocities, and presumably tidal range, with time. The Lower Member was deposited during a marine transgression, therefore the shelf was probably widening with time. Howarth (1982) has shown that tidal range may be amplified by resonant effects when the shelf width is 1/4, 3/4, 5/4 etc. of the tidal wavelength, therefore the transition from a mesotidal barrier island and shelf sequence to a macrotidal shelf sequence may be a result of the Lower Member shelf approaching resonance as the shelf widened.

The mesotidal barrier island and shoreface system of associations A and B were probably lateral time equivalents of facies 1C, 2C, and 3C only (summarised in Fig. 2.29). The macrotidal conditions necessary to produce the large sandwaves of facies 4C would have precluded barrier island development and resulted in a coastal system of macrotidal flats and estuaries.

Fig. 2.29 Summary diagram of the depositional elements of the Lower Member.

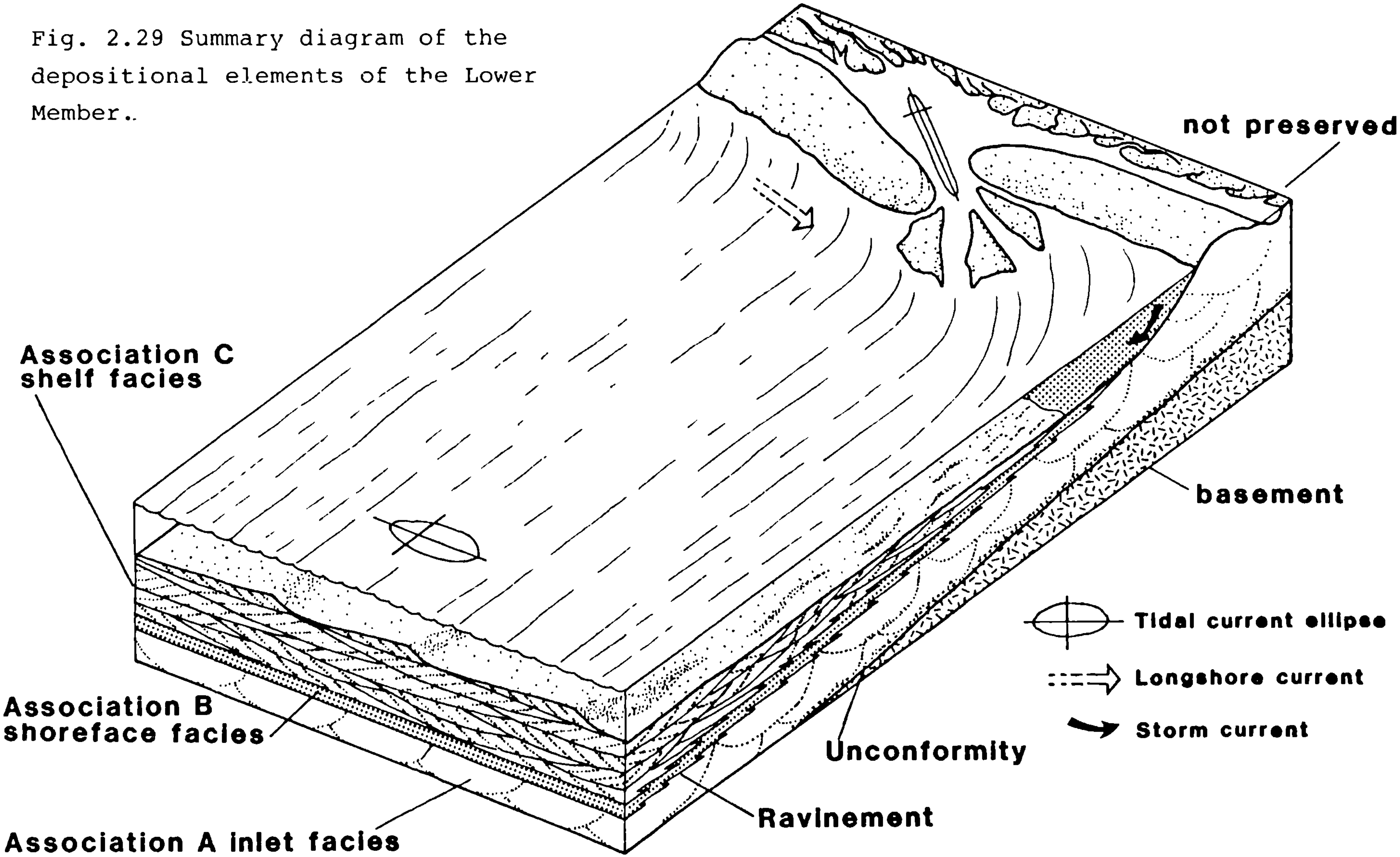

Chapter 3

The sedimentology of the Pipe Rock

Facies	Typical log	Grain size	Coset/set thickness	Coset/set length	Internal structure	Set surfaces	Other features	Interpretation
5	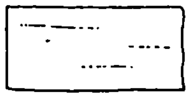	MS	Coset 4m thick, sets 25cm thick	Present over several km	Massive			Produced by seismic activity
4	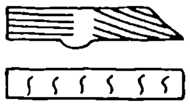	FS-CS	0.5-50cm	10-30m	Parallel or cross lamination	Planar, erosional	Gutter casts, rip up clasts, skolithos monocraterion,	Predominantly tempestites
3		MS-CS	5-100cm	5-25m	Rare tabular cross beds			
2	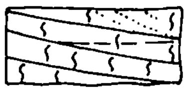	MS-CS	Cosets 1.5-3m thick. sets 0.2-1m	40m	Sets dip at 6-9°	Planar, with stylolites	Thin muds along bedding planes	Small shelf sandwaves
1	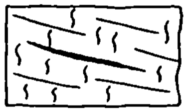	MS-CS	Cosets 4-7m sets 10-50cm thick	40m	Sets 1-7m long dipping at 6-10°	Planar, with stylolites	Mud drapes up to 2cm thick on bedding planes	Large shelf sandwaves

All facies have skolithos present

Table 3.1

3.1 INTRODUCTION

The Pipe Rock conformably overlies the Lower Member and consists of 75-100m of mature, highly burrowed quartzarenites. Muds are present but do not constitute a major part of the facies sequence. The Pipe Rock is so-called because of the abundant Skolithos burrows which are dense enough to obscure the internal structure of virtually all the beds in the sequence. Hallam and Swett (1966) interpreted these burrows as the dwelling burrows of suspension feeding worm-like animals. Monocraterion is locally abundant and has been interpreted by Hallam and Swett as escape burrows produced by the same animal responsible for the Skolithos burrows in response to rapid influxes of sediment. Peach et al. (1907) used the various morphologies and relative abundances of Skolithos and Monocraterion to subdivide the Pipe Rock into five zones. These zones consist of two lower Skolithos zones, a central Monocraterion zone and two upper Skolithos bearing zones. These zones were subsequently found to be discontinuous both laterally and vertically (Hallam and Swett 1966). This study confirms the discontinuous nature of the zones as described by Peach et al. However, the Monocraterion zone does appear to be a distinct lithlogical zone regardless of whether Monocraterion is abundant or not.

The contact with the Lower Member is always abrupt; marked by a single bedding plane above which Skolithos burrows are densely packed and below which they are absent. Burrows may occasionally penetrate a few centimetres into the Lower Member.

3.2 FACIES DESCRIPTIONS

The facies subdivisions of the Pipe Rock are summarised in table 3.1

Facies 1: Thick compound sets

This facies consists of cosets 4-7m thick comprising 10-50cm thick sets of medium to coarse sand with rare sets 50-100cm thick composed of medium to very coarse sand. Grains are predominantly monocrystalline quartz and are subrounded to well rounded in shape. Accessory muscovite is normally present. Sets dip at 6-10 degrees and are defined by discontinuous bounding surfaces 1-7m long (Fig. 3.1) with occasional short, subhorizontal surfaces enclosed between them. The majority of bedding planes have stylolites along them with very thin mud films. Mud drapes may be up to 2cm thick and occasionally thicken down-dip. Skolithos burrows are very dense, generally less than 1cm apart (Fig. 3.2) and vary in diameter from 0.5-1.0cm. Rarely, vague tabular cross-bedding is visible where burrows are less dense. Burrowing can obscure bedding planes as well as cross-bedding to the extent that outcrops are reduced to a sequence of short, discontinuous bounding surfaces with dips ranging from 0-10 degrees with no immediately apparent pattern. The horizontal surfaces defining the cosets and some dipping bounding surfaces are usually persistant enough to indicate the presence of this facies.

Facies 2: Thin compound sets

Cosets of this facies range from 1.5-3.0m in thickness and consist of inclined sets 20-100cm in thickness. These sets dip at 6-9 degrees and are defined by laterally persistent bounding surfaces 5-14m long (Fig. 3.3a). One example of this facies (at NG 623 143) shows an exhumed inclined bounding surface with sparse superimposed small dune form sets (Fig. 3.3b and c). Occasional discontinuous surfaces less than 2m long define thinner, 10cm thick sets. Grain sizes range from medium to coarse sand and grain shape and composition is similar to facies 1. Sets are generally ungraded, although reverse graded and, more rarely, normally graded examples occur. Skolithos burrows are usually too dense to permit preservation of any set internal structures but occasionally down-dip oriented tabular cross-bedding is visible (Fig. 3.3a). As with facies 1 very thin mud drapes are frequently present on bed tops, which may be stylolitised. On very rare occasions horizontal erosion surfaces are present and may have a topography of up to 1m (Fig. 3.4) which may represent channeling.

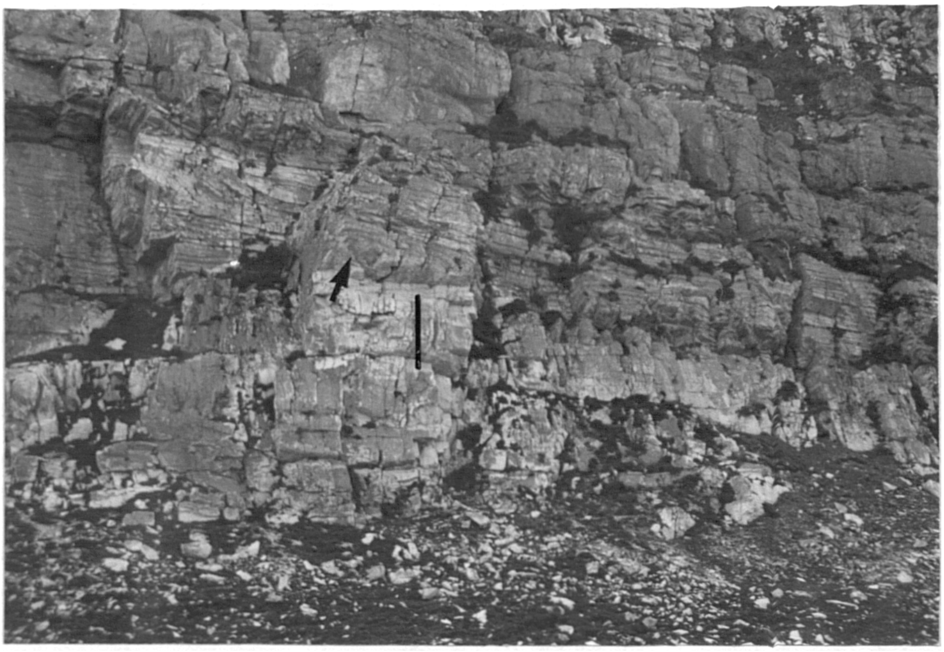

Fig. 3.1 Facies 1 thick compound coset, Ben Arnaboll, NC 456 595. Note large dipping sets. Scale bar 3m long.

Fig. 3.2 Typical field appearance of Skolithos burrows, An t-Sròn, NC 445 582.

Fig. 3.3 Facies 2, thin compound sets.

Fig. 3.3a Tracing from a field photograph of a coset with tabular cross-bedding visible in less densely burrowed sets. Ord, NG 623 643.

Fig. 3.3b Exhumed dipping surface of a facies 2 coset, Ord, NG 623 143. Scale bar 1m long.

Fig. 3.3c Same surface as 3.3b showing superimposed form sets.

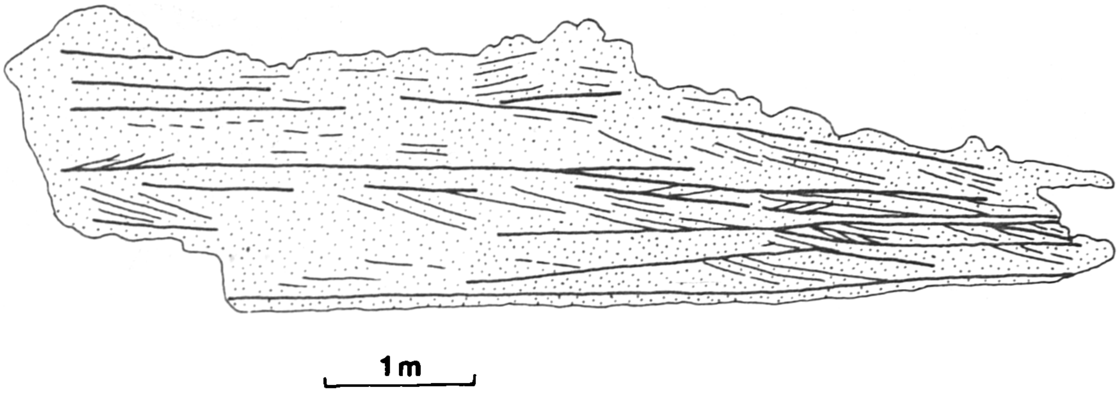
1m

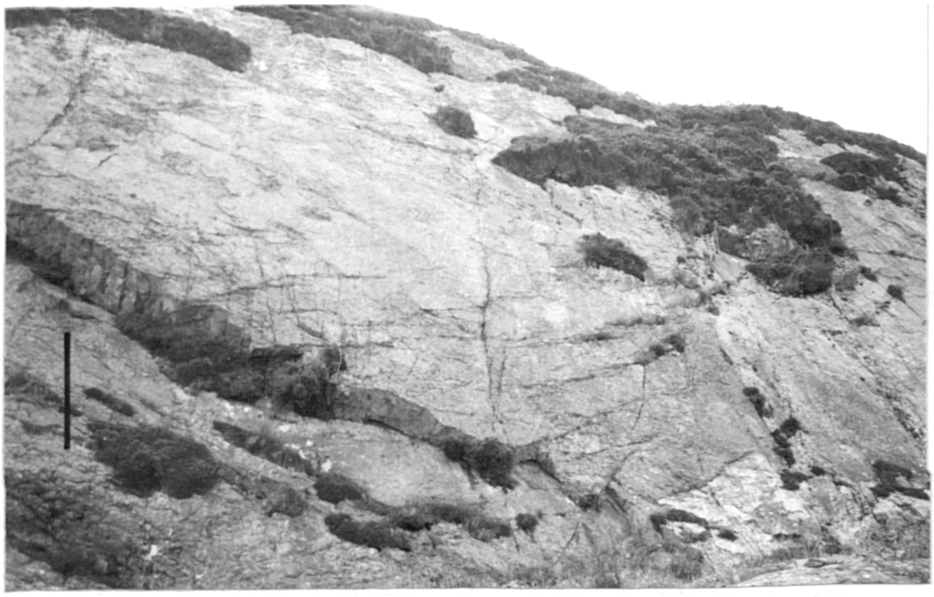

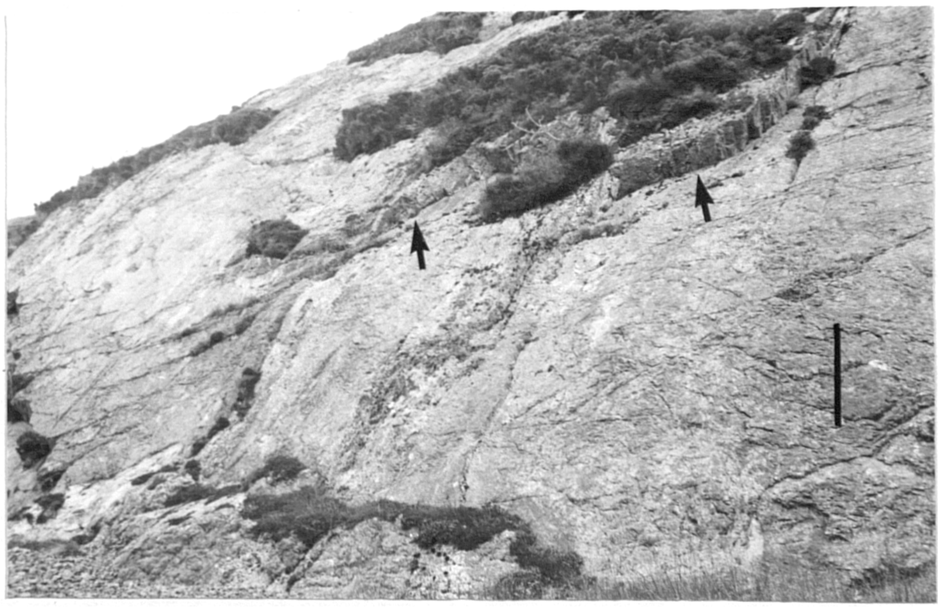

Fig. 3.4 Large erosion surface within facies 2, Ord, NG 624 143. Scale 1m long.

Facies 3: Thick horizontal sets

These laterally persistent horizontal sets (Fig. 3.5a) range in thickness from 5-100cm and consist predominantly of medium to coarse sand with rare examples consisting of very coarse sand. Grains are mostly monocrystalline quartz, with accessory muscovite, and are typically rounded in shape with occasional well rounded examples (Fig. 3.5b). Beds are normally ungraded although winnowed granule lags may be present on set tops or bases. Reverse graded sets are rare, but are more common than normally graded sets. The planar, horizontal bounding surfaces defining sets may be traced over 5-25m laterally. Most surfaces are stylolitised and have very thin mud drapes which, in exceptional cases, may be up to 2cm thick. Skolithos burrows are generally dense enough to obscure all set internal structures but in exceptional cases may show faint tabular cross-bedding. Occasionally foresets decrease in dip laterally (Fig. 3.5c) and may pass into parallel laminated beds. Glauconite is extremely rare, occuring as solitary rounded pellets.

Facies 4: Thin horizontal sets

Thin horizontal sets of this facies range in thickness from 0.2-50cm and consist of fine to coarse sand. Beds are generally ungraded although normally graded examples are frequent. Muds are occasionally present, ranging in thickness from a few millimetres up to 4cm, and occur interbedded with thinner sets and at the top of graded beds. Bed soles often have gutter casts, up to 15cm deep and a few ten's of centimetres wide, and may also have a lag of mud and fine silt angular rip-up clasts. Sets frequently show low angle tabular cross-bedding and, less frequently, parallel laminations (Fig. 3.6a). Bed tops have decimetre wavelength undulations or symmetrical wave rippling (Fig. 3.6b). Skolithos burrows are common in this facies but are generally not dense enough to obscure set internal structures. Many burrows have concave-up spreiten or deflect laminae near the margins along the full burrow length (Fig. 3.6a). Monocraterion is locally very abundant (Fig. 3.6c) and Planolites burrows are occasionally present associated with the

Fig. 3.5 Facies 3 thick horizontal sets.

Fig. 3.5a Typical appearance, Skiag Bridge, NC 235 245. Scale 1m long.

Fig. 3.5b Thin section showing the well rounded nature of many of the grains of this facies, Skiag Bridge, NC 235 245. Field of view 2.78mm wide.

Fig. 3.5c Cross-bedded set of facies 3 with foreset dip decreasing from left to right interbedded with typical facies 3 sets, Ben Arnaboll, NC 460 596. Scale bar 1m long.

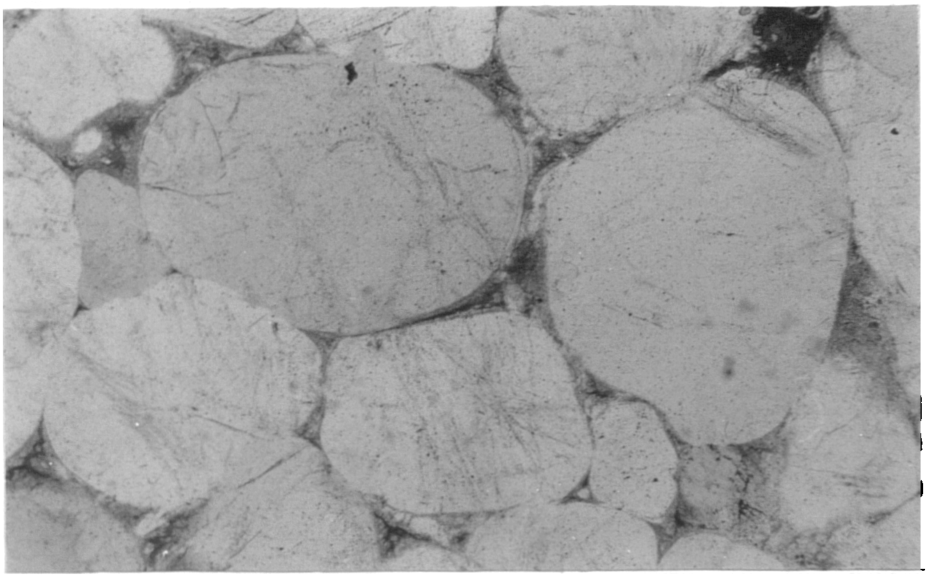

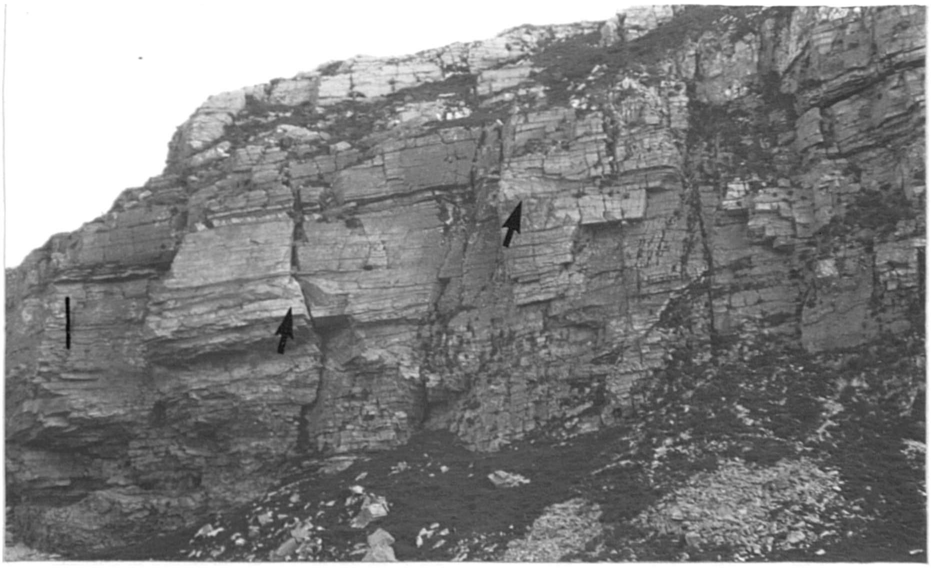

Fig. 3.6 Facies 4 thin horizontal sets.

Fig. 3.6a Tabular cross-bedded set with foresets deflected around burrows, Ord, NG 623 143. Lens cap 5cm wide.

Fig. 3.6b Wave rippled set, Ord, NG 623 143.

Fig. 3.6c Concentric tops of Monocraterion burrows, Assynt, NC 231 255.


SIGMA

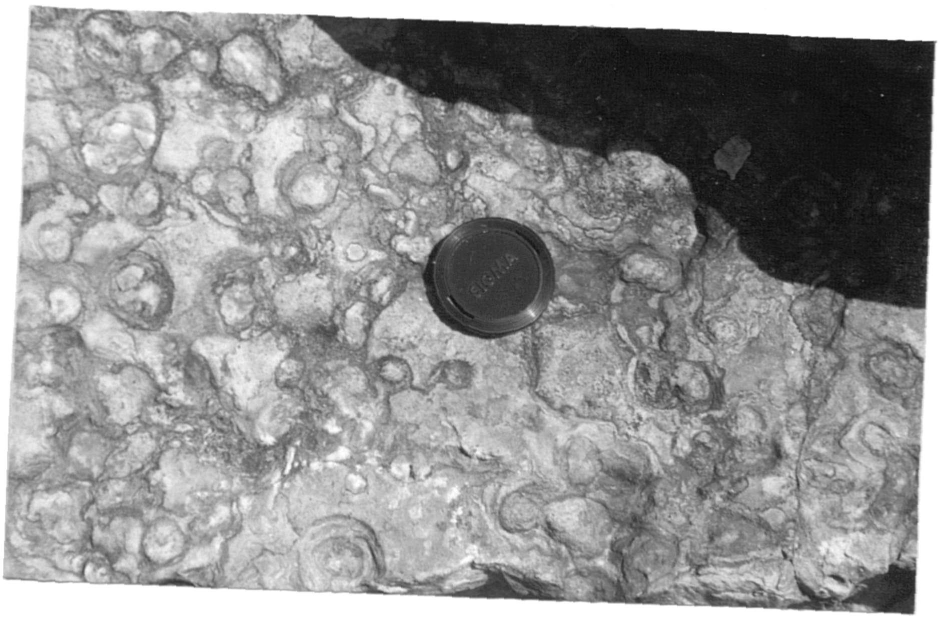

fine sands and muds.

Individual sets rarely show all the features described but generally display at least two. An exception is a particularly abundant suite of beds which simply occur as thin beds up to 2cm thick which stand out as being thinner and coarser than other beds, but have no other distinguishing features.

Facies 5: Massive sands

This facies was only observed at one locality (NC 231 255). It consists of 4-5m of medium sand with vague, discontinuous bedding planes up to 25cm apart. No other structures are visible.

3.3 FACIES DISTRIBUTION

The vertical distribution of the various facies described is illustrated in Fig. 3.7. There is a vertical gradation from facies 1, at the Lower Member-Pipe Rock contact through facies 2 and 3 to facies 4 near the middle of the sequence. This zone of facies 4 concentration corresponds to the "Monocraterion" zone of Peach et al. (1907) although the presence of Monocraterion is not a necessary component. There then follows a more rapid transition via facies 2 and 3 back to facies 1. The rest of the sequence shows a gradual transition via facies 2 and 3 to the top of the Pipe Rock sequence. Well rounded grains appear to be particularly well developed in facies 3 at the top of the sequence. These facies changes are spectacularly displayed on the north shore of Little Loch Broom (NG 117 881, Fig. 3.8). There is no pronounced facies changes along the length of outcrop except in the area of the "Assynt window". In this area the massive sands of facies 5 mark a rapid increase in the proportion of muds and a decrease in bed thickness before a return to a facies distribution similar to elsewhere along outcrop (Fig. 3.9a and b).

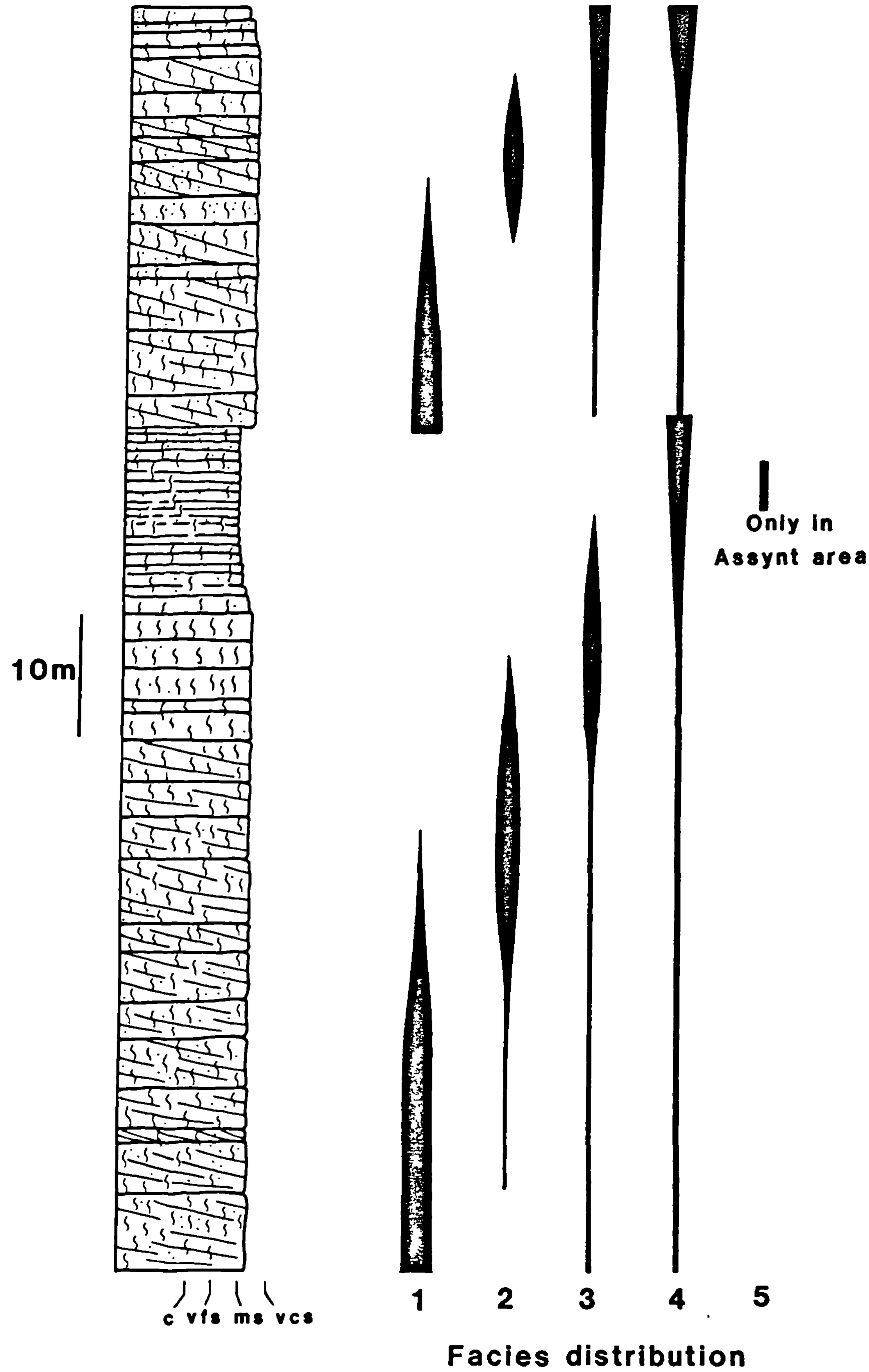

Fig. 3.7 The vertical distribution of Pipe Rock facies.

Fig. 3.8 A well exposed Pipe Rock sequence (Dundonell, NG 117 881) showing the upward thinning and then thickening of sets. The rapid transition from facies 4 to facies 1 is indicated. The complete sequence is approximately 90m thick.

Fig. 3.9a,b Sratigraphic logs of the Assynt Pipe Rock

Fig. 3.9c Photograph of the thinly bedded, muddy sequence just above the massive sands of facies 5. scale 1m long.

Fig. 3.9a

Fig. 3.9b

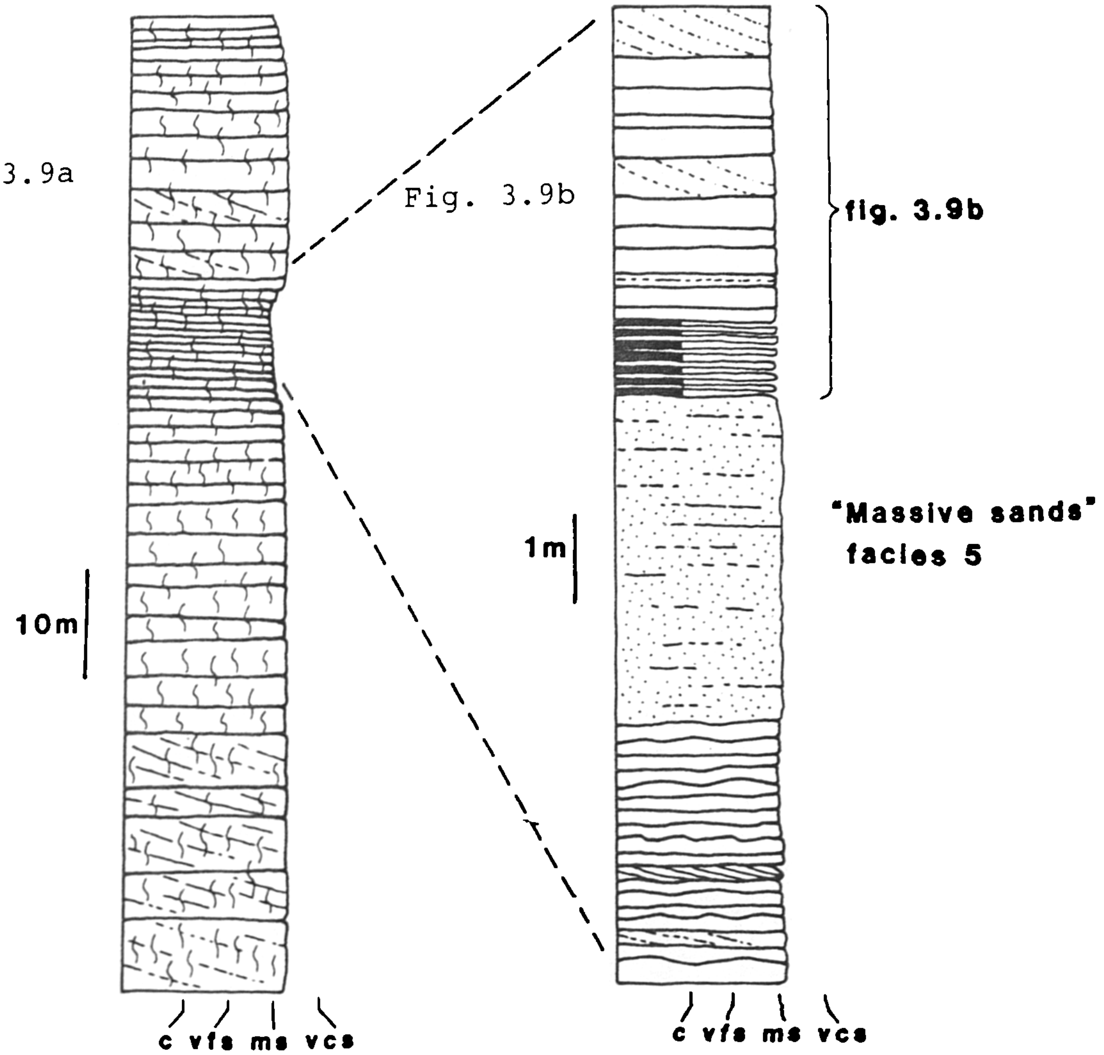

3.4 PALAEOCURRENTS

The extensive bioturbation precludes the collection of a large number of palaeocurrent readings from cross-bedding therefore the inclined bounding surfaces of facies 1 and 2 were used. The palaeocurrents are crudely bimodal on a local and regional scale (Fig. 3.10) and are similar to the palaeocurrents for the shelf facies of the Lower Member. A regional north-south orientation is indicated except in the Loch Eriboll area where the palaeocurrents swing around to an east-west orientation. Channels within facies 2 are very rare but appear to be parallel to subparallel to the palaeocurrents.

3.5 FACIES INTERPRETATION

The crude bimodality of the palaeocurrents and abundant trace fossil fauna suggest that the Pipe Rock is a continuation of the tidal shelf facies interpreted for the Lower Member. The large cosets of facies 1 are probably bioturbated equivalents of the large sandwave cosets of facies 3C in the Lower Member. These cosets are of a similar scale and have analogous dipping bounding surfaces. These inclined surfaces were probably produced by storm erosion, planing of dunes during the subordinate tide or by erosion in the lee of descending dunes. Dune overtaking would produce the shorter subhorizontal surfaces. The mud drapes present are unlikely to have been deposited during one tidal cycle (McCave 1970) and are probably the result of large suspended sediment concentrations deposited during waning storms. The rare cross-bedded sets are identical to the bioturbated sets in every other way suggesting that all sets were originally cross-bedded before colonisation by suspension feeders. Colonisation was likely to have been on the more stable stoss side of dunes and, since most burrows are longer than the set thickness, the apparently dense burrowing was the cumulative effect of burrows descending from overlying beds and repeated colonisation of dunes through time. Sets with fewer burrows and visible cross-bedding indicate that rapid dune migration and overtaking buried sets before

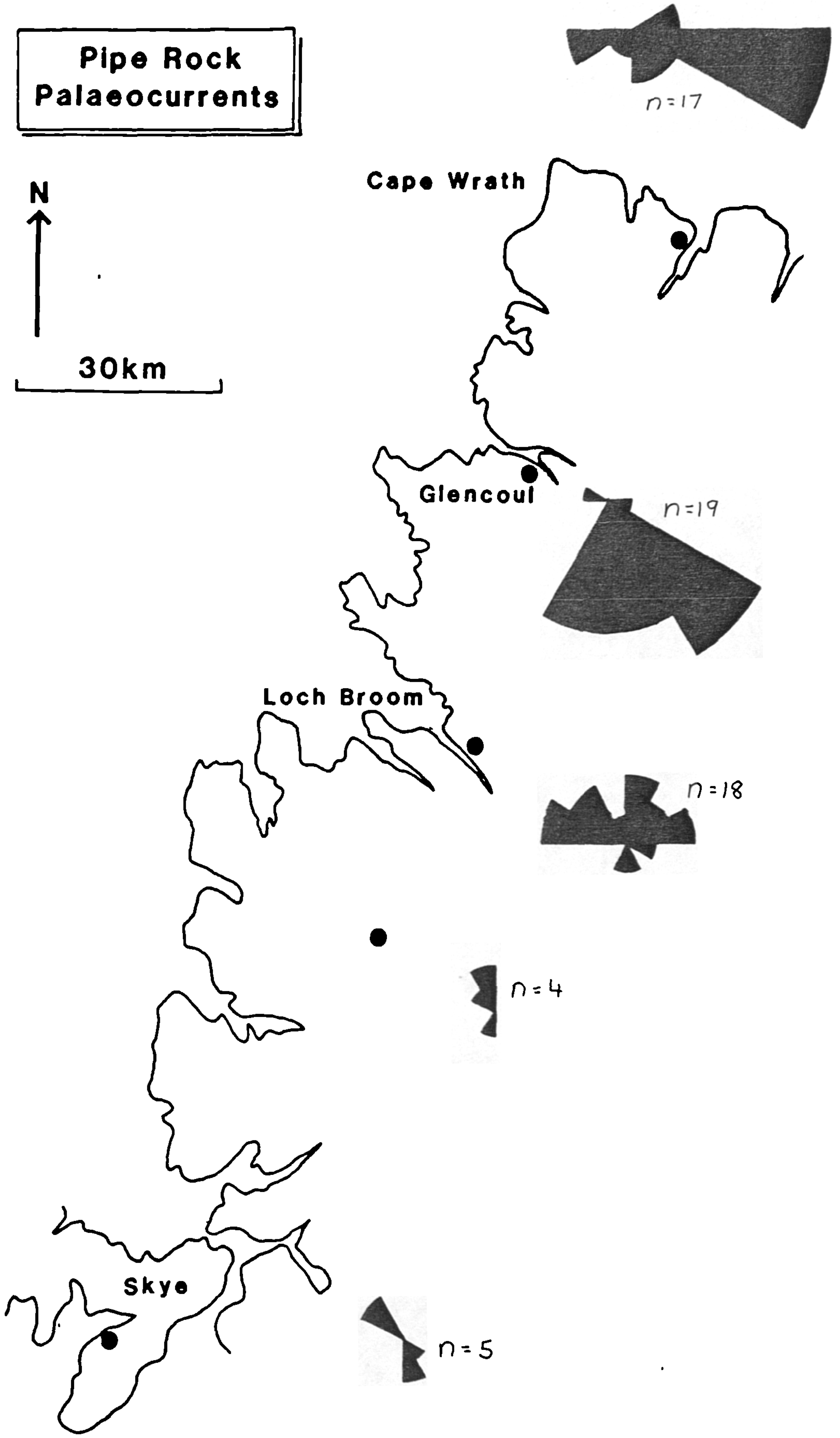

Fig. 3.10 Pipe Rock palaeocurrents.

bioturbation was complete, possibly as a result of storm enhanced tidal currents. The general absence of cross-bedding within individual cosets makes it impossible to make any statement about the velocity asymmetry of the tidal currents involved in constructing these sandwaves, however the similarity in geometry with the Lower Member cosets and overall bimodality of the palaeocurrents suggest that currents were as velocity symmetrical as those of the Lower Member. These cosets then, may be analogous to the type V sandwaves of Allen (1980). The smaller cosets of facies 2 may have been produced by smaller sandwaves under relatively weaker tidal currents than facies 1. The more laterally persistent inclined bounding surfaces of this facies indicate that the subordinate tide, or storm currents, were more able to erode the entire lee of these smaller sandwaves and that this erosion plane was less liable to reworking during fairweather conditions. The undulose erosion surfaces observed in this facies are similar to those of the Lower Member and the type 1 erosion surfaces of Anderton (1976) and were probably the result of widespread erosion during storms, with currents occasionally strong enough to concentrate flow into wide shallow channels.

The discrete sets of facies 3 were probably deposited by the migration of simple dunes or sandwaves with no superimposed smaller bedforms on the lee slope. The bedforms were low enough and possibly migrated sufficiently slowly to allow total burrowing of the sets to take place. The rare cross-bedded sets with downcurrent decreasing foreset dips indicate rapid dune migration preventing escape of buried animals and colonisation, probably as a result of storm or storm enhanced tidal currents. Anderton (1976) has interpreted similar sets from the Jura Quartzite as the result of accelerating currents indicating that dune migration took place during storm build-up rather than waning storms.

The association of thin, laterally persistent beds with gutter casts, vertical grading and wave rippling is strongly suggestive of storm dominated deposition for facies 4. Most beds are parallel laminated or have low angle cross-bedding suggesting a dominance of strong unidirectional over wave currents during bed deposition. Wave rippled bed tops indicate that these currents waned with time resulting in wave reworking of set upper surfaces. The Monocraterion burrows associated with this facies have been interpreted as being the result of vertical movement of the Skolithos producing suspension feeder in response to a sharp increase in sedimentation rates (Hallam and Swett 1966), although some controversy exists as to how the funnel shaped top of these burrows could have been produced (eg. Crimes et al. 1977). Since these burrows were probably produced during storms the rapid increase in non-organic suspended material would probably have induced suspension feeders to retract into their burrows for protection during peak storm conditions. If the burrow walls were not mucous cemented, as seems to be the case, the retraction of the animal into it's burrow would allow the upper burrow walls to collapse producing the observed funnel (Fig. 3.11a). As the storm waned the suspension feeders would penetrate the plugged burrow top and newly deposited tempestite bed to reach the new sediment-water interface and produce a simple Skolithos burrow continuous with the central "pipe" running through the Monocraterion burrow. Monocraterion burrows should therefore indicate the "instantaneous" population density on the sea floor at the time of storm deposition. These burrows are generally more widely spaced, but are typically less than 15cm apart implying that the Pipe Rock shelf was very densely populated. Skolithos coexisting with Monocraterion on the same beds were probably the result of penetration from overlying beds of post storm arrivals.

Vertical Skolithos burrows with spreiten and no funnel at the top may have been produced during weaker storms when suspended clastic material was minimal and the suspension feeders did not retract into their burrows. The vertical spreiten indicate incremental vertical movement within the burrow, perhaps in an effort to keep pace with sedimentation rates eg. dune migration over the burrow entrance. Possibly these moderately agitated conditions marked a time of maximum suspended organic matter providing an incentive for the suspension feeders to maintain contact with the water column (Fig. 3.11b). Burrows which have deflected laminae along their full length may represent an intermediate behavioural response to storms

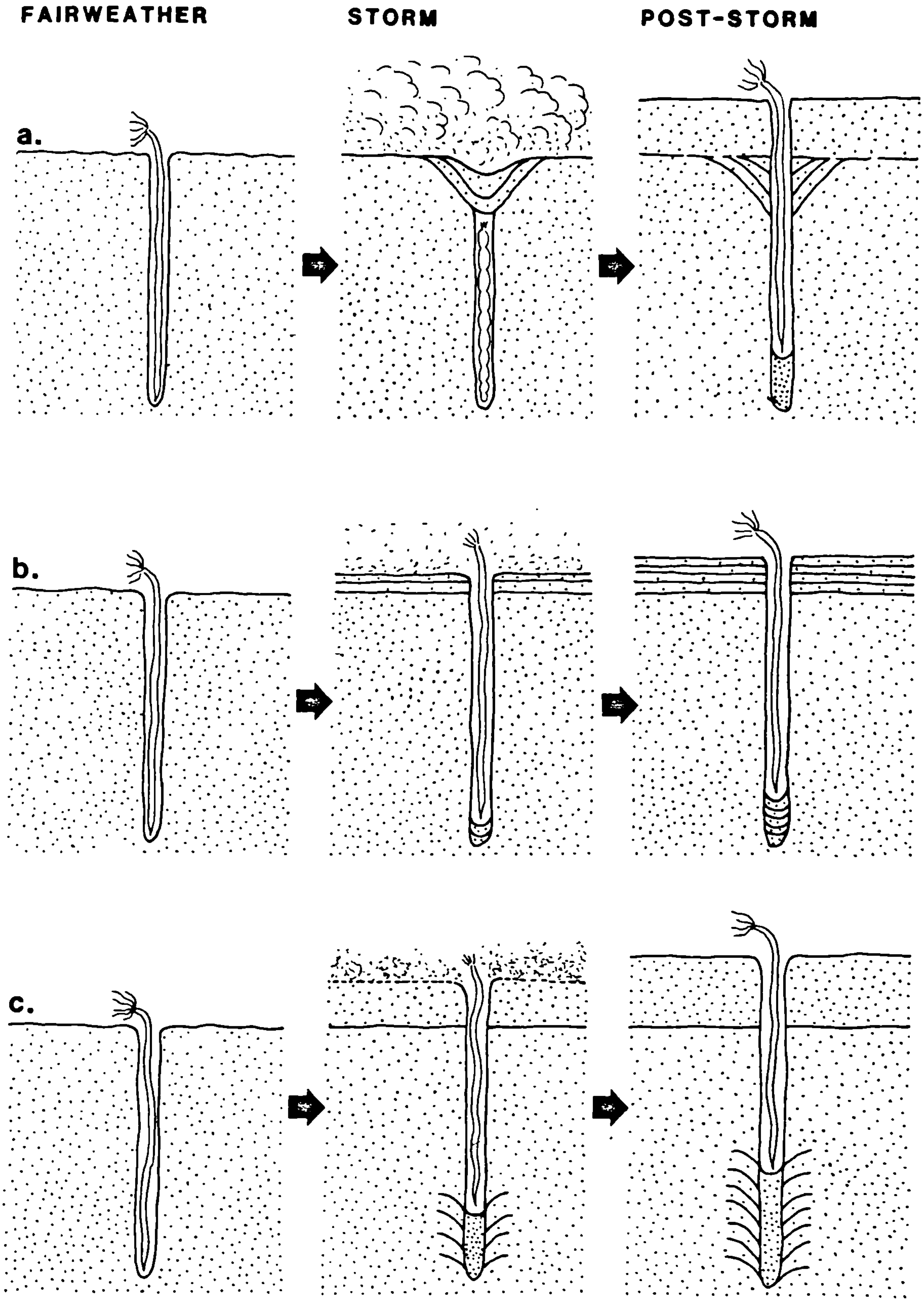

Fig. 3.11 Conceptual models for the development of the various burrow types found within the Pipe Rock.
a. Monocraterion, b. Skolithos with spreiten, c. Skolithos which deflect cross-bedding.

in which the animal did not retract into it's burrow but may have rapidly ascended causing collapse of the full burrow length in response to very rapid burial (Fig. 3.11c). During fairweather periods new arrivals of suspension feeders produced simple Skolithos burrows which penetrated down into the beds containing Monocraterion and other "escape" burrows.

The thinnest beds of fine sand with mud drapes represent the most distal tempestites, or the product of smaller storms, and were probably deposited out of suspension under negligable current or wave activity as storms waned. This facies tends to be concentrated in the Assynt area and also marks a faunal transition from suspension feeders to deposit feeders suggesting that deposition was in a distal, deep water location rather than simply recording relatively less intense storm events.

The particularly frequent series of beds within this facies consisting of featureless sands less than 2cm thick may be tempestites or, alternatively, may represent the winnowed material which was excavated by the burrowing annelids when constructing the fairweather Skolithos burrows.

The relative distribution of facies indicates a vertical transition from large sandwaves, not unlike the forms at the top of the Lower Member, via smaller sandwaves formed under weaker tidal currents to the tempestite dominated "Monocraterion" zone. These facies changes are gradual and probably related to continual deepening and widening of the shelf with possibly a reduction in resonant amplification of tides. The general lack of facies changes along the length of outcrop indicates uniform deepening, except in the Assynt area. Here there is an abrupt increase in mud content and decrease in bed thickness in the beds overlying the massive sands of facies 5. Miller (1984) has suggested that such massive beds in mature quartzarenites are the result of intense bioturbation, however the association in this case with such rapid facies changes suggests bed homogenisation was seismically induced, with faulting producing the rapid subsidence. The tempestite dominated "Monocraterion zone" is followed by a more rapid return to facies 1 and 2 indicating a more rapid shallowing before a continued gradual deepening indicated by the transition to facies 3. The Pipe Rock therefore, applying Walther's Law, appears to have been a "graded shelf" with proximal areas characterised by large fairweather tidal sandwaves and storm erosion and distal areas characterised by smaller tidal dunes and sandwaves and thin, finer grained tempestites (Fig. 3.12).

The sudden appearence of Skolithos at the Lower Member-Pipe Rock boundary does not appear to mark a significant change in sediment type, bedforms or tidal energy. The abundance of burrows and lack of other trace fossils or shelly fauna suggests that the sudden appearance of Skolithos is an evolutionary development with suspension feeding annelids proliferating across the shelf unrestricted by competitors or predators. The relative spacing of Monocraterion burrows indicates that the shelf was densely populated therefore there must have been sufficient suspended organic material to support a large population. Brasier (1980) and Cook and Shergold (1984) have suggested that the widespread occurence of phosphorites in the Lower Cambrian worldwide may have been related to phytoplankton blooms, in which case the Lower Cambrian seas would have provided a rich source of organic material for suspension feeders. The Pipe Rock shelf was too agitated and oxygenated for the preservation of phosphorites, however in the lower energy facies of the Lower Member and the Fucoid Beds collophane is abundant and stands testament to the presence of abundant suspended organic matter capable of settling given sufficiently low current activity.

The very high degree of roundness and sphericity of many of the Pipe Rock grains and well sorted nature suggests that these shelf sands are reworked aeolian sands. Russell and Allison (1985) suggested that the mineralogical maturity of the Eriboll Sandstone is a result of in-situ weathering of the Lewisian basement to quartz and "agalmatolite" mica. If this was the case the agalmatolite clay is likely to have been blown westwards, in the absence of sediment binding plants, by the prevailing tradewinds (Dalrymple et al. 1985) leaving a mature quartz sand to form aeolian dune fields. When these aeolian sands were reworked the absence of fines would contribute towards a very clear water column in which case the newly evolved suspension feeders may not have had to develop sophisticated

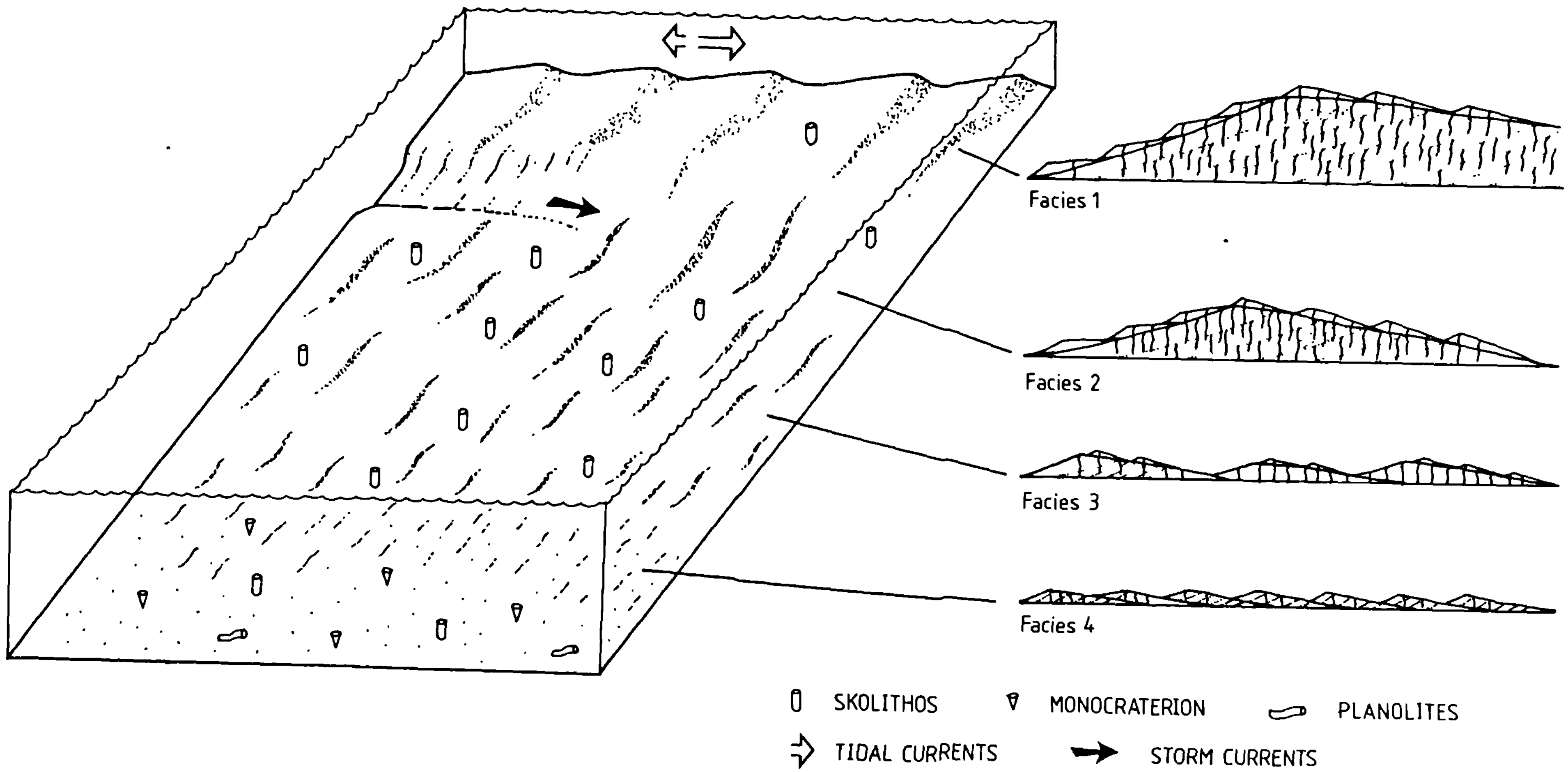

Fig. 3.12 Summary diagram of the depositional elements within the Pipe Rock.

mechanisms for sorting organic and clastic suspended material. In addition a clear water column would have aided algal blooms by providing a deeper photic zone.

The Lower Member is marginally less mature than the Pipe Rock (Swett 1965) and less well sorted with more angular grains suggesting that aeolian sands were a less significant component in the source area. A possible explanation is that initial transgression reworked a coastal lithosome of more fluvio-deltaic dominated sands before proceeding inland and flooding aeolian dune fields and producing the maximum development of well rounded grains in the Pipe Rock during times of maximum transgression. The coexistance of aeolian and fluvial environments in the absence of land plants has been suggested for the Cambro-Ordovician clastic sediments of the northern Mississippi Valley (Dott et al. 1986).

In summary therefore (Fig. 3.12), the Pipe Rock appears to have been a "graded shelf" with proximal zones characterised by large tidal sandwaves and dunes. The most distal part of the shelf was dominated by deposition by rare storm events. Storm effects in nearshore areas were more erosive.

Chapter 4

The sedimentology of the Fucoid Beds

4.1 INTRODUCTION

The Fucoid Beds is a 12-27m thick sequence of thinly bedded muds, dolomitic silts and siliciclastic sands with minor shelly beds. The top and bottom few metres are mostly siliciclastic in composition with the rest of the sequence consisting of thinly bedded dolomitic silts and minor siliciclastic silts. Muds are mainly concentrated near the middle to top of the sequence.

Although exposure is poor, especially within the more muddy parts of the sequence, it was possible to log near complete sections along strike at roughly 30km intervals. Where available, smaller sections were examined between the larger outcrops and within the thrust zone to confirm the overall facies changes. On a more detailed scale, samples of representative facies were slabbed to elucidate the processes responsible for the deposition of beds since the Fucoid Beds appear to be an accumulation of deposits from numerous discrete events.

Most beds within the sequence are bioturbated (Fig. 4.1), especially within the finer-grained facies. However, there are sufficient unburrowed beds to allow the identification of broad facies changes. Unburrowed beds occur, on average, vertically on a decimetre scale. The bioturbated beds show a similar range of lithologies and bed thicknesses to the unburrowed facies suggesting that they were probably of a similar origin and do not represent a unique facies.

4.2 FACIES DESCRIPTIONS AND INTERPRETATION

The Fucoid Beds facies are summarised in table 4.1.

Facies A: Parallel laminated quartzarenite beds

Beds of this facies range from 5-15cm in thickness and consist of quartzose medium sand with horizontal to sub-horizontal planar laminations (Fig 4.2a). The upper few centimetres of individual beds, where preserved, may have current or wave ripple cross-laminations although erosion of bed tops makes this a rare occurence.

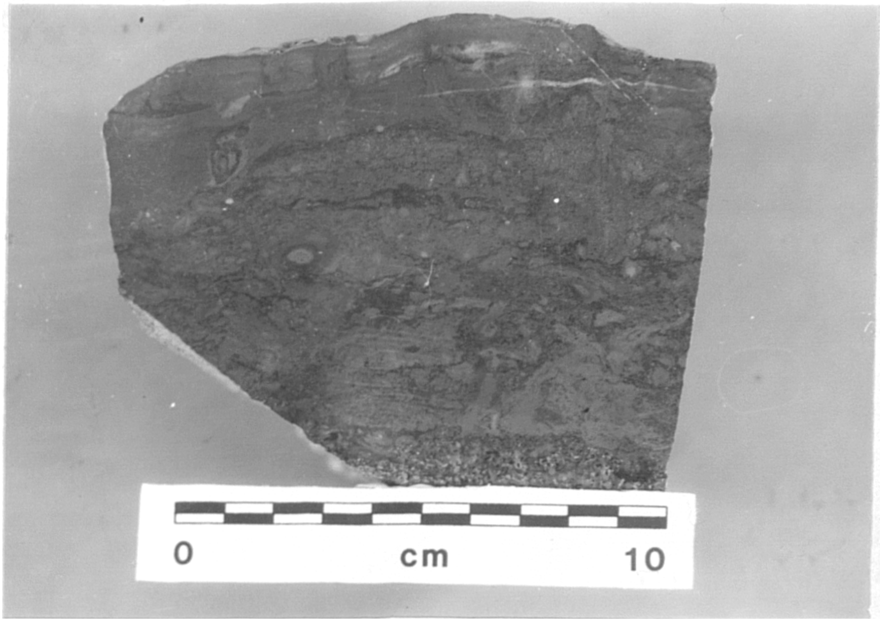

Fig. 4.1 Typical bioturbated appearance of most of the Fucoid Beds. Sample from NC 250 159.

Facies	Typical log	Grain size	Set thickness	Set surfaces	Internal structure	Other features	Interpretation
H	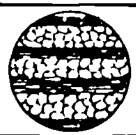	VF Silt + mud	Up to 0.03cm	Planar, non-erosional		Cyclic variations in bed thickness	Settling of airborne dust on shelf. Possible seasonal control
G	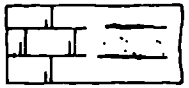	CS-VCS	5-65cm	Planar, non-erosional	Rare cross-bedding or wave ripples	Salterella, Hyolithes echinoderms and trilobites present	Fairweather echinoderm patches
F		Silt + mud	Few mm up to 2cm	Planar, non-erosional	Delicate grading, well burrowed	Abundant framboidal pyrite	Deposition of storm suspended sediment below wave-base
E		VFS-Silt + mud	4-12cm	Planar, erosional	Wave ripples, symmetrical and asymmetrical	Abundant vertical "escape" burrows	Wave dominated shelf tempestite
D		VFS-Silt + mud	4-12cm	Planar, erosional with gutter casts	Ripple lamination, horizontal and climbing	Vertical "escape" burrows. Bimodal palaeocurrents	Shelf tempestite deposited under strong wave currents
C		VFS-Silt + mud	1-5cm	Planar, erosional	Planar laminations	Vertical "escape" burrows	Shelf tempestite deposited under very strong wave currents
B		FS-VCS	10-40cm	Planar, erosional	Tabular cross bedding. Occasional rippled top	Monomorphichnus, Rusophycus and "escape" burrows	Proximal tempestite possibly deposited by combined currents
A		MS	5 15cm	Planar, erosional	Planar or low angle lamination. Rare rippled top	May form amalgamated units up to 1m thick	Proximal tempestite possibly deposited by combined currents

Table 4.1

Occasionally beds may be amalgamated, forming units up to 1m thick (Fig. 4.2b). Where wave ripples are present they are mostly form-concordant types analagous to the "swell and pinch" forms of DeRaaf et al. (1977).

The presence of wave rippling associated with parallel laminated beds is suggestive of a storm origin for this facies. Similar beds have been observed in recent shelf sediments (Goldring and Bridges 1973, Kumar and Sanders 1976, Aigner and Reineck 1982) and in the ancient record (Brenchley and Pickerill 1980, Brenchley and Newall 1982, Tunbridge 1983) and have been interpreted as having been deposited by storm driven flows. Kumar and Sanders (1976) have suggested that such beds were deposited under conditions of strong current or wave induced near bed shear velocities and high suspended sediment concentrations. The presence of wave or current ripples on bed tops indicates that as these currents waned and as suspended sediment concentrations were reduced ripple modification of the bed surface took place.

In terms of "tempestite proximality" (Aigner and Reineck 1982) facies A represents the most proximal storm beds in the Fucoid Beds sequence, deposited under the most intense storm currents.

Facies B: Tabular cross-bedded quartzarenites

This facies occurs exclusively in the top and bottom few metres of the Fucoid Beds sequence. There are sufficient differences between the beds at the top and bottom to warrant separate descriptions.

Facies B is variably distributed along the base of the sequence where it consists of 10-40cm thick, dolomite cemented, tabular cross-bedded sets of fine to very coarse sand (Fig. 4.3). Pelletal glauconite is occasionaly present and is of the same grain-size as the clastic grains. The cross-bedding varies in dip from as low as 10 degrees up to angle of repose and is frequently opposed in adjacent sets. Individual foresets are rarely more than a few millimetres thick. Beds may be normally graded or ungraded. The bases of these beds are frequently erosive and may have a lag of fragmented trilobites, echinoderm plates and Salterella. Less than 5% of these beds have a parallel laminated base and in rare cases, where

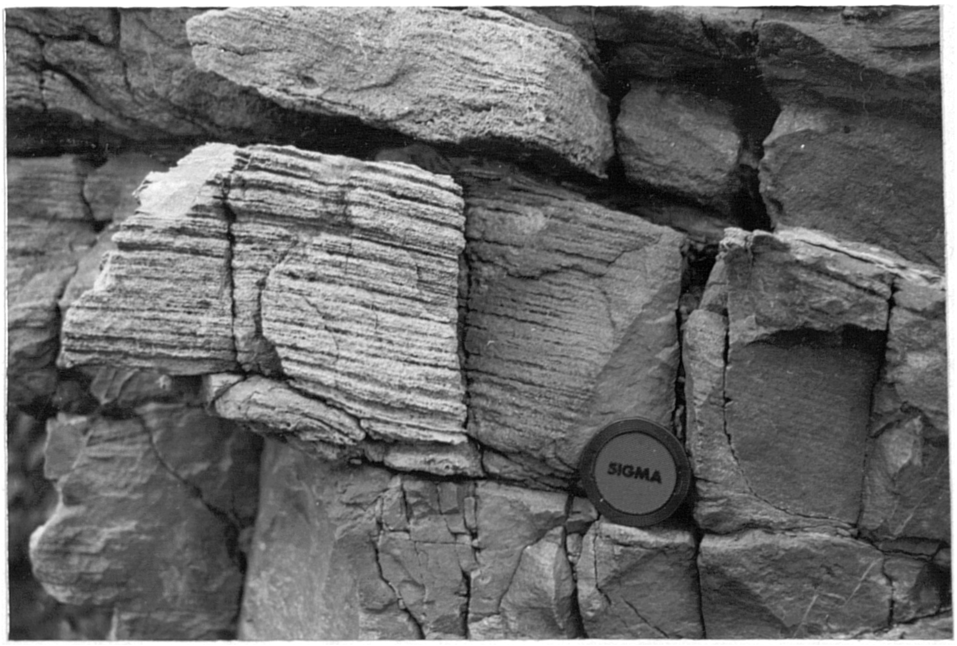

Fig. 4.2a Parallel laminated bed of facies A, An t-Sròn, NC 440 582. Lens cap 5cm wide.

Fig. 4.2b Amalgamated sequence of parallel laminated sets. An t-Sròn, NC 440 582.

Fig. 4.3 Facies B sets.

Fig. 4.3a Tabular cross-bedded set of facies B, An t-Sròn, NC 440 582. Lens cap 5cm wide.

Fig. 4.3b Set with highly erosive base, An t-Sròn, NC 440 582. Lens cap 5cm wide.

Fig. 4.3c Low angle tabular cross-bedding. An t-Sròn, NC 440 582. Scale 1m long.

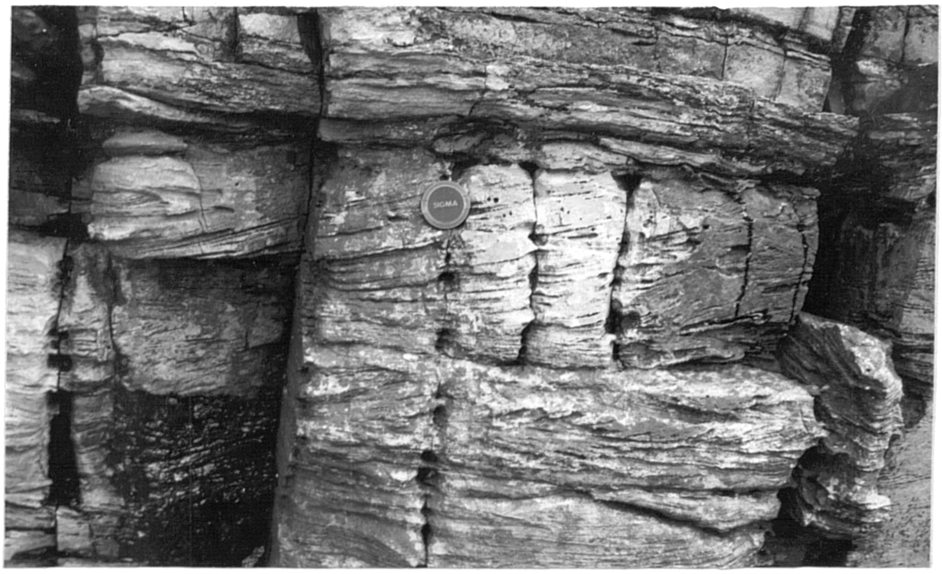
SIGMA

SIGMA


the top has not been truncated by erosion, may have a current or wave rippled top. Rusophycus and Monomorphichnus occur on the soles of beds (Fig. 4.4), which are occasionally cross-cut by vertical "escape" burrows with well developed spreiten. Planolites burrows may be present and cross-cut all other burrows.

At the top of the Fucoid Beds sequence facies B sets are similar in thickness and have similar trace fossils and internal structures to the sets at the base of the sequence. They differ, however, in that they form a complex arrangement of beds which erode deeply into underlying ones and can rarely be traced laterally over distances greater than a few metres (Fig. 4.5a). These beds also differ in lithology, consisting of a heterogenous mix of quartz sand, dolomitic silt, pelletal glauconite and various shell fragments (Fig. 4.5b). As with sets at the base of the sequence foresets are frequently opposed, forming herringbone sets.

The association of erosive based, graded beds with wave ripples is again strongly suggestive of a storm origin for this facies. In addition the "tiering" (Aigner 1985) of trace fossils suggests very rapid deposition followed by slow post-depositional colonisation. The erosive bases of these beds were probably cut by peak storm currents. During this stage clustered Rusophycus suggests that trilobites burrowed into the sediment to protect themselves. Monomorphichnus trails suggest that many trilobites were plucked from the sea floor and swept along by storm currents (Crimes 1970), perhaps after their burrows were exposed by storm erosion. As the storm currents waned dune migration rapidly buried those animals still on the sea floor. These would have strived to reach the surface and produced the vertical escape burrows. Further waning of storm currents resulted in the modification of dune surfaces by ripples or wave ripples. A return to fairweather conditions allowed colonisation by annelids producing Planolites burrows. The presence of herringbone cross-bedding suggests a weak tidal influence on storm currents although the abscence of features indicative of large scale bedforms implies that tidal currents alone were too weak to exceed the sediment threshold velocity and required enhancement by storm

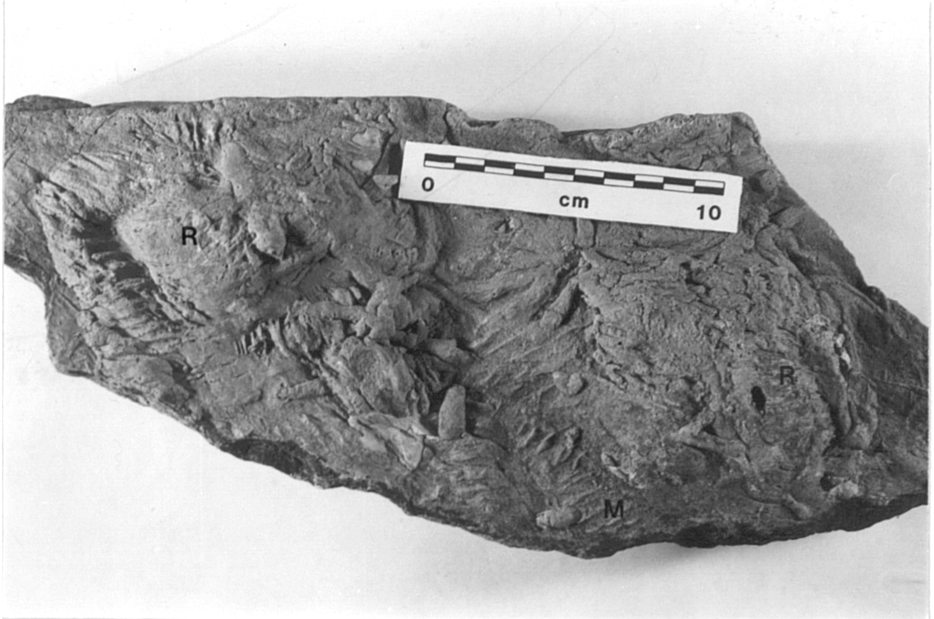

Fig. 4.4a Facies B bed sole with Rusophycus (R) and Monomorphichnus (M). An t-Sròn, NC 440 582.

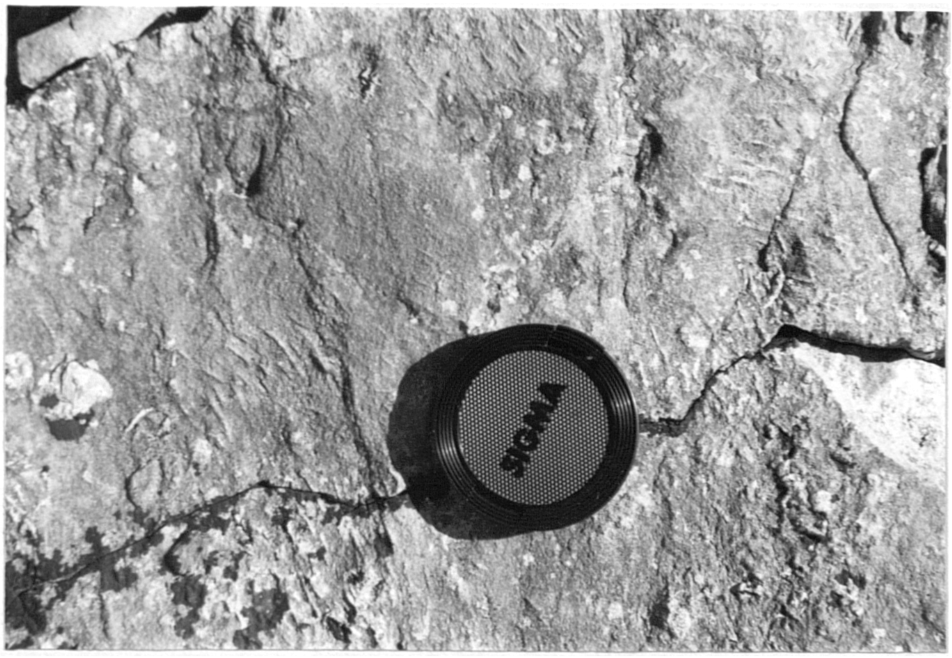

Fig. 4.4b Monomorphichnus on bed sole, An t-Sròn, NC 440 582. Lens cap 5cm wide.

Fig. 4.5a Tracing from field photograph of condensed facies B2 sets, An t-Sròn, NC 440 582.

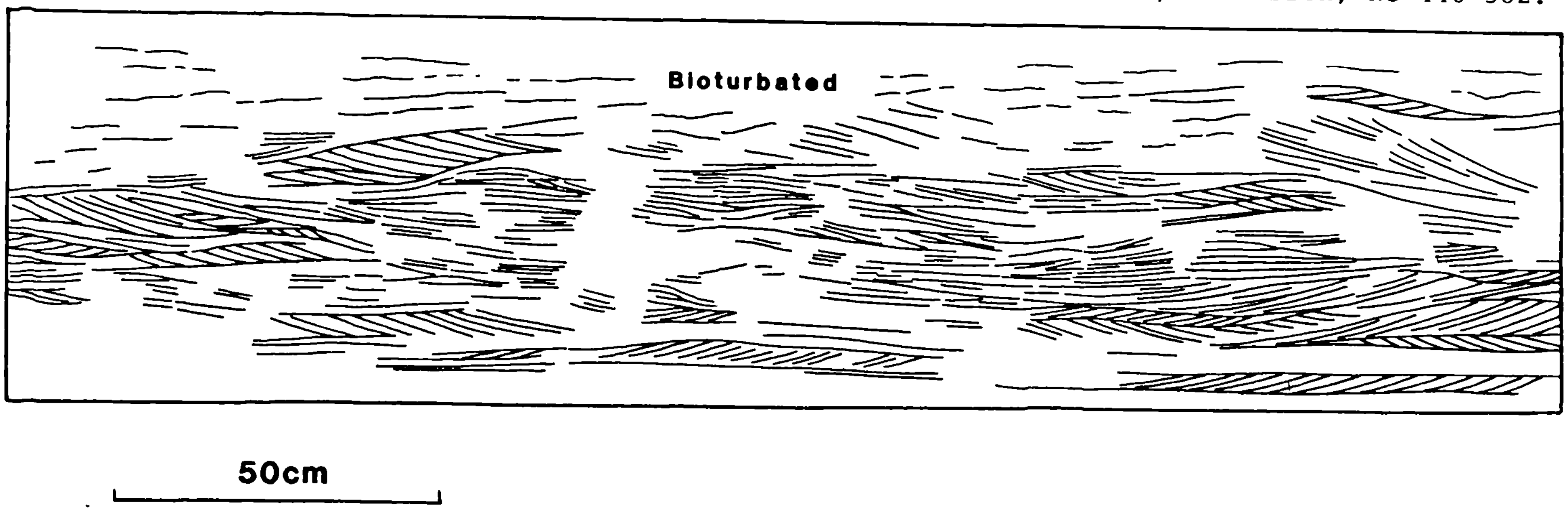

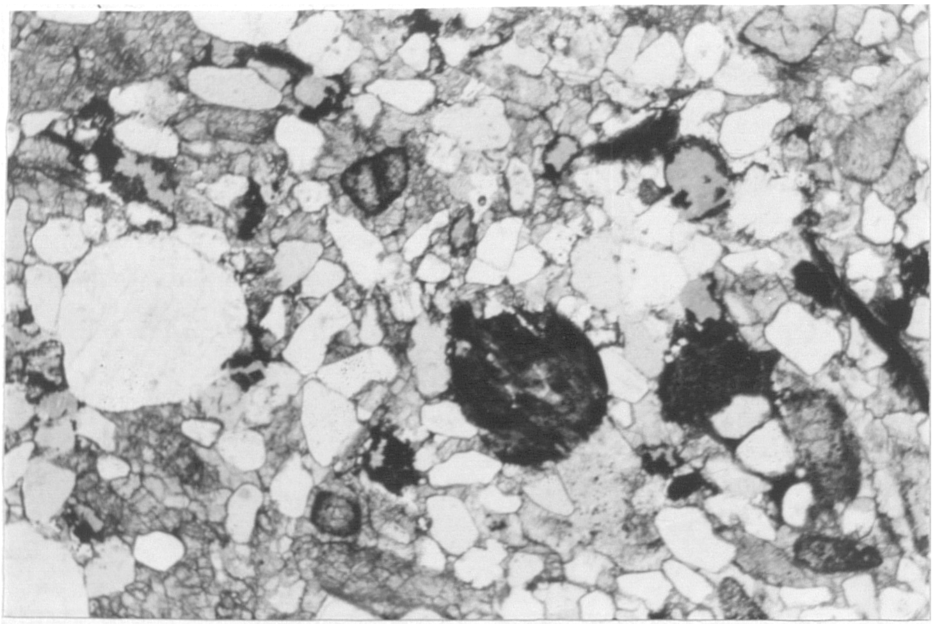

Fig. 4.5b Thin section of facies B2 showing a mix of large rounded and small angular quartz grains (white), dolomitic silt (grey), shell fragments and glauconite. Field of view 2.78mm wide.

currents to transport sediment.

Recent examples of storm induced dunes have been observed in Norton Sound, Alaska (Nelson 1982), the Adriatic Sea (Cavaleri and Stephanon 1980) and on the eastern seaboard of the USA (Swift et al. 1979).

These beds are interpreted as more distal tempestites than those of facies A, deposited under less intense unidirectional or combined currents, although the presence of wave rippling of similar dimensions to those of facies A suggests that during late stages of storm decay wave energy was similar for both facies. The level of erosion during peak storm currents was probably less in this more distal facies and therefore the observed bed thickness range is greater. This facies is not always present at the base of the sequence and may therefore represent storm reworked material from the crests of relict Pipe Rock bedforms. Facies B may also be absent at the top of the Fucoid Beds sequence, but is probably related to the variable depth of erosion at the base of the overlying Salterella Grit (Chapter 5).

Facies C: Parallel laminated silt

Beds of this facies are 1-5cm thick and consist of erosive-based, parallel laminated, graded or ungraded very fine dolomitic sand to silt (Fig. 4.6). A lag of shelly material is sometimes present. The laminations are generally horizontal, but may be gently inclined and may pass laterally into ripple cross-laminations. These silts fine upwards into muds which may be up to 1cm thick.

Vertical "escape" burrows are abundant and are truncated by downward penetrating bioturbation from the bed tops.

This facies is similar to the recent laminated sands described by Reineck and Singh (1971) from several shelf environments, which they attributed to storm suspended sediment clouds which settled out as wave energy decreased. In contrast Kumar and Sanders (1976) suggested that such laminated sands were produced in higher energy conditions by a combination of strong near-bed shear velocities and high suspended sediment concentrations. This higher energy scenario

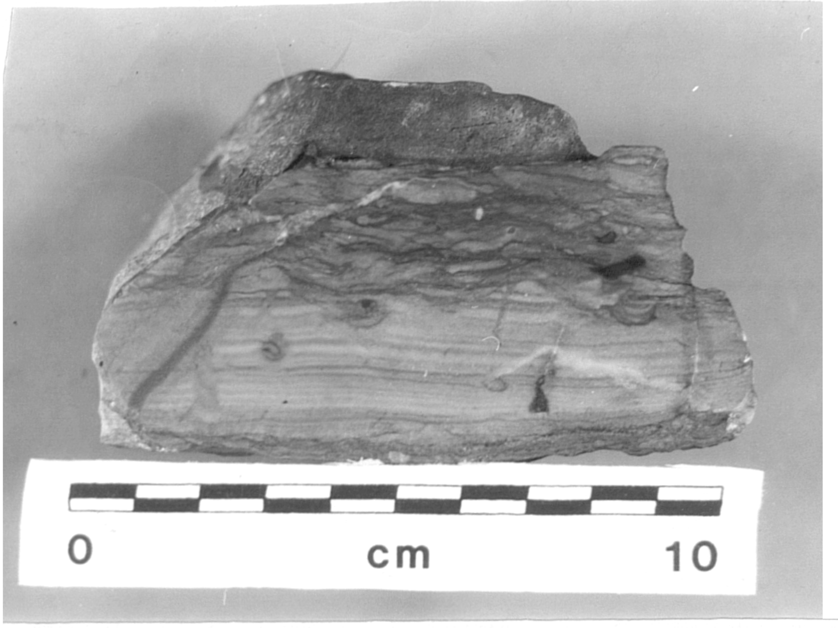

Fig. 4.6a Parallel laminated bed of facies C, Ord River, NG 621 130. Note downward penetrating bioturbation.

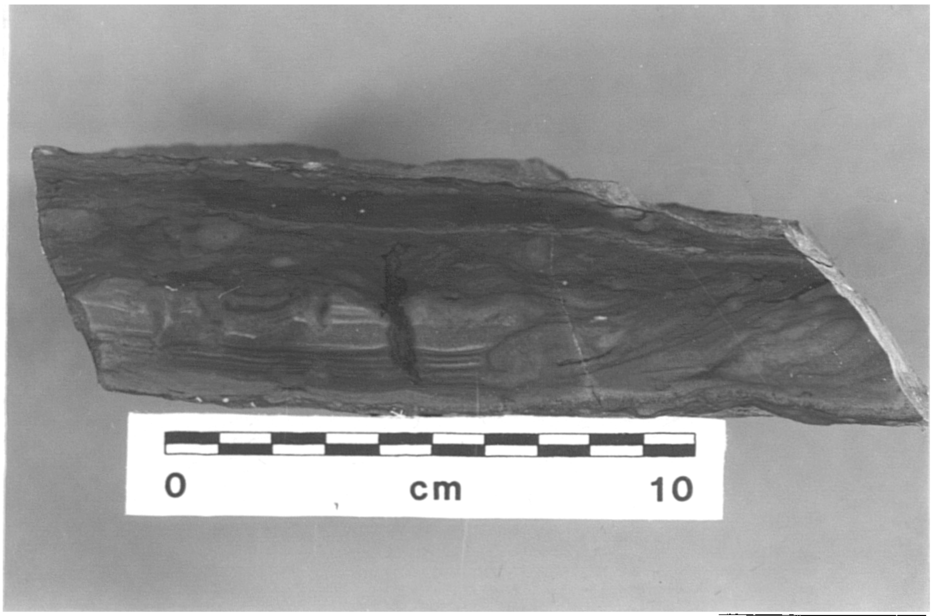

Fig. 4.6b Parallel laminated bed of facies C, Ord River, NG 621'130. Note downward penetrating bioturbation truncating vertical "escape" burrows.

is considered more likely for this facies due to the erosive nature of these beds and the coarse lag occasionally associated with them. Again a waning storm sequence is implied consisting of erosion during peak storm currents, rapid deposition of parallel laminated silts and deposition of mud as storm currents waned followed by post-storm bioturbation of the bed surface. The lateral transition to ripple laminations (Facies D) implies that currents during deposition were unsteady.

An abrupt change in the type of sediment which was being supplied to the Fucoid Beds shelf, from facies A and B to facies C, has resulted in a break in the otherwise linear progression of proximal to distal tempestites. Facies C, although it contains similar structures to facies A and has a broadly similar hydrodynamic interpretation, was probably deposited in a more distal shelf location as shown by the thinner bedding, greater mud content and increased bioturbation. However, the finer grain size has allowed these similar structures to be deposited by weaker currents in a more distal shelf location.

Facies D: Ripple laminated silts

Beds of this facies are 4-12cm in thickness and consist of graded or ungraded ripple laminated very fine sand to silt (Fig. 4.7). These beds are generally erosive-based, may show gutter casts and frequently have a lag of shell fragments. Ripple laminations generally dip at 15-30 degrees and may be horizontal or climbing. Foresets may be opposed within the same bed and bottomsets are occasionally scalloped (Fig. 4.8a). These beds may pass laterally into laminated beds of facies C or may pass into wave ripple laminations (facies E). Bed tops, where preserved, may have up to 1cm of unlaminated mud draping and preserving the undulose rippled surfaces. The upper few centimetres of these beds are often burrowed by dense Planolites burrows (Fig. 4.8b). This downward excavating bioturbation truncates vertical "escape" burrows which have well developed spreiten (Fig. 4.8c).

This is a predominantly dolomitic facies although some clastic quartz and feldspar is always present. Entirely quartzose beds

Fig. 4.7a Facies D ripple laminated silts, An t-Sròn, NC 441 582.

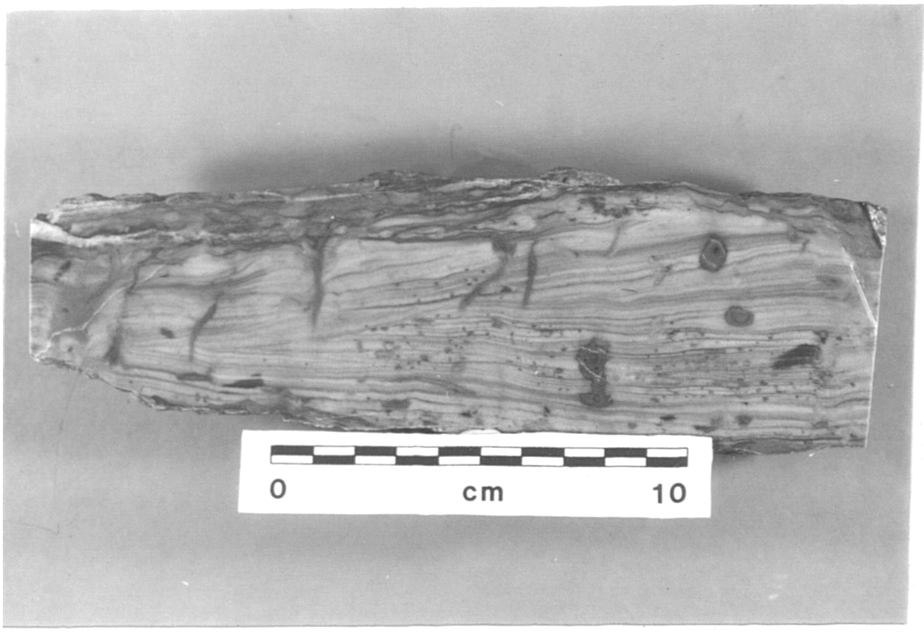

Fig. 4.7b Low angle ripple laminated silts of facies D, NC 250 159.

Fig. 4.8a Ripple laminated silts with scalloped bases, NC 250 159.

Fig. 4.8b Downward penetrating Planolites burrows on bed top, An t-Sròn, NC 441 582.

Fig. 4.8c Vertical "escape" burrow. Note downward deflection of laminae. NC 250 159.

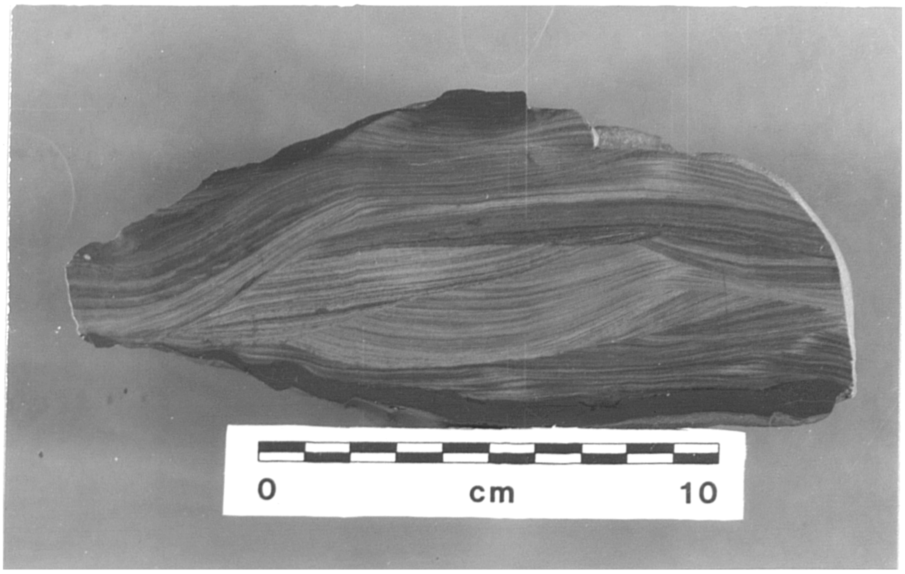
0
cm
10


0
cm
10

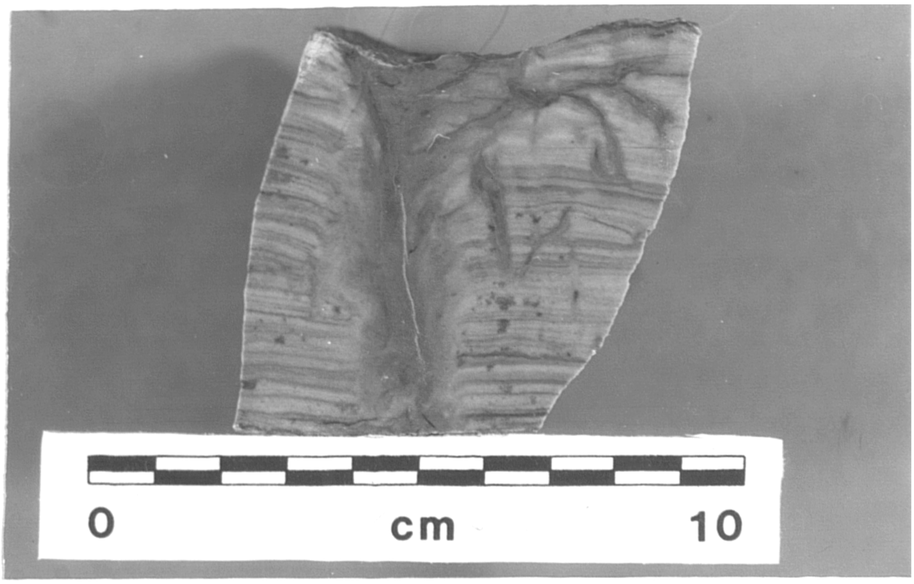
0
cm
10

comprise less than 10% of this facies. Collophane and framboidal pyrite occur in association with the bioturbation and are indicative of the former presence of abundant organic matter in the sediment which provided a food source for the burrowing annelids.

The vertical progression from erosive, scoured soles to ripple laminated beds with escape burrows overlain by thin mud drapes implies deposition from decelerating currents. The lateral association with wave ripple laminations and opposed current ripple laminations within a short distance suggests that the currents were predominantly wave induced. That these currents were markedly unsteady is shown by lateral changes into parallel laminations and wave ripple laminations and the presence of scalloped bottomsets (Rubin 1987). The inferred current unsteadiness and strong wave influence suggests a storm origin for this facies. The thinner bedding, finer grainsize and presence of mud drapes imply lower storm current velocities than those associated with facies A,B and C.

The unlaminated nature of the mud drapes is indicative of very rapid deposition. Cacchione and Drake (1982) attributed similar muds in Norton Sound, Alaska, to a rapid drop in bed shear stress as the near bed suspended sediment concentration reached a critical value resulting in a sudden drop in turbulent flow intensity and rapid mud deposition. The relative abundance of escape burrows in this facies is probably due to the fact that these beds were thin enough for benthic animals to burrow through following burial, in contrast to the thicker beds of facies A and B.

Recent beds similar to this facies and interpreted as storm beds have been described by Nelson (1982) and in the ancient record by Tucker (1982), Turnbridge (1983) and Hobday and Morton (1984).

Facies D beds therefore appear to have been the product of less intense flows than facies A,B and C and represent deposition further offshore under predominantly wave induced currents.

Facies E: Wave rippled silts

These beds are 4-12cm thick, erosive-based and are generally graded from very fine sand to fine silt, although ungraded examples do occur. A basal lag of shell debris is sometimes present. This facies is similar in composition to facies C and D in that it consists almost entirely of dolomitic detritus, although quartz and feldspar silt is normally present. Drapes of unlaminated mud from 0.5-3.0cm thick preserve the ripple forms, which range in wavelength from 6 to 18cm. Vertical "escape" burrows, as with the other fine grained-facies, are truncated by bioturbation along the bed tops. In the less muddy facies Curvolithus and Didymaulichnus occur on bed tops.

The internal structure of the wave ripples can be subdivided into three broad types on the basis of symmetry and degree of current ripple laminations present.

Type 1 wave ripples are symmetrical in cross-section (Fig. 4.9a) and consist internally of form-concordant laminations and are similar to the "swell and pinch" forms of DeRaaf et al. (1977). These ripples may show vertically accreting or translatory crestlines in cross-section and may show internal erosive discordances.

These ripples represent fallout of suspended sediment under relatively weak, symmetrical wave currents although those with translatory crestlines may have experienced some asymmetry in wave currents. Accelerations of these currents may have produced the internal erosion surfaces.

Type 2 wave ripples are symmetrical in cross-section, but have form discordant internal laminations (Fig. 4.9b,c and d). These form discordant laminations take the form of a central core of ripple laminations, similar to facies D, which are moulded into a symmetrical shape by form-concordant laminations. Occasionally the crests of these ripples are "spill-over" forms (nomenclature of Seilacher 1982). Thin stringers of silt, a few millimetres thick and up to 5cm long, extend from the silt crest of an individual ripple into the draping muds infilling the ripple trough. Unlike Seilacher's examples, some of these "spill-over" laminations tend to extend in one preferred direction rather than being symmetrical about the ripple crest.

Type 2 ripples were probably formed either by combined unidirectional and wave currents, where the unidirectional component of flow waned through time with respect to the oscillatory component,

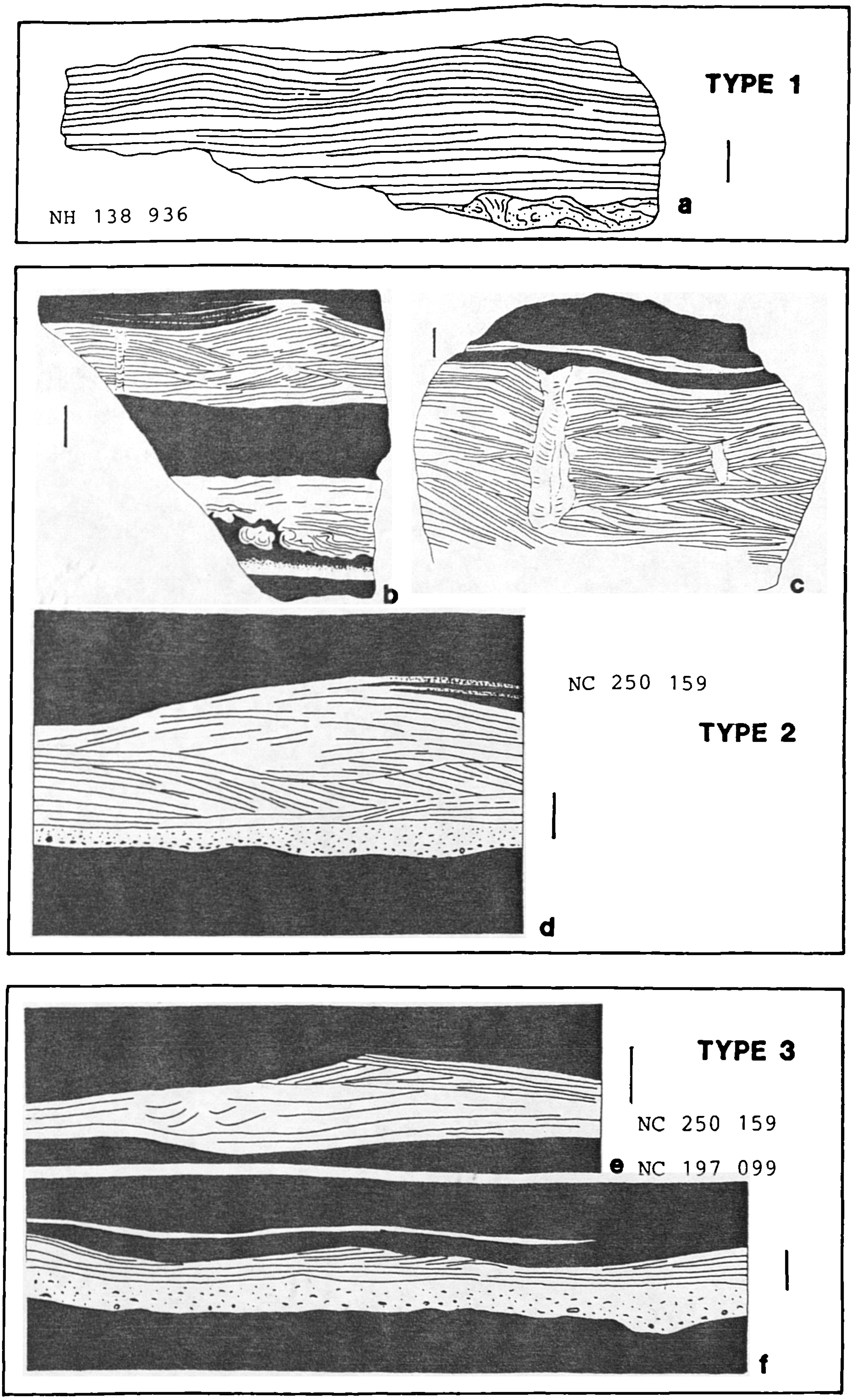

Fig. 4.9 Various wave ripple types from facies E. Scale bars 1cm long.

or were formed by very strong wave currents which produced asymmetrical ripples during peak storm currents which were moulded into symmetrical forms as currents waned and wave orbital diameters were reduced. As will be shown in section 4.4 the latter case is more likely. During the final stages of deposition mud came out of suspension but pulses in current strength were occasionally strong enough to transport silt from the exposed ripple crests into the partly mud filled troughs. Asymmetry in these "spill-over" ripples suggests either asymmetry in wave currents or a superimposed unidirectional current on symmetrical wave currents.

Type 3 wave ripples are asymmetric in profile but may be recognised as wave ripples by the form-discordant internal lamination (Fig. 4.9e and f).

These ripples may represent a more extreme case of strong rectilinear wave currents or wave currents coupled with a weak superimposed unidirectional current.

These classes of wave ripples represent an arbritrary subdivision of a continuous spectrum of forms ranging from the purely oscillatory current induced type 1, and possibly type 2 ripples, to type 2 and type 3 ripples which were deposited under predominantly oscillatory currents but with a possible unidirectional componant.

In summary facies E was deposited under waning storm conditions by predominantly wave currents. The presence of pyrite framboids along wave ripple laminae and within the draping muds implies that abundant organic matter fell out of suspension with the sediment and provided a food source for the post-depositional burrowers and surface grazers. The dominance of wave over current processes, greater mud content, greater faunal diversity and presence of abundant detrital organic matter again suggest a more distal location for this facies than those described earlier.

Facies F: Unlaminated muds

This is a predominantly muddy facies. Beds consist of up to a few millimetres of structureless, predominantly quartzose, silt which fines upwards into unlaminated muds ranging from a few millimetres to 20cm in thickness (Fig. 4.10). The base of these beds is not erosive.

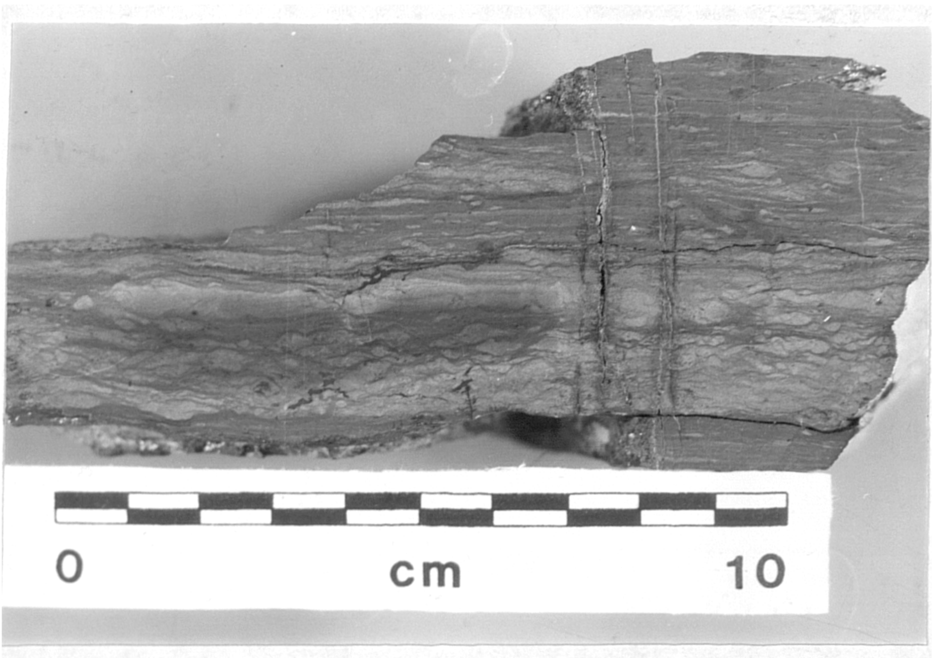

Fig. 4.10 Facies F interbedded silts and muds, Ord River, NG 621 130.

Fig. 4.10b Relatively thickly bedded facies F silts and muds, Ullapool, NH 138 963. Sequence 14cm thick.

The silts are often disturbed by isolated Planolites burrows rather than by a dense bioturbate texture. Pyrite occurs as framboids in many beds.

The delicate grading of this facies suggests that these beds were deposited from decelerating density flows of suspended sediment. Within the context of a storm depositional system these beds represent deposition below storm wave base as turbid flows; possibly analagous to those described by Komar et al. (1974) from the Oregon continental shelf. Similar beds have also been noted from the German Bight (Reineck 1969, Reineck and Singh 1971, Aigner and Reineck 1982).

Facies G: Echinoderm grainstones

Grainstone beds are 5-65cm thick and consist almost entirely of disarticulated and dolomitised echinoderm plates with lesser amounts of trilobite fragments, Hyolithes and Salterella (Fig. 4.11, 4.12a). Individual beds may be normally graded, reverse graded or ungraded and consist of very coarse sand sized fragments. Unlaminated muds up to 1cm thick often subdivide stacked grainstone beds, although isolated beds are more common. Closely spaced logs in the Ullapool area show that these beds pinch out over less than 1km laterally. The bases of thin grainstone beds, where they overlie muds, occasionally incorporate rip-up clasts of these muds, (Fig. 4.12). In general no structures are visible within these beds, but occasional tabular cross-bedding or wave rippling is present. Glauconite is common within the grainstones either as a microcrystalline replacement of echinoderm plates or as microcrystalline, rounded pellets. Glauconite is absent north of Assynt, but appears south of this area as a pale green shell replacement. Further south, especially between Loch Maree and Skye, the glauconite takes on a more emerald green, pelletal form.

These shell beds are considered to represent carbonate deposition below fairweather wave base. No intact echinoderms are found, probably because echinoderm tests spontaneously disintegrate shortly after the animal's death (Paul 1979). Many shell beds within storm depositional systems have been considered to be winnowed lags

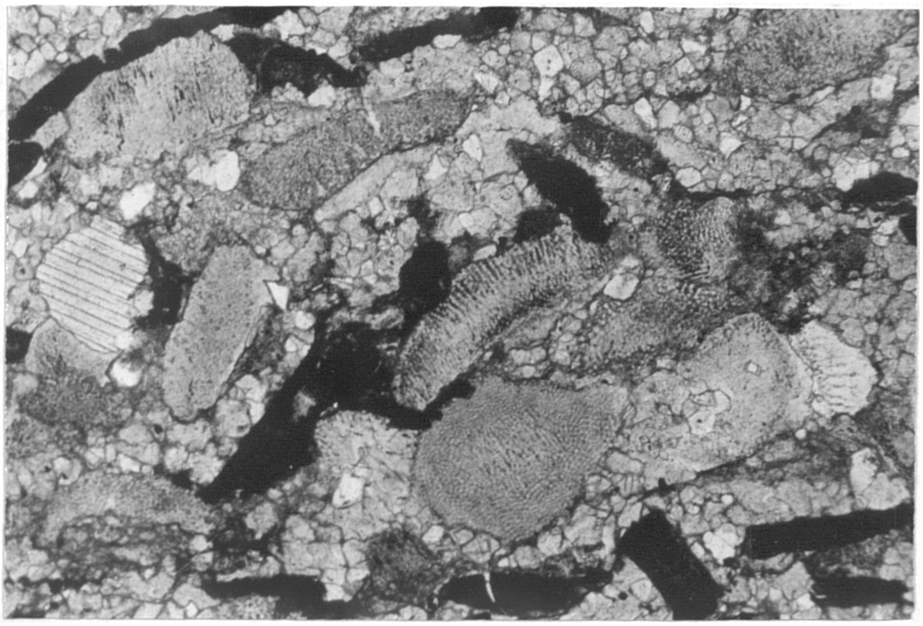

Fig. 4.11a Thin section of facies G grainstone, Ullapool, NH 143 927. Note bioturbation has incorporated some detrital silt which allows greater definition of bioclasts. Field of view 2.78mm wide.

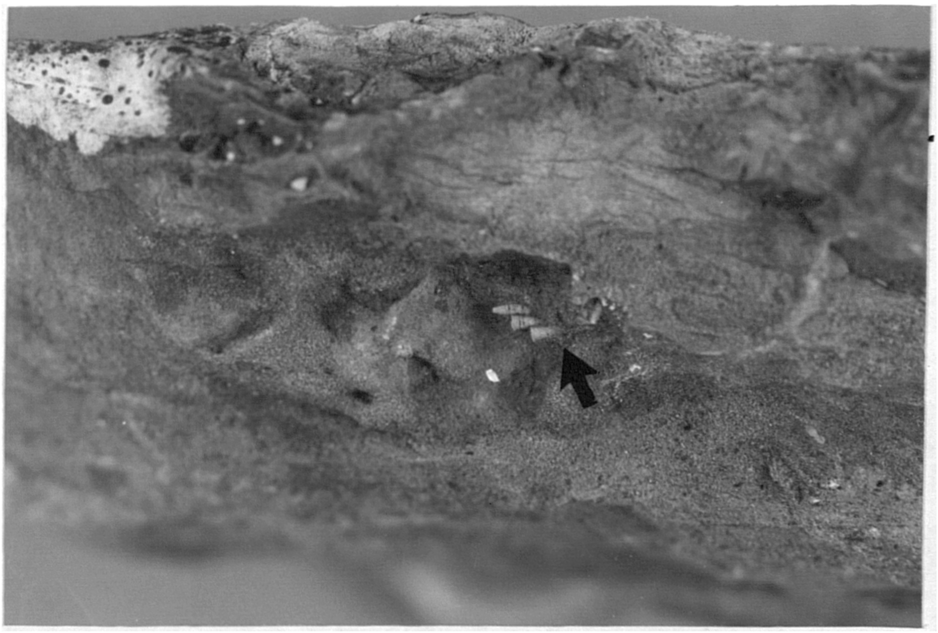

Fig. 4.11b Salterella within burrowed facies G grainstone, Ullapool, NH 137 948. Shells 3mm long.

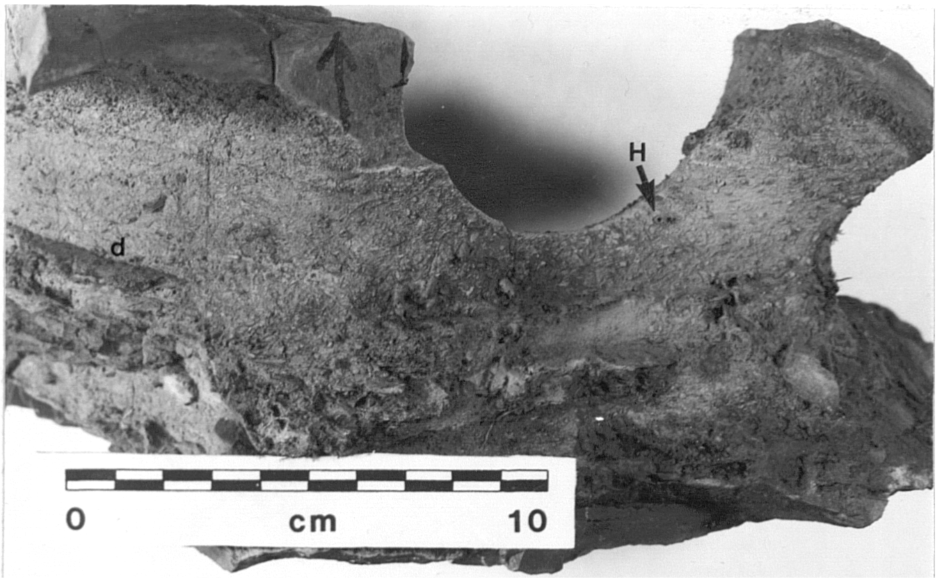

Fig. 4.12a Grainstone with <u>Hyolithes</u> (H). Note thin, discontinuous mud drapes (d). Achnegie, NH 093 795.

Fig. 4.12b Erosive-based grainstone with rip-up clasts, Ullapool, NH 137 948.Lens cap 5cm wide.

of erosive storm events (Kreisa 1981, Kreisa and Bambach 1982, Brett 1983). However, these beds are lithologically distinct from the surrounding sediments, which are not fairweather accumulations but storm derived, and therefore could not be winnowed from them. These grainstone beds most probably accumulated by the post-death disintegration of echinoderms. Peach et al. (1907) record *Eocystites* from the Fucoid Beds which may be from these beds. Cystoids were mostly sessile animals (Clarkson 1979) which suggests that these laterally restricted beds were formed by patch-like thickets of sessile, probably cystoid, echinoderms. These patches also hosted a fauna of trilobites, *Hyolithes* and *Salterella*. During major storms some winnowing and transport of the shell debris is indicated by the occasional presence of cross-bedding, wave ripples and rip-up clasts. A similar mechanism has been proposed by Specht and Brenner (1979) for shelly beds in the Jurassic Redwater Shale of North America.

The thin shelly lags within some beds of facies C to E may have been produced by the deposition of the winnowed fines "downstream" from these thickets. As storms waned mud would have come out of suspension and smothered the thickets, perhaps killing off the echinoderms, although the stacking of these beds suggests that even if this was the case they remained favourable sites for recolonisation. The presence of glauconite suggests that pore waters were slightly reducing within the disaggregated shell beds, although too well oxygenated to form pyrite or collophane.

Facies H: Micro-laminated silts and muds

This facies is comparitively rare. It consists of up to 3cm of non-erosive, rhythmic alternations of very fine quartzose silts and delicately laminated muds (Fig. 4.13a) which often stand out in sharp contrast lithologically to the surrounding dolomitic tempestites and grainstones. Individual silt-mud couplets never exceed 0.03cm in thickness and over a scale of a few metres laterally these beds are scoured out.

The thinness of individual beds, the totally clastic lithology, fine grain-size and absence of fossils or trace fossils suggests that

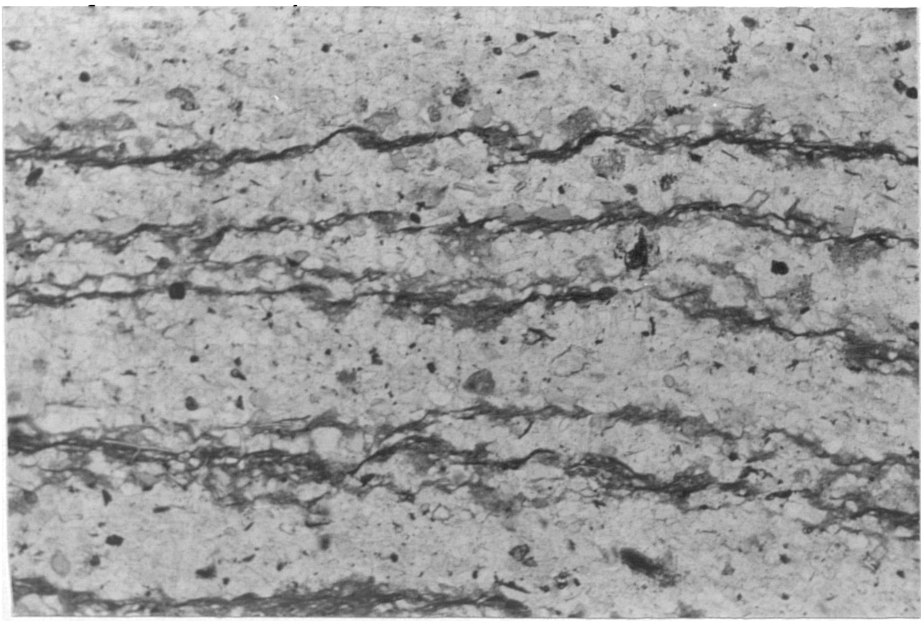

Fig. 4.13a Micro laminated silts and muds of facies H, Knockan, NC 197 099. Field of view 2.78mm wide.

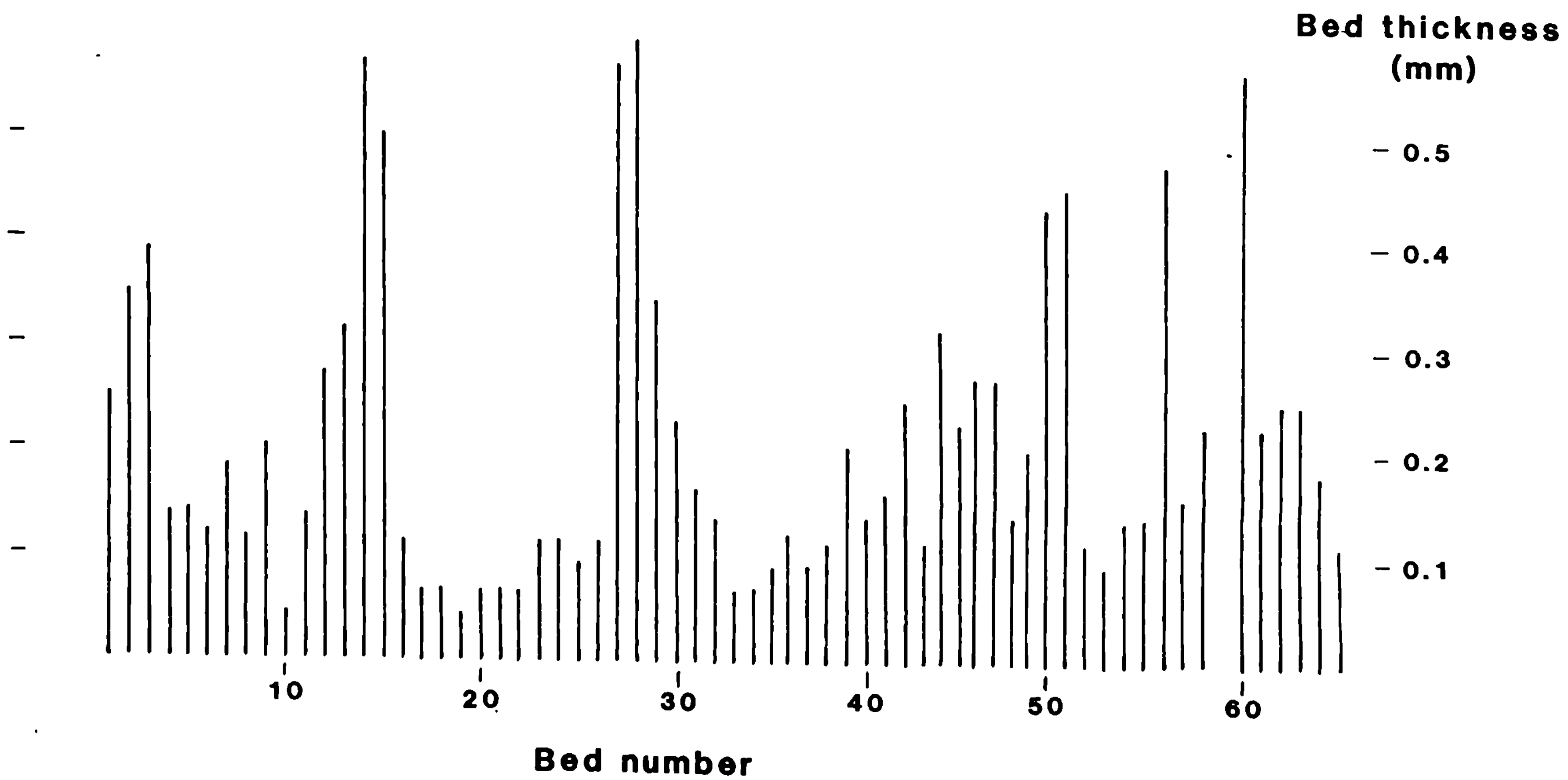

Fig. 4.13b Plot of silt laminae thickness (same sample as in Fig. 4.13a).

this facies is analagous to recent deposits of wind blown silts and muds which have settled offshore in the Arabian Gulf (Foda et al. 1985) and are found in the Tertiary of the Atlantic (Lever and McCave 1983). In the absence of terrestrial plant life such dust storms could have been much more common in the Lower Palaeozoic (Dalrymple et al. 1985, Dott et al. 1986). The presence of a trade wind belt in the Cambrian (Drewry et al. 1974) however, would have transported much of this material westwards across the craton, therefore only rare dust storms moving eastward off the craton would have deposited this facies. Once deposited such beds would have been extremely vulnerable to reworking by burrowers and storm currents; contributing to their relative scarcity in the sequence.

The presence of a crude periodicity in individual bed thicknesses (Fig. 4.13b) is suggestive of seasonal fluctuations. Cycles of beds have a mean thickness of approximately 2.5mm which corresponds to modern rates of annual accumulation (Foda et al. 1985, Khalaf and Hashash 1983) which may imply that the observed periodicity is of an annual scale.

4.3 FACIES DISTRIBUTION

On a large scale the Fucoid Beds, with the exception of the northernmost outcrop at An t-Sron, shows an upward progression from sands of facies A and B through facies C,D and E to muds of facies F. This sequence is abruptly reversed over the top few metres of the section with a return to a condensed sequence of facies A and B, which contain reworked lithologies from other facies. The An t-Sròn section is atypical in that it consists of facies A and B at the top and bottom few metres, but with the rest of the section comprising almost exclusively of facies C and D silts.

Along strike there is little change in facies south of An t-Sròn (Fig. 4.14). Between An t-Sròn and Assynt the mud content of the Fucoid Beds increases dramatically. South of Assynt facies F muds gradually increase in proportion towards Skye where they reach a maximum. Grainstone beds increase in frequency slightly from Assynt to Ullapool, where they reach their greatest thickness. South of

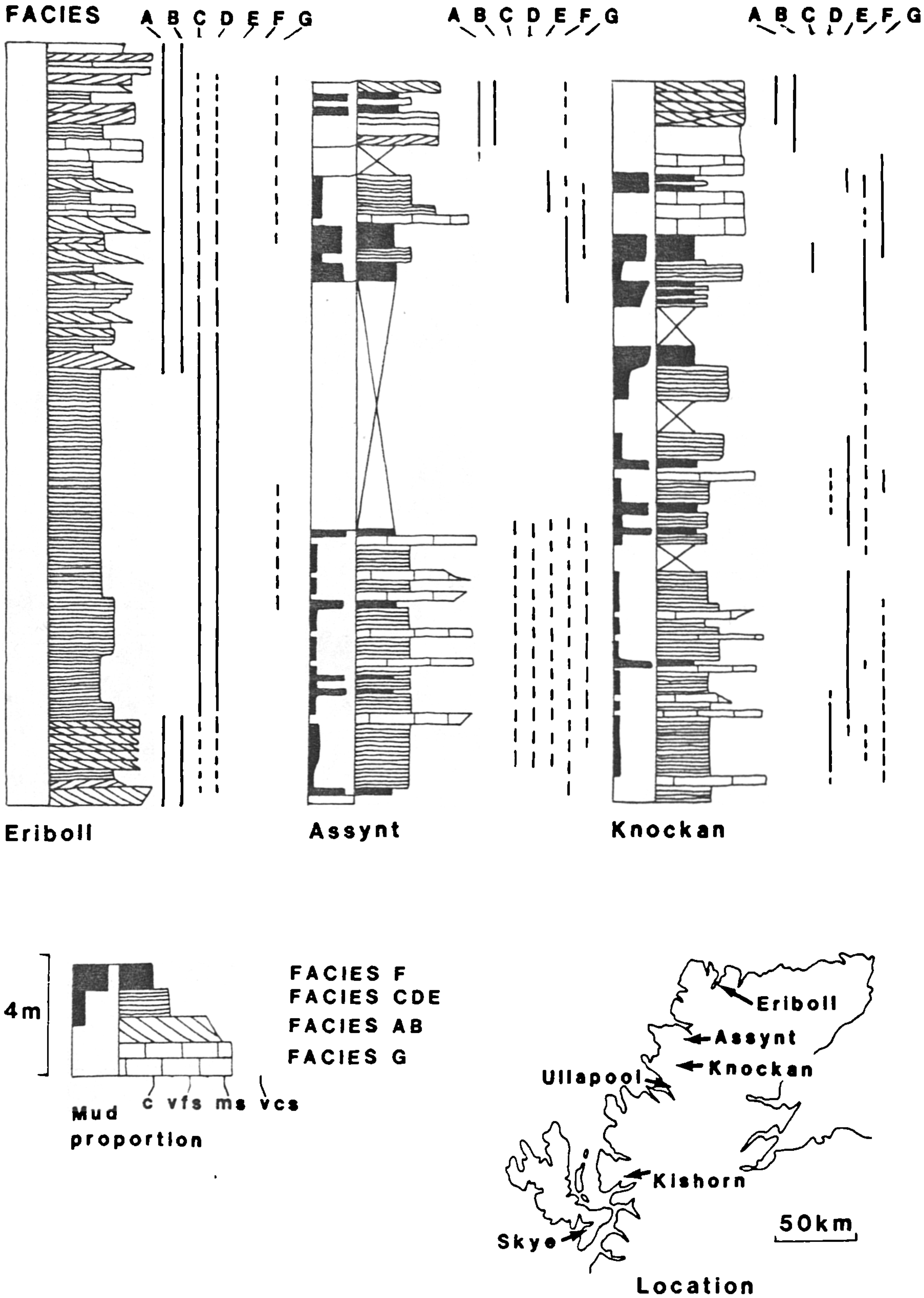
FACIES
A B C D E F G
A B C D E F G
A B C D E F G
Eriboll
Assynt
Knockan
4m
FACIES F
FACIES CDE
FACIES AB
FACIES G
c vfs ms vcs
Mud proportion
Eriboll
Assynt
Knockan
Ullapool
Kishorn
Skye
50km
Location

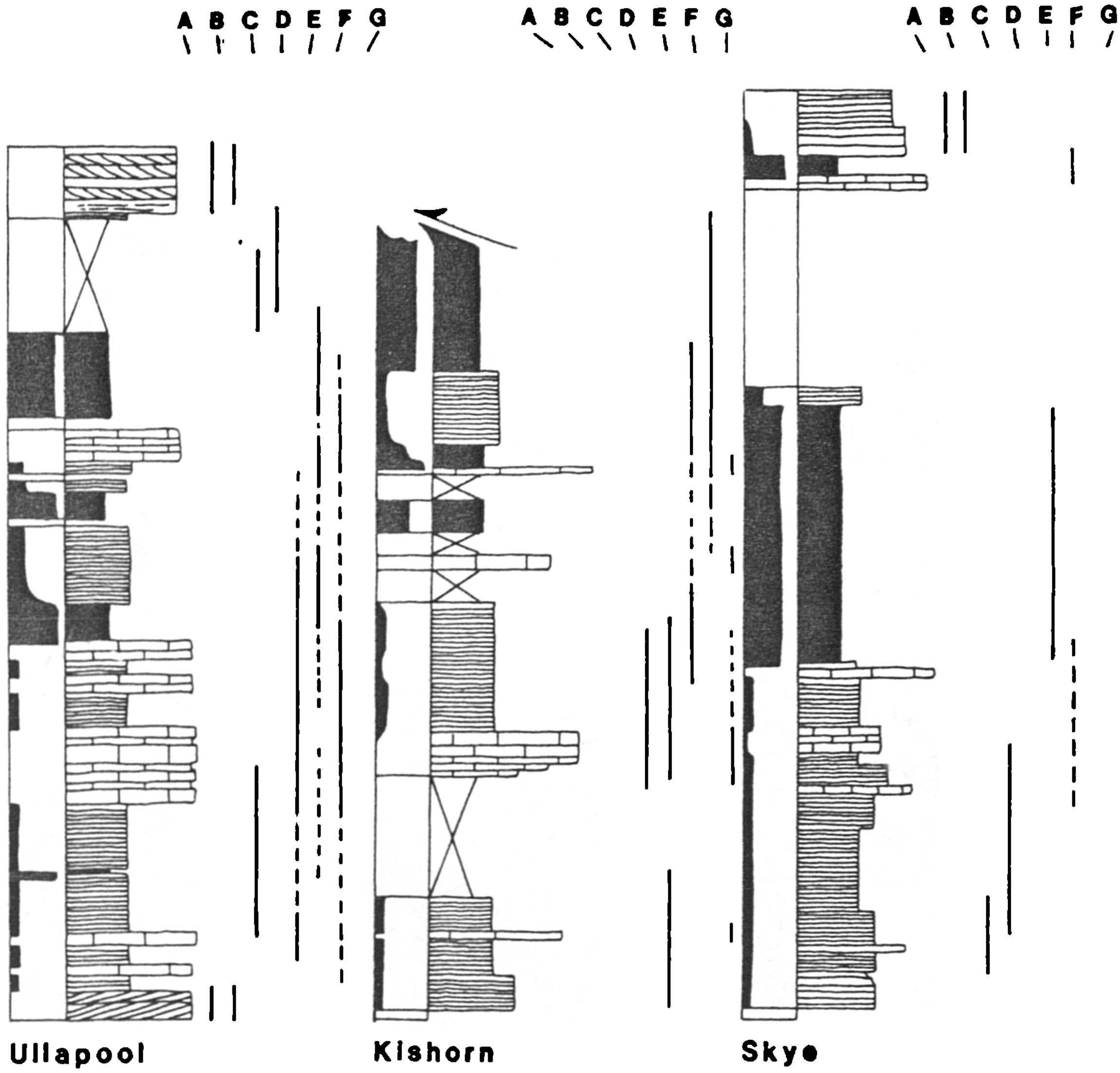

Fig. 4.14 Representative logs of the Fucoid Beds at approximately 30km intervals. Note southwards increase in proportion of muds between Eriboll and Assynt and Ullapool and Kishorn.

Ullapool grainstone beds decrease in frequency.

A closer examination of the facies distribution on a metre scale reveals a more random bed by bed pattern of facies A to F. Facies H is too rare to make any comment on its distribution. Individual beds may on occasion show combined vertical and lateral sequences of facies C to E. Vertical sequences are randomly distributed but tend to have facies C at the base and facies E at the top.

In terms of tempestite proximality (Aigner and Reineck 1982, Aigner 1985) facies A to F represent storm deposition at increasing water depth and distance from the shoreline, all other factors being equal. The Fucoid Beds therefore show a broad transgression reflected by a vertical transition from facies A to F accompanied by an increasing mud content. This transgression is abruptly terminated near the top of the sequence, where a regression is indicated by a very rapid change to a more proximal assemblage of highly condensed beds of mainly facies A and B. This transgressive-regressive cycle is also reflected in changes in acritarch species through the Fucoid Beds sequence (Downie 1984).

Along strike facies changes indicate that the shoreline remained relatively close to An t-Sròn throughout the deposition of the Fucoid Beds. South of Assynt the lack of pronounced facies changes, particularly in the lower 10m, and the palaeocurrent pattern suggest that the palaeoshoreline must have been almost parallel to outcrop and at a greater distance than at An t-Sròn, although in the middle of the sequence the increased mud content and more distal tempestites between Kishorn and Skye suggests that it veered westwards at this time in this area.

On a smaller scale, the more random distribution of facies is a function of the random nature of storm events. The facies present at a particular locality would have been a function of (1) the magnitude of the storm and (2) the distance from the shoreline (Aigner and Reineck 1982). During major storms proximal facies would extend further seawards than during smaller storms. On the smallest scale, the random lateral and vertical facies changes within individual beds reflects the extremely unsteady nature of storm currents.

4.4 PALAEOCURRENTS

Due to the extensive bioturbation and poor exposure, palaeocurrent data is limited. Readings were taken on wave ripple crests, gutter casts and ripple laminations (Fig. 4.15a). These readings were generally taken from the less muddy basal 10m of the succession, which shows no pronounced facies variations between Assynt and Skye. In order to gain an overview of wave ripple crest and current ripple orientations for this region the data was grouped together (Fig. 4.15b). Ripple orientations show a bimodal distribution which is perpendicular to wave ripple crests and suggests that the bulk of facies C ripples were produced by strong, reversing wave induced currents flowing at a distance from, and parallel to, the palaeoshoreline.

The Eriboll area consistently displays more proximal facies suggesting that the palaeoshoreline changed from being parallel to outcrop to a more east-west orientation north of this area. This is reflected in the change in palaeocurrent data. Wave ripple crestlines show a possible change in orientation of a few tens of degrees in an anticlockwise direction which may be related to wave refraction within this shallower northern area. Ripple orientations show a greater dispersal but may be roughly subdivided into a bimodal set perpendicular to the wave ripple crests and modes oriented roughly parallel to the wave ripple crests with a predominantly easterly direction. These data suggest a strong, shore perpendicular, wave influence coupled with alongshore currents generally flowing in an easterly direction.

Gutter cast orientations are few, but appear to be perpendicular to the wave ripple crests suggesting that they were produced by wave currents.

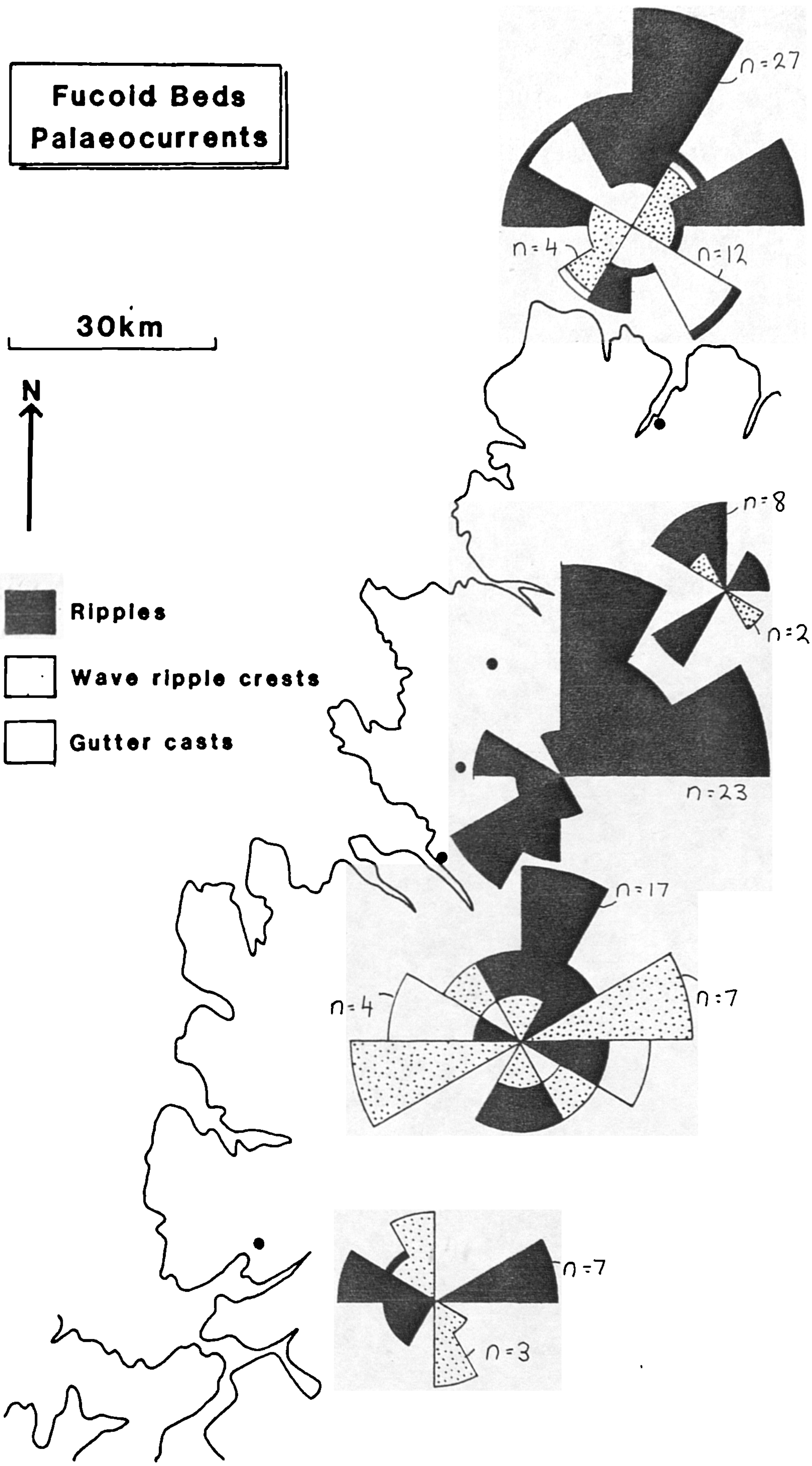

Fig. 4.15a Fucoid Beds palaeocurrents.

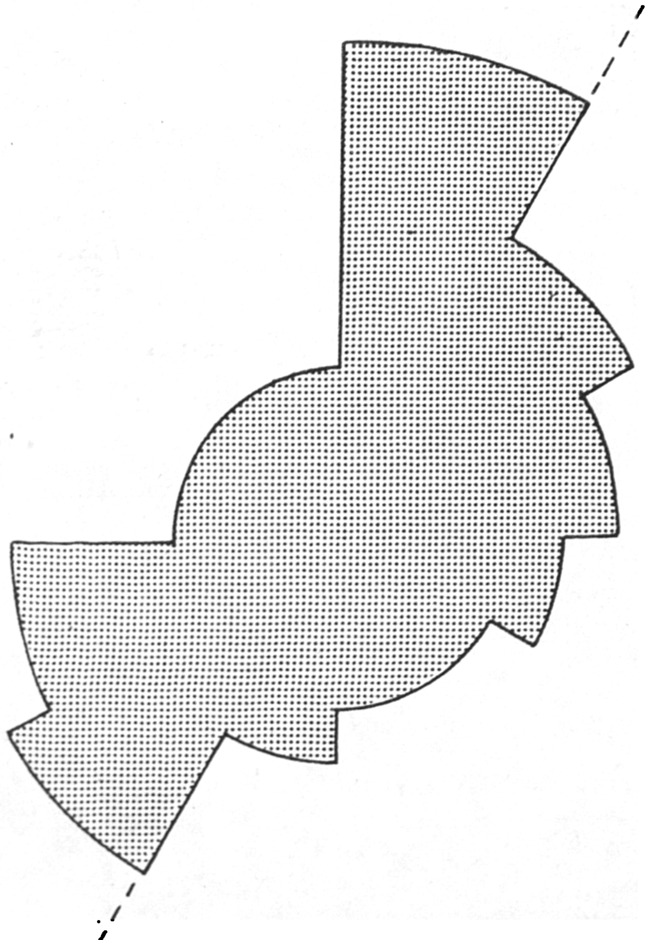

Fig. 4.15b Total ripple palaeocurrents for Assynt to Kishorn.

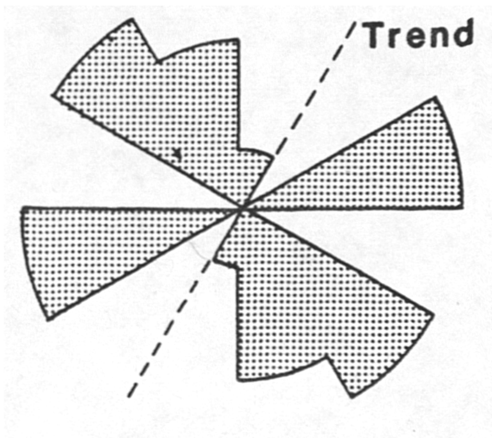

Fig. 4.15c Total wave ripple crest orientations for Assynt to Kishorn. The lack of pronounced facies changes for this area suggests that outcrop is parallel to the palaeoshoreline.

4.5 DEPOSITIONAL ENVIRONMENT

4.5.1 Storm depositional model

A variety of hydrodynamic models have been proposed to account for ancient and recent sequences of storm beds. The nett offshore transport of sediment has been variously ascribed to ebbing storm surges (Hayes 1967, Mount 1982), wind induced gradient currents (Forristall 1974, Swift and Freeland 1978, Nelson 1982), wind enhanced tidal currents (Reineck 1969, Anderton 1976), and combined wave and gradient currents (Allen 1982, Cacchione and Drake 1982, Aigner 1985).

Within the Fucoid Beds the palaeocurrents suggest that for facies C to F two forms of storm depositional system were operating; a nearshore system near Eriboll and an offshore system between Assynt and Skye. Facies A and B are significantly different in lithology, grainsize and structures to warrant being treated separately and will be discussed later. Applying Walther's Law to the transgressive-regressive components of the Fucoid Beds sequence it is possible to reconstruct the depositional processes operating during a storm's passage over the Fucoid Beds shelf.

Between Assynt and Skye Facies D and E indicate a very strong wave influence in comparison with unidirectional currents. These facies may change laterally within the same bed to facies C suggesting that this facies too was likely to have been wave produced. Type 2 and 3 wave ripples suggest either asymmetrical wave currents or a small superimposed unidirectional current. Beds of these facies are generally erosive based and may also have gutter casts. This major erosion must have taken place during peak storm conditions when wave currents were at a maximum. During this stage of rapid increase in current strength benthic animals would have been plucked from the sea floor (eg. trilobites), rip-up clasts would be transported and grainstone shell debris would be winnowed. Subsequent sedimentation would only take place when the storm began to wane and sediment came out of suspension. Suspension fallout in the Assynt to Skye area was dominated by wave currents which produced parallel laminated beds in proximal, shallow water and grading offshore into rippled and then purely wave rippled beds in deeper water where wave currents were weaker. The lateral grading of different facies within individual beds suggests that these currents were markedly unsteady, probably in response to variations in wind strength. In the deepest offshore areas, below storm wave base, suspended sediment would have formed bottom hugging turbid flows. These flows were mud dominated since the coarser silts would have come out of suspension nearer the shoreline.

As the storm waned further wave currents would become weaker and wave base would rise. As this happened proximal laminated beds would become overlain by wave ripples, current ripples would be moulded into symmetrical ripples by wave currents with more circular orbitals with a smaller radius, and further offshore mud would be sedimented as wave-base left the sea floor. The presence of spill-over ripples implies that currents continued to be unsteady. The final stages of storm sedimentation would have been the deposition of suspended muds over the whole shelf as wave base approached a fairweather level, although little would take place in more proximal areas as most mud would have been swept offshore. These processes are summarised in Fig. 4.16. In addition to this offshore grading of facies a similar zonation would have taken place in a shore parallel direction from the storm centre towards its fringes. Rodolfo et al. (1971) noted the thinning of a tempestite bed, attributed to Hurricane Gerda, both in an offshore direction and laterally away from the storm's locus.

The Eriboll area differs from the rest of the Fucoid Beds in the proportion of different facies present and in the palaeocurrents. The abundance of proximal facies and greater thickness of the sequence as a whole suggests that this area was nearer the coastline and may therefore provide an indication of storm current dynamics nearer the Fucoid Beds palaeoshoreline. The bipolar set of palaeocurrent modes suggests that wave induced currents were still a significant feature of deposition within this area, but appear to have been combined with strong along shore currents. Wave ripple orientations from the rest of the Fucoid Beds suggests that most

Fig. 4.16 A temporal and spacial model for storm deposition on the Fucoid Beds shelf. Letters refer to the dominant facies being deposited.

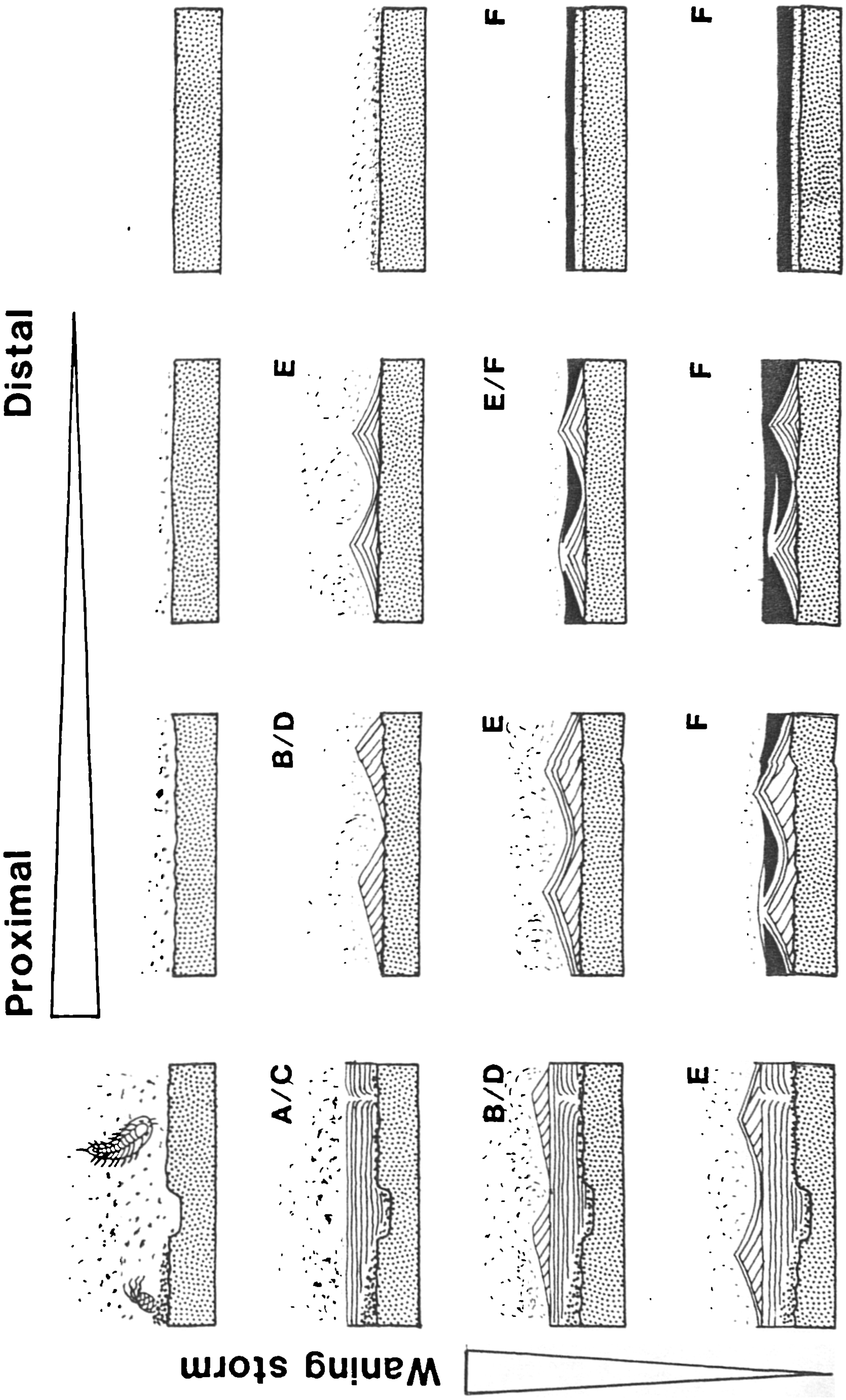
Proximal
Distal
Waning storm
A/C
B/D
E
B/D
E
F
E
E/F
F
F
F

storm waves (and winds) travelled either northwards or southwards. A northwards direction would have induced a set-up of sea level against the coast north of Eriboll. Swift (1976) and Swift et al. (1987) have shown that such a set up will induce a downwelling current in response to the cross shelf pressure gradient which, on being balanced by frictional and Coriolis effects, results in an along-shore geostrophic current. During the Cambrian northwest Scotland was in the southern hemisphere which would imply that the Coriolis force acted to deflect currents to the left and hence would produce a geostrophic current flowing in what is now an eastwards direction. Winds blowing in a southerly direction would have induced a set down of sea level against the northern coast producing a geostrophic current flowing westwards.

It is now possible to integrate both areas of Fucoid Beds into one deposititional model (Fig. 4.17). Between Skye and Assynt northwards blowing winds would have induced a bulk transport of water towards the west which would have produced a storm surge against this coast. The resultant downwelling and shore parallel geostrophic current would have flowed northwards. Within the present area of outcrop this current must have been too weak to significantly affect sedimentary structures, but may have contributed to wave current asymmetry and was still capable of supplying wave suspended silt and mud to the shelf. At Eriboll flow was dominated by combined shore perpendicular wave currents and alongshore geostrophic currents as a result of waves piling water up against this northern coast, and possibly by geostrophic currents flowing northwards and eastwards round the inferred bend in the coastline. Southwards blowing winds would cause a general eastward transport of water which would not be capable of significantly transporting sediment from the western coast and, because of the restricted wave fetch, would have a limited effect on the northern coast.

Facies A and B occur at the top and bottom few metres of the Fucoid Beds sequence, stratigraphically adjacent to the Pipe Rock and Salterella Grit which are interpreted as being essentially tidal in origin. The coarse grainsize, bed thickness and internal structures of these facies suggests that waves alone could not have produced

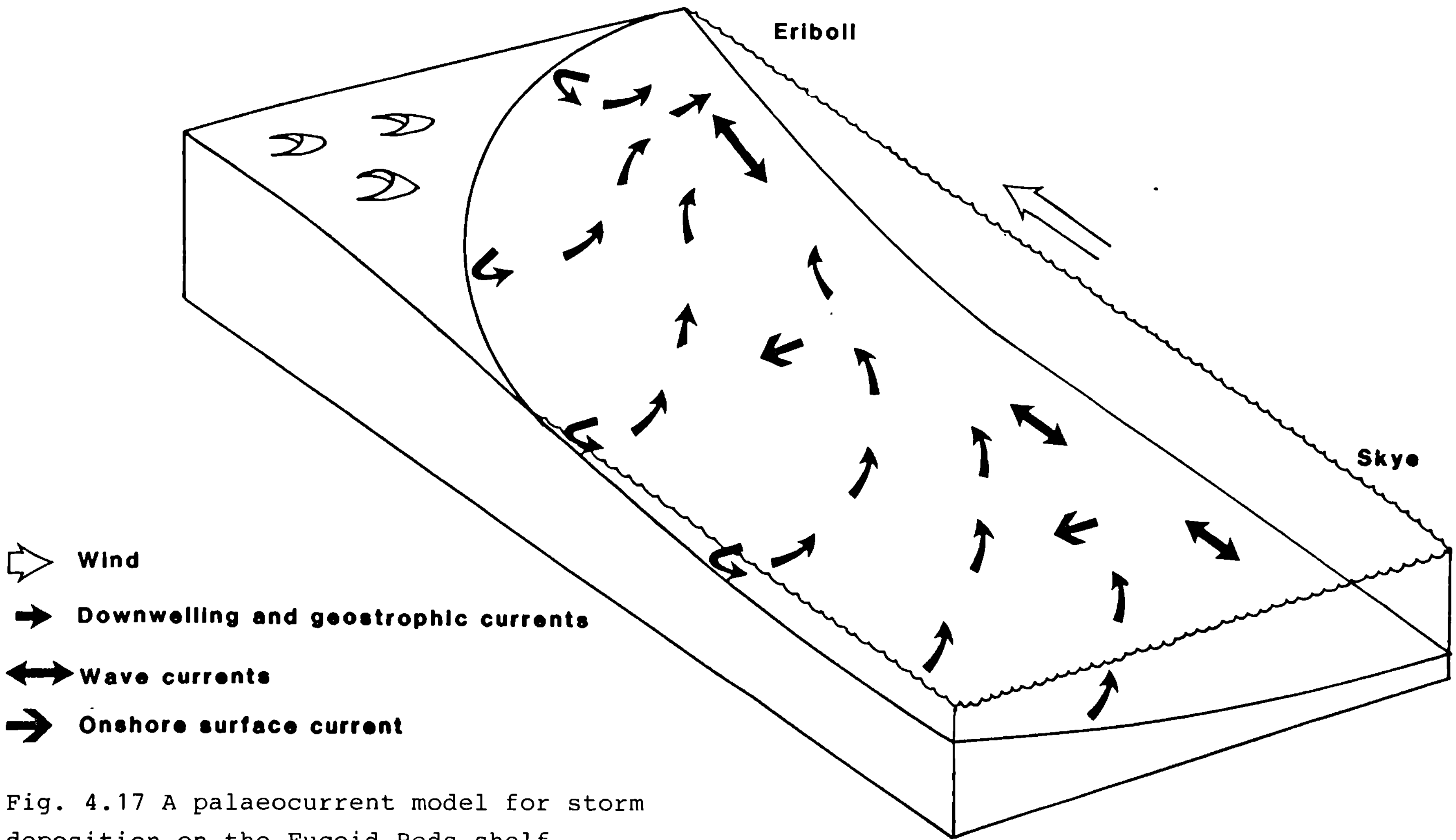

Fig. 4.17 A palaeocurrent model for storm deposition on the Fucoid Beds shelf.

them. It is likely therefore that facies A and B were deposited by combined wave and tidal currents, with possibly some contribution by geostrophic currents, although tides were probably too weak to transport sediment without the aid of storms.

The geologically most significant storms are likely to have been tropical hurricanes and mid-lattitude anticyclones (Marsaglia and Klein 1983, Duke 1985). Palaeogeographic reconstructions of the Laurasian continent (eg. Smith et al. 1981) generally place Scotland at a lattitude of approximately twenty degrees south, which would be within a Cambrian tropical hurricane belt (Marsaglia and Klein 1983). In addition, it's position on an east facing coast would render it susceptable to westward travelling hurricanes crossing the Iapetus Ocean, a situation analagous to that on the modern Gulf of Mexico and Florida coastlines. A hurricane origin for the Fucoid Beds tempestites is therefore likely.

4.5.2 Fairweather environment

A return to fairweather conditions allowed the tempestite beds to be burrowed over by annelids, probably feeding off organic detritus which settled out of suspension together with the fine silts and muds. There appears to be two forms of Planolites within the Fucoid Beds; small forms 1-2mm in diameter which are sinuous on a centimetre scale and penetrate beds to a depth of up to 10cm and large forms 1-2cm in diameter which tend to be restricted to the upper few centimetres of beds. The larger forms were probably produced by large annelids unable to penetrate the deeper, more compacted sediment because of their large size. Alternatively these large animals may have stayed near the surface because they were predators. Cowie and McNamara (1982) noted signs of predation on olenellid trilobites from the Fucoid Beds. After storms echinoderms would have resumed colonisation of the sea floor, most likely on the sites of previous echinoderm patches either because of the survival of animals on these sites or, since they were most likely to have been sessile forms, due to the coarser substrate allowing easier colonisation. The occasional rip-up clasts of echinoderm debris suggests that hardgrounds were forming during fairweather periods. The fairweather Fucoid Beds environment is summarised in Fig.4.18.

The general absence of tidal reworking, abundance of authigenic minerals requiring reducing conditions, sparseness of echinoderms and number of unburrowed beds suggests that the Fucoid Beds shelf may have been extremely quiescent and possibly disaerobic at times. Paul (1979) noted that Cambro-Ordovician echinoderms have particularly well developed thecal pores in relation to their subvective systems which he considered to be a result of these early Palaeozoic shelves being relatively stagnant, with a low concentration of dissolved oxygen and a high organic matter content. This has also been suggested by Wilde (1987). Other examples of unbarred, storm dominated shelves where organic matter was abundant and periods of anoxia common include the Silurian-Devonian Arisaig Group of Nova Scotia (Cant 1980) and the Jurassic Fjerritslev Formation of Denmark (Pederson 1985). Bioturbation is greatest in the shallower water proximal facies C,D and E despite the fact that organic matter appears to have been more abundant in the more distal facies F muds. This may imply that oxygenation of the water column was greatest near fairweather wave base and closer to the shoreline.

The presence of opposed cross-bedding in the upper part of the sequence suggests a weak tidal overprint to the tempestites appearing as the shelf shallowed and probably became more oxygenated. This weak tidal influence marks a transition from the tempestite dominated Fucoid Beds to the macrotidal Salterella Grit.

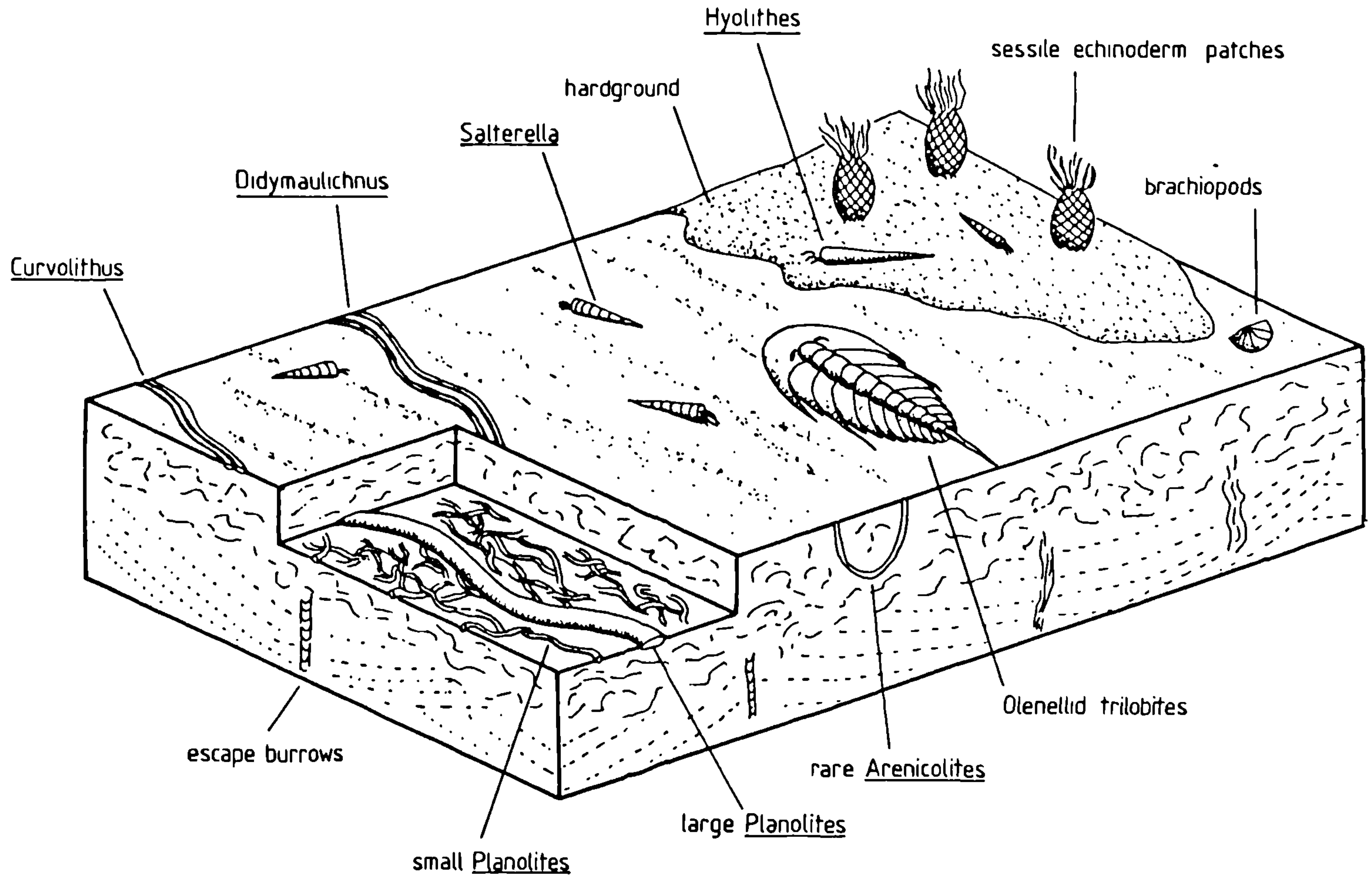

Fig. 4.18 The Fucoid Beds fairweather environment.

Chapter 5

The sedimentology of the Salterella Grit

5.1 INTRODUCTION

The Salterella Grit forms the uppermost part of the clastic sequence. It ranges from 5-15m in thickness and is composed predominantly of cross-bedded quartzarenites with a variable mud and faunal content.

This member shows the greatest variation in lithology along the length of outcrop, but may be subdivided into four general facies associations; three of which represent end-member divisions of a continuously varying suite of lithologies found along most of the length of outcrop and perpendicular to this direction eastwards into the Moine Thrust Zone.

5.2 Facies association A

5.2.1 Introduction

This association is the most common within the Salterella Grit and forms coarsening and thickening upwards sequences up to 15m thick. The facies for this association are summarised in table 5.1.

5.2.2 Facies descriptions

Facies 1A: Laminated muds and sands

This facies consists of up to 70cm of interbedded muds and sands (Fig. 5.1a). The muds are dark grey and fissile and range from 5-25cm in thickness. These muds are interbedded with parallel laminated sands ranging in grain size from angular silt to subrounded medium sand. Beds vary in thickness from a few millimetres up to 7cm. The sandy beds are composed predominantly of quartz grains with a variable proportion of pelletal collophane and glauconite (Fig. 5.1b). Trilobite fragments are comparatively rare. Planolites burrows are common and may be so dense as to totally bioturbate the sediment.

Facies	Typical log	Grain size	Coset/set thickness	Coset/set length	Internal structure	Set surfaces	Other features	Interpretation
6A	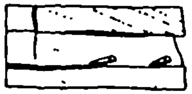	FS-CS	Cosets 1m, sets 5-10cm thick	10m	Vague ripple lamination, bioturbated	Planar, erosive	Shell lags common, *Skolithos* present	Storm sand sheet deposited between banks
5A		FS-MS	Cosets 4m sets 15-50cm thick	10m	Tabular cross bedding	Planar, erosive, horizontal to inclined	Abundant *Skolithos*	Moribund sand bank facies deposited on bank flanks
4A		MS-CS	Cosets 1-10m sets 0.5-1.5m thick	20m	Tabular cross bedding	Planar, erosive inclined at 2-5°	Palaeocurrents along or up inclined surfaces	Prograding steep slope of active tidal sandbank
3A		VFS-MS	4-15cm	10m	Parallel lamination	Planar, erosive	Occasional wave rippled top	Tempestite, deposited by combined currents
2A	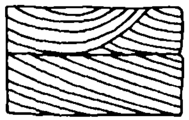	MS-CS	5-25cm	Few metres	Tabular or trough lamination	Planar, erosive	*Planolites*	Deposited by 2-D and 3-D ripples on bank margin
1A	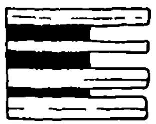	Silt + MS + mud	Cosets 70cm muds 5-25cm sands 7cm	Few metres	Sands parallel laminated	Planar, non-erosive	Bioturbated, abundant *Planolites*	Interbank muds and (storm deposited?) sands

Table 5.1

Fig. 5.1a Interbedded mud and sands of facies 1A, Skiag Bridge, NC 235 245. Lens cap 5cm wide

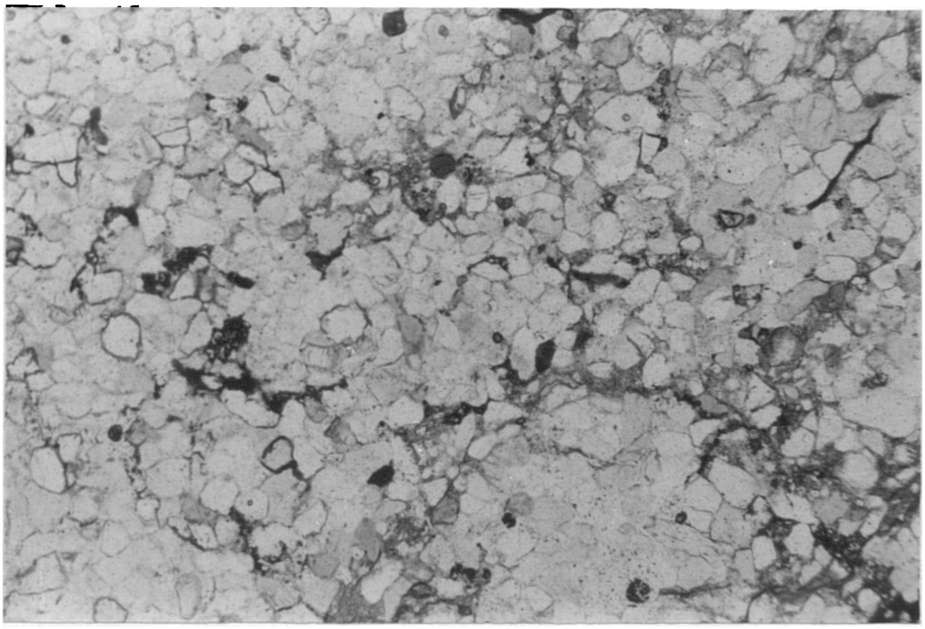

Fig. 5.1b Thin section of sands of facies 1A showing dark, pelletal collophane, Skiag Bridge, NC 235 245. Field of view 2.78mm wide.

Facies 2A: Ripple laminated quartzarenites

Sets of this facies range from 5-25cm in thickness and may be arranged in cosets up to 100cm thick. The cross-laminations are tabular in form, millimetre thick and generally have angular bottomsets (Fig. 5.2a). Trough cross-laminated sets are comparatively rare. Grains vary in size from medium to coarse sand and are composed predominantly of rounded to subrounded quartz. Sets are generally ungraded, although rare normally graded examples occur. Minor quantities of rounded collophane pellets and angular to subrounded collophane cemented siltstone clasts also occur (Fig. 5.2b and c). Abraded and collophane replaced echinoderm and trilobite fragments are present. Planolites burrows are common and may totally bioturbate the sediment.

Facies 3A: Parallel laminated quartzarenites

This facies is relatively rare in association A. It consists of 4-15cm thick beds of very fine to medium sand sized grains with a composition similar to facies 2A. Beds are generally ungraded and are comprised of thin, millimetre thick parallel laminations throughout the bed thickness. Rare beds may have form-concordant wave ripple laminations in the upper few centimetres.

Facies 4A: Cross-bedded quartzarenites

Sets of this facies range in thickness from 50-150cm (Fig. 5.3a and b) although rare examples may be up to 200cm thick. Sets are arranged in cosets 1-10m thick. Grain sizes range from medium to coarse sand and are composed mainly of well sorted, rounded to subrounded quartz. Accessory amounts of collophane pellets, abraded and phosphatised echinoderm and trilobite fragments and collophane cemented siltstone clasts occur along foresets (Fig. 5.3b) and as a winnowed lag on the base of beds. Beds are generally ungraded although reverse graded examples occur, and very rarely, normally graded examples. Foresets are generally steep "avalanche" forms although dips may be as low as twenty degrees. Individual foreset laminations may be up to 0.5cm thick. Bottomsets are mostly

Fig. 5.2a Facies 2A ripple laminated sands overlying facies 1A muds and silts. Scale 0.5m long. Skiag Bridge, NC 235 245.

Fig. 5.2b Phosphatic clasts within facies 2A. Skiag Bridge, NC 235 245.

Fig. 5.2c Thin section showing collophane cemented siltstone clasts. Field of view 2.78mm wide. Skiag Bridge, NC 235 245.

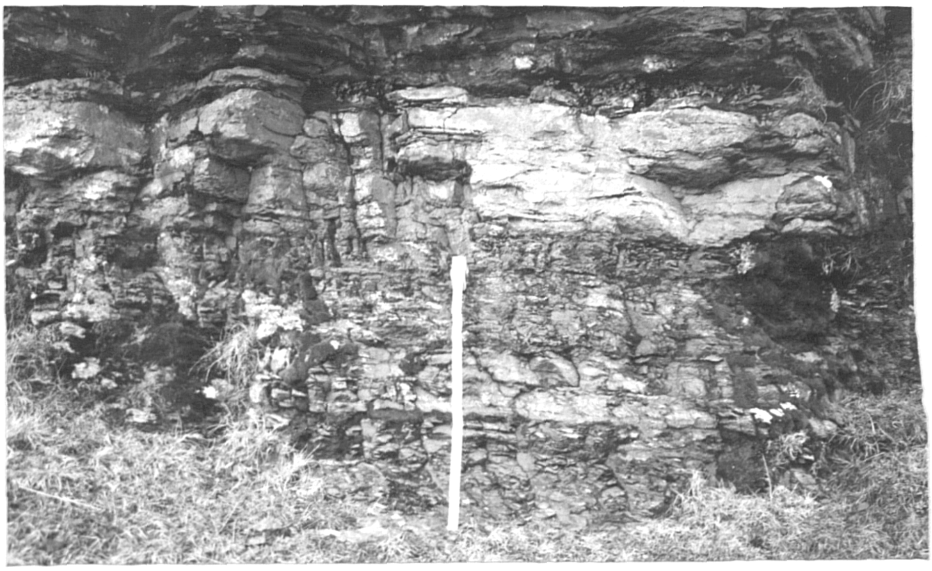

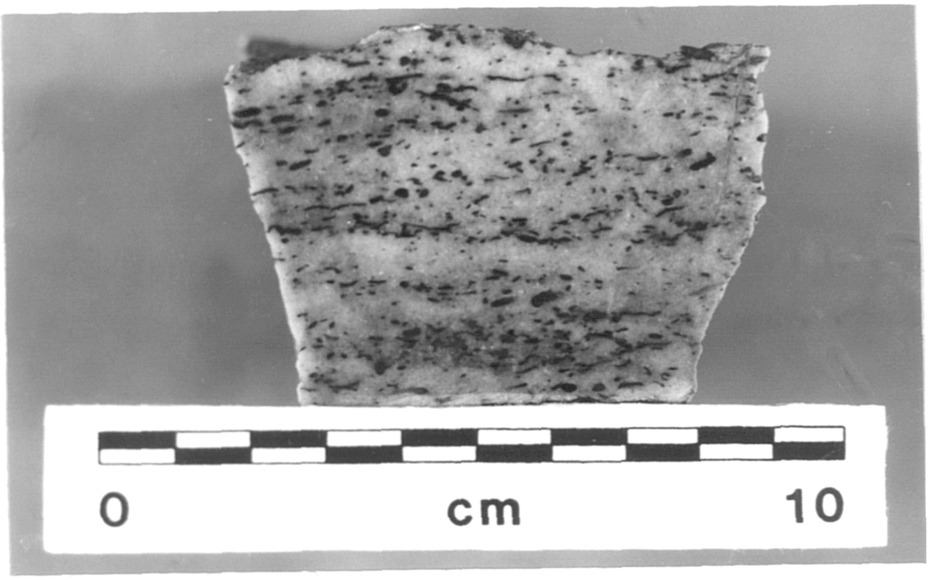
0
cm
10

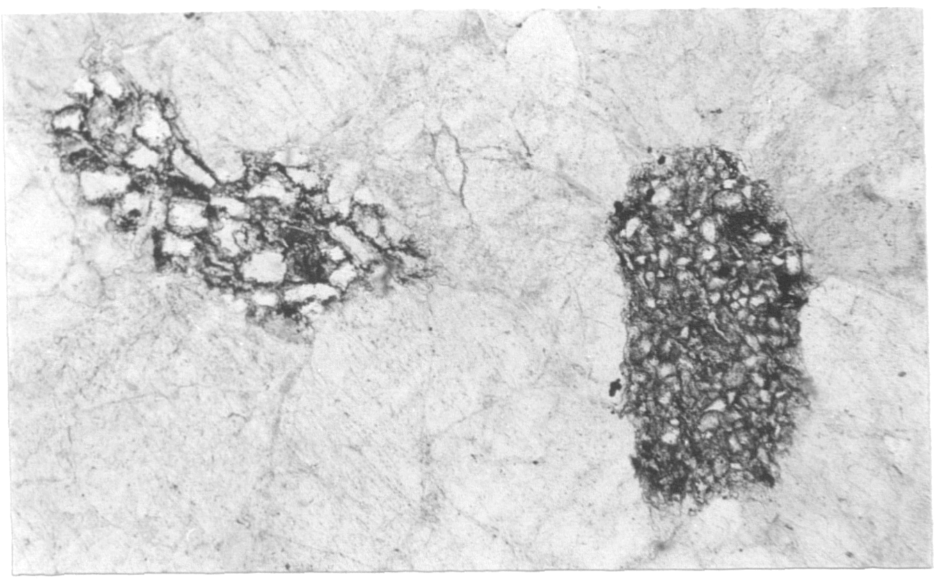

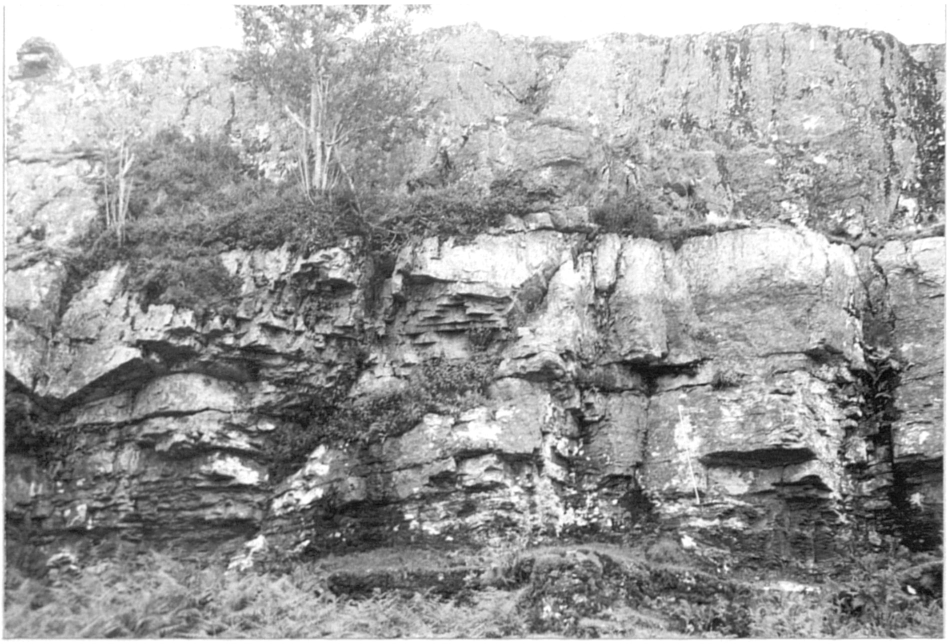

Fig. 5.3a Large tabular cross-bedded set of facies 4A, Skiag Bridge, NC 235 245. Scale 1m long.

Fig. 5.3b Phosphatic clasts defining cross-bedding, in facies 4A set, Skiag Bridge, NC 235 245. Lens cap 5cm wide.

tangential although angular forms are also common. Backflow ripples occasionally occur on low angle bottomsets. Individual cross bedded sets may be traced laterally over several tens of metres before being truncated by convex-up reactivation surfaces with dips as low as ten degrees. Skolithos burrows are variably distributed both vertically and laterally and range from 1cm to several centimetres in diameter and may be tens of centimetres long (Fig. 5.3c). At one locality (NC 235 244) this facies is cut by a channel, up to 150cm deep and traceable laterally over 16m, which has a concordant infill of tabular cross-bedded sets up to 30cm thick which thicken into the channel trough. Skolithos burrows are particularly abundant within this trough (Fig. 5.3d).

Facies 5A: Burrowed quartzarenites

This facies consists of up to 4m of 15-50cm thick beds of poorly sorted, rounded to angular, fine to medium sand with abundant Skolithos burrows which frequently obscure earlier structures (Fig. 5.4). These burrows range in size from large forms tens of centimetres long and up to 2cm in diameter to small burrows a few centimeters long and up to 0.5cm in diameter. Many have concave-up spreiten and deflect foreset laminations downwards near the burrow walls. Occasionally the base of beds is unburrowed and shows tabular cross-bedding, frequently with tangential bottomsets. Foreset dips range from "avalanche" forms to as low as twenty degrees. Collophane pellets and collophane replaced shelly material occurs occasionally along foresets. Salterella occurs sporadically within this facies.

Facies 6A: Fossiliferous quartzarenites

This facies consists of up to 1m of vaguely ripple laminated 5-10cm thick beds of poorly sorted fine to coarse sand (Fig. 5.5a). The finer grain sizes tend to be angular whilst the coarser sands are well rounded in shape. Discontinuous, millimetre-thick mud beds occasionally separate beds. Collophane cemented siltstone clasts, similar to those in facies 4A, are common (Fig. 5.5b). Beds are

Fig. 5.3c Dense Skolithos burrows within facies 4A, Skiag Bridge, NC 235 245. Lens cap 5cm wide.

Fig. 5.3d Downcutting channel margin, Skiag Bridge, NC 235 245. Section 2.5m high.

Fig. 5.4a Burrowed quartzarenites of facies 5A, Skiag Bridge, NC 235 245. Scale 0.5m long.

Fig. 5.4b Very dense Skolithos within facies 5A, NC 246 225. Lens cap 5cm wide.

Fig. 5.4c Large Skolithos burrows in facies 5A, Stronchrubie, NC 250 195. Note weathering of dolomite cemented outer burrow walls. Lens cap 5cm wide.

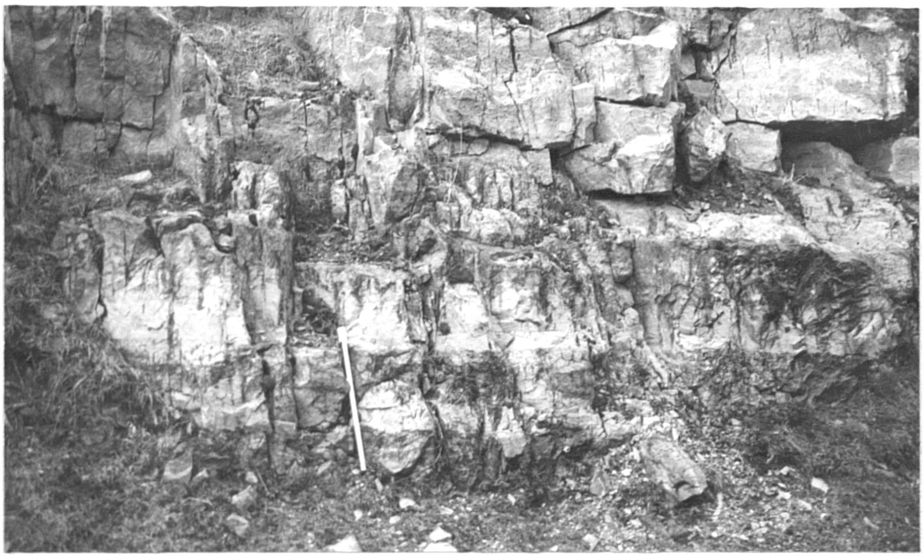

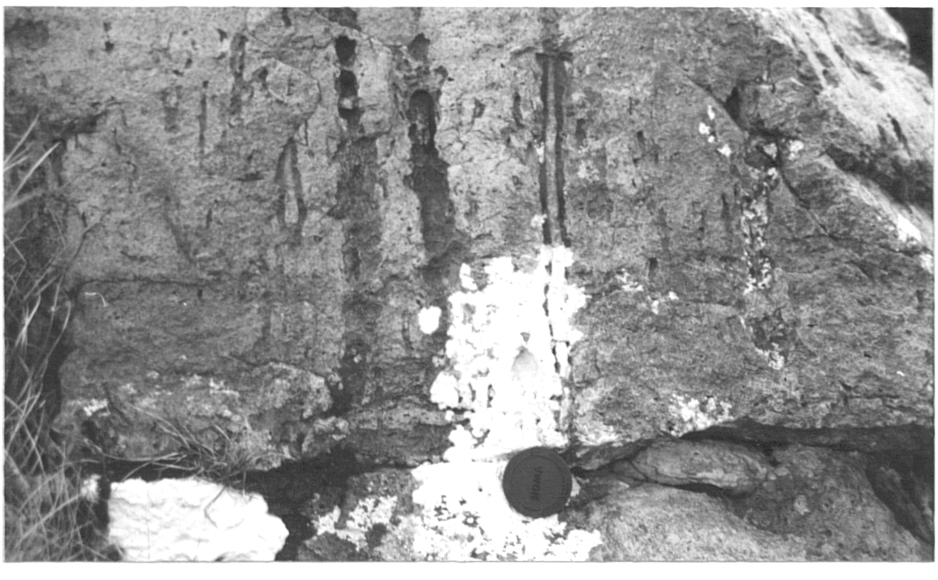

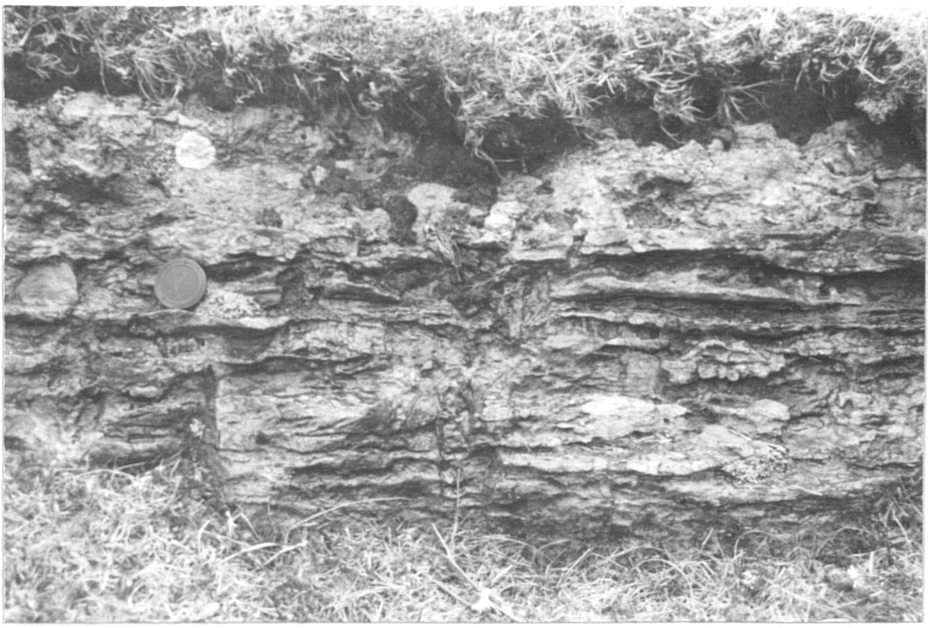

Fig. 5.5a Thinly bedded quartzarenites of facies 6A, Stronchrubie, NC 250 195. Lens cap 5cm wide.

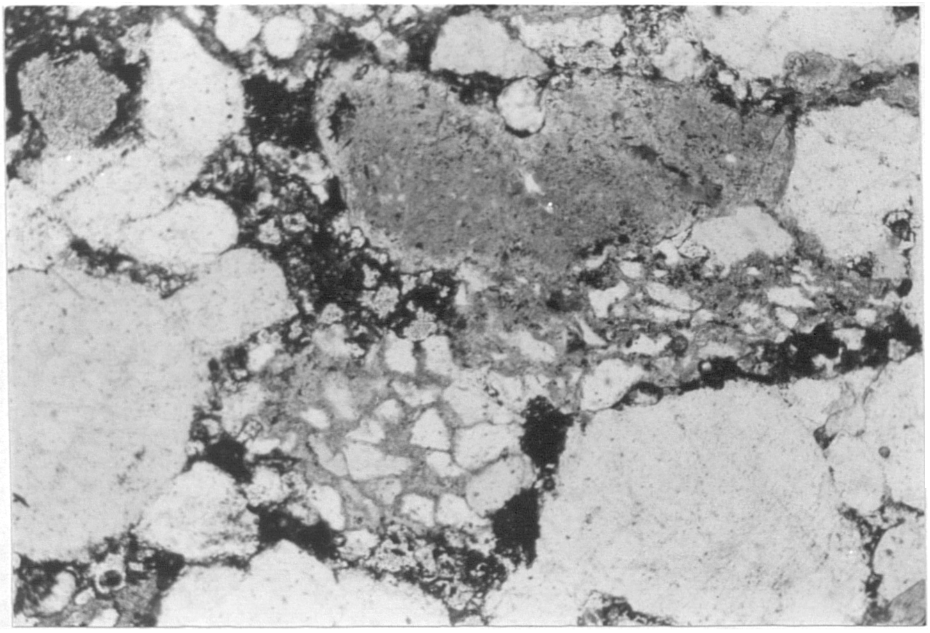

Fig. 5.5b Thin section showing abundant dark phosphatic material. Field of view 2.78mm wide.

frequently bioturbated, although on rare occasions discrete Skolithos burrows are visible. Both the large and small forms of Skolithos occuring in facies 5A are found in this facies although the smaller forms are more common. Salterella tests frequently occur concentrated at the base of beds and may show a preferred orientation. Glauconite pellets are occasionally present and framboidal pyrite occurs associated with the bioturbation.

5.2.3 Facies arrangement

Much of association A comprises coarsening and thickening upwards successions ranging from 1-15m in thickness. The vertical sequence of facies, which varies laterally, consists of facies 1A at the base passing upwards into facies 2A with randomly distributed beds of facies 3A. Facies 4A forms the bulk of these sequences and individual cosets tend to thicken upwards (Fig. 5.6). Facies 5A is present at the top of coarsening and thickening upwards sequences thinner than 10m. As these sequences decrease in thickness the proportion of facies 5A increases; reaching a maximum of 3m when overlying the thinnest sequences (Fig. 5.6). Facies 5A is always thinner than 3m when directly overlying the Fucoid Beds. Facies 6A always occurs overlying facies 5A, but does not vary significantly in thickness.

On a kilometer scale laterally, as association A sequences decrease in thickness and the relative proportion of facies 5A increases, there is an overall reduction in bed thickness for each facies and an increase in the number of Skolithos burrows within facies 4A.

These changes in the relative proportions of facies present and set thicknesses occur on a scale of 0.5-3.0 km in a direction perpendicular to the local palaeocurrent direction. On a lateral scale of tens of metres facies 3A and 4A are seen to be enclosed by gently dipping bounding surfaces inclined at 0-5 degrees which are planar to slightly concave-up (Fig. 5.7a and b). Foreset orientations in these facies tend to be unidirectional (see section 5.6) and are oriented in a direction perpendicular or opposite to the direction of

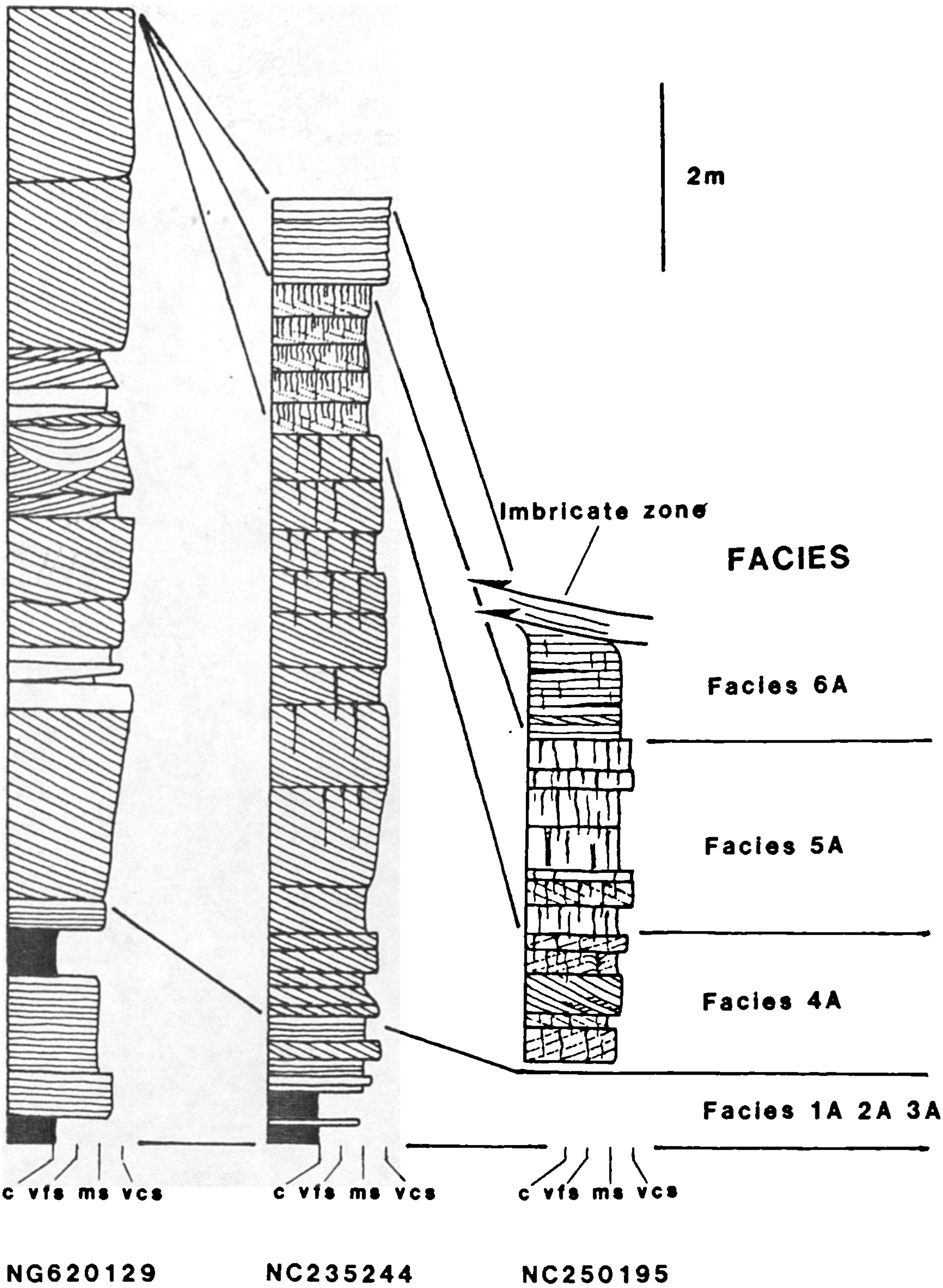

Fig. 5.6 Representative logs showing the changes in the proportion of each facies of association A along outcrop.

Fig. 5.7 Tracing of the Skiag Bridge section showing the inclined bounding surfaces and the cross-bedding orientations with respect to them.

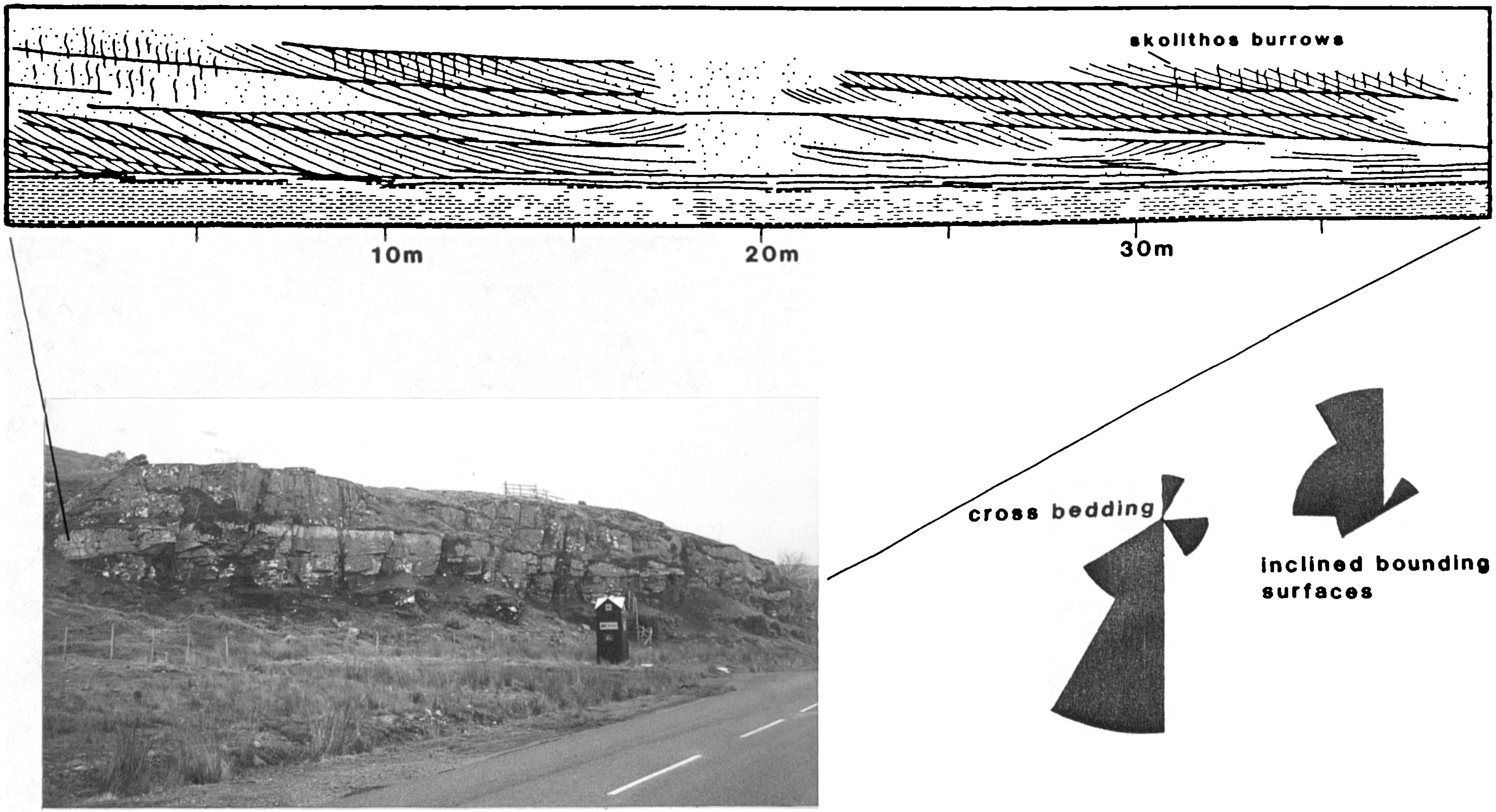

Fig. 5.8 Burrowed sands of facies 5A resting on a truncated Fucoid Beds sequence of facies F muds and silts (southeast slope of Beinn nam Ban, NG 117 883). Contact is not a thrust plane. Hammer 30cm long.

dip of the bounding surfaces.

Where facies 5A and 6A occur overlying facies 4A these facies have a barely perceptable dip, too low to derive an accurate vector mean with respect to the other facies. Sequences consisting entirely of facies 5A and 6A have no perceptable dip. These sequences frequently rest on a truncated Fucoid Beds sequence where the proximal facies A and B, normally found at the top of the Fucoid Beds, are absent (Fig. 5.8).

5.2.4 Interpretation of association A

The coarsening upwards sequences, kilometre-scale lateral facies changes and faunal content suggests that this association was deposited by a very large migrating marine bedform. The relationship of the foreset orientations to the inclined bounding surfaces is typical of linear shelf sandbanks or sandridges produced by tide or storm induced flows (Hobday and Reading 1972, Hobday and Tankard 1978, Johnson 1977). As will be shown in facies association B a tidal sandbank origin is the most likely interpretation for this association, although the contribution of wind enhanced currents to bedform migration may have been significant (Lees 1983).

The gently inclined surfaces in association A may be analogous to the gently dipping reflectors observed in sparker profiles of recent sandbanks (Houbolt 1968, Lapierre 1975, Yang and Sun 1985) and observed in the linear sandbodies of the North American Cretaceous (Boyles and Scott 1982). Within the context of laterally migrating sandbanks the basal muds and silts of facies 1A represent the fine sediment occurring between the banks and over which they migrated. Facies 2A was probably deposited by migrating ripples at the fringes of the sandbanks. The parallel laminated sands of facies 3A are similar to the parallel laminated and wave rippled sands of the Eriboll Sandstone and Fucoid Beds and were probably deposited by waning storm currents or storm enhanced tidal currents. These beds were probably reworked by fairweather tidal currents higher up on the sandbanks and were only preserved on the fringes and between banks. Facies 4A represents the migration of large dunes or sandwaves along and up the prograding steep slope of the sandbanks and probably reflect migration under the subordinate tidal current (Kenyon et al. 1981, McCave and Langhorne 1982). Palaeocurrents are mostly unidirectional due to the segregation of the opposing tidal streams by the sandbanks (Caston and Stride 1970) and by reworking by subordinate current bedforms. The dominant tidal current also reworked subordinate tidal bedforms to produce reactivation surfaces. Although tides were probably the dominant control on bedform migration, the absence of any periodicity in foreset thickness or reactivation surface spacing suggests that sand transport only took place during spring tides or wind enhanced tides. Periodically the bank slopes were colonised by suspension feeding organisms. The variable distribution and mutually exclusive nature of the large and small Skolithos burrows suggests that several different species of annelid formed patch-like colonies on the bank slopes. This increase in faunal diversity and decrease in population (compared with the Pipe Rock) follows the pattern outlined by Brasier (1982) for evolving communities.

The channel found in facies 4A is oriented parallel to the direction of dip of the inclined surfaces and was probably produced by storm induced currents accelerating across the the shallower water of the sandbank. The resultant storm scoured channel was infilled laterally by along-bank migrating ripples and dunes. During infill the channel appears to have been a favourable site for annelid colonisation, perhaps because it afforded some shelter from strong tidal currents. Similar storm induced channels were inferred for the Sussex Sandstone of Wyoming (Brenner and Davies 1974) and although later refuted (Brenner et al. 1985) the mechanism remains valid.

Facies 5A represents a transition to lower energy conditions resulting in thinner sets, finer grain sizes and greater colonisation by suspension feeders. The reduced dips of the bounding surfaces in this facies and inferred lower energy conditions may be analogous to the deposits of moribund sandbanks of the Celtic Sea (Stride et al. 1982) and East China Sea (Yang and Sun 1985) which were active when sea level was lower than at present and tides were correspondingly stronger (Belderson et al. 1986). These moribund banks are characterised by greatly reduced slopes, reduced height, finer grain sizes and an increased proportion of shelly debris (Bouyse et al. 1976, Kenyon et al. 1981). The reduced bank height is a result of storm erosion of the crest and the inability of the weaker tides to restore bank height.

The thick Salterella Grit sequences without facies 5A and 6A probably represent the bank crests where sediment was eroded during this moribund stage of development. These sequences may be traced perpendicular to the facies 4A palaeocurrent direction and pass into thinner sequences with facies 5A and 6A within 0.5-3.0km. These thinner sequences represent the bank flanks where crest derived sediment was deposited by storms or storm enhanced tides. Thin sequences consisting of facies 5A resting on the Fucoid Beds directly represent deposition of moribund bank sands as drapes extending off the active banks into the "channels" between them. The presence of collophane cemented siltstone clasts and phosphatised and abraded shell debris of Fucoid Beds affinities in the active bank facies suggests that erosion of the Fucoid Beds took place. This is also implied by the similarity in acritarch faunas for these two members (Downie 1981) in spite of the extreme differences in environment. The presence of moribund bank facies lying directly on truncated Fucoid Beds sequences suggests that this erosion took place as scouring between the active banks; probably to a depth of several metres. Such erosion was noted by Off (1963) as depressions between banks in the Gulf of Korea.

Facies 6A represents a progression from facies 5A to conditions of even weaker tidal currents as shown by the increased bioturbation, thinner, ripple laminated sets and appearance of thin muds. The presence of oriented Salterella concentrated at the base of graded beds suggests that storms were the main depositional agent with fairweather processes restricted to bioturbation by infauna and colonisation by Salterella. Storm currents, as indicated by Salterella alignment (section 5.6), may have been directed offshore and across the moribund banks and were probably downwelling gradient currents induced by coastal set-up (Allen 1982). The presence of pelletal glauconite indicates that fairweather sedimentation was negligible.

Facies 6A therefore represents the final moribund stage in the bank evolution before burial under the carbonate sediments of the Ghrudaidh Member. The sedimentology, fauna and authigenic minerals suggests that this facies represents a return to conditions not unlike those responsible for the proximal facies A and B of the Fucoid Beds. The development of the Salterella Grit banks is summarised in Fig. 5.9.

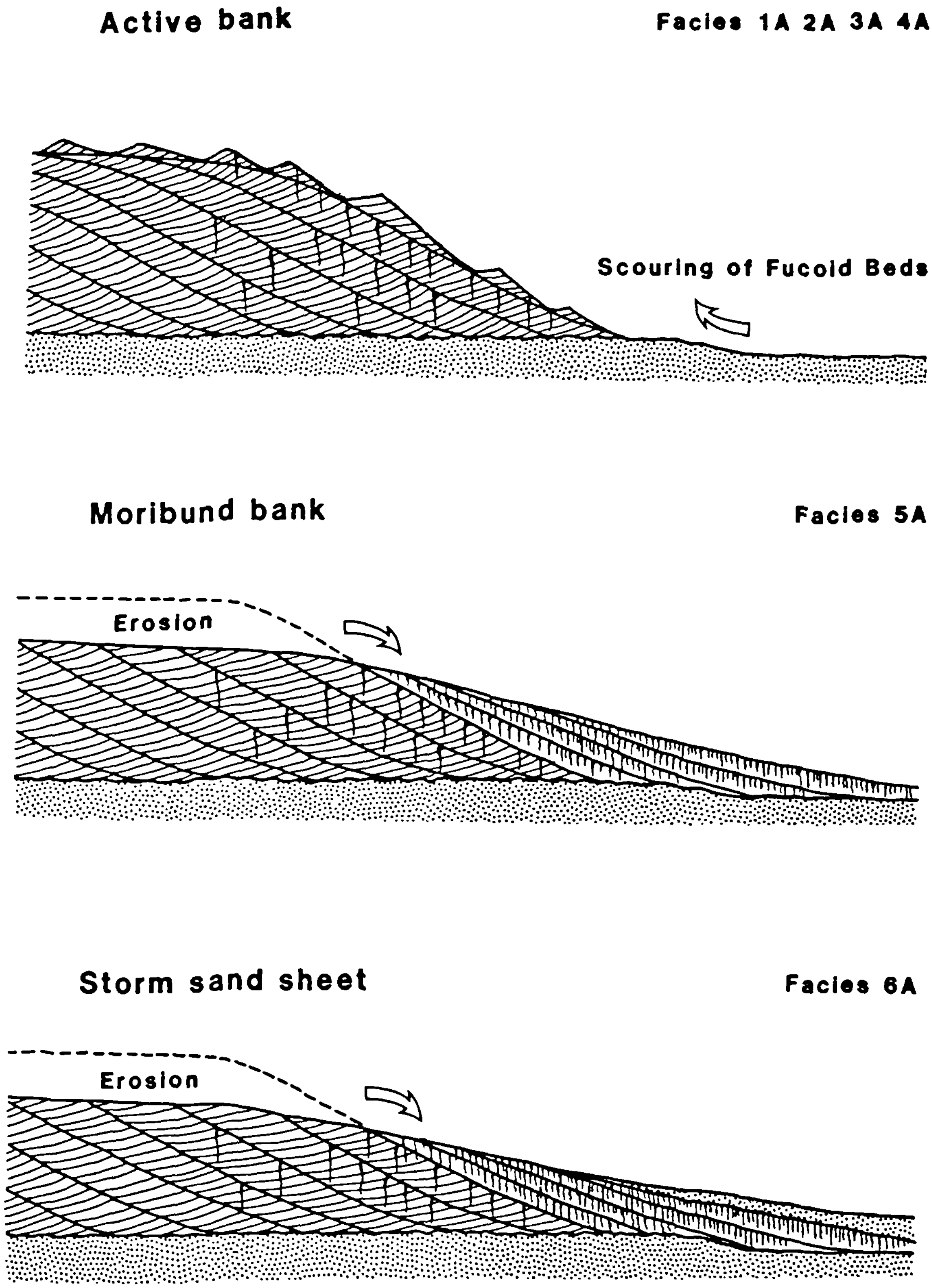

Fig. 5.9 Summary diagram of Salterella Grit bank evolution in cross-section.

Facies	Typical log	Grain size	Coset/set thickness	Coset/set length	Internal structure	Set surfaces	Other features	Interpretation
6A	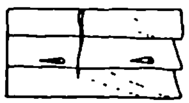	FS-MS	Sets 5 10cm cosets imbricated	10m	Vague ripple lamination, bioturbated	Planar, erosive	Shell lags common, <u>Skolithos</u> present	Storm sandsheet
4B	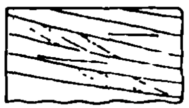	MS-CS	Cosets 2m sets 5 20cm thick	5m	Sets dip at up to 10°. Bioturbated	Planar, erosive	Vague tabular cross bedding	Small sandwaves on bank apron
3B		VFS MS	Up to 3cm	Few metres	Parallel lamination	Planar, erosive		Tempestite beds deposited by combined currents
2B		VFS-MS	Sets 1-10cm	Few metres	Tabular cross lamination	Planar, erosive	Palaeocurrents bimodal, diverse fauna	Rippled sands of bank apron
1B		Mud	0.5-15cm	20m	Burrowed	Planar, non-erosive	Horizontal beds or draping foresets. <u>Planolites</u> present	Interbank muds

Table 5.2

5.3 FACIES ASSOCIATION B

5.3.1 Introduction

This facies association is less common than association A. There is no obvious arrangement of facies and there is a greater proportion of muds, thinner bedding and a greater faunal diversity. The facies for this association are summarised in table 5.2.

5.3.2 Facies descriptions

Facies 1B: Thin muds

Mud beds range from 0.5-15cm in thickness (Fig. 5.10). Thicker beds may be traced laterally over several tens of metres but thinner beds are discontinuous over a scale of a few metres. This facies is generally burrowed, with sand filled Planolites burrows frequently present in thinner beds.

Facies 2B: Cross-laminated quartzarenites

Beds of this facies range in thickness from 1-10cm and consist of very fine to medium sand. The cross-laminations are tabular in form, dip at fifteen to twenty degrees and are generally less than 0.5cm in thickness, although rare examples may be up to 1cm thick. Pelletal collophane and collophane replaced shell debris is occasionally concentrated along foresets. Palaeocurrents are bimodal (section 5.6). This facies is often bioturbated and may contain abundant Skolithos (Fig. 5.11a), Planolites and occasionally Aulichnites on bed tops or low angle foresets. Rusophycus is rarely present on bed soles (Fig. 5.11b). Salterella is sparsely distributed along with rare shell valves of unknown origin. Beds may be traced laterally over several metres before being truncated by convex-up reactivation surfaces. Discontinuous drapes of facies 1B muds or fine silts occur on reactivation surfaces or on foresets.

Fig. 5.10 Interbedded facies 1B muds and 2B sands, Loch Dubh, NH 150 995. Lens cap 5cm wide.

Fig. 5.11a Skolithos burrows in facies 2B sands, Loch Dubh, NH 150 995. Lens cap 5cm wide.

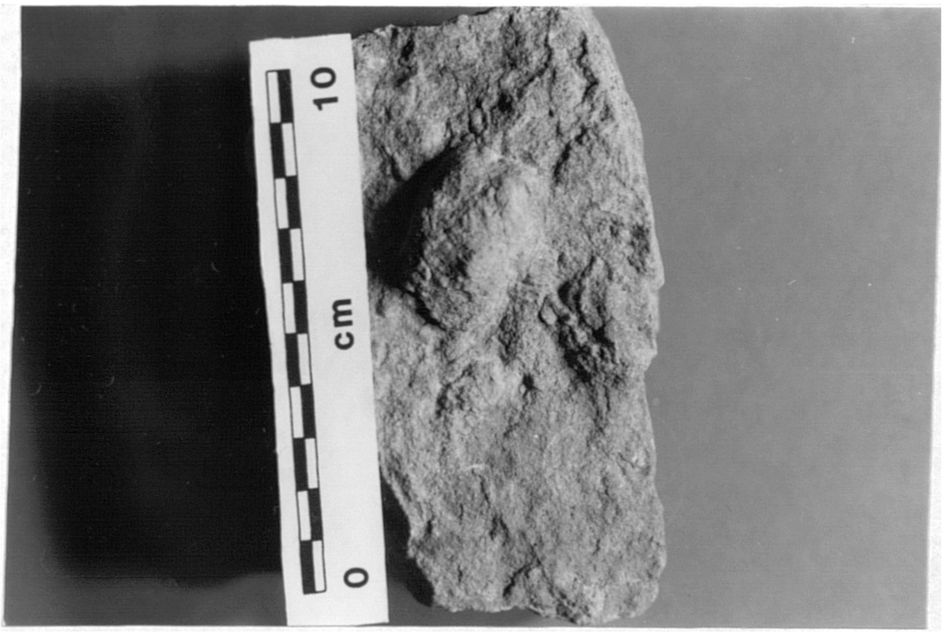

Fig. 5.11b Rusophycus from facies 2B (Loch Dubh).

Facies 3B: Parallel laminated sands

This facies is relatively uncommon. Beds may be up to 3cm thick and consist of graded medium to fine sand which is parallel laminated on a millimetre scale. These beds are discontinuous on a metre scale due to truncation by the erosive bases of facies 2B sets.

Facies 4B: Compound cosets

This facies was only observed at Loch Dubh (NH 151 996). It consists of cosets up to 2m thick comprising inclined sets 5-20cm thick dipping at approximately ten degrees and composed of strongly bioturbated medium to coarse sand (Fig. 5.12). Occasionally vague down-dip oriented ripple laminations are visible. Surfaces with dips of 0-20 degrees are occasionally present defining the inclined sets and are dipping in the same direction.

Facies 6A: Fossiliferous quartzarenites

Within association B this facies consists of beds 5-10cm in thickness, composed of vaguely cross-laminated fine to medium sand. <u>Salterella</u> is abundant and <u>Skolithos</u> is present.

5.3.3 <u>Facies arrangement</u>

Association B appears to take two forms; form 1 (Fig. 5.13a) with abundant facies 1B muds (up to 20% of the vertical sequence) in which sands are grouped into "packages" up to 100cm thick, and form 2 (Fig. 5.13b) in which muds are generally sparse. Facies 2B is the most abundant facies in association B. Facies 3B and 4B are too rare for any pattern in distribution to be deduced. Facies 6A only occurs at the tops of sequences.

5.3.4 <u>Interpretation of association B</u>

The absence of coarsening upwards cycles, major inclined surfaces and large scale cross-bedding suggests that this association was not produced by the migration of a large scale bedform.

Fig. 5.12 Compound coset showing gently dipping sets, Loch Dubh, NH 150 995. Scale is 1m long.

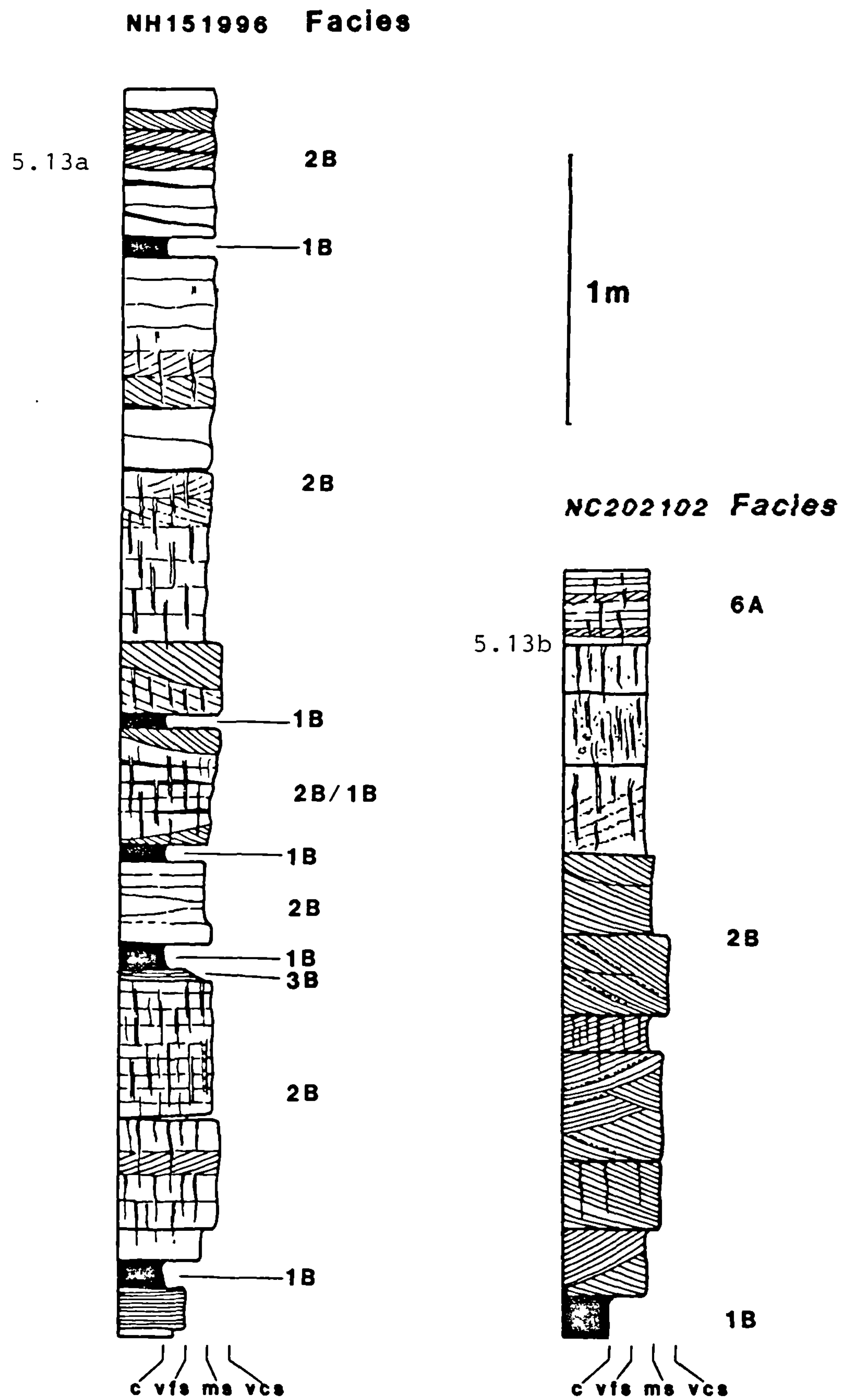

Fig. 5.13 Representative logs of Association B

Association B passes, in an up or down palaeocurrent direction with respect to the bank facies, into association A within 3-15km suggesting that this association represents a bank apron (Caston 1981) facies rather than an interbank facies (see facies 1A).

Facies 2B represents the migration of ripples and small dunes on the bank apron. A tidal origin for this facies is indicated by the well developed bimodal palaeocurrents, reactivation surfaces and mud and silt foreset drapes. The increased faunal diversity indicates that bedform migration was less frequent due to the expanded flows being weaker off the main bank sequence. The facies 1B muds probably represent the interbank shelf mud blanket described in association A. The "packaging" of facies 2B apron sands within these shelf muds may indicate that in some cases the bank apron expanded and contracted, possibly in a manner similar to that suggested for the Leman and Ower Banks (Caston 1972) and Haisborough Sand (McCave and Langhorne 1982) where the bank aprons may have extended over a time scale of several decades. Alternatively, muddy association B sequences may simply be more distal apron deposits than the less muddy sequences. The closest bank apron sequence to a main bank sequence is one of the muddiest observed suggesting that the former alternative is more likely. The parallel laminated sands of facies 3B were deposited under higher energy conditions; possibly by storms, large spring tides or wind enhanced tides. Fairweather reworking was extensive, resulting in a low preservation potential. The large cosets of facies 4B, with down-dip oriented cross-laminations, were probably deposited by small asymmetric sandwaves. Facies 6A was again probably deposited by storms during the final moribund stage in bank evolution, indicating that this storm sand sheet facies extended in all directions off the sandbanks.

The thick apron sequence in Fig. 5.13a rests on the facies F muds of the Fucoid Beds, indicating that erosion and channeling took place occasionally at the ends of banks as well as between them. Such channeling has been observed at both the head and tail of North Sea banks (Robinson 1966). The subsequent infill of these channels would contribute to the greater thickness of some apron sequences.

Facies	Typical log	Grain size	Coset/set thickness	Coset/set length	Internal structure	Set surfaces	Other features	Interpretation
6A	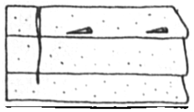	FS-CS	Cosets 1m sets 5-10cm	10m	Bioturbated	Planar, erosive	Shell lags common *Skolithos* present	Storm sand sheet
2C		Mud	2cm	20m		Planar, non-erosive		Storm suspended muds deposited on end of bank
1C		MS-CS	5-25cm	20m	Tabular cross bedding	Planar, erosive dipping at up to 4°	Palaeocurrents bimodal, along and down set surfaces	Dunes or sandwaves on end of tidal sandbank

Table 5.3

5.4 FACIES ASSOCIATION C

5.4.1 Introduction

This association was only observed in one locality (NH 148 959) forming a 5m thick sequence. Facies for this association are summarised in table 5.3.

5.4.2 Facies descriptions

Facies 1C: Cross-bedded quartzarenites

This facies forms the bulk of association C. Beds range from 5-25cm in thickness and consist of medium to coarse sand with rare very coarse sand beds. Foresets are tabular, less than 0.5cm thick and range from 20-25 degrees in dip. Collophane pellets and shell fragments are occasionally concentrated along foresets. Occasionally bed tops show symmetrical wave rippling. Skolithos burrows are common, with burrows ranging from large forms up to 1cm in diameter and tens of centimetres long to small burrows a few millimetres in diameter and a few centimetres long (Fig. 5.14a), but are rarely dense enough to obscure the cross-bedding. Beds without Skolithos are generally concentrated in the basal 2m but may extend up to 4m above the base of the sequence.

Facies 2C: Thin muds

Muds are sparse in this association. Beds may be up to 2cm thick, occur at the base of the sequence and sporadically between facies 1C as discontinuous drapes.

Facies 6A: Fossiliferous quartzarenites

Within this association facies 6A consists of up to 1m of 5-10cm beds of poorly sorted fine to coarse sand, frequently with a winnowed lag of aligned Salterella at the base. Bioturbation is intense, but with occasional Skolithos burrows present (Fig. 5.14b).

Fig. 5.14a Facies 1C cross-bedded quartzarenite set with small <u>Skolithos</u> burrows, Ullapool River, NH 148 958. Lens cap 5cm wide.

Fig. 5.14b Facies 6A sands. Note <u>Skolithos</u> burrow and abundant <u>Salterella</u>, Ullapool River, NH 148 958.

5.4.3 Facies distribution

Association C consists almost entirely of facies 1C. As with association A, sets are enclosed by very gently inclined bounding surfaces although maximum dips in this association are three degrees. Unlike association A the cross-bedding shows modes directed both up and down as well as along the inclined bounding surfaces (Fig. 5.15). Facies 6A occurs in the uppermost metre of the sequence and is horizontally bedded.

5.4.4 Interpretation of association C

Association C occurs a few kilometres "downstream" of an association B bank apron facies. This relationship, the decreased mud content and presence of inclined bounding surfaces, but with smaller sets than association A, suggests that this association was deposited near the end of a tidal sandbank. The smaller bedforms and increased burrowing, relative to association A, indicates flow deceleration off the main bank sequence but still with greater velocity than the bank apron facies. Wave rippled set tops indicate possible storm wave reworking of the bank slopes.

As with association A there is a palaeocurrent mode directed along the bank axis (as defined by the inclined bounding surfaces), but unlike association A there is a second mode directed down the bank slope and possibly a minor mode directed up this slope. The along-bank mode probably reflects the subordinate tide and, because it is only a few kilometres "downstream" of a bank apron facies, it has experienced little deflection towards the bank crest due to acceleration of the cross-bank component of flow (Caston 1972, Huthnance 1982). The down dip palaeocurrent mode may have been the result of the dominant tide. Since this tide has already traversed the bank axis it is very strongly deflected in a direction perpendicular to the bank crest. Consequently when this component of flow crosses the bank crest it produces sandwaves oriented down the steep bank slope (Fig. 5.15). This style of palaeocurrent pattern does not occur in association A which may imply that the dominant

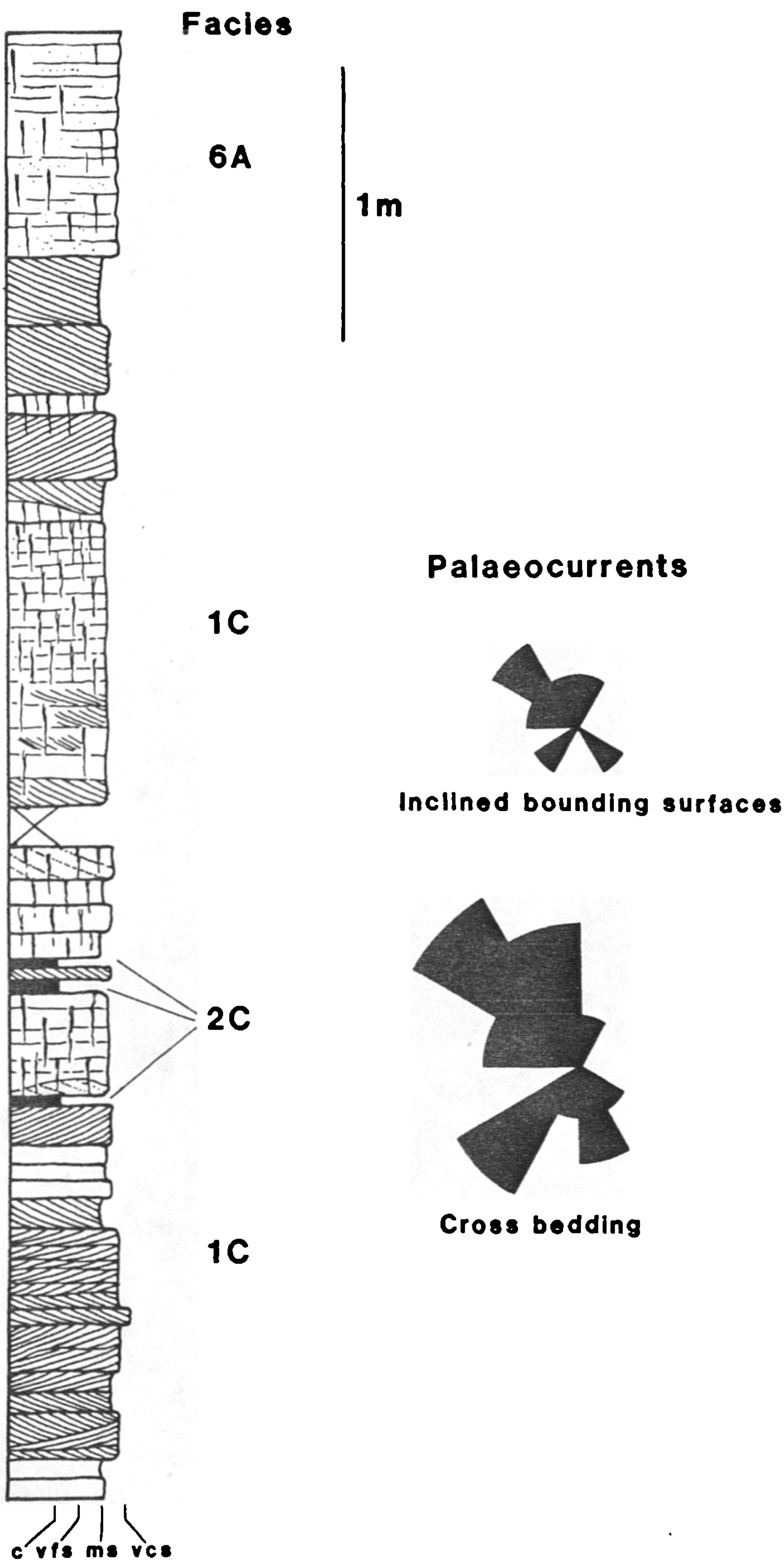

Fig. 5.15 Vertical sequence of association C and relationship of cross-bedding to inclined bounding surfaces.

tide occured during low water, in which case it would have been unable to cross the the bank except at the lower head and tail. The possible minor mode directed up-dip may reflect slight crestal veering of sandwaves produced by the subordinate tide.

As with association A there is a vertical increase in burrowing either reflecting decreasing tidal current velocities or migration of the bank away from this locality. Facies 6A was deposited by very weak tidal currents or storm currents. This facies forms part of the ubiquitous storm sand sheet facies occurring within all bank facies sequences with the exception of the bank crest. The Salterella Grit bank depositional system is summarised in Fig. 5.16.

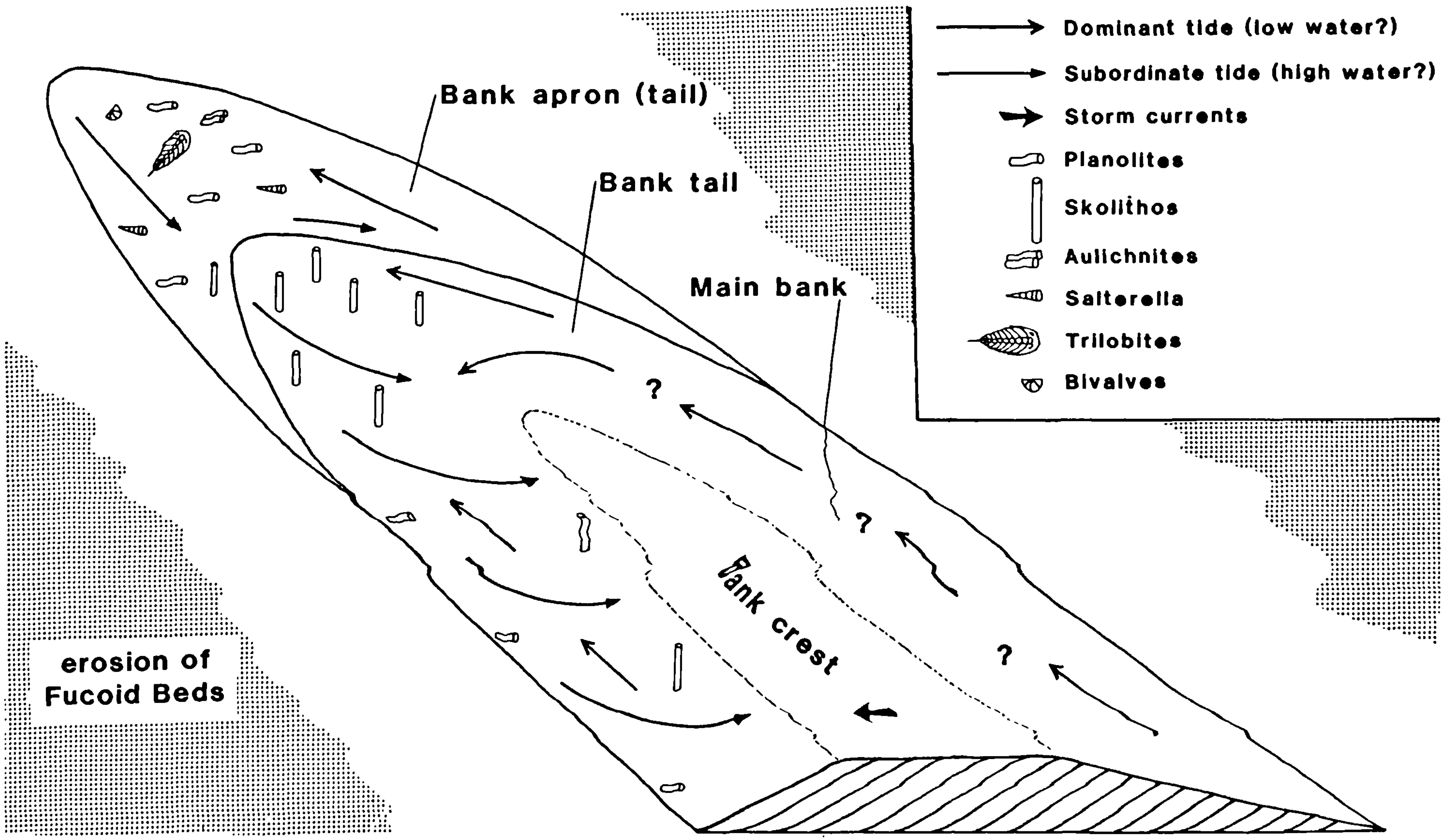

Fig. 5.16 Summary diagram of the Saltcrella Grit bank depositional system.

Facies	Typical log	Grain size	Coset/set thickness	Coset/set length	Internal structure	Set surfaces	Other features	Interpretation
6A	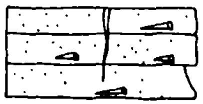	FS-VCS	Cosets 2m sets up to 20cm thick	30m	Bioturbated	Planar, erosional	Rare Skolithos	Proximal storm sandsheet
3D	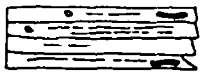	MS-CS	Cosets 15cm sets 1-10cm thick	20m	Vague parallel lamination	Planar, erosional	Burrowed. Planolites, Aulichnites	Sandwave trough facies
2D	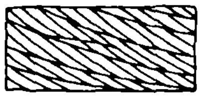	MS-CS	Cosets 2m sets 8-40cm thick	20m	Sets dip at 10-15°	Planar, erosional	Sets tabular cross bedded. Skolithos present	Small sandwaves forming tidal sandsheet
1D		Mud	50cm	20m	Burrowed	Planar	Planolites present	Northern part of early bank mud sheet

Table 5.4

5.5 FACIES ASSOCIATION D

5.5.1 Introduction

This facies association is restricted to the northernmost outcrops at Loch Eriboll and Durness. This association is poorly exposed and is disturbed by thrusting but is approximately 6m thick. The facies for this association are summarised in table 5.4.

5.2.2 Facies descriptions

Facies 1D: Thin muds

The transition from the Fucoid Beds to the Salterella Grit is marked by up to 50cm of fissile green mudstone with accessory quantities of very fine quartz grains. Planolites burrows and vertical burrows deflecting laminations are present.

Facies 2D: Compound cosets

This facies consists of cosets up to 2m thick composed of sets 8-40 cm thick defined by inclined bounding surfaces which dip at ten to fifteen degrees. Sets consist of tabular cross-bedded medium to coarse, rounded to subangular quartz sand with occasional clasts of collophane cemented siltstone. Foresets are generally less than 0.5cm thick, have both angular and tangential bottomsets and are oriented down the inclined bounding surfaces. the cross-bedding is enclosed by horizontal to subhorizontal bounding surfaces enclosed by the dipping surfaces. Convex-up reactivation surfaces occasionally truncate the cross-bedding. Skolithos is present and may be dense enough to obscure the other structures.

Facies 3D: Burrowed sands

This facies consists of up to 15cm of 1-10cm thick beds of medium to coarse sand. Beds are generally bioturbated, although vague parallel laminations are occasionally visible. Planolites burrows are common and Aulichnites (Fig. 5.18) is occasionally visible on

Fig. 5.17 Compound coset of facies 2D. Cross-bedding obscured by abundant *Skolithos*. Note thrust plane in bottom right of photograph. An t-Sròn, NC 440 581. Scale 1m.

Fig. 5.18a Aulichnites from facies 3D, An t-Sròn, NC 440 581.

Fig. 5.18b Pelletal collophane and collophane cemented siltstone clasts, An t-Sròn. Field of view 2.78mm wide.

Fig. 5.18c Phosphatic pellet containg acritarch tests, An t-Sròn. Field of view 2.78mm wide.


0
cm
10

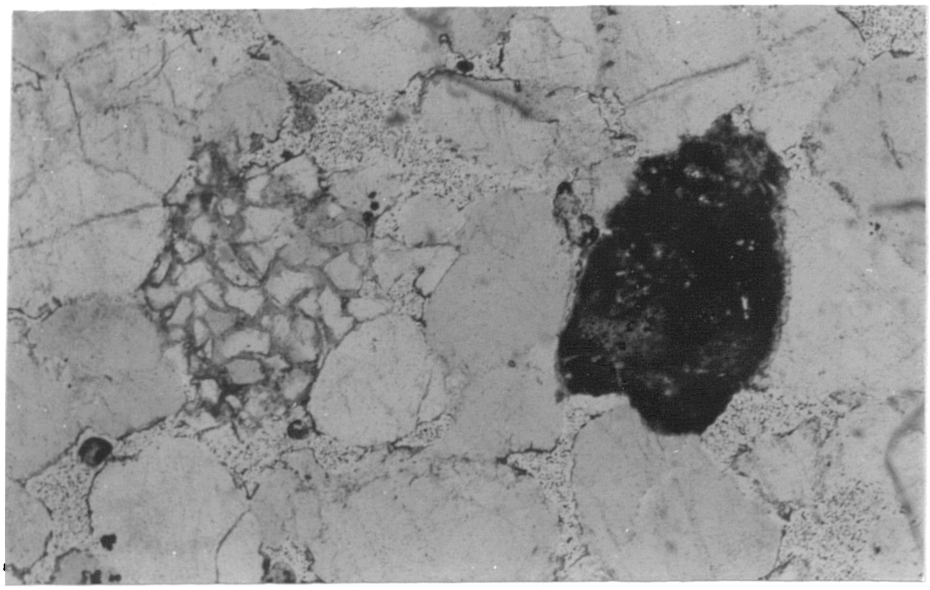

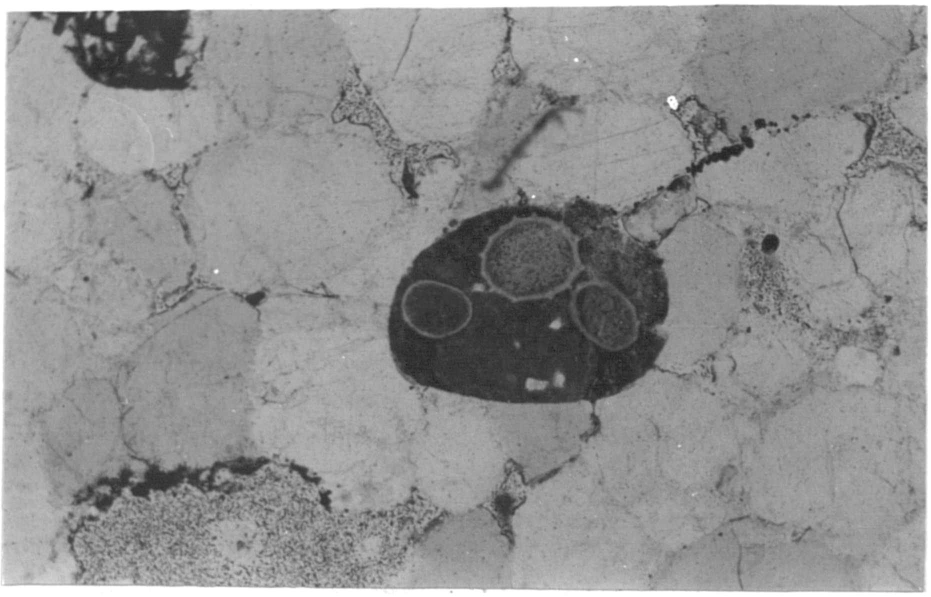

bed tops. These beds are composed predominantly of rounded quartz grains with rare clasts of pelletal collophane (in one instance containing acritarch tests-Fig. 5.18) and abraded, collophane replaced, echinoderm and trilobite fragments (Fig. 5.18).

Facies 6A: Fossiliferous quartzarenites

Within association D this facies consists of up to 2m of 20cm thick beds of graded or ungraded fine to very coarse sand. The base of beds frequently contains a lag of oriented Salterella tests (Fig. 5.19). Clasts consist of well rounded quartz grains, although smaller grain sizes tend to be more angular. Occasional collophane pellets and collophane cemented siltstone clasts are present. Well rounded pellets of microcrystalline glauconite are present in some beds. Beds are generally bioturbated, with framboidal pyrite associated with burrowing. Skolithos burrows are rare.

5.5.3 Facies distribution

The muds of facies 1D occur only at the base of association D. The bulk of the sequence consists of facies 2D cosets interbedded with facies 3D. Cosets are unburrowed at the base of the sequence and have the most dense bioturbation at the top (Fig. 5.20). Facies 6A forms the top of the succession. This association rests on the thickest, most complete Fucoid Beds succession.

5.5.4 Interpretation of association D

The muds of facies 1D correlate with the basal muddy facies of associations A,B and C indicating that at the beginning of Salterella Grit deposition the shelf on which the tidal sandbanks were initiated was covered with a thin mud blanket.

Facies 2D is similar to the theoretical Type IV and V sandwaves of Allen (1980) and those of the Precambrian of northern Norway (Levell 1980). The inclined surfaces may have been produced by erosion during the subordinate tide, storm erosion or by erosion in the lee of the descending dunes and ripples. Current reversals are

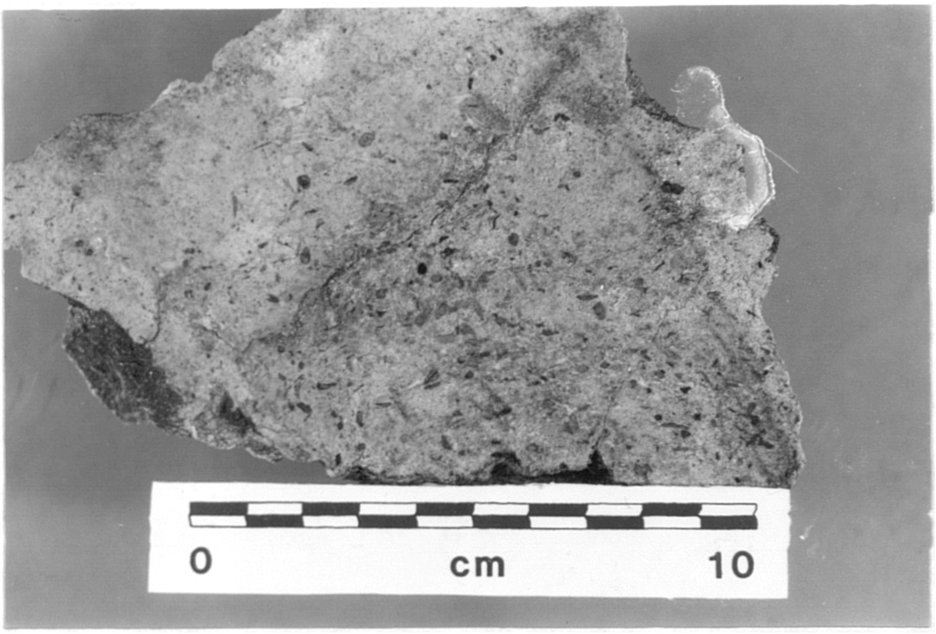

Fig. 5.19 Slab of a facies 6A bed showing a lag of Salterella. An t-Sròn, NC 440 581.

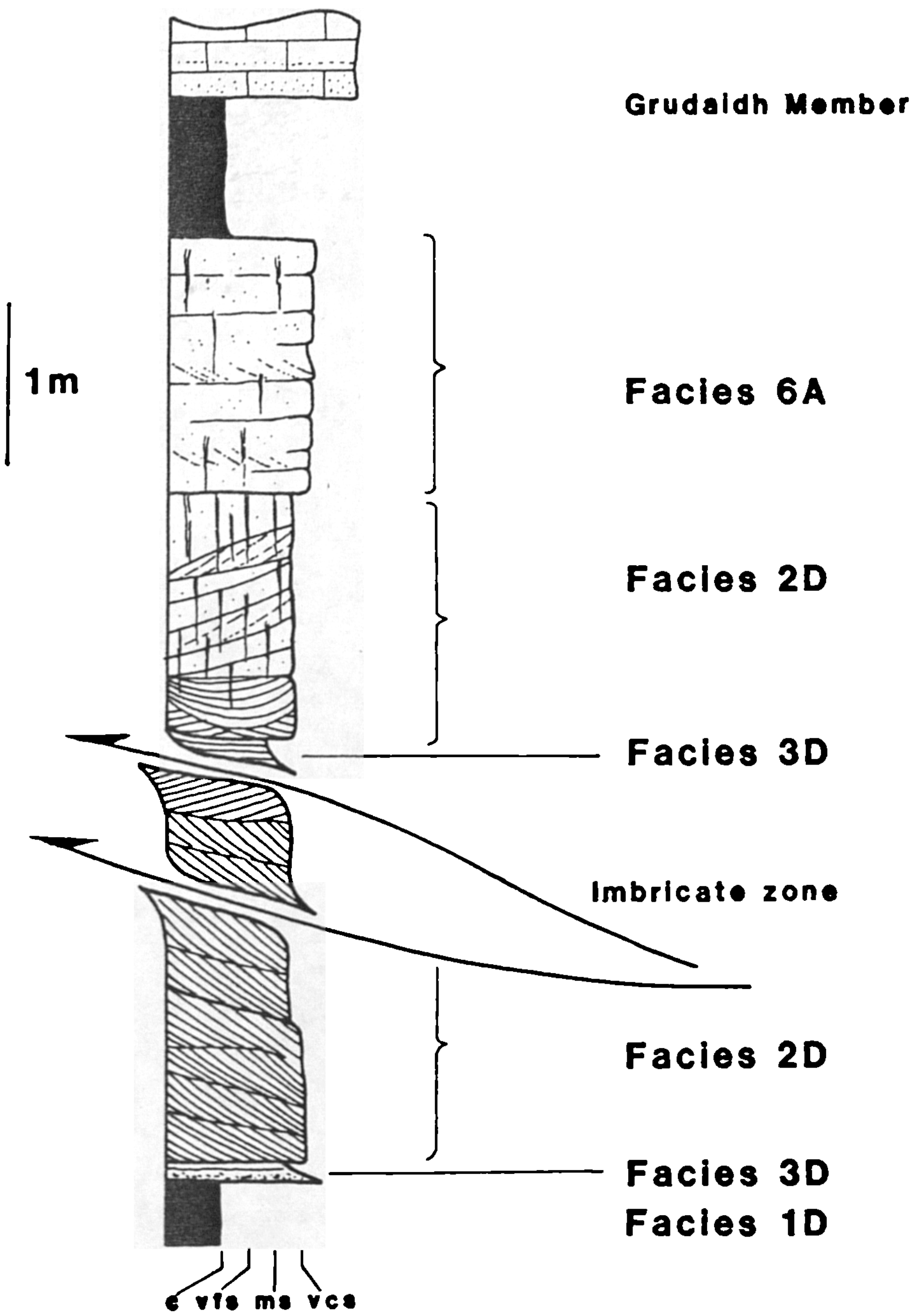

Fig. 5.20 Log of the An t-Sròn section showing the typical facies distribution for the Durness-Loch Eriboll area.

probably indicated by the convex-up reactivation surfaces. The general lack of opposed cross-bedded sets indicates a pronounced velocity asymmetry to the tidal currents producing this facies.

The finer, horizontally bedded and burrowed, sands of facies 3D were probably deposited in the troughs between sandwaves where the currents were comparatively weaker. As with facies associations A,B and C, the collophane cemented siltstone clasts and abraded shelly material indicates reworking of the Fucoid Beds although the lack of obvious erosion and truncation of the underlying Fucoid Beds sequence indicates either transport of this material from the bank facies, or more laterally restricted channeling not exposed in this area. Facies 2D and 3D indicate that a sandsheet developed in the north, in contrast to the bank facies associations which always migrated over a muddy shelf.

Again the presence of graded beds and lags of oriented Salterella indicate in facies 6A a more storm influenced environment although the overall greater thickness of this facies and greater thickness of individual beds indicates that facies 6A in this association may be the most proximal example within the Salterella Grit sequence. The proximality of this facies and the relative thinness of association D and general lack of mud suggests that this northern area remained closest to the shoreline throughout Salterella Grit deposition; which may also have been the case during Fucoid Beds deposition.

The vertical sequence of this association from cross-bedded cosets to cosets with abundant Skolithos to a storm dominated sandsheet facies is reminiscent of the facies progression in associations A,B and C of active bank facies to moribund bank facies to storm sandsheet facies. The Salterella Grit therefore appears to have been the product of strong tidal currents initiated during the regression noted at the top of the Fucoid Beds. The shelf subsequently appears to have undergone a progressive decrease in tidal current velocities, probably due to deepening and widening of the shelf, resulting in banks becoming moribund, increased colonisation of bedforms and eventually a return to a storm dominated environment not unlike the more proximal facies of the Fucoid Beds.

Although the Ghrudaidh Member is essentially a carbonate depositional environment, the base of this sequence appears to be an extension of this storm dominated shelf as suggested by the presence of thin, laterally persistant beds with rip-up clasts (Sepkoski 1982) and a *Salterella* fauna (Fig. 5.21).

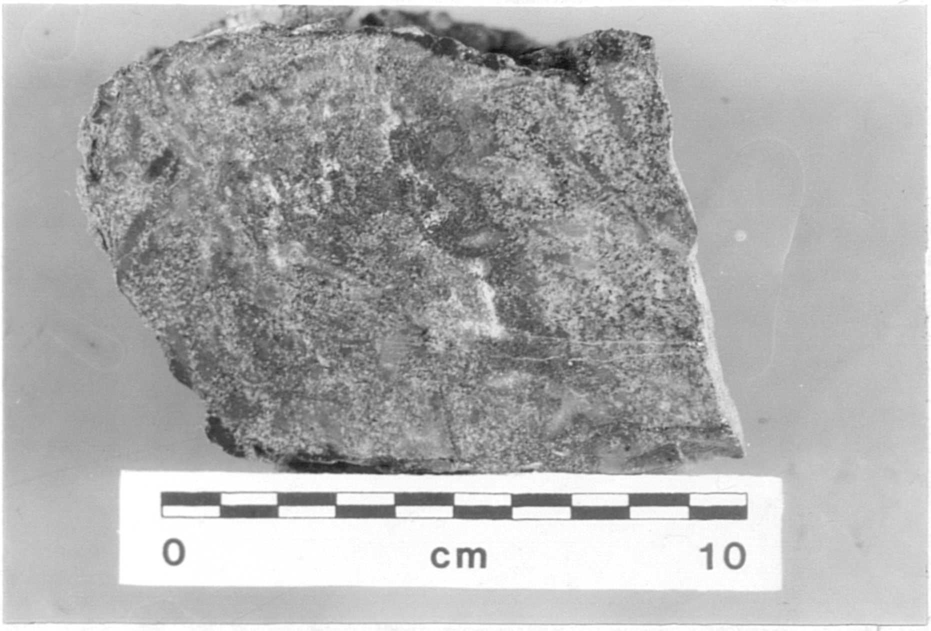

Fig. 5.21 Slab from the basal 5m of the Grudaidh Member showing rip-up clasts, An t-Sròn, NC 440 581.

5.6 REGIONAL PALAEOCURRENTS

Palaeocurrent roses for associations A,B,C and D are presented in Fig. 5.22. The sandwave facies in the north shows a crude easterly mode. Southwards, and further further away from the palaeoshoreline, the bank facies palaeocurrents and master bedding orientations (Associations A and C) indicate a southwest to southerly orientation to the banks as far south as Ullapool. Further south the banks show a more easterly orientation. Kenyon et al. (1981) and McCave and Langhorne (1982) have suggested that the cross-bedding preserved within tidal sandbanks will reflect the subordinate tide, therefore the regional sand transport direction preserved will be opposite to that indicated by the palaeocurrents. Reversing the palaeocurrents for associations A and C allows a regional sand transport direction to be deduced which is consistent for both the bank facies in the south and the sandwave facies in the north and indicates a dominant tide transporting sand northwards and eastwards.

This pattern is departed from in the vicinity of Cnoc Daimh where the palaeocurrent pattern is opposite to the regional one. This may be due to a bed load parting in this area where the local tidal asymmetry was reversed. Association B bank apron palaeocurrents indicate currents flowing along and across the apron, with the bimodal pattern a result of exposure to both tidal streams.

The alignment of Salterella (using the criteria of Futterer (1978) for conical shells) in the storm sandsheet facies indicates possible offshore directed currents for facies 6A in response to downwelling storm induced gradient currents.

5.7 OUTCROP DISTRIBUTION

South of Ullapool, where the palaeocurrents suggest that the banks were aligned roughly in an east-west direction perpendicular to the Moine Thrust, the pattern of outcrop of the Salterella Grit changes from being nearly continuous to one of isolated lenses (Fig. 5.23). The upper contact of these lenses is defined by thrust planes,

Cross bedding
Association A,C

Inclined bounding surfaces
Association A,C

Cross bedding Association B

Cross bedding Association D

Salterella alignment

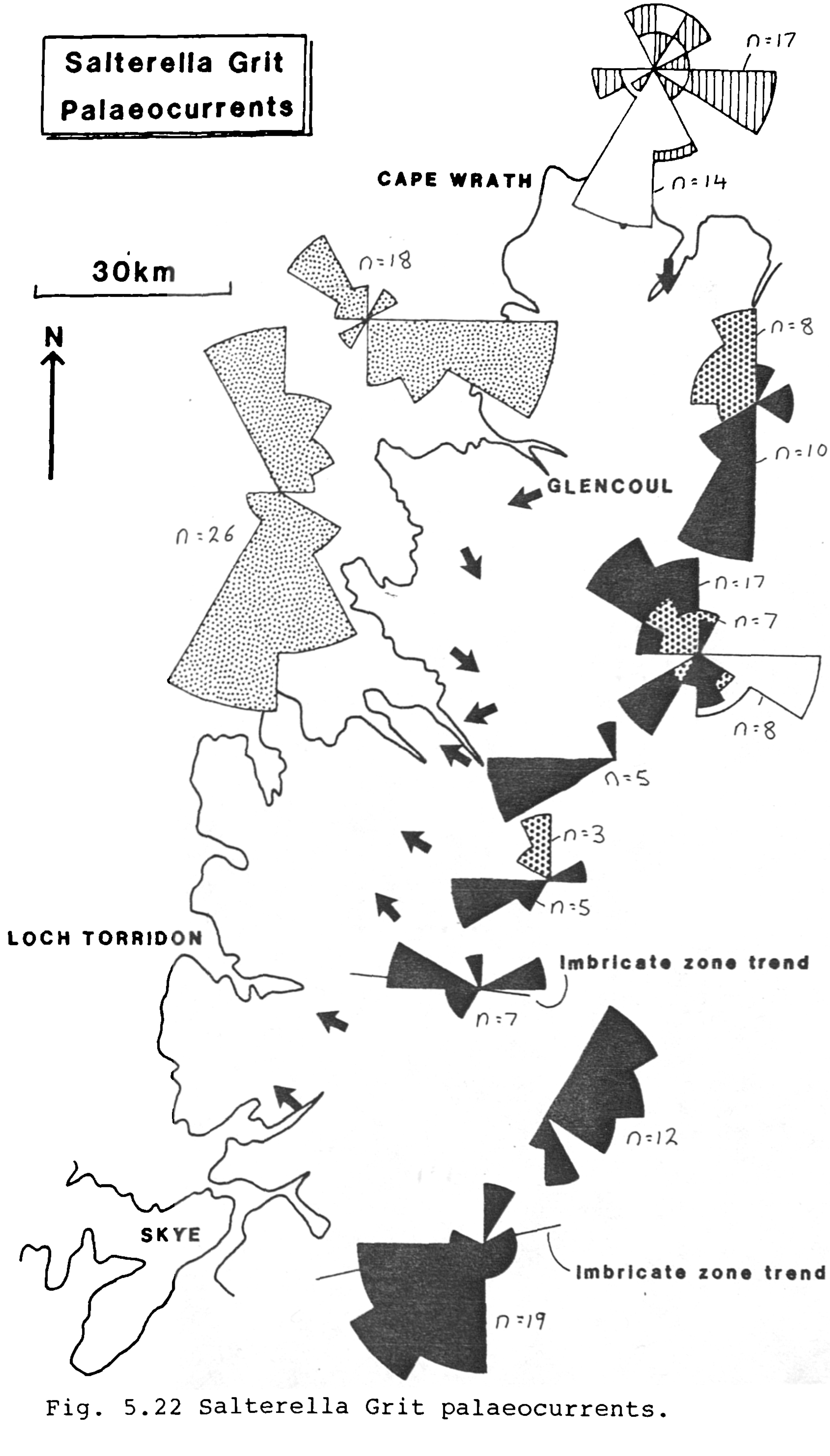

Fig. 5.22 Salterella Grit palaeocurrents.

Fig. 5.23 Outcrop distribution of the Salterella Grit between Little Loch Broom and Kishorn. The Salterella Grit is in black with the rest of the Cambro-Ordovician stippled.

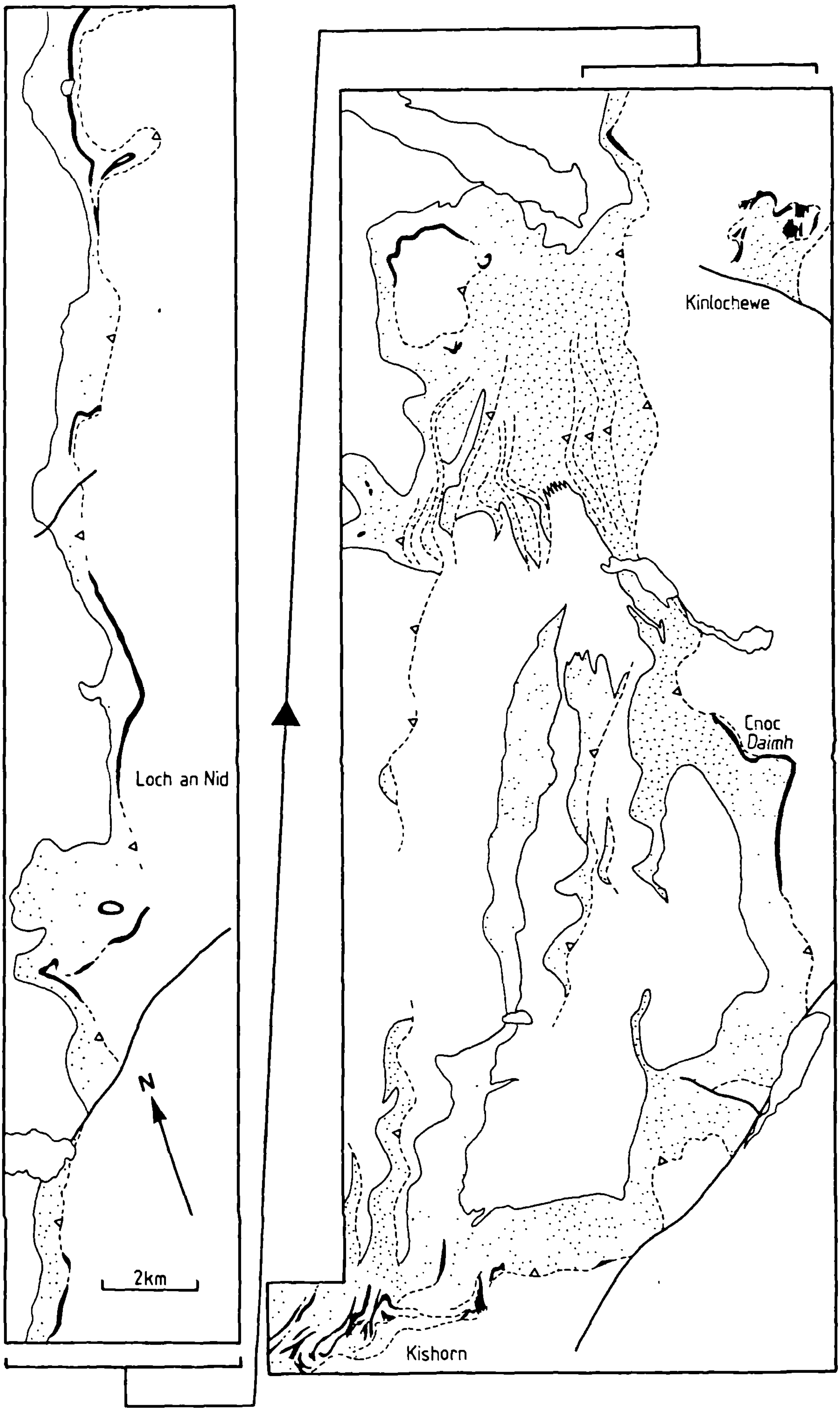
Loch an Nid
N
2km
Kinlochewe
Cnoc
Daimh
Kishorn

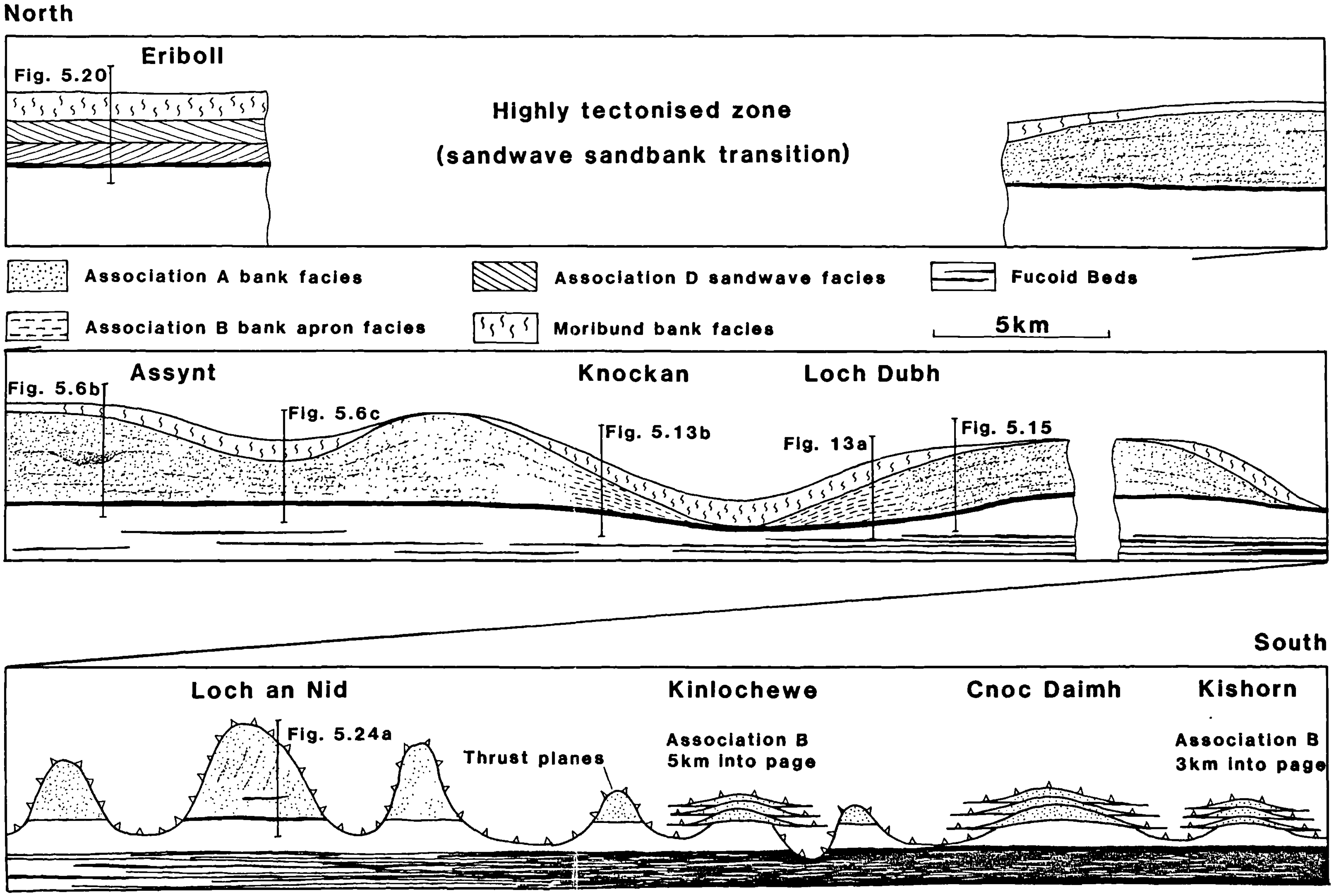

Fence diagram of Salterella Grit along Moine Thrust but these may reflect a lithological control on thrust emplacement which would in turn have been controlled by the sand-body geometry.* It is likely that the sandbanks would have presented a more competent suite of lithologies than the interbank lithologies in which case thrust faults may have been forced to ramp over the banks, but would have been unimpeded in the less competent interbank areas. Where the Salterella Grit is present in imbricate thrust zones the thinner bedded facies of associations B or C dominate and the imbricate zone has an axis roughly parallel to the palaeocurrent direction (see Fig. 5.22). This suggests imbrication of the end of the sandbanks before thrust ramping over the main bank sequence.

The Salterella Grit outcrop lenses show a regular spacing very similar in scale to that exhibited by modern active and moribund banks (Chakhotin et al. 1972, Belderson et al. 1982). The outcrop lens at Loch an Nid (Fig. 5.23) is considerably wider than the other lenses and has a vertical sequence consisting of two coarsening upwards cycles (Fig. 5. 24a). This may suggest amalgamation of two banks in a manner similar to that described by Evans (1970) (Fig. 5.24b) or lateral oscillation of the bank crestline as observed by Smith (1969) (Fig. 5.24c) or a hierarchical arrangement of banks (Pantin and Evans 1984, Hoogendoorn and Dalrymple 1986) (Fig. 5.24d). Considering that the upper coarsening upward cycle is thick, and the width of this lens, then an amalgamation of banks is more likely.

Assuming that the lenses reflect the original bank forms then the spacing of the lenses may be used to calculate water depth. Huthnance (1982) has shown that bank spacing = 250 x the mean water depth. Using a mean spacing of 6.3km (measured from the centre of each lens and perpendicular to the palaeocurrent direction) a water depth of approximately 25m is implied. Allen (1968) presents a graph of bank spacing against water depth for which water depths of between 6m and 35m, with a mean of 20m, is suggested for these examples. The thickness of the bank coarsening upwards cycles exceed the lower limit of this range of values suggesting that a value of 25m using Huthnance's method is the best approximation. One implication of Huthnance's formula is that bank spacing should increase with increasing water depth. Proximality trends in the Fucoid Beds

* SEE OPPOSITE PAGE

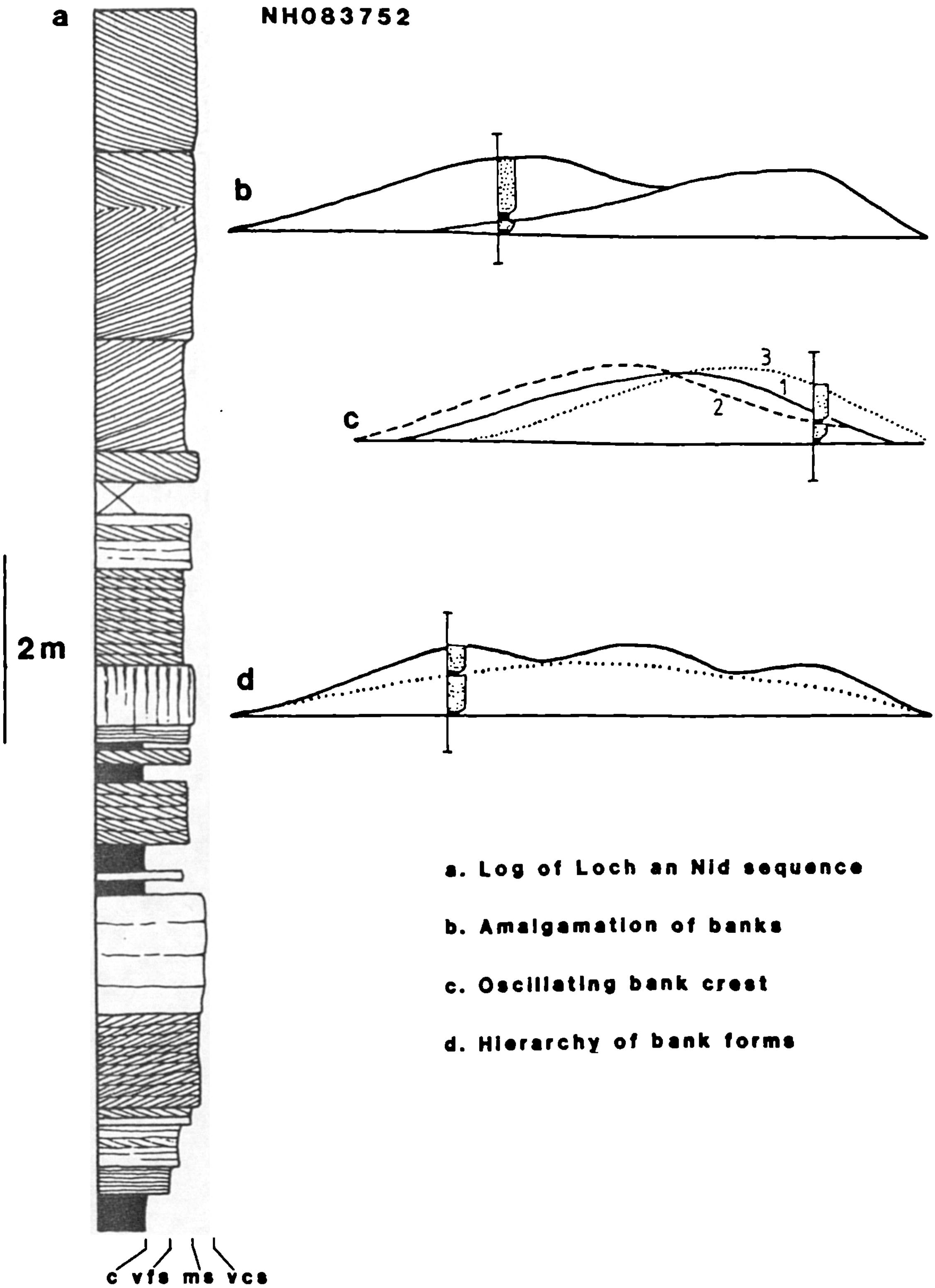

Fig. 5.24 a. Log of the Loch an Nid section.
b-d. Possible explanations for the width of outcrop lens and double coarsening upwards cycle.

indicate a deepening southwards between Ullapool and Skye. A moving average plot of Salterella Grit outcrop spacing (Fig. 5.25) indicates an increase southwards suggesting a similar deepening between Ullapool and Kishorn. Extrapolation of this line, assuming a bank positioned in the Kyle of Lochalsh (between Kishorn and Skye), predicts the position of the Ord bank crest facies to within 0.5km (Fig. 5.25).

Huthnance (1982) also shows that bank height = 0.0038 x bank spacing. This relationship would imply that the active Salterella Grit banks had heights of approximately 23m and therefore may have grown very near the sea surface, a situation very common among recent active banks and noted by Allen (1982b, p38). This would have limited the cross bank component of flow during low water contributing to the lack of cross bank palaeocurrents except in association C and implies removal of approximately 10m of sediment from the bank crest during the moribund stage of bank evolution to be redeposited on the bank flanks.

Using the active bank height, the observed moribund bank heights and bank "lee" slopes and assuming that the preserved lenses approximate to the original width of the moribund banks, the cross-sectional shape of both the active and moribund banks may be very roughly reconstructed. It is necessary however to use values for the unobserved "stoss" slope from those quoted for recent banks (Stride et al. 1982). Therefore an active bank "stoss" slope of 2 degrees and a moribund slope of 0.5 degrees were selected as plausible values. The reconstructed bank cross-sections are presented in Fig. 5.26 based on a stylised bank shape. From these hypothetical sections it appears that the Salterella Grit banks were probably flat topped forms approximately 1.4km wide and 23m high with the flat crest 0.5km wide. The maximum distance observed between a bank apron and a main bank sequence which is likely to be part of the same bank is between Assynt and Knockan, a distance of 20km. This bank must terminate before the sandwave facies at Eriboll, a distance of 40km, suggesting that in this case the bank was 20-40km long. Comparing these bank dimensions with the data on global tidal sandbank dimensions of Chakhotin et al. (1972) the Salterella Grit banks are

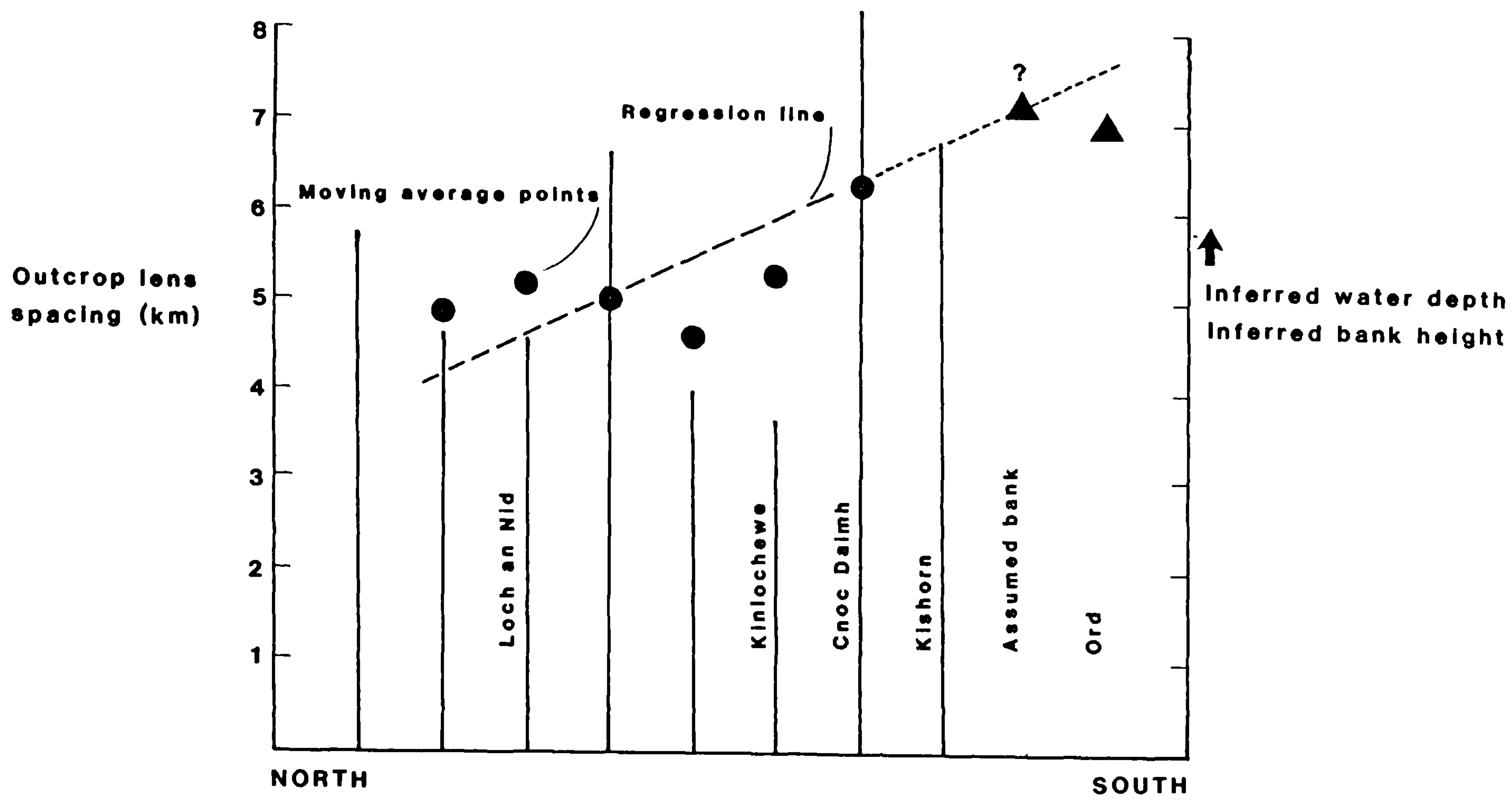

Fig. 5.25 Plot of outcrop lens spacing with the position of the Ord bank included based on the assumption of a bank near Kyle of Lochalsh.

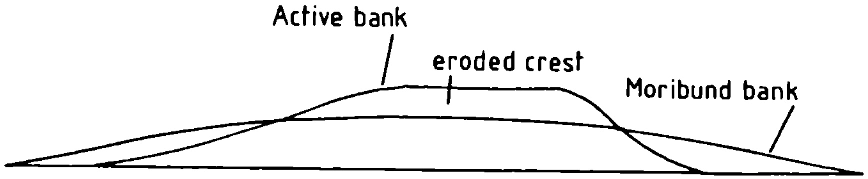

Fig. 5.26a Approximation to original bank shape.

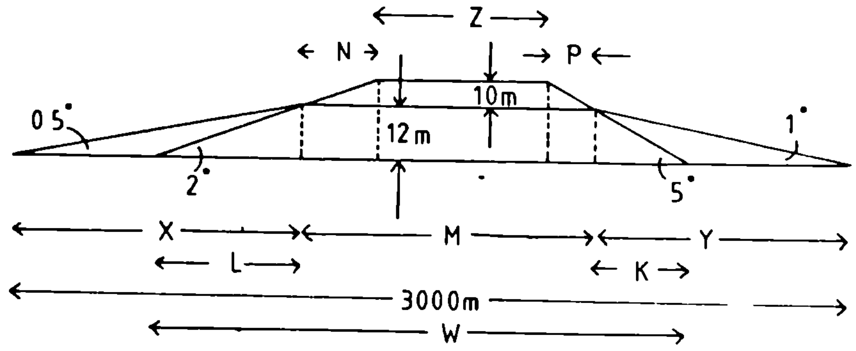

$X = 12/\tan 0{\cdot}5$ $\quad Y = 12/\tan 1$ $\quad N = 10/\tan 2$ $\quad P = 10/\tan 5$

$L = 12/\tan 2$ $\quad K = 12/\tan 5$

$M = 3000 - X - Y = 938m$

$Z = M - N - P = 540m$

$W = M + K + L = 1419m$

Fig. 5.26b Idealised bank shape with calculated and assumed dimensions.

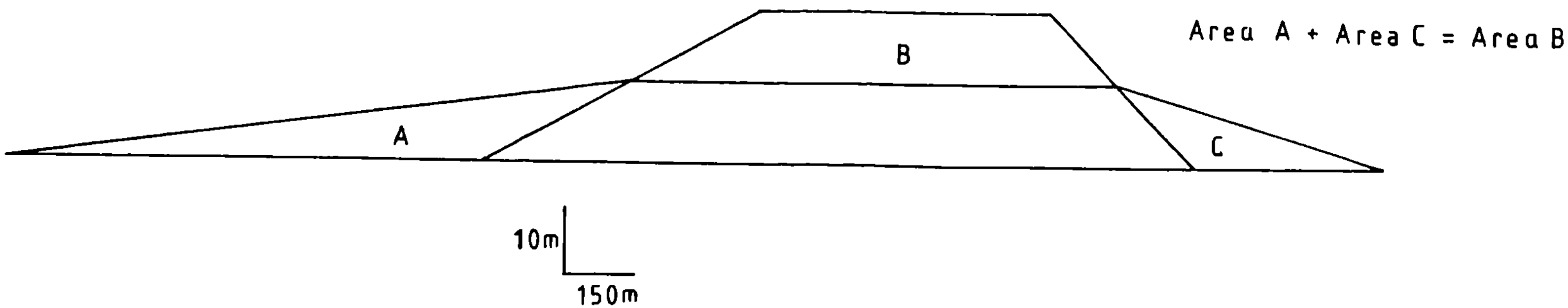

Fig. 5.26c Calculated bank shape, note different vertical and horizontal scales.

broadly similar to those of Korea Bay, Malay Strait and the Gambia River Mouth.

During the transition to a moribund morphology the bank height was reduced and sediment deposited on the flanks. On the reconstructed cross-section the area representing the material removed from the crest is the same as the sum of the areas representing material deposited on the flanks. This may suggest that the conjectural shape is a close approximation to the original shape, although it does not take into account along bank transport of sediment during the moribund stage.

Transferring the cross-sectional area of the bank into a channel 2m deep would require a channel width of approximately 5km. Channeling of approximately 2m deep has already been estimated for erosion into the Fucoid Beds and a width of approximately 5km could be accomodated between 1-2km wide banks spaced at 4-6km apart with any discrepancies accommodated by erosion at the bank heads and tails. This would suggest that much of the sediment comprising the Salterella Grit banks could have been derived by reworking of the Fucoid Beds and would imply that these banks were essentially palimpsest (Swift et al. 1971) sandbodies. This is also implied by the quantity of shell and lithic clasts of probable Fucoid Beds affinities found in the Salterella Grit sands. The Salterella Grit palaeogeography and regional sediment transport paths is summarised in Fig. 5.27.

Fig. 5.27 Salterella Grit palaeogeography.

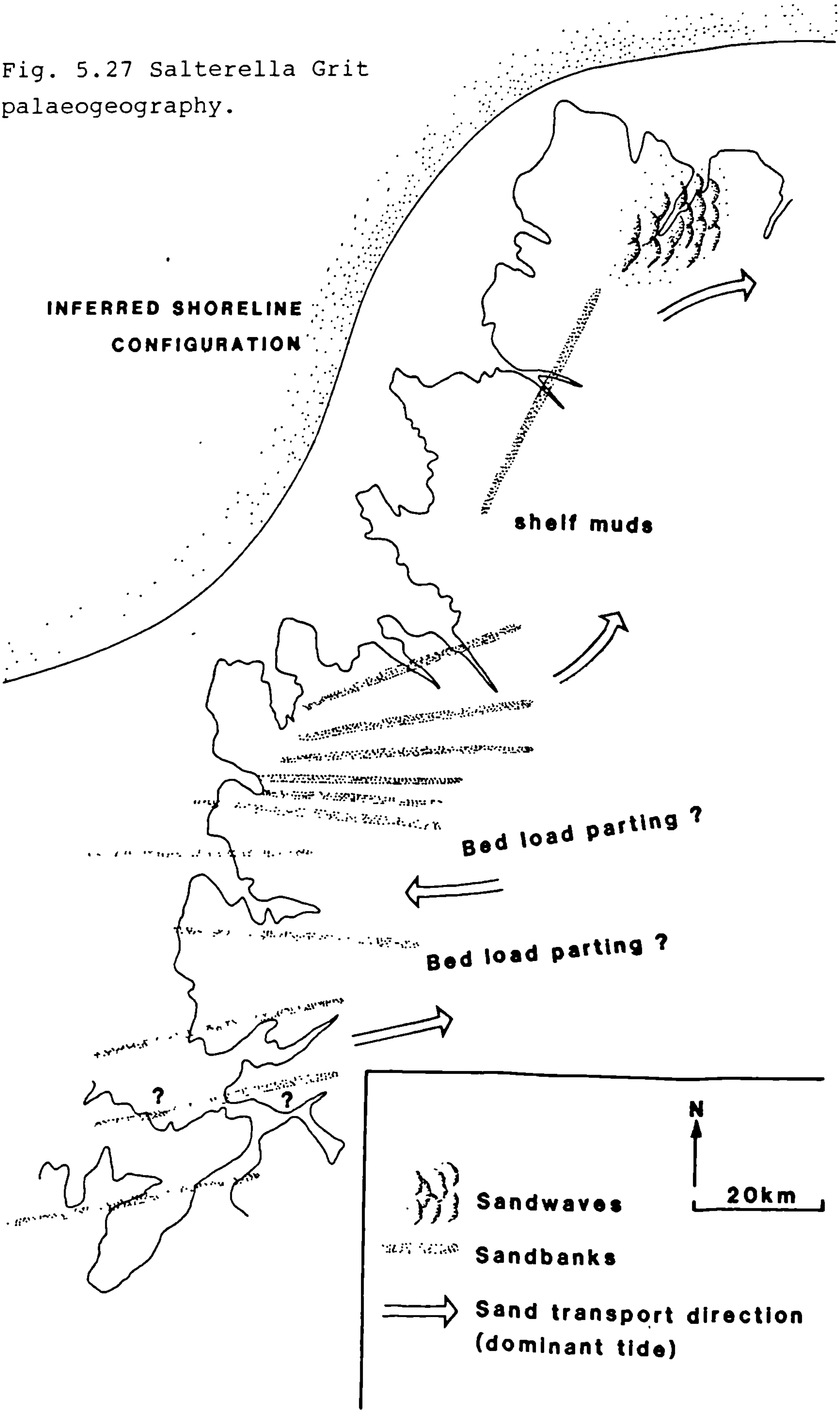

Chapter 6

Controls on the deposition of the clastic sequence

6.1 INTRODUCTION

The stratigraphic sequence described shows no evidence of synsedimentary faulting, rapid facies changes, evidence of frequent seismic events or contemporaneous igneous activity suggesting that deposition took place at a distance from the probable rifted margin of the Laurentian continent and possibly some time after rifting took place. It is unlikely that the Eriboll Sandstone, Fucoid Beds and Salterella Grit were lateral time equivalents because of the wide differences in sediment types and inferred depositional processes. The similarities with sequences of the same age in Labrador, western Newfoundland and eastern Greenland suggest a common origin, probably as a result of shelf-wide tectonic and eustatic changes and varying degrees of tidal amplification.

In order to delineate the relative contributions of these factors in producing the observed vertical facies changes it is necessary to determine the changes in water depth and associated changes in tidal and wave influence which took place during deposition of the sequence. Palaeodepth estimates were made using wave ripples, inferred bedform dimensions and authigenic mineral distributions. Wave ripple calculations were made using the method of Diem (1985), which is derived from simple Airy wave theory. Only vortex ripples (Allen 1979) which showed no form asymmetry or internal evidence of a preferred direction of migration were used, ensuring that the currents during deposition were predominantly oscillatory. These constraints limited the number of usable beds to nine throughout the clastic sequence (Fig. 6.1). Following the recommendation of Diem (1985) only the range of values for maximum calculated depths are presented. Additional depth constraints are as follows (numbers refer to those on depth plot of Fig. 6.1a):

(1) The shoreface facies of the Lower Member is assumed to have a maximum depth of approximately 16m, in keeping with recent lower shoreface environments (Oertel 1985).

(2) The large sandwaves at the top of the Lower Member were probably high in relation to water depth (section 2.4.4). Belderson et al.

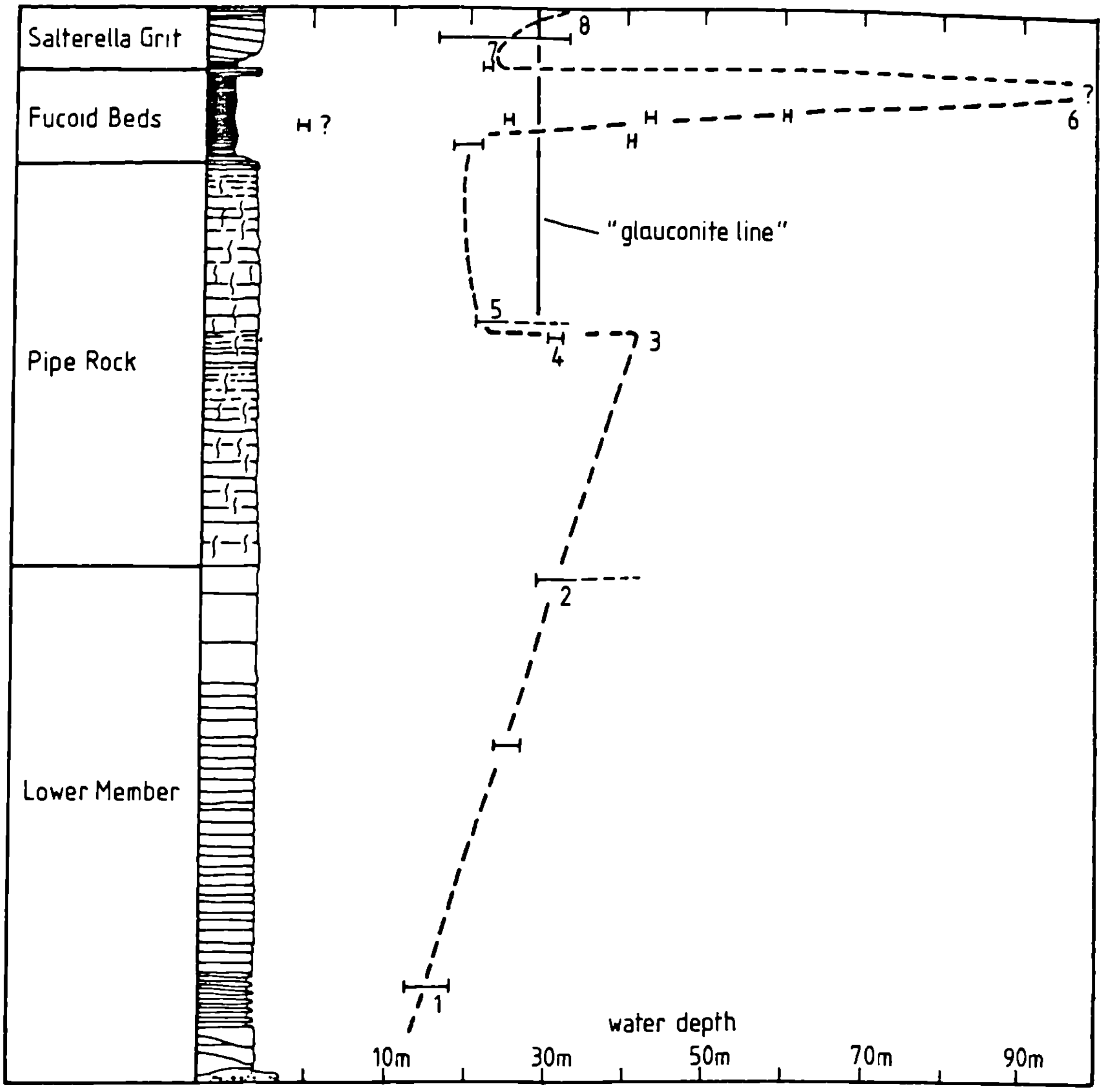

Fig. 6.1 Palaeodepth plot for the clastic sediments.

Locality	Member	Ripple spacing (cm)	Grain size (μm)	Orbital diameter (cm)	Wave period (s)	Water depth (m)	Orbital velocity (cms^{-1})
NH130963	LM	20	385	31	5·2	23-24	18·7
NG625143	PR	23	350	35 5	5 8	30-32	19
NG875453	FB	11	100	17	4·6	17-21	11·5
NC445582	FB	11	95	17	4·7	-22	11·3
NC197099	FB	18	125	27·7	6·4	-41	13·7
NG87543	FB	15	180	23	5	24-25	14·5
"	FB	20	150	30·7	6·5	42-44	14·8
"	FB	25	150	38·5	7·7	-62	15·7
"	FB	7	130	10·7	3·1	7-9	10·9

Fig. 6.1b Wave ripple data.

(1982) have shown that sandwaves may grow to a maximum height of one thira of the water depth, implying a depth of the order of 30m for the top of the Lower Member.

(3) The point of maximum water depth in the Pipe Rock is the result of extrapolating the Lower Member water depths. If subsidence and sea level rise were constant for this part of the sequence then, because this tempestite dominated part of the sequence experienced reduced sedimentation rates, the extrapolated depth will be an underestimate.

(4) This wave ripple derived depth is from the uppermost bed of a series of condensed tempestites at the top of the shallowing episode indicated, and therefore represents part of a range of depths encapsulated within this short stratigraphic interval. The value of 30m provides a maximum value for the shallower water after this interval.

(5) The large sandwave facies within this interval was deposited by sandwaves with a maximum height of 7m. There is no data to show whether these bedforms were large in proportion to the water depth but using the same criterion as under point (2) a depth of 21m would be a minimum estimate for this facies.

(6) This part of the Fucoid Beds sequence was mainly deposited below storm wave base, therefore there are no data on palaeodepths. Maximum depths of storm wave penetration on recent shelves range from 182m in the North Sea (Draper 1980) to 204m on the eastern seaboard of North America (Komar et al. 1972), but is more typically 125m (Komar 1976). The relatively short period calculated for storm waves in the clastic succession (Fig. 6.1b) suggests that storm wave-base was probably nearer 100m than 200m although the calculated wave periods may be due to local hurricane generation, may reflect waning storm conditions or may be biased towards the particular waves which produced ripples suitable for palaeowave climate calculations.

(7) A depth of approximately 25m has been calculated for the active bank facies of the Salterella Grit (section 5.7).

(8) The storm sand sheet facies of the Salterella Grit is physically very similar to the more proximal facies of the Fucoid Beds and is assumed to have been deposited in similar water depths.

(9) This line represents an approximation to the minimum depth of glauconite formation (Porrenga 1967). Glauconite formation in the deeper facies of the Pipe Rock "Monocraterion zone" was probably suppressed by relatively high sedimentation rates and oxygenation of the sediment pores by weak tidal currents. Within lower energy facies the presence of glauconite is important at the top of the Pipe Rock, within the Fucoid Beds and at the top of the Salterella Grit.

The resultant palaeobathymetric plot generated using these parameters is presented in Fig. 6.1. All other data points not mentioned are based on wave ripple calculations. The overall shape of the curve is dictated by the relative facies changes with the inferred depths used to provide a rough numerical scale. The plot ignores local departures from the more typical facies of each member and the tendency of the northernmost outcrops to consistently display more proximal facies.

6.2 CONTROLS ON FACIES DEVELOPMENT

The clastic sequence shows a record of gradual deepening (accelerating in tempestite facies as sedimentation rates decreased) punctuated by two periods of rapid shallowing near the middle of the Pipe Rock and at the top of the Fucoid Beds. A prime contributor to the transgressive nature and gradual deepening recorded by these sediments would have been the global rise in sea level which occured throughout the Cambrian (Matthews and Cowie 1979). This sea level rise has been attributed to an increase in mid-ocean ridge volume following the break-up of the "Eocambrian" supercontinent (Donovan and Jones 1979). This sea level rise and the resultant emplacement of several hundred metres of sediment would have induced isostatic loading of the shelf. It is unlikely, however, that sea level rise and loading can fully account for the total subsidence history of this area and subsidence due to cooling, following the opening of the

Iapetus Ocean, is likely to have produced much of the subsidence recorded by the clastic sediments.

The two rapid shallowing events are probably partly enhanced by condensation of the sequence due to successive storm events increasing in their erosive capability and failing to preserve a complete record of successively more proximal facies. In spite of this it is likely that the rates of shallowing were considerably greater than the rates of deepening. Periods of rapid shallowing in the stratigraphic record have been ascribed to expansion of polar ice caps (Donovan and Jones 1979, Pitman and Golovchenko 1983), infilling of dessicated cratonic basins (Cisne 1985) or, for passive continental margins, variations in intraplate stress fields (Cloetingh et al. 1985, Cloetingh 1986). There is little evidence of sufficiently large polar ice caps in the Cambrian to produce large sea level changes and flooding of cratonic basins is unlikely to have produced shallowing of up to 70m, which appears to have taken place at the top of the Fucoid Beds. Intraplate stress field variations therefore appear to be the mechanism most likely to have produced the two shallowing events. Cloetingh (1986) has shown that uplift of basin edges of up to 50m may be achieved by, for example, a change in the intraplate stress field from up to one kilobar of tension to compression of a similar order of magnitude. Such stress changes may be local in nature, related to sediment loading, or may be produced by changes in ridge push in adjacent oceanic crust. The shallowing event within the Pipe Rock may have been produced by such a change in spreading rate by mid-ocean ridges in the Iapetus Ocean. This event may be approximately synchronous with a stratigraphic break in northeast Greenland, although eastern Greenland does not show evidence of any hiatus at this time (Cowie 1971). The eastern Greenland sequence may be associated with a terrain to the north of Scotland which appears to have been more resistant to subsidence or external tectonic influences.

The shallowing event at the top of the Fucoid Beds, leading to deposition of the Salterella Grit, appears to have been a more dramatic event with a relative fall in sea level probably in excess of 50m. The Salterella Grit may be correlated with the Hawke Bay

Formation of western Newfoundland (Swett and Smitt 1972) and possibly with erosional disconformities in northeast Greenland (Cowie 1971). Palmer and Jones (1980) have shown that the Hawke Bay Formation is representative of a widespread shallowing event along the western margin of the Iapetus Ocean which resulted in the deposition of thin nearshore clastic sequences along the length of the Appalachians. The Cambrian of Morocco, which may have been situated approximately on the opposite margin of the Iapetus Ocean from the Scottish and North American sequences (Jell 1974), also shows an increase in proximal facies at roughly the same time (Brasier 1982). Spitzbergen does not appear to show a similar regressive phase (Swett 1981) and may have been outwith the area affected by the "Hawke Bay Event". The magnitude of the relative sea level fall in Scotland and the widespread occurence of proximal sands along the western, and possibly the eastern, margins of the Iapetus Ocean suggests, using the Cloetingh model, that a major lithospheric plate reorganisation took place at this time. Possible shallowing events of slightly different ages and durations in California and Western Canada associated with a decrease in faunal diversity (Brasier 1982) may have been related to the same event.

On a more local scale, minor along-strike facies changes indicate tectonic controls at shallower crustal levels. Deepening appears to have taken place in the Assynt district during deposition of the Pipe Rock, south of Loch Maree during deposition of the middle Fucoid Beds and south of Loch Broom during deposition of the Salterella Grit (Fig. 6.2). The Lewisian basement has a well developed tectonic "grain" of Laxfordian origin which may have allowed vertical fault displacements of the order of a few ten's of metres producing the inferred deepening. The Loch Maree fault, which was active in Torridonian times (Stewart 1967) and during the Caledonian orogeny, and its continuation offshore as the mid-Minch High (Stein in prep.) probably controlled the deepening in Fucoid Beds times and may have provided sufficient topography during deposition of the Lower Member shelf facies to deflect tidal currents. The faulting active during Pipe Rock deposition in the Assynt area may be located at the sites of the northwest/southeast

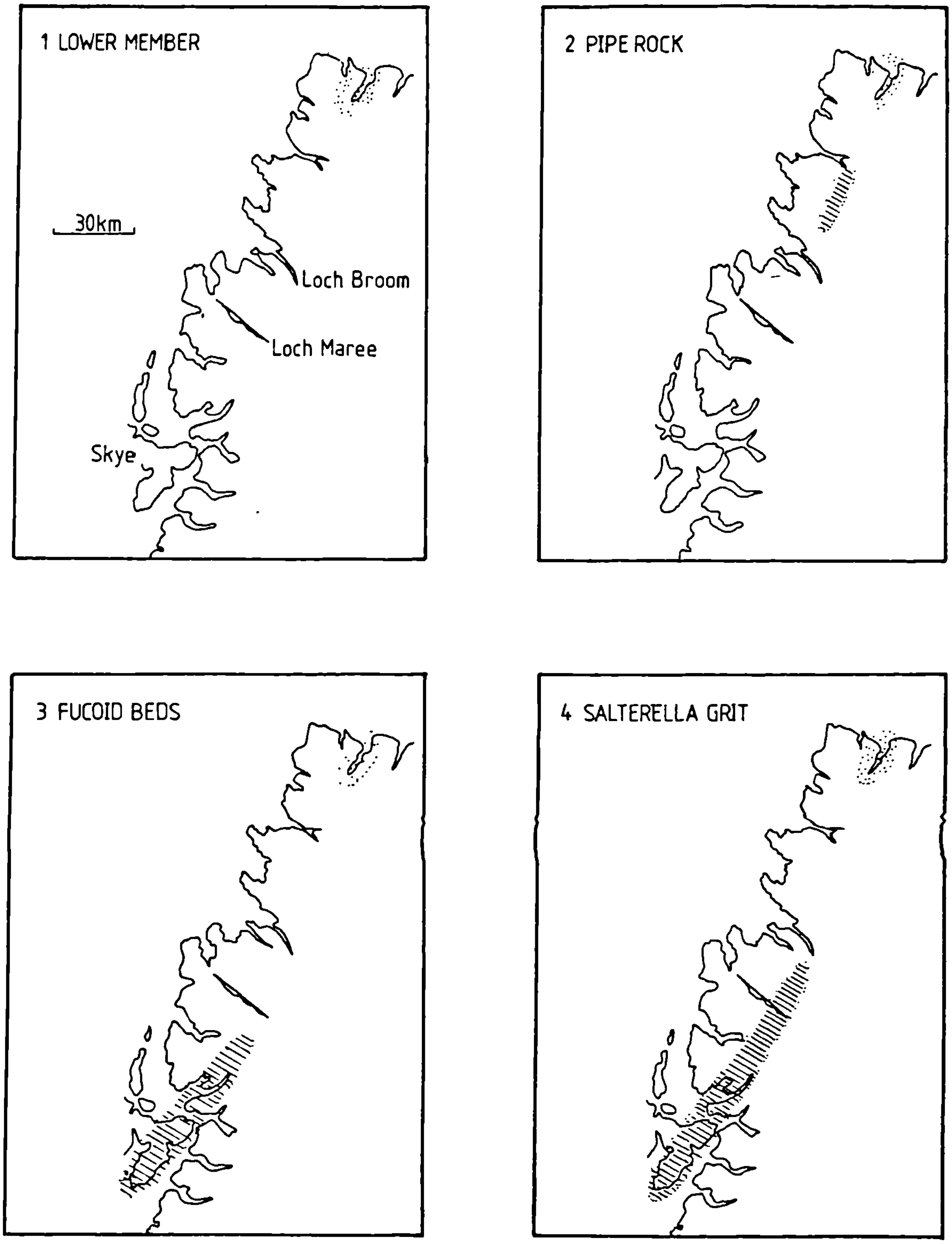

Fig. 6.2 Areas of local deepening (cross hatched) and shallowing (stippled) during deposition of the clastic sequence.

lineaments defining the "Assynt window". Loch Broom also has a similar trend to the other northwest/southeast trending lineaments and may be underlain by a Laxfordian trending fault which contributed to deflection of tidal currents during Salterella Grit deposition, although the mid-Minch High was probably the dominant control at this time. These faults were unlikely to have had throws in excess of a few ten's of metres and were probably activated in response to sediment and water loading resulting in local isostatic equilibration.

A recurring feature throughout the deposition of the clastic sequence is the presence of more proximal facies in the northernmost outcrops coupled with a change in palaeocurrent directions implying a coastline which changed from an outcrop parallel direction to an east-west direction. It is likely that north of this area there was a more stable crustal block which was less susceptible to subsidence induced by local sediment loading. This stable crustal block may have influenced Caledonian thrust faulting. Coward (1986) has postulated an east-west oriented tear fault or lateral ramp between Sutherland and Orkney, to account for a sinistral offset of the the main Caledonian crustal ramp in this area in excess of 50km.

The changes in water depth, shelf width and coastline shape produced by thermal, tectonic and eustatic processes appear to have had a strong control on the relative influences of tides and waves on sediment transport. Proudman (1953) has shown that the shelf tide will be resonantly amplified when the shelf width is 1/4, 3/4, 5/4 etc. of the tidal wavelength, an effect noted by Cram (1979) who demonstrated a positive relationship for modern shelves between shelf width and tidal range. Figure 6.3 shows a plot of palaeodepth against a subjective assessment of the relative degree of tidal influence throughout the Cambrian clastic sequence. The Lower Member shows an inferred increase in tidal range between the mesotidal barrier inlet facies at the base of the sequence and the macrotidal sandwave facies at the top which may have been produced by the widening shelf approaching a resonant width. The presence of tidal sandbanks in the Salterella Grit implies greatest amplification in this facies, which may be related to the presence of a large coastal embayment (of which

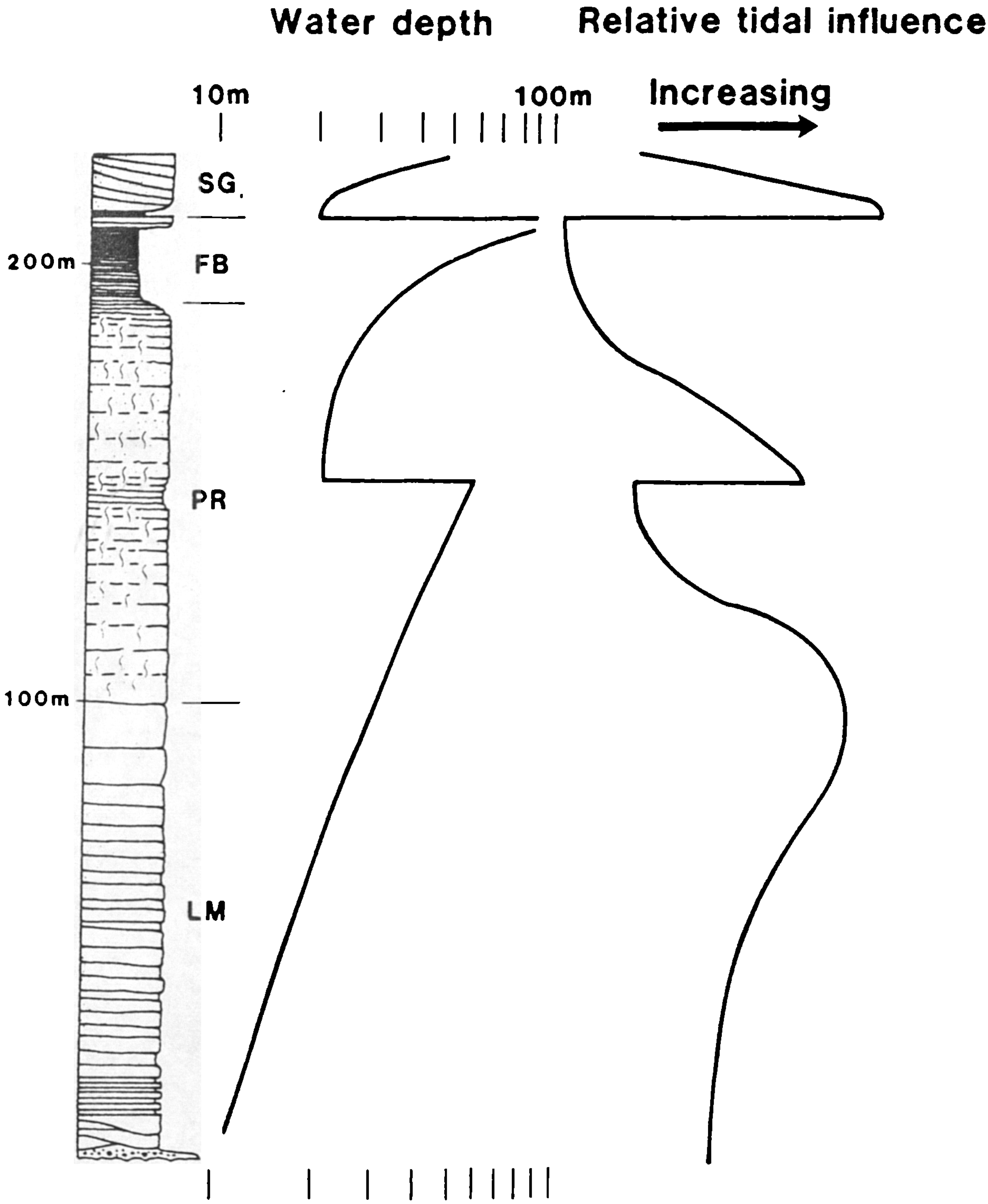

Fig. 6.3 Plot of water depth with a subjective estimate of the relative degree of tidal influence for each member of the clastic sequence.

only the northern portion is indicated in the northwest Highlands) constricting and further amplifying tides. The more tempestite dominated "Monocraterion zone" of the Pipe Rock shows a weaker tidal influence, probably as a result of being deposited in greater water depths than other parts of the Eriboll Sandstone sequence. The abundance of coarse sand indicates that regular sediment transport was probably taking place in shallower nearshore areas. In contrast the Fucoid Beds shows a profound change in grainsize, sediment type and degree of oxygenation of the shelf without an initially great increase in water depths suggesting that tidal currents were very much weaker. There is no evidence of a physical barrier to tides: the amount of clastic material incorporated in the Fucoid Beds implies a cratonic source area with no indication of sediment input from an offshore carbonate bank as envisaged for the Cambrian of the Canadian Rocky Mountains (Aitken 1978). Neither is there evidence for the seismicity which would be associated with movement of fault blocks nearer the rifted craton margin *which would have restricted tidal* currents. The large wavelength of many Fucoid Beds wave ripples suggests an unrestricted shelf (Tanner 1971). It is possible that continued transgression produced a shelf which was approximately one half of the tidal wavelength which would have resulted in a partial reduction in the magnitude of tidal currents (Proudman 1953). That the western margin of the Iapetus Ocean at this time appears to have had very little tidal influence is suggested by the similar facies in the Forteau Formation of Newfoundland and the Bastion Formation of eastern Greenland which consist essentially of carbonate bioherms, thinly bedded silts and shales and minor glauconitic sands (Cowie 1971, Swett and Smitt 1972). Transgression therefore appears to have produced a very wide, essentially tideless, shelf dominated by storms and which may have developed into a carbonate platform if the clastic input was reduced and the water column more oxygenated.

Lithospheric flexure probably played a role in the early subsidence history of the clastic sequence, but eventually transgression may have penetrated into the interior of the craton where gradients were very low and flexural rigidity high. The Eriboll Sandstone may have been deposited on the flexural margin of the shelf and possibly the fine-grained dolomitic Fucoid Beds were deposited as the transgression began to onlap onto the craton interior. Assuming an initial water depth (h) of 30m for the Fucoid Beds and a Cambrian tidal period (T) of ten hours then, using the relationship;

$$\text{Tidal wavelength}=(gh)^{1/2}T$$

then a tidal wavelength of approximately 500km is indicated for the Fucoid Beds shelf. If this shelf was in a non-resonant mode then a shelf width of approximately 250km is indicated. This corresponds well to the estimated maximum flexural shelf width of 300km estimated by Watts (1982) for a crustal thickness of 31.2km, a thickness which is close to the 30km estimated by Soper and Barber (1982) for the pre-Caledonian crust in the Moine Thrust area. This suggests that the Fucoid Beds were deposited as the transgression onlapped the flexural limit of the shelf. Further transgression onto the peneplained craton interior would have resulted in detrital sources receding rapidly and allowing the development of carbonate platform sequences (i.e. the Ghrudaidh Member). The well rounded quartz grains present at the base of this member (and also in facies 3 and 4 of the Pipe Rock and facies 6A of the Salterella Grit) may be reworked sands of inland aeolian dunes flooded during times of maximum transgression across the craton interior. The development of the clastic sequence is summarised in Fig. 6.4. The Ghrudaidh Member consists of thin, laterally persistant beds with echinoderm grainstones present (Wright 1985) which may represent an environment similar to the Fucoid Beds but with a more oxygenated water column, perhaps as a result of the Hawke Bay Event altering the shelf configuration enough to allow slight tidal circulation, but without significant clastic transport.

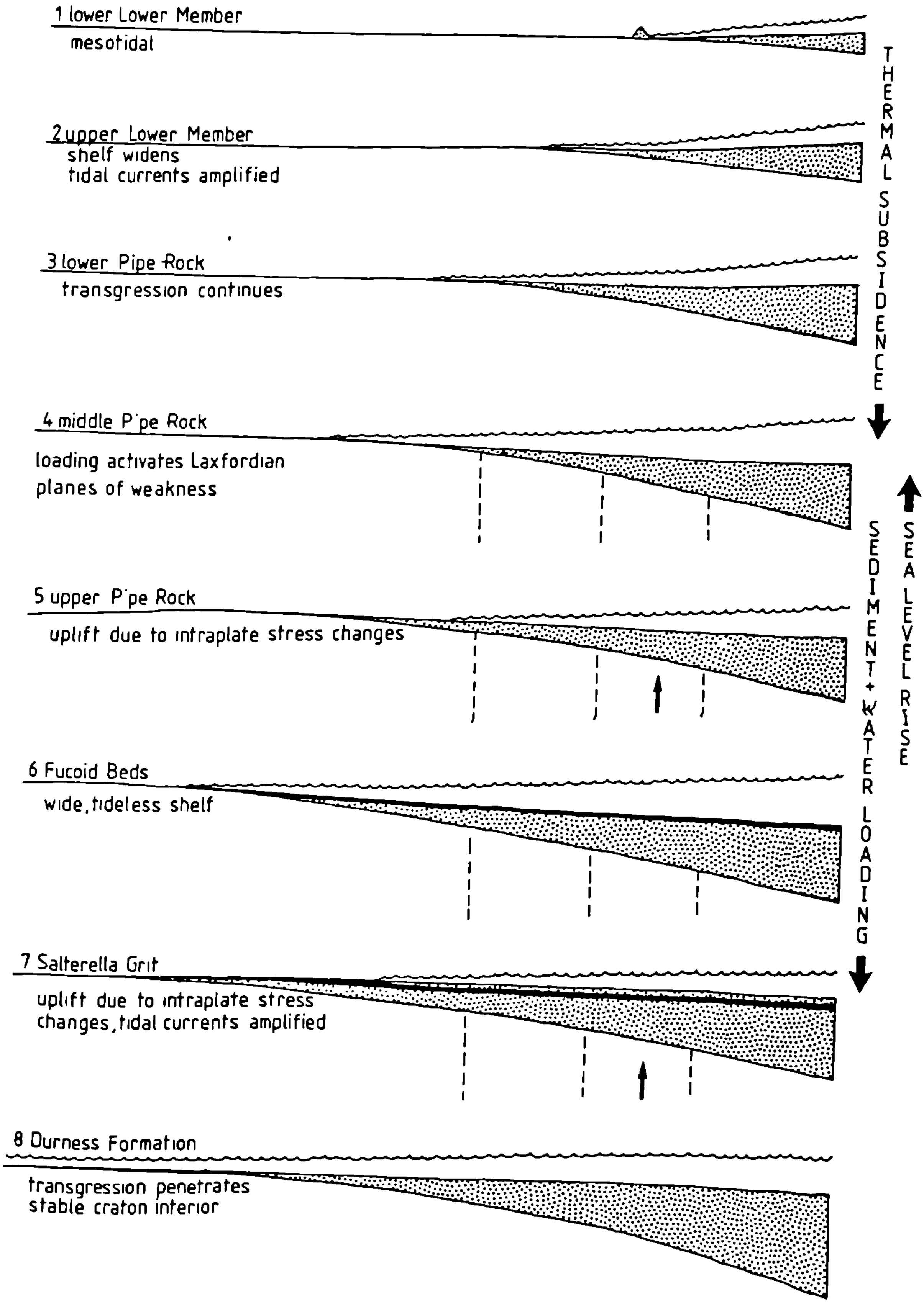

Fig. 6.4 Summary diagram of the main controls on the deposition of the Cambrian clastic sediments.

Chapter 7

Potassium feldspar occurrences in the clastic sequence

7.1 INTRODUCTION

Perhaps the most intriguing aspect of the Cambrian clastic succession is the anomalously high concentration of potassium feldspar found within the Fucoid Beds (Bowie et al. 1966) and it's correlatives in Newfoundland and eastern Greenland (Swett and Smit 1972), Spitzbergen (Swett 1981) and along the length of the Appalachians (Buyce and Friedman 1975). Various models have been proposed to explain this widespread development of potassium feldspar in Cambro-Ordovician marine shales of the western margin of the Iapetus Ocean. Ranganathan (1983) and Dalrymple et al. (1985) have suggested that the abundance of feldspar is a function of the widespread acid gneiss source areas developed at the time and that deposition was a result of offshore transport by dust storms. In contrast Braun and Freidman (1969) and Allison and Russell (1985) advocated a syndepositional model where potassium feldspar was precipitated on the sea floor, perhaps in an evaporitic setting. A late diagenetic model has been proposed by Swett (1968), Hearn and Sutter (1985) and Hearn et al. (1987).

During the course of this investigation large concentrations of K-feldspar were discovered within the muddy facies of the Lower Member and the Salterella Grit indicating that feldspar distribution is more widespread than originally indicated by Bowie et al. (1966).

7.2 POTASSIUM FELDSPAR DISTRIBUTION AND PETROLOGY

Within the Lower Member, feldspar occurs within the dark, fine-grained silts and muds of facies 6A in association with abundant collophane (partly recrystallised to dahlite), "floating" corroded grains of quartz, occasional grains of plagioclase feldspar and rare laths of muscovite (Fig. 7.1). X-ray diffraction analysis shows the feldspar to be a monoclinic form. Visually however, the potassium feldspar has a phyllosilicate appearence similar to fine-grained muscovite or sericite with laths 0.1-0.01mm in length. It differs from the larger, variably distributed muscovite laths present in that it has a much lower birefringence, particularly round grain edges,

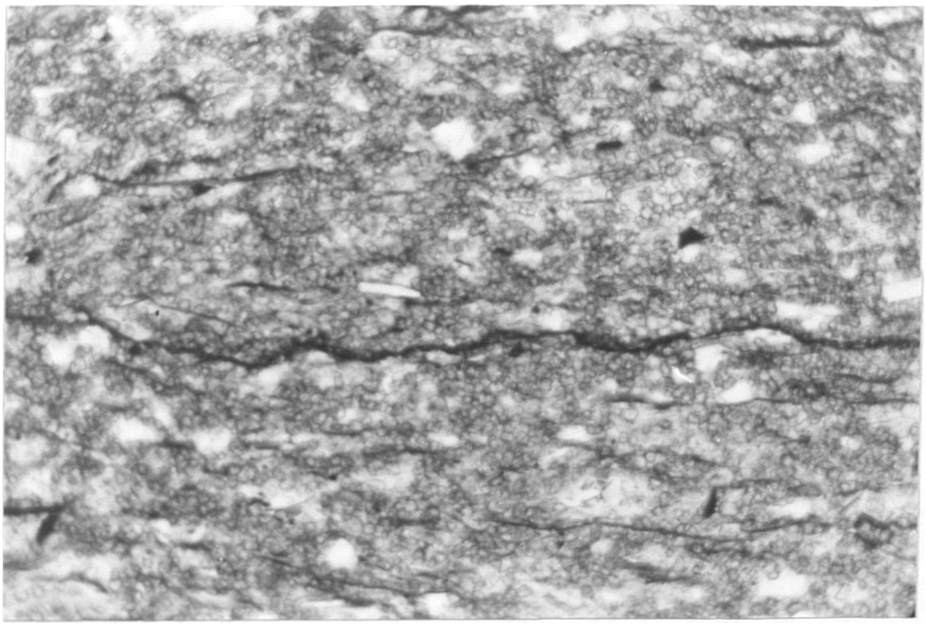

Fig. 7.1a General view of Lower Member feldspathic silts showing carbonaceous laminae, equant dahlite crystals and corroded quartz grains (white). Field of view 2.78 mm wide. Creag na Feòla, NH 130 963.

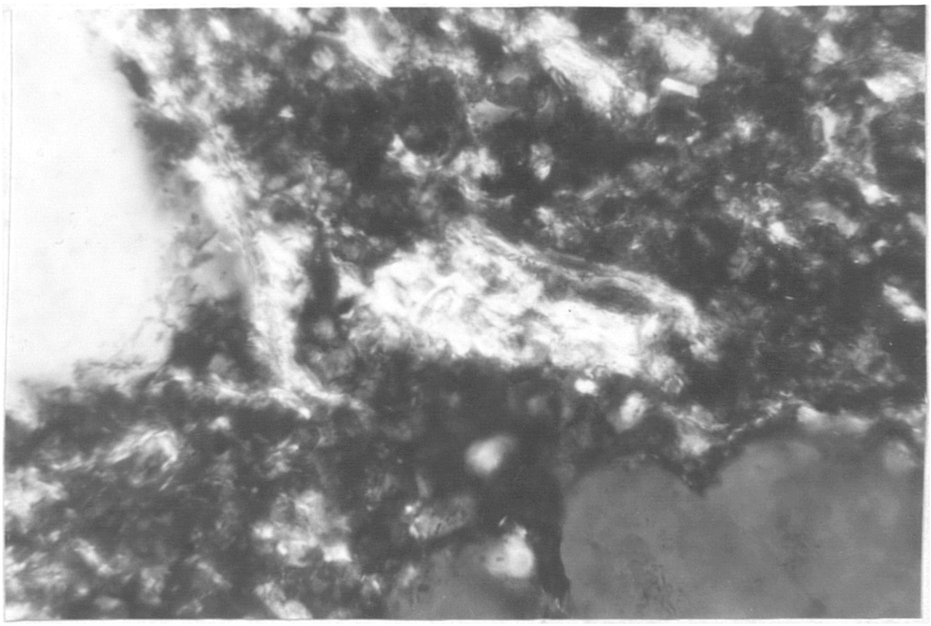

Fig. 7.1b Altered muscovite and corroded quartz in a collophane/dahlite groundmass. Field of view 0.27mm wide. Creag na Feòla.

and with a less well developed cleavage (Fig. 7.1). Adularia-type overgrowths also occur on detrital microcline grains in the sandstones throughout the Lower Member sequence and also within the Pipe Rock (Fig. 7.2) and have a "dirty" appearance due to numerous inclusions.

The Fucoid Beds Member contains the greatest development of K-feldspar within the clastic sequence, averaging 11.5% K_2O (Bowie et al. 1966), the bulk of which is contained within dark grey feldspar muds capping the top of graded tempestite beds or forming mud rip-up clasts on bed soles. Muscovite does not make a significant contribution to the K_2O content. These muds have similar XRD diffractogram patterns to the Lower Member muds (Fig. 7.3) and have a similar phyllosilicate appearance, although laths are smaller in size, ranging from 0.01-0.001mm in length. Adularia forms overgrowths on detrital grains (Fig. 7.2b) and also replaces shell fragments.

As with the Fucoid Beds all the Salterella Grit muds are composed almost entirely of potassium feldspar which has the same sericitic appearance , yellow-grey interference colours and XRD diffractogram pattern (Fig. 7.3). Adularia overgrowths on detrital cores occur, but are uncommon. Both the overgrowths and fine muds throughout the clastic sequence are non-lumeiescent.

7.3 INTERPRETATION

The extensive quartz dissolution within the Lower Member feldspathic muds is a feature unique within the Eriboll Sandstone and suggests that at some time in their history they experienced a pore fluid chemistry unlike that of the rest of the sequence. The phyllosilicate appearance of the K-feldspar suggests that it formed by the alteration of a mica-like precursor. Such thin, laterally impersistant beds could only have experienced a different fluid chemistry during deposition when they were laid down in abandoned inlet channels, and possibly back barrier channels, physically isolated from the regular tidal exchange with normal sea water but with a continued input from continental groundwaters. The Lower Member inlets were mesotidal which suggests that flood tidal deltas

Fig. 7.2a Adularia overgrowths on detrital potassium feldspars, Lower Member, Loch na Gainmhich, NC 239 292. Field of view 0.67mm wide.

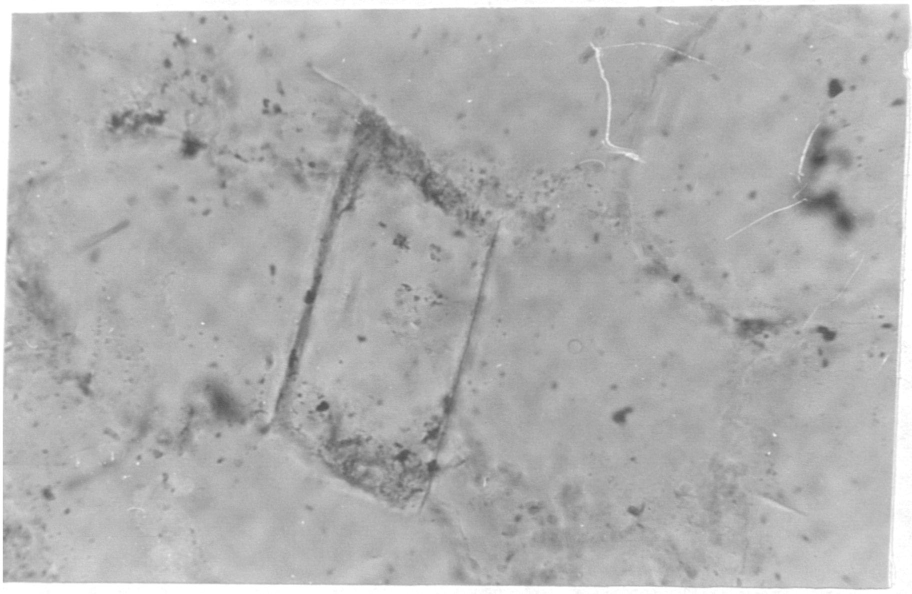

Fig. 7.2b Adularia overgrowths on detrital potassium feldspars, Pipe Rock, An t-Sròn, NC 445 582. Field of view 0.27mm wide.

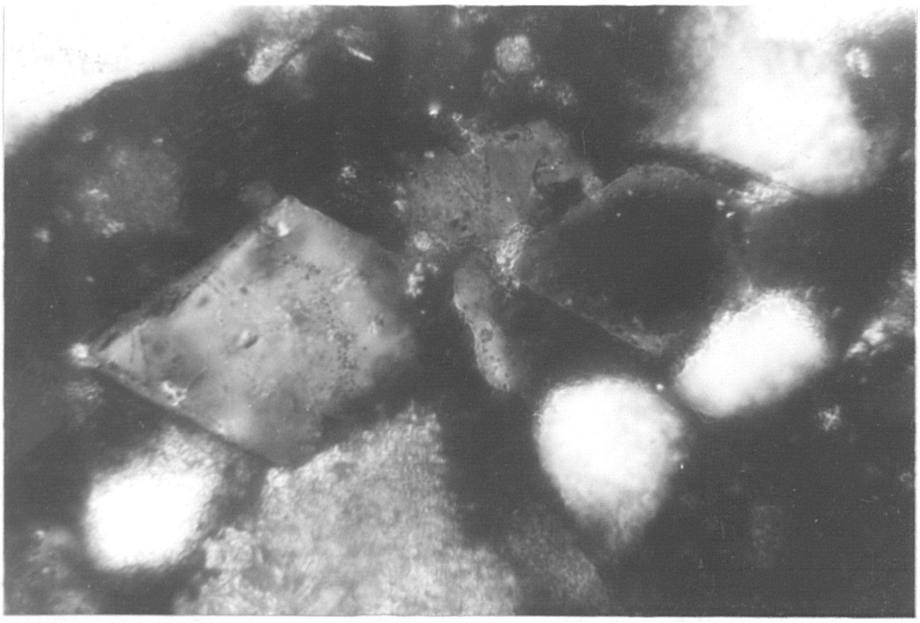

Fig. 7.2c Adularia overgrowths on detrital potassium feldspars, Fucoid Beds, An t-Sròn, NC 445 582. Field of view 0.27mm wide.

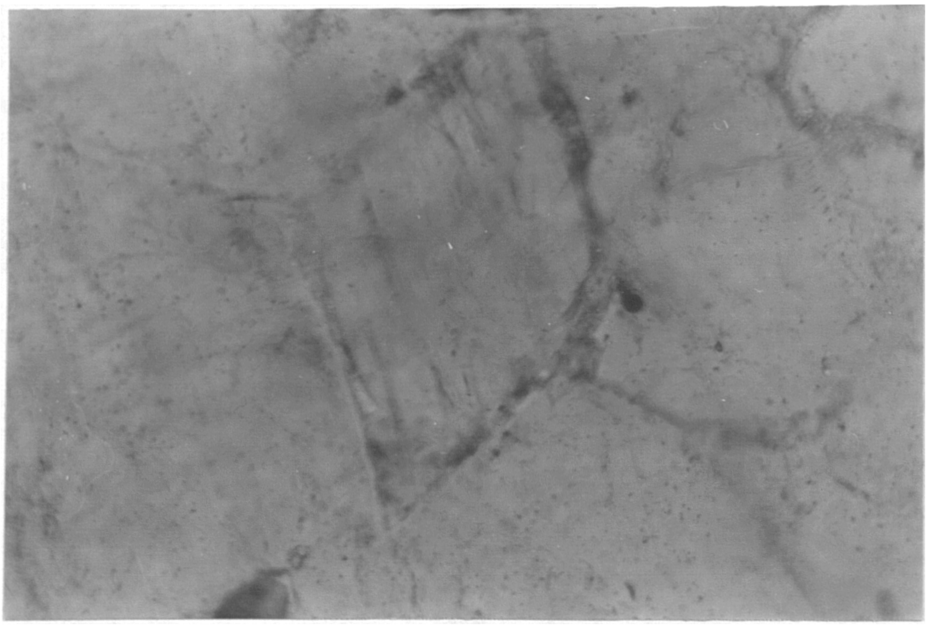

Fig. 7.2d Adularia overgrowths on detrital potassium feldspars, Salterella Grit, An t-Sròn, NC 445 582. Field of view 0.67mm wide.

Fig. 7.3 XRD diffractograms of feldspathic muds from the Lower Member, Fucoid Beds and Salterella Grit. All peaks are monoclinic potassium feldspar peaks with the exception of the peak at 10° 2θ which is a muscovite peak.

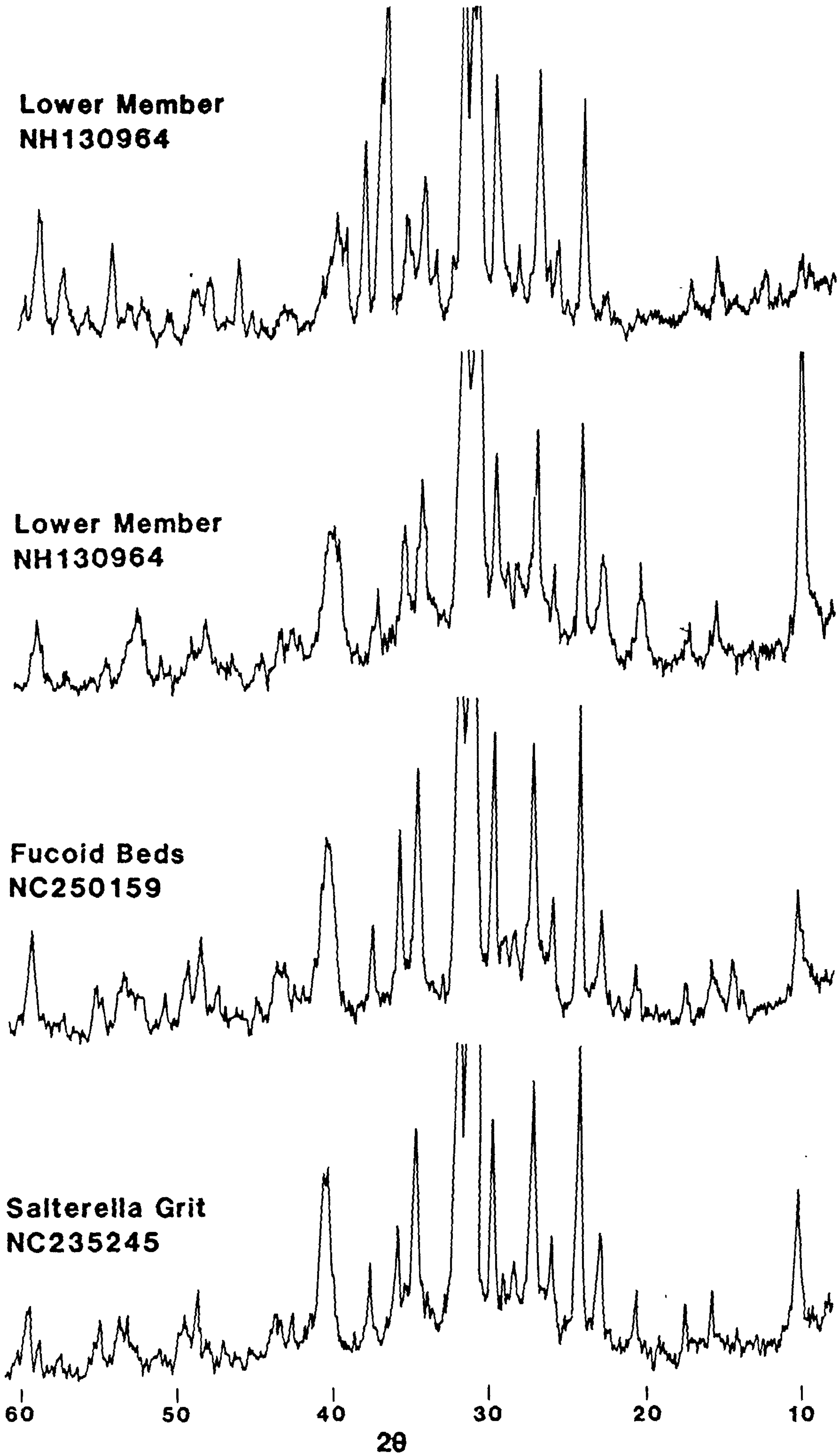
Lower Member
NH130964
Lower Member
NH130964
Fucoid Beds
NC250159
Salterella Grit
NC235245
60
50
40
30
20
10
2θ

and backbarrier lagoons were poorly developed and that the landward side of the barrier islands would have had a network of intertidal channels and tidal flats with bays developed behind inlets (Hayes 1980). Following inlet abandonment spit accretion and swash bar migration would close the inlet throat isolating the back barrier bays and producing the small enclosed "lagoons" within which the potassium feldspar could form. The degraded phyllosilicate habit of the feldspar suggests that it formed from the "reverse weathering" (Mackenzie and Garrels 1966) of a detrital muscovite precursor. Kastner and Siever (1979) have suggested the reaction-

$$KAl_2(AlSi_3)O_{10}(OH)_2 + 2K^+ + 6H_4SiO_4 \rightarrow 3KAlSi_3O_8 + 12H_2O + 2H^+$$

for the conversion of muscovite to potassium feldspar and shown that the reaction is primarily dependant on the concentration of dissolved silica and the K^+/H^+ ratio of the water involved. The dissolved silica is likely to have been supplied by the in-situ dissolution of detrital quartz grains. Russell and Allison (1985) have suggested that weathering of the Lewisian basement by alkaline groundwater (in the absence of plant derived humic acids) produced a quartz and muscovite soil and fluids enriched in potassium ions. This alkaline, K^+ rich groundwater would have found it's way to the back barrier lagoons where, possibly under evaporating conditions, it would have raised the K^+/H^+ ratio and the pH sufficiently to begin to dissolve quartz. This weathering process would also have been the ultimate source of the mature quartz sands of the Eriboll Sandstone (Russell and Allison 1985) and of the muscovite shales found within the active channel and open shelf facies of this formation. X-ray diffractograms of these shales are frequently identical to the muscovites of the Lewisian palaeosol (Fig. 7.4). The large pristine muscovite laths occasionally present within this facies may represent original metamorphic muscovite, possibly less amenable to reverse weathering than the palaeosol muscovite. The Lower Member model is summarised in Fig. (7.5).

The similarity in habit of the Fucoid Beds feldspar muds to those of the Lower Member and the presence of feldspathic mud rip-up clasts, which must have lithified very early, suggests a similar

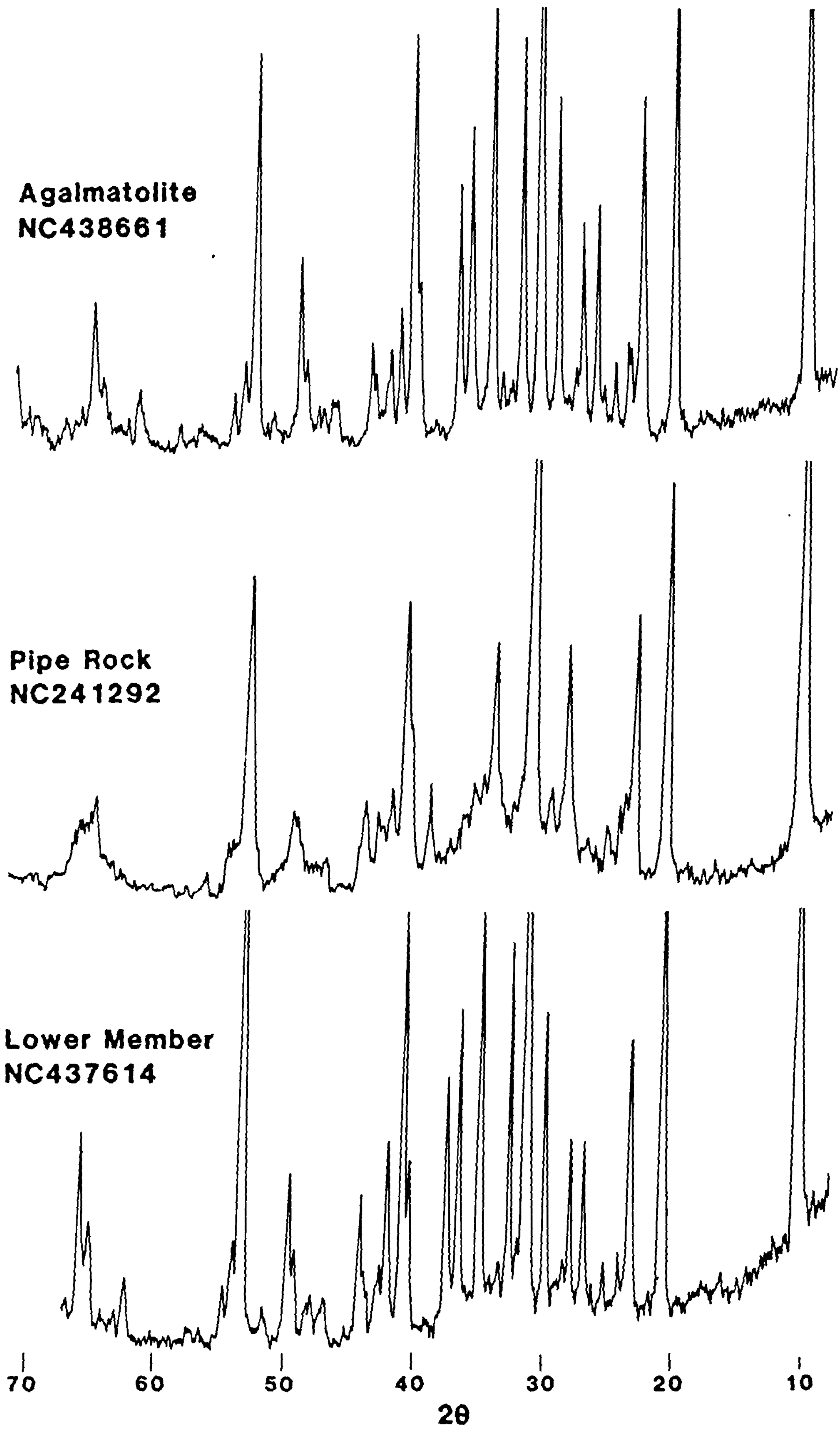
Agalmatolite
NC438661
Pipe Rock
NC241292
Lower Member
NC437614
70
60
50
40
30
20
10
2θ

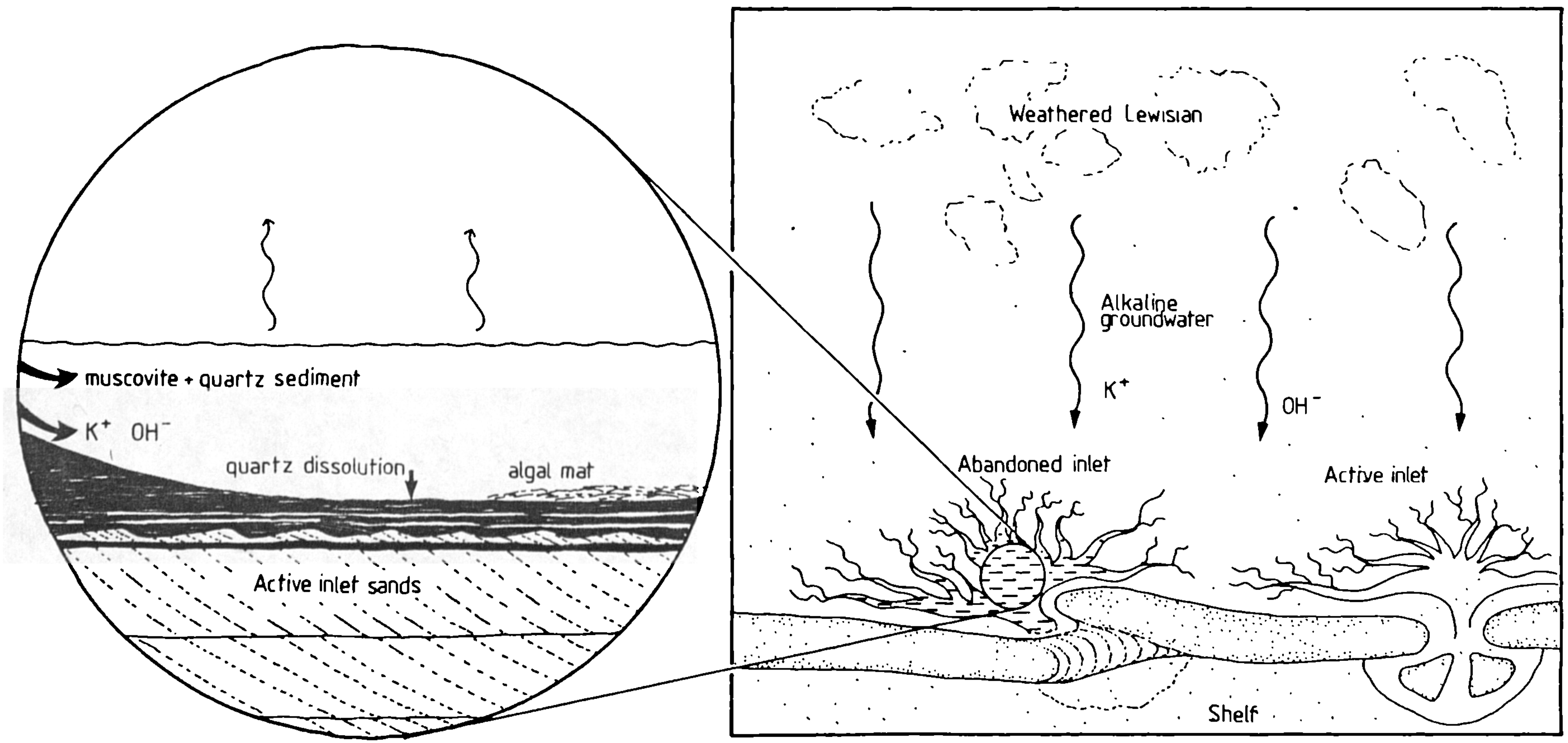

Fig. 7.5 A summary diagram of the model to explain the Lower Member feldspathic mud occurences.

origin by "reverse weathering" of detrital muscovite early in the depositional history. It is unlikely that alteration was post-depositional due to the extremely low permeability these beds would have had (enhanced by early lithification of muds and grainstones) and the huge volumes of pore water which would have been required to achieve 100% conversion of greater than 50% of the total volume of the Fucoid Beds whilst leaving the Pipe Rock muds totally unaffected.

The Fucoid Beds depositional environment however, would have been unable to produce the extreme geochemical environment required for such mass production of potassium feldspar and it is more probable that these muds were transported and deposited on the shelf as feldspar muds. The delicate fabric preserved in the Fucoid Beds tempestites, in contrast to the extensive neomorphism of the grainstone beds which were deposited in-situ, suggests that they were transported as dolomitic sediment. The Fucoid Beds coastal zone was likely to have consisted of very wide and extensive storm flats and salinas where possibly the "reverse weathering" processes outlined for the Lower Member could have operated on a much larger scale. The complete dolomitisation and "reverse weathering" of these sediments would have been facilitated by the long intervals between storm events. Dolomitisation of the grainstone beds is likely to have been a later event, perhaps related to the dolomite replacement of the quartz cemented facies 6A sands of the Salterella Grit. This dolomitisation may have been due to reflux of sabkha brines from the overlying Durness Group and appears to have only affected the Salterella Grit moribund bank and storm sand sheet facies where the presence of Salterella allowed dolomite to precipitate. Dolomite replacement appears to have penetrated these facies to gain access to the Fucoid Beds via Skolithos burrows, which may have been more permeable. The subsequent dolomitisation of the Fucoid Beds grainstones may have produced the anhydrite described by Allison and Russell (1985) which appears to infill solution vughs and is almost entirely restricted to the grainstones. Similar anhydrite nodules unrelated to the depositional environment of the host sediments have been noted by Milliken (1978), Berg and Wayne (1978) and Maliva

(1987) infilling solution vughs in turbiditic and shallow marine limestones.

The Salterella Grit sediments are essentially palimpsest in origin and the feldspathic muds of this member may simply be reworked Fucoid Beds feldspathic muds derived from between the sandbanks.

The adularia overgrowths ubiquitous throughout the sequence must have formed much later after deposition. It is unlikely that there was a nearby thick sequence of basinal sediments which, on compaction, would supply fluids capable of precipitating feldspar overgrowths. Overgrowths are best developed within the Fucoid Beds and basal Salterella Grit where feldspathic muds are most common. Overgrowth formation, and shell replacement within the Fucoid Beds, may have been controlled by localised fluid movements dissolving and reprecipitating the feldspars of the Fucoid Beds and Salterella Grit within the overlying and underlying quartzarenites and may have been driven by Caledonian heating and thrust movements.

Appendix

Appendix 1- Lower Member bundle sequence data

(a) Creag na Feòla (NG 130 963)

Bundle thickness (cm)	Grainsize (mm)	Set thickness (cm)
5.5	0.40	
11.0	0.50	
7.0	0.40	
6.0	0.40	
8.0	0.60	68
11.0	0.80	
6.0	0.50	
5.0	0.30	
3.0	0.40	68
3.0	0.50	
7.5	0.75	
12.5	0.40	
11.0	0.35	
5.0	0.50	
6.5	0.40	
7.0	0.30	68
7.0	0.25	
6.5	0.37	
10.0	0.50	
4.0	0.50	
5.5	0.50	
3.5	0.40	

(b) Meall a'Ghiubhais (NG 977 657)

Bundle thickness (cm)	Grainsize (mm)	Set thickness (cm)
4.0	0.50	
2,2	0.50	
1.0	0.50	
1.3	0.50	
2.0	0.50	37
4.5	0.50	
4.5	0.60	
5.5	0.75	
2.0	0.50	
4.8	0.75	
7.0	0.75	
2.5	0.50	
7.0	0.75	
4.0	0.75	21
7.0	0.75	
12.0	1.00	
4.0	0.60	
4.0	0.50	
7.0	0.60	
4.5	0.75	
4.0	1.00	
4.0	0.75	
2.8	0.75	
1.0	0.50	
2.0	0.50	
2.0	0.50	
4.0	1.00	
1.0	0.50	33
1.5	0.50	
5.0	0.75	
3.0	0.75	
4.5	1.00	
2.0	0.75	

(c) Meall a' Ghiubhais (NG 978 658)

Bundle thickness (cm)	Grainsize (mm)	Set thickness (cm)
13.0	0.37	47
11:5	"	
17.0	"	
gap	"	
14.5	"	
12.0	"	40
4.0	"	
7.0	"	
4.0	"	33
14.0	"	
7.0	"	

References

Aigner, T. (1985) Storm depositional systems. Lecture notes in the Earth Sciences vol. 3. Springer-Verlag. 174 pp.
Aigner, T. and Reineck, H.E. (1982) Proximality trends in modern storm sands from the Helgoland Bight (North Sea) and their implications for basin analysis. Senckenberg. marit., 14, 183-215.
Aitken, J.D. (1978) Revised models for depositional grand cycles, Cambrian of the southern Rocky Mountains, Canada. Bull. Can. Petroleum Geology, 26, 515-542.
Allen, J.R.L. (1968) The nature and origin of bed-form hierarchies. Sedimentology, 10, 161-182.
Allen, J.R.L. (1973) Features of cross stratified-units due to random and other changes in bed-forms. Sedimentology, 20, 189-202.
Allen, J.R.L. (1979) A model for the interpretation of wave ripple-marks using their wavelength, textural composition and shape. J. geol. Soc. London, 136, 673-682.
Allen, J.R.L. (1980) Sand waves: a model of origin and internal structure. Sediment. Geol., 26, 281-328.
Allen, J.R.L. (1981) Palaeotidal speeds and ranges estimated from cross-bedding sets with mud drapes. Nature, 293, 394-396.
Allen, J.R.L. (1982a) Sedimentary structures: their character and physical basis. Developments in Sedimentology, 30A(1), Elsevier, Amsterdam.
Allen, J.R.L. (1982b) Sedimentary structures: their character and physical basis. Developments in Sedimentology, 30A(2), Elsevier, Amsterdam.
Allen, P.A. and Homewood, P. (1984) Evolution and mechanics of a Miocene tidal sandwave. Sedimentology, 31, 63-82.
Allison, I. and Russell, M.J. (1985) Anhydrite discovered in the Fucoid Beds of Northwest Scotland. J. sedim. Petrol., 55, 917-918.
Anderton, R. (1976) Tidal-shelf sedimentation: an example from the Scottish Dalradian. Sedimentology, 23, 429-458.
Anderton, R. (1985) Clastic facies models and facies analysis. In: Sedimentology, Recent developments and applied aspects (Ed. by P.J. Brenchley and B.P.J. Williams), pp. 31-47. Spec. Publ. geol. Soc. London. Blackwell, Oxford.
Barwis, J.H. and Makurath J.H. (1978) Recognition of ancient tidal

inlet sequences: an example from the Upper Silurian Keyser Limestone in Virginia. Sedimentology, 25, 61-82.

Belderson, R.H., Johnson, M.A. and Kenyon, N.H. (1982) Bedforms. In: Offshore tidal sands (Ed. by A.H. Stride), pp. 27-57. Chapman and Hall.

Belderson, R.H., Pingree, R.D. and Griffiths, D.K. (1986) Low level tidal origin of Celtic Sea sand banks- evidence from numerical modelling of M_2 tidal streams. Mar. Geol., 73, 99-108.

Belknap, D.F. and Kraft, J.C. (1981) Preservation potential of transgressive coastal lithosomes on the U.S. Atlantic shelf. Mar. Geol., 42, 429-442.

Belknap, D.F. and Kraft, J.C. (1985) Influence of antecedent geology on stratigraphic preservation potential and evolution of Delaware's barrier systems. Mar. Geol., 63, 235-262.

Berg, R.R. and Wayne, M.A.H.R. (1978) Turbidite origin for anhydritic dolomites in Bell Canyon Formation, Delaware Basin, New Mexico. Bull. Am. Ass. Petrol. Geol., 62, p496.

Blakey, R.C. (1984) Marine sandwave complex in the Permian of central Arizona. J. sedim. Petrol., 54, 29-51.

Bouysse, P., Horn, R., Lapierre, F., and Le Lann, F. (1976) Etude des grands bancs de sable du sud-est de la Mer Celtique. Mar. Geol., 20, 251-275.

Bowie, S.H.U., Dawson, J., Gallagher, M.J. and Ostle, D. (1966) Potassium rich sediments in the Cambrian of Northwest Scotland. Trans. Inst. Min. Metal., 75B, 125-145.

Boyles, J.M. and Scott, A.J. A model for migrating shelf-bar sandstones in the Upper Mancos Shale (Campanian), Northwestern Colorado. Bull. Am. Ass. Petrol. Geol., 66, 491-508.

Brasier, M.D. (1980) The Lower Cambrian transgression and glauconite phosphate facies in western Europe. J. geol. Soc. London, 137, 695-703.

Brasier, M.D. (1982) Sea-level changes, facies changes and the Late Precambrian-Early Cambrian evolutionary explosion. Precamb. Res., 17, 105-123.

Braun, M. and Friedman, G.M. (1969) Carbonate lithofacies and environments of the Tribes Hill Formation (Lower Ordovician) of the

Mohawk Valley, New York. J. sedim. Petrol., 39, 113-135.
Brenchley, P.J. and Newall, G. (1982) Storm influenced inner-shelf sand lobes in the Caradoc (Ordovician) of Shropshire, England. J. sedim. Petrol., 52, 1257-1269.
Brenchley, P.J. and Pickerill, R.K. (1980) Shallow subtidal sediments of Soudleyan (Caradoc) age in the Berwyn Hills, North Wales, and their palaeogeographic context. Proc. Geol. Ass., 91, 177-194.
Brenner, R.L. and Davies, D.K. (1974) Oxfordian sedimentation in Western Interior United States. Bull. Am. Ass. Petrol. Geol., 58, 407-428.
Brenner, R.L., Swift, D.J.P. and Gaynor, G.C. (1985) Re-evaluation of coquinoid sandstone depositional model, Upper Jurassic of central Wyoming and south-central Montana. Sedimentology, 32, 363-372.
Brett, C.E. (1983) Sedimentology, facies and depositional environments of the Rochester Shale (Silurian; Wenlockian) in Western New York and Ontario. J. sedim. Petrol., 53, 947-971.
Briden, J.C., Drewry, G.E. and Gilbert-Smith, A. (1974) Phanerozoic equal-area world maps. J. Geol., 82, 555-574.
Bruun, P. (1962) Sea-level rise as a cause of shore erosion. J. Waterw. Harbors Div. (ASCE), 88, 117-130.
Butler, R.W.H. and Coward M.P. (1984) Geological constraints, structural evolution and deep geology of the Northwest Scottish Caledonides. Tectonics, 3, 347-366.
Buyce, M.P. and Friedman, G.M. (1975) Significance of authigenic K-feldspar in Cambrian-Ordovician carbonate rocks in North America. J. sedim. Petrol., 45, 508-521.
Cacchione, D.A. and Drake, D.E. (1982) Measurements of storm-generated bottom stresses on the continental shelf. J. geophys. Res., 87, 1952-1960.
Cant, D.J. (1980) Storm dominated shallow marine sediments of the Arisaig Group (Silurian-Devonian) of Nova Scotia. Can. J. Earth Sci., 17, 120-131.
Caston, V.N.D. (1971) Linear sand banks in the southern North Sea. Sedimentology, 18, 63-78.
Caston, V.N.D. (1981) Potential gain and loss of sand by some sandbanks in the southern bight of the North Sea. Mar. Geol., 41,

239-250.
Caston, V.N.D. and Stride, A.H. (1970) Tidal sand movement between some linear sand banks in the North Sea of northeast Norfolk. Mar. Geol., 9, M38-M42.
Cavaleri, L. and Stefanon, A. (1980) Bottom features due to extreme meteorological events in the northern Adriatic Sea. Mar. Geol., 36, 49-64.
Chakhotin, P.S., Medvedev, V.S. and Longinov, V.V. (1972) Sand ridges and waves on the shelf of tidal seas. Oceanology, 12, 386-394.
Chowdhuri, K.R. and Reineck, H.E. (1978) Primary sedimentary structures and their sequence in the shoreface of barrier island Wangerooge (North Sea). Senckenberg. marit., 10, 15-29.
Cisne, J.L. (1985) Depth dependant sedimentation and the flexural edge effect in epeiric seas: measuring water depth relative to the lithosphere's flexural wavelength. J. Geol., 93, 567-576.
Clarkson, E.N.K. (1979) Cystoid ecology. In: Invertebrate palaeontology and evolution. pp. 227. George Allen and Unwin.
Cloetingh, S. (1986) Tectonics of passive margins: implications for the stratigraphic record. Geologie Mijnb., 65, 103-117.
Cloetingh, S., McQueen, H. and Lambeck, K. (1985) On a tectonic mechanism for regional sea-level variations. Earth planet. Sci. Lett., 75, 157-166.
Cook, P.J. and Shergold, J.H. (1984) Phosphorous, phosphorites and skeletal evolution at the Precambrian-Cambrian boundary. Nature, 308, 231-236.
Coward, M.P. (1986) Moine Thrust structures. In: The Caledonides (Ed. by A.L. Harris and D. Fettes). NATO ASI.
Cowie, J.W. (1971) The Cambrian of the North American Arctic regions. In: Lower Palaeozoic rocks of the world: The Cambrian of the New World (Ed. by C.H. Holland), pp. 325-384. Wiley Interscience.
Cowie, J.W. (1974) The Cambrian of Spitzbergen and Scotland. In: Lower Palaeozoic rocks of the world: The Cambrian of the British Isles, Norden and Spitzbergen (Ed. by C.H. Holland), pp. 123-155. Wiley Interscience.
Cowie, J.W. and McNamara, K.J. (1978) Olenellus (Trilobita) from the Lower Cambrian of north-west Scotland. Palaeontology, 21,

615-634.
Cowie, J.W. and Rushton, A.W.A. (1974) Palaeogeography of the Cambrian of the British Isles. In: Lower Palaeozoic rocks of the world: The Cambrian of the British Isles, Norden and Spitzbergen (Ed. by C.H. Holland), pp. 177-183. Wiley Interscience.
Cowie, J.W., Rushton, A.W.A. and Stubblefield, C.J. (1972) A correlation of Cambrian rocks in the British Isles. Geol. Soc. London Spec. Report no. 2. Scottish Academic Press.
Cram, J.M. (1979) The influence of continental shelf width on tidal range: palaeo-oceanographic implications. J. Geol., 87, 441-447.
Crimes, T.P. (1970) Trilobite tracks and other trace fossils from the Upper Cambrian of North Wales. Geol. J., 7, pp. 47.
Crimes, T.P., Legg,I., Marcos, A. and Arboleya, M. (1977) ?Late Precambrian-low Lower Cambrian trace fossils from Spain. In: Trace fossils 2 (Ed. by T.P. Crimes and J.C. Harper), pp. 91-138. Geol. J. Spec. Issue no. 9, Seel House Press. 351 pp.
Dalrymple, R.W., Narbonne, G.M. and Smith, L, (1985) Eolian action and the distribution of Cambrian shales in North America. Geology, 13, 607-610.
DeRaaf, J.F.M. and Boersma, J.R. (1971) Tidal deposits and their sedimentary structures. Geologie Mijnb., 50, 479-504.
DeRaaf, J.F.M., Boersma, J.R. and van Gelder, A. (1977) Wave generated structures and sequences from a shallow marine succession, Lower Carboniferous, County Cork, Ireland. Sedimentology, 24, 451-483.
Diem, B. (1985) Analytical method for estimating palaeowave climate and water depth from wave ripple marks. Sedimentology, 32, 705-720.
Donovan, D.T. and Jones, E.J.W. (1979) Causes of world wide changes in sea-level. J. geol. Soc. London, 136, 187-192.
Dott, R.H., Byers, C.W., Fielder, G.W., Stenzel, S.R. and Winfree, K.E. (1986) Aeolian to marine transition in Cambro-Ordovician cratonic sheet sandstones of the northern Mississippi Valley, U.S.A. Sedimentology, 33, 345-368.
Downie, C. (1982) Lower Cambrian acritarchs from Scotland, Norway, Greenland and Canada. Trans. Roy. Soc. Edin., 72, 257-285.
Draper, L. (1980) Wave climatology of the U.K. continental shelf. In:

The N.W. European shelf seas: the seabed and the sea in motion, Vol. II: Physical and chemical oceanography and physical resources (Ed. by F.T. Banner, M.B. Collins and K.S. Massie), pp. 353-368. Elsevier Amsterdam. 638 pp.
Drewry, G.E., Ramsay, A.T.S. and Gilbert-Smith, A. (1974) Climatically controlled sediments, the geomagnetic field and trade wind belts in Phanerozoic time. J. Geol., 82, 531-553.
Duke, W.L. (1985) Hummocky cross-stratification, tropical hurricanes and intense winter storms. Sedimentology, 32, 167-194.
Evans, W.E. (1970) Imbricate linear sandstone bodies of Viking Formation in Dodsland-Hoosier area of southwestern Saskatchewan, Canada. Bull. Am. Ass. Petrol. Geol., 54, 469-486.
Foda, M.A., Khalaf, F.I. and Al-Kadi, A.S. (1985) Estimation of dust fallout rates in the northern Arabian Gulf. Sedimentology, 32, 595-603.
Forristall, G.Z. (1974) Three-dimensional structure of storm-generated currents. J. geophys. Res., 79, 2721-2729.
Futterer, E. (1978) Studien über die Einregelung, Anlagerung und Einbettung biogener Hartteile im Strömungskanal. N. Jb. Geol. Palaont. Abh., 156, 87-161.
Gadow, S. and Reineck, H.E. (1969) Ablandiger sandtransport bei Sturmfluten. Senckenberg. marit., 1, 63-78.
Glaeser, J.D. (1978) Global distribution of barrier islands in terms of tectonic setting. J. Geol., 86, 283-297.
Goldring, R. and Bridges, P. (1973) Sublittoral sheet sandstones. J. sedim. Petrol., 43, 736-747.
Hallam, A. and Swett, K. (1966) Trace fossils from the Lower Cambrian Pipe Rock of the north-west Highlands. Scott. J. Geol., 2, 101-106.
Hayes, M.O. (1967) Hurricanes as geological agents, South Texas coast. Bull. Am. Ass. Petrol. Geol., 51, 937-942.
Hayes, M.O. (1980) General morphology and sediment patterns in tidal inlets. Sediment. Geol., 26, 139-156.
Hine, A.C. (1977) Lily bank, Bahamas: History of an active oolite sand shoal. J. sedim. Petrol., 47, 1554-1581.
Hearn, P.P. and Sutter, J.F. (1985) Authigenic potassium feldspar in Cambrian carbonates: evidence of Alleghanian brine migration.

Science, 228, 1529-1531.
Hearn, P.P., Sutter, J.F. and Belkin, H.E. (1987) Evidence for Late Palaeozoic brine migration in Cambrian carbonate rocks of the central and southern Appalachians: Implications for Mississippi Valley-type sulphide mineralişation. Geochim. Cosmochim. Acta, 51, pp. 1323.
Hobday, D.K. and Morton, R.A. (1984) Lower Cretaceous shelf storm deposits, Northeast Texas. In: Siliciclastic shelf sediments (Ed. by R.W. Tillman and C.T. Siemers). Spec. Publs. Soc. econ. Paleont. Miner., Tulsa, 34, 205-214.
Hobday, D.K. and Reading, H.G. (1972) Fair weather versus storm processes in shallow marine sand bar sequences in the Late Precambrian of Finnmark, North Norway. J. sedim. Petrol., 42, 318-324.
Hobday, D.K. and Tankard, A.J. (1978) Transgressive-barrier and shallow-shelf interpretation of the Lower Palaeozoic Peninsula Formation, South Africa. Bull. geol. Soc. Am., 89, 1733-1744.
Hoogendoorn, E.L. and Dalrymple, R.W. (1986) Morphology, lateral migration and internal structures of shoreface-connected ridges, Sable-Island Bank, Nova Scotia, Canada. Geology, 14, 400-403.
Houbolt, J.J.H.C. (1968) Recent sediments in the southern bight of the North Sea. Geologie Mijnb., 47, 245-273.
Howard, J.D. and Reineck, H.E. (1972) Physical and biogenic sedimentary structures of the nearshore shelf. Senckenberg. marit., 4, 81-124.
Howarth, M.J. (1982) Tidal currents on the continental shelf. In: Offshore tidal sands (Ed. by A.H. Stride), pp. 10-26. Chapman and Hall, London.
Hoyt, J.H. and Henry, V.J. (1967) Influence of island migration on barrier island sedimentation. Bull. geol. Soc. Am., 78, 77-86.
Hubbard, D.K., Oertel, G. and Nummedal, D. (1979) The role of waves and tidal currents in the development of tidal inlet sedimentary structures and sand body geometry: examples from North Carolina, South Carolina and Georgia. J. sedim. Petrol., 49, 1073-1092.
Huthnance, J.M. (1982) On one mechanism forming linear sand banks. Est. Coastal Mar. Sci., 14, 79-99.
Jell, P.A. (1974) Faunal provinces and possible planetary

reconstruction of the Middle Cambrian. J. Geol., 82, 319-350.
Johnson, H.D. (1977) Shallow marine sand bar sequences: an example from the late Precambrian of North Norway. Sedimentology, 24, 245-270.
Kastner, M. and Seiver, R. (1979) Low temperature feldspars in sedimentary rocks. Am. J. Sci., 279, 435-479.
Kenyon, N.H., Belderson, R.H., Stride, A.H. and Johnson, M.A. (1981) Offshore tidal sand banks as indicators of net sand transport and as potential deposits. In: Holocene marine sedimentation in the North Sea basin (Ed. by S.-D. Nio, R.T.E. Shüttenhelm and Tj.C.E. van Weering). Spec. Publs. Int. Ass. Sediment. 5, 257-268.
Khalaf, F. and Al-Hashash, M. (1983) Aeolian sedimentation in the north-western part of the Arabian Gulf. J. Arid Env., 6, 319-332.
Komar, P.D. (1976) The transport of cohesionless sediments on continental shelves. In: Marine sediment transport and environmental management (Ed. by D.J. Stanley and D.J.P. Swift), pp. 107-125. John Wiley and Sons, New York.
Komar, P.D., Kulm, L.D. and Harlett, J.C. (1974) Observations and analysis of bottom turbid layers on the Oregon continental shelf. J. Geol., 82, 104-111.
Komar, P.D., Neudeck, R.H. and Kulm, L.D. (1972) Observations and significance of deep water oscillatory ripple marks on the Oregon continental shelf. In: Shelf sediment transport: process and pattern (Ed. by D.J.P. Swift and O.H. Pilkey), pp. 601-619. Dowden, Hutchinson and Ross, Stroudsburg.
Kreisa, R.D. (1981) Storm-generated sedimentary structures in subtidal marine facies with examples from the Middle and Upper Ordovician of Southwestern Virginia. J. sedim. Petrol., 51, 823-848.
Kreisa, R.D. and Bambach, R.K. (1982) The role of storm processes in generating shell beds in Paleozoic shelf sediments. In: Cyclic and event stratification (Ed. by G. Einsele and A. Seilacher), pp. 200-207. Springer-Verlag.
Kumar, N. (1973) Modern and ancient barrier sediments: new interpretations based on stratal sequence in inlet-filling sands and on recognition of nearshore storm deposits. Ann. N. Y. Acad. Sci., 220, 247-340.

Kumar, N. and Sanders, J.E. (1970) Are basal transgressive sands chiefly inlet-filling sands? Marit. Sedim., 6, 12-14.
Kumar, N. and Sanders, J.E. (1976) Characteristics of shoreface storm deposits: modern and ancient examples. J. sedim. Petrol., 46, 145-162.
Lambeck, K. (1978) The Earth's palaeorotation. In: Tidal friction and the Earth's rotation (Ed. by P. Brosche and J. Sundermann), pp. 144-153. Springer-Verlag.
Lapierre, F. (1975) Contribution à l'étude géologique et sédimentolgique de la Manche orientale. Phil. Trans. R. Soc., A279, 177-187.
Leatherman, S.P. (1983) Barrier island evolution in response to sea-level rise: a discussion. J. sedim. Petrol., 53, 1026-1031.
Lees, B.J. (1983) The relationship of sediment transport rates and paths to sandbanks in a tidally dominated area off the coast of East Anglia, U.K. Sedimentology, 30, 461-483.
Levell, B.K. (1980) A Late Precambrian tidal shelf deposit, the Lower Sandfjord Formation, Finnmark, North Norway. Sedimentology, 27, 539-557.
Lever, A. and McCave, I.N. (1983) Eolian componants in Cretaceous and Tertiary North Atlantic sediments. J. sedim. Petrol., 53, 811-832.
Mackenzie, F.T. and Garrels, R.M. (1966) Chemical mass balance between rivers and oceans. Am. J. Sci., 264, 507-575.
Maliva, R.G. (1987) Quartz geodes: Early diagenetic silicified anhydrite nodules related to dolomitization. J. sedim. Petrol., 57, 1054-1059.
Marsaglia, K.M. and Klein, DeVries G. (1983) The paleogeography of Paleozoic storm depositional systems. J. Geol., 91, 117-142.
Matthews, S.C. and Cowie, J.W. (1979) Early Cambrian transgression. J. geol. Soc. London, 136, 133-135.
McCave, I.N. (1970) Deposition of fine grained suspended sediment from tidal currents. J. geophys. Res., 75, 4151-4159.
McCave, I.N. and Langhorne, D.N. (1982) Sandwaves and sediment transport around the end of a tidal sandbank. Sedimentology, 29, 95-110.
Miller, M.C., McCave, I.N. and Komar, P.D. (1977) Threshold of

sediment motion under unidirectional currents. Sedimentology, 24, 507-528.
Miller, M.F. (1984) Bioturbation of intertidal quartz-rich sands: a modern example and it's sedimentologic and palaeoecologic implications. J. Geol., 92, 201-216.
Milliken, K.L. (1978) Non-sabkha evaporites (silicified) from Carboniferous limestones of Southern Kentucky and Northern Tennessee. Bull. Am. Ass. Petrol. Geol., 62, pp. 544.
Moslow, T.F. and Tye, R.S. (1985) Recognition and characterisation of Holocene tidal inlet sequences. Mar. Geol., 63, 129-151.
Mount, J.M. (1982) Storm-surge-ebb origin of hummocky cross-stratified units of the Andrews Mountain Member, Campito Formation (Lower Cambrian), White-Inyo Mountains, Eastern California. J. sedim. Petrol., 52, 941-958.
Nelson, C.H. (1982) Modern shallow water graded sand layers from storm surges, Bering Shelf: a mimic of Bouma sequences and turbidite systems. J. sedim. Petrol., 52, 537-545.
Nio, S.-D., Siegenthaler, C. and Yang, C.S. (1983) Megaripple cross-bedding as a tool for the reconstruction of the palaeo-hydraulics in a Holocene subtidal environment, SW Netherlands. Geologie Mijnb., 62, 499-510.
Oertel, G.F. (1985) The barrier island system. Mar. Geol., 63, 1-18.
Off, T. (1963) Rhythmic linear sand bodies caused by tidal currents. Bull. Am. Ass. Petrol. Geol., 47, 324-341.
Olsen, H.W., Clukey, E.C. and Nelson, C.H. (1982) Geotechnical characteristics of bottom sediment in the northeastern Bering Sea. Geologie Mijnb., 61, 91-103.
Palmer, A.R. and James, N.P. (1980) The Hawke Bay Event: a circum-Iapetus regression near the Lower Middle Cambrian boundary. In: The Caledonides in the U.S.A. (Ed. by D.R. Wones). Dept. of Geological Sciences, Virginia Polytechnic Institute and State University Memoir no. 2, 15-18.
Panageotou, W. and Leatherman, S.P. (1986) Holocene-Pleistocene stratigraphy of the inner shelf off Fire Island, New York: implications for barrier island migration. J. sedim. Petrol., 56, 528-537.

Pantin, H.M. and Evans, C.D.R. (1984) The Quaternary history of the central and southwestern Celtic Sea. Mar. Geol., 57, 259-293.
Paul, C.R.C. (1979) Caledonian echinoderms of the British Isles. In: The Caledonides of the British Isles-reviewed (Ed. by A.L. Harris, C.H. Holland and B.E. Leake), pp. 453-456. Geol. Soc. London Spec. Publs. 8, Scottish Academic Press. 768 pp.
Peach, B.N., Horne, J., Gunn, W., Clough, C.T., Hinxman, L.W. and Teall, J.J.H. (1907) The geological structure of the Northwest Highlands of Scotland (Ed. by Sir A. Geikie). Memoir of the Geological Survey of Great Britain. 668 pp.
Pederson, G.K. (1985) Thin, fine-grained storm layers in a muddy shelf sequence: an example from the Lower Jurassic in the Stenlille 1 well, Denmark. J. geol. Soc. London, 142, 357-374.
Penland, S., Suter, J.R. and Boyd, R. (1985) Barrier island arcs along abandoned Mississippi river deltas. Mar. Geol., 63, 197-233.
Pitman III, W.C. and Golovchenco, X. (1983) The effect of sea level change on the shelf edge and slope of passive margins. In: The shelfbreak: critical interface on continental margins (Ed. by D.J. Stanley and G.T. Moore). Spec. Publs Soc. econ. Paleont. Miner., Tulsa, 33, 41-58.
Porrenga, D.H. (1967) Glauconite and chamosite as depth indicators in the marine environment. Mar. Geol., 5, 495-501.
Proudman, J. (1953) Dynamical oceanography. Methuen, London.
Ranganathan, V. (1983) The significance of abundant K-feldspar in potassium-rich Cambrian shales of the Appalachian Basin. Southeastern Geol., 24, 139-146.
Reineck, H.E. and Singh, I.B. (1971) Genesis of laminated sand and graded rhythmites in storm sand layers of shelf mud. Sedimentology, 18, 123-128.
Robinson, A.H.W. (1966) Residual currents in relation to shoreline evolution of the East Anglian coast. Mar. Geol., 4, 57-84.
Rodolfo, K.S., Buss, B.A. and Pilkey, O.H. (1971) Suspended sediment increase due to hurricane Gerda in continental shelf waters off Cape Lookout, North Carolina. J. sedim. Petrol., 41, 1121-1125.
Rubin, D.M. (1987) Formation of scalloped cross-bedding without unsteady flows. J. sedim. Petrol., 57, 39-45.

Russell, M.J. and Allison, I. (1985) Agalmatolite and the maturity of sandstones in the Appin and Argyle Groups and Eriboll Sandstone. Scott. J. Geol., 21, 113-122.
Scrutton, C.T. (1978) Periodic features in fossil organisms and the length of the day and month. In: Tidal friction and the Earth's rotation (Ed. by P. Brosche and J. Sundermann), pp. 154-196. Springer-Verlag.
Seilacher, A. (1982) Distinctive features of sandy tempestites. In: Cyclic and event stratification (Ed. by A. Seilacher and G. Einsele). Springer-Verlag.
Siegenthaler, C. (1982) Tidal cross-strata and the sediment transport rate problem: a geologist's approach. Mar. Geol., 45, 227-240.
Smith, A.G., Hurley, A.M. and Briden, J.C. (1981) Phanerozoic palaeocontinental world maps. Cambridge University Press.
Smith, J.D. (1969) Geomorphology of a sand ridge. J. Geol., 77, 39-55.
Soper, N.J. and Barber, A.J. (1982) A model for the deep structure of the Moine Thrust Zone. J. geol. Soc. London, 139, 127-138.
Specht, R.W. and Brenner, R.L. (1979) Storm wave genesis of bioclastic carbonates in Upper Jurassic epicontinental mudstones, East-Central Wyoming. J. sedim. Petrol., 49, 1307-1322.
Spizharski, T.N., Zhuravleva, I.T., Repina, L.N., Rosanov, A.Yu., Tchernysheva, N.Ye. and Ergaliev, G.H. (1986) The stage scale of the Cambrian system. Geol. Mag., 123, 387-392.
Stein, A.H. (in prep.) Basement controls upon Hebridean Basin development, N.W. Scotland. Basin Research.
Stewart, A.D. (1967) Torridonian rocks of Scotland reviewed. In: North Atlantic-geology and continental drift (Ed. by M. Kay), pp. 595-608. Am. Ass. Petrol. Geol. Memoir no. 12.
Stride, A.H., Belderson, R.H., Kenyon, N.H. and Johnson, M.A. (1982) Offshore tidal deposits: sand sheet and sand bank facies. In: Offshore tidal sands: processes and deposits (Ed. by A.H. Stride), pp. 95-124. Chapman and Hall.
Swett, K. (1965) Petrology of the Cambro-Ordovician succession of the Northwest Highlands of Scotland. Unpublished Ph.D thesis. University of Edinburgh. 186 pp.

Swett, K, (1968) Authigenic feldspars and cherts resulting from dolomitisation of illitic limestones: a hypothesis. J. sedim. Petrol., 38, 128-135.
Swett, K. (1969) Interpretation of depositional and diagenetic history of Cambrian-Ordovician succession of Northwest Scotland. In: North Atlantic-geology and continental drift (Ed. by M. Kay), pp. 630-646. Am. Ass. Petrol. Geol. Memoir no. 12.
Swett, K. (1981) Cambro-Ordovician strata in Ny Friesland, Spitzbergen and their paleotectonic significance. Geol. Mag., 118, 225-336.
Swett, K., Klein, Devries G. and Smit, D.E. (1971) A Cambrian tidal sand body-the Eriboll Sandstone of Northwest Scotland. J. Geol., 79, 400-415.
Swett, K. and Smit, D.E. (1972) Paleogeography and depositional environments of the Cambro-Ordovician shallow marine facies of the North Atlantic. Bull. geol. Soc. Am., 83, 3223-3248.
Swift, D.J.P. (1968) Coastal erosion and transgressive stratigraphy. J. Geol., 76, 444-456.
Swift, D.J.P. (1976) Coastal sedimentation. In: Marine sediment transport and environmental management (Ed. by D.J. Stanley and D.J.P. Swift), pp. 255-310. John Wiley and Sons, New York.
Swift, D.J.P. and Freeland, G.L. (1978) Current lineations and sand waves on the Inner Shelf, Middle Atlantic Bight of North America. J. sedim. Petrol., 48, 1257-1266.
Swift, D.J.P., Freeland, G.L. and Young, R.A. (1979) Time and space distribution of megaripples and associated bedforms, Middle Atlantic Bight, North American Atlantic Shelf. Sedimentology, 26, 389-406.
Swift, D.J.P., Hudelson, P.M., Brenner, R.L. and Thomson, P. (1987) Shelf construction in a foreland basin: storm beds, shelf sandbodies and shelf-slope depositional sequences in the Upper Cretaceous Mesaverde Group, Book Cliffs, Utah. Sedimentology, 34, 423-458.
Swift, D.J.P., Niederoda, A.W., Vincent, C.E. and Hopkins, T.S. (1985) Barrier island evolution, Middle Atlantic Shelf, U.S.A. Part 1: shoreface dynamics. Mar. Geol., 63, 331-361.
Swift, D.J.P., Sanford, R.B., Dill, C.E. and Avignone, N.F. (1971) Textural differentiation on the shoreface during retreat of an

unconsolidated coast, Cape Henry to Cape Hatteras, North Carolina. Sedimentology, 16, 221-250.

Swift, D.J.P., Young, R.A., Clarke, T.L., Vincent, C.E., Niedoroda, A. and Lesht, B. (1981) Sediment transport in the Middle Atlantic Bight of North America: synopsis of recent observations. In: Holocene marine sedimentation in the North Sea Basin (Ed. by S.-D. Nio, R.T.U. Shüttenhelm and Tj.C.E. van Weering). Spec. Publs. Int. Ass. Sedim., 5, 361-383. Blackwell Scientific Publications.

Tanner, W.F. (1971) Numerical estimates of ancient waves, water depth and fetch. Sedimentology, 16, 71-88.

Tavener-Smith, R. (1982) Prograding coastal facies associations in the Vryhead Formation (Permian) at Effingham Quarries near Durban, South Africa. Sediment. Geol., 32, 111-140.

Terwindt, J.H.J. (1981) Origin and sequences of sedimentary structures in inshore mesotidal deposits of the North Sea. In: Holocene marine sedimentation in the North Sea Basin (Ed. by S.-D. Nio, R.T.U. Shüttenhelm and Tj.C.E. van Weering). Spec. Publs. Int. Ass. Sedim, 5, 4-26. Blackwell Scientific Publications.

Teyssen, T. (1984) Physical model and FORTRAN IV program to estimate paleotidal flow velocities from features of sandwaves. Comp. Geosci., 10, 237-244.

Tucker, M.E. (1982) Storm surge sandstones and the deposition of interbedded limestone: Late Precambrian, Southern Norway. In: Cyclic and event stratification (Ed. by G. Einsele and A. Seilacher), pp. 363-370. Springer-Verlag.

Tunbridge, I.P. (1983) The Middle Devonian shoreline in North Devon, England. J. geol. Soc. London, 140, 147-158.

Tye, R.S. (1984) Geomorphic evolution and stratigraphy of Price and Capers Inlets, South Carolina. Sedimentology, 31, 655-674.

Watts, A.B. (1982) Tectonic subsidence, flexure and global changes in sea level. Nature, 297, 469-474.

Wilde, P. (1987) Model of progressive ventilation of the Late Precambrian-early Palaeozoic ocean. Am. J. Sci., 287, 442-459.

Wright, S.C. (1985) The study of the depositional environments and diagenesis in the Durness Group of Northwest Scotland. Unpublished Ph.D. thesis. Oxford University.

Villas, F., Sopena, A., Rey, L., Amos, A., Nombela, M.A. and Arche, A. (1985) The Corrubedo tidal inlet: processes and facies, Galicia, NW Spain. In: IAS Symposium on modern and ancient clastic tidal deposits, Comparative Sedimentology Division, University of Utrecht (abstracts), pp. 150-153.

Yang, Chang-shu and Sun, Jia-song (1985) Tidal sand ridges on the shelf of East China Sea. In: IAS Symposium on modern and ancient tidal deposits, Comparative Sedimentology Division, University of Utrecht (abstracts), pp. 166-168.

Yochelson, E.L. (1983) Salterella (Early Cambrian; Agmata) from the Scottish Highlands. Palaeontology, 26, 253-260.

```
$
$ TY TMTIDE.FOR
c       PROGRAM VELEST
C
C       PROGRAM FOR ESTIMATION OF PALEOTIDAL VELOCITIES
C       FROM CROSS BEDDING SETS WITH MUD DRAPES USING AN
C       ITERATIVE METHOD.
C       AUTHOR : T.TEYSSEN, BONN 1982
C
        DIMENSION DAT1(11),DAT2(11)
        REAL  I,J,PI,LLIMIT,LEST,K
        PI=3.141592654
        IT=0
C             IFPRT=1 CAUSES DETAILED OUTPUT
        IFPRT=1
        IFCON=1
        NNLST=0
        IEX=1
        RANINT=1.5
        DIF=99999999.
        SAVDIF=DIF
        READ(1,99999)UCES
        READ(1,99999)D
        READ(1,99999)GAMMA
        READ(1,99999)H
        READ(1,99999)K
        LLIMIT=1.1
        ULIMIT=10.
        DGH2K=(D*H*GAMMA)/(2.*K)
   10 STEP1=(ULIMIT-LLIMIT)/10.
        STEP2=(UCES*ULIMIT-UCES*LLIMIT)/10.
        IGRENZ=INT((ULIMIT-LLIMIT)/STEP1)+1
        DO 40 II=1,IGRENZ
          I=LLIMIT+(II-1)*STEP1
          IF(I.GT.ULIMIT) GOTO 40
C
C         EUMS IS INITIAL ESTIMATE OF THE VELOCITY
C
          EUMS=UCES*I
          ARG=UCES/EUMS
C
C         EVALUATION OF LIMITS OF INTIGRATION T1 AND T2 AS
C         FUNCTION OF THE INITIAL ESTIMATE EUMS
C
          T1=(10.0/(2.*PI))*ARSIN(ARG)
          T2=.5*10.0-T1
          IF(IFPRT.EQ.1)WRITE(2,99997) II,EUMS
C
C         EVALUATION OF ACTUAL VALUES OF THE COEFFICIENTS
C         OF POLYNONE (6)
C
          AA=A(T2)-A(T1)
          BB=B(T2)-B(T1)
          CC=C(T2)-C(T1)
          D=(UCES**3)*(T2-T1)-DGH2K
          BB=BB/AA
          CC=CC/AA
          DD=D/AA
          JGRENZ=INT((UCES*ULIMIT-UCES*LLIMIT)/STEP2)+1
          DO 20 JJ=1,JGRENZ
            J=UCES*LLIMIT+(JJ-1)*STEP2
C
C           POLYNOME OF EQUATION (6)
C
            ZERO=J**3-BB*UCES*J**2-CC*J*UCES**2-DD
            DAT1(JJ)-J
            DAT2(JJ)=ZERO
   20   CONTINUE
        IF(IFPRT.EQ.1)WRITE(2,99996) (DAT1(M),M=1,JGRENZ)
        IF(IFPRT.EQ.1)WRITE(2,99993) (DAT2(M),M=1,JGRENZ)
```

```
C
C          POLYNOME OF EQUATION (6)
C
           ZERO=J**3-BB*UCES*J**2-CC*J*UCES**2-DD
           DAT1(JJ)=J
           DAT2(JJ)=ZERO
   20   CONTINUE
        IF(IFPRT.EQ.1)WRITE(2,99996) (DAT1(M),M=1,JGRENZ)
        IF(IFPRT.EQ.1)WRITE(2,99993) (DAT2(M),M=1,JGRENZ)
C
C       DETERMINE WHETHER A ZERO VALUE EXISTS
C
        DO 25 M=2,JGRENZ
           IF((DAT2(M-1).GT.0..AND.DAT2(M).LT.0.).OR.
      &    (DAT2(M-1).LT.0..AND.DAT2(M).GT.0.)) GOTO 26
   25   CONTINUE
        GOTO 30
   26   CONTINUE
        IFCON=0
C
C       EVALUATION OF ZERO VALUES
C
        CALL NLST(DAT2,DAT1,II,YY,EUMS,INLST,IS)
        IF(INLST.LE.NNLST) GOTO 27
        NNLST=INLST
        ISI=IS
   27   CONTINUE
        DIFF=ABS(EUMS-YY)
        IF(DIFF.GT.DIF) GOTO 30
        DIF=DIFF
        SAVEII=II
        SAVEYY=YY
        SAVEEU=EUMS
   30   CONTINUE
   40   CONTINUE
        IF(IFPRT.EQ.1)WRITE(2,99994) LLIMIT,ULIMIT,DIF,SAVEII
       &SAVEYY,SAVEEU
        IT=IT+1
        IF(DIF.EQ.SAVDIF)IFCON=1
        DIF=SAVDIF
        IF(IFCON.EQ.1) SAVEII=5.
        IF(IFCON.EQ.1) RANINT=3.
        IF(IFCON.EQ.0) RANINT=1.5
        LEST=(LLIMIT*UCES+(SAVEII-1)*STEP1*UCES)/UCES
C
C       REDUCE RANGE OF THE INTERVAL OF POSSIBLE SOLUTIONS OF
C       THE MODEL
C
        LLIMIT=LEST-(STEP1*RANINT)
        IF(LLIMIT.LE.1.) LLIMIT=1.1
        ULIMIT=LEST+(STEP1*RANINT)
        IF(IT.GT.5) GOTO 50
        GOTO 10
   50   CONTINUE
         CONF=ABS(SAVEEU-SAVEYY)
        IF(IFCON.EQ.1) WRITE(2,99995)
        WRITE(2,99998) SAVEEU,CONF
        IF(NNLST.LE.1) GOTO 100
        IEX=IEX+1
        IF(IEX.GT.5) GOTO 100
        WRITE(2,99992)
        IT=0
        IF(ISI.GT.1) GOTO 60
        LLIMIT=1.1*(SAVEEU/UCES)
        ULIMIT=10.
        IF(IEX.GE.3.AND.IFCON.EQ.1) ULIMIT=LLIMIT+4.*UCES
        GOTO 70
   60   LLIMIT=1.1
        ULIMIT=.9*(SAVEEU/UCES)
        IF(IEX.GE.3.AND.IFCON.EQ.1) LLIMIT=ULIMIT-4.*UCES
        IF(LLIMIT.LE.1.) LLIMIT=1.1
   70   CONTINUE
        GOTO 10
```

```
      II=0
      IF(ISI.GT.1) GOTO 60
      LLIMIT=1.1*(SAVEEU/UCES)
      ULIMIT=10.
      IF(IEX.GE.3.AND.IFCON.EQ.1) ULIMIT=LLIMIT+4.*UCES
      GOTO 70
   60 LLIMIT=1.1
      ULIMIT=.9*(SAVEEU/UCES)
      IF(IEX.GE.3.AND.IFCON.EQ.1) LLIMIT=ULIMIT-4.*UCES
      IF(LLIMIT.LE.1.) LLIMIT=1.1
   70 CONTINUE
      GOTO 10
  100 CONTINUE
99999 FORMAT(F10.0)
99998 FORMAT(1x,//' THE PALEOTIDAL PEAK VELOCITY WAS ',F8.4,
     &' +-',f8.4,'M/SEC' )
99997 FORMAT(1H0,//'II=',I4,10X,'EUMS=',F10.3)
99996 FORMAT(1x,//'      J=',6F11.2/6X,5F11.2)
99995 FORMAT(1H ,//' WARNING : NO STEADY CONVERGENCE OF THE MODEL,',
     &/,' THE RESULT MAY ONLY BE A ROUGH ESTIMATE.')
99994 FORMAT(//,5X,6F14.4,/,1H ,126('='))
99993 FORMAT(1x,//' F(J)=',4F16.4/6X,4F16.4/6X,3F16.4)

99992 FORMAT(1H),126('='),//,1H ,' EVALUATION OF THE NEXT',
     &' SOLUTION OF THE MODEL')
      STOP
      END
C
      FUNCTION A(T)
C
C     EVALUATION OF COEFFICIENT A OF EQUATION (5)
C
      PI=3.141592654
      A=(10.0/(24.*PI))*COS(6.*PI*T)-(((3.*10.0)/(8.*PI))
     &*COS(2.*PI*T))
      RETURN
      END
C
      FUNCTION B(T)
C
C     EVALUATION OF COEFFICIENT B OF EQUATION (5)
C
      PI=3.141592654
      B=((3.*T)/2.)-((3.*10.0)/(8.*PI))*SIN((PI*T)/10.0)
      RETURN
      END
C
      FUNCTION C(T)
C
C     EVALUATION OF COEFFICIENT C OF EQUATION (5)
C
      PI=3.141592654
      C=((3.*10.0)/(2.*PI))*COS((2.*PI*T)/10.0)
      RETURN
      END
C
      FUNCTION ARSIN(ARG)
C
C     COMPUTATION OF THE ARCSIN FUNCTION OF THE ARGUMENT
C
      IF(ARG.EQ.0.) GOTO 10
      IF(ARG.EQ.1.) GOTO 20
      ARSIN=ATAN(ARG/SQRT(1.-ARG**2))
      GOTO 30
   10 ARSIN=0.
      GOTO 30
   20 ARSIN=1.5707963
   30 RETURN
      END
C
C
      SUBROUTINE NLST(X,Y,N,YY,EST,INLST,IS)
C
C     DETERMINATION OF ZERO VALUES OF FUNCTION Y(X)
```

```
      GOTO 30
   10 ARSIN=0.
      GOTO 30
   20 ARSIN=1.5707963
   30 RETURN
      END
C
C
      SUBROUTINE NLST(X,Y,N,YY,EST,INLST,IS)
C
C     DETERMINATION OF ZERO VALUES OF FUNCTION Y(X)
C     TABLE LOOK UP  USING SEQUENTIAL SEARCH  .
C     LINEAR INTERPOLATION BETWEEN TABLE VALUES USED
C
C     X      VECTOR OF INDEPENDANT VALUES (ARGUMENTS)
C     Y      VECTOR OF DEPENDENT VARIABLES (FUNCTION VALUES)
C     N      NUMBER EF TABLE ENTRIES
C     YY     INTERPOLATED FUNCTION OF ARGUMENT 0. IF MORE THAN
C            ONE ZERO VALUE EXISTS, YY IS THE FUNCTION OF THAT
C            VALUE, FOR WHICH Y(VALUE) EUMS IS MINIMAL
C     EST    ESTIMATE OF VELOCITY AS IN MAIN PROGRAM
C     INLST  NUMBER OF ZERO VALUES
C     IS     INDICATES WHICH ZERO VALUE IS NEAREST TO EUMS
C
C
      DIMENSION X(N),Y(N),ZERO(11)
      XX=0
      J=0
      DO 10 I=2,N
         IF((X(I-1).GT.0..AND.X(I).GT.0.).OR.
     &   (X(I-1).LT.0..AND.X(I).LT.0.)) GOTO 10
         YY=Y(I-1)+(Y(I)-Y(I-1))*(XX-X(I-1))/(X(I)-X(I-1))
         J=J+1
         ZERO(J)=YY
   10 CONTINUE
      INLST=J
      DIF=99999999.
      DO 20 I=1,J
      DIFF=ABS(ZERO(I)-EST)
      IF(DIFF.LT.DIF) GOTO 15
      GOTO 20
   15 YY=ZERO(I)
      DIF=DIFF
      IS=I
   20 CONTINUE
      WRITE(2,1000)
 1000 FORMAT(1H ,'$')
      RETURN
      END
```

EXAMPLE OF PALAEOTIDAL CALCULATION: METHOD OF NIO ET AL. (1982)

This palaeotidal calculation utilises the method of Nio et al. (1982) to which the reader should refer for the theory behind this method. The calculations follow steps 1-4 on p.504-505 of this paper.

Step (1) Determination of the dimensionless version of the bed load transport (V) per unit width.

$$V=2\pi fh\rho_g g\rho^{1/2}/(T\sin\beta(r_gD)^{3/2})=0.38$$

Where: f = bundle height = 8cm

h = megaripple thickness = 68cm

T = tidal period = 10 hours

β = foreset dip = 25°

D = grainsize = 0.06cm

r_g = submerged specific weight of sediment = /3

ρ = density of water = $1g/cm^{-3}$

ρ_g = bulk density of sediment = $2.65g/cm^{-3}$

Step (2) Calculation of the dimensionless version of the peak value of the bed load transport rate (ϕ).

$$\phi=V/r=0.36$$

Where r is an approximation to the time-velocity pattern of the tide ($=\pi/3$)

Step (3) Calculation of the peak value of the shear velocity (U_*) during the dominant tide and its dimensionless version (Y) using the bed load transport function where a and n are dimensionless factors with values of 15.6 and 2.77 respectively. These values are derived from Fig. 8 in Nio et al. (1983) and are based on data from the modern Oosterschelde.

$$Y=(\phi/a)^{1/n}=0.26$$

The shear velocity is given by-

$$U=(Y\gamma_g D/\rho)^{1/2}=5.0cm/s$$

Step (4) Calculation of the peak value of flow velocity (U_{100}) 1.0m above the seabed.

$$U_{100}=U_*/0.0547=91cms^{-1}$$

This method is relatively insensitive to the input data f, D and h. For example, by doubling the values of these parameters 2f yields a velocity of 102cm/s, 2h yields the same value and 2D yields a tidal velocity of 108cm/s. This reflects the narrow range of current speeds within which these bundle sequences probably develop. In addition the calculation of the shear velocity in step (4) is held within a narrow range by the inverse relationship of Y and D.

EXAMPLE OF PALAEOTIDAL CALCULATION: METHOD OF TEYSSEN (1984)

This method is based on that of Allen (1981) which is a kinematic version of Bagnold's bedload transport equation:

(1) $$U(t)=U_m \sin(2\pi t/T)$$

Where $0<t<T/2$

U_m=peak current speed

t=time

T=tidal period

Allen (1981) has shown that the bedload transport rate, J(U), may be defined by:

(2) $$J(U)=k(U(t)-U_{ces})^3$$

Where $U>U_{ces}$

J=dry mass per unit width and time

k=empirically derived dimensional coefficient

U_{ces}=threshold velocity for bedload transport

The speed of sandwave advance, V(J) is given by:

(3) $$V(J)=2J/HY$$

Where H=sandwave height

Y=sediment dry bulk density

Bundle spacing, d, is obtained by substitution of equations (1) and (2) in equation (3) and integration, thus defining bundle spacing in terms of the sediment transport rate and the rate of advance of the sandwave within the tidal period.

$$(4) \qquad d=2k/HY\int_{t_1}^{t_2}(U_m \sin(2\ \ t/T)-U_{ces})^3 dt$$

Where t_1 and t_2 are the times during flow of the dominant current when $U(t)=U_{ces}$.

Evaluation of equation (4) leads to:

$$(5) \qquad d=\Big[(2k/HY)(U_m^3 A-U_m^2 U_{ces} B-U_m U_{ces}^2 C-U_{ces}^3 t)\Big]_{t_1}^{t_2}$$

With: $A=(T/24\pi)\cos(6\pi t/T)-(3T/8\pi)\cos(2\pi t/T)$

$B=3t/2-(3T/8\pi)\sin(\pi t/T)$

$C=(3T/2\pi)\cos(2\pi t/T)$

Teyssen's program utilises an iterative procedure whereby an initial estimate of U_m is used to calculate t_1 and t_2, determine U_m from substitution in equation (5) and iterate to improve the original estimate. The iteration proceeds until U_m, t_1 and t_2 are in general agreement with an assumed sinusoidally varying current speed.
Substitution of the coefficients A,B and C and subtraction:

$\bar{A}=A(t_2)-A(t_1)$

$\bar{B}=B(t_2)-B(t_1)$

$\bar{C}=C(t_2)-C(t_1)$

leads to a third degree polynomial in U_m:

(6) $$0=U_m^3-U_m^2U_{ces}(\bar{B}/\bar{A})-U_mU_{ces}^2(\bar{C}/\bar{A})-(U_{ces}^3(t_2-t_1)-dHY/2k)/\bar{A}$$

Where U_{ces}=threshold velocity (m/s)

H=sandwave height (m)

d=bundle spacing (m)

Y=dry sediment bulk density (kg/dm^3)

k=dimensional coefficient estimated from graphs presented by Teyssen (1984)

A sample printout is given of Teyssen's FORTRAN program. Using this method with the following input data gave a palaeotidal velocity of 1.1m/s.

U_{ces}=0.55m/s

d=0.08m

Y=1.6kg/dm^3

H=0.68m

k=8.0kgs^2/m^4